Approaches to Outfitting an Inflatable Habitat

Moon to Mars Exploration Systems and Habitat (M2M X-hab) 2022 Academic Innovation Challenge

Final Report
University of Maryland

Dr. David L. Akin
June 1, 2022

University of Maryland ENAE484 XHab Senior Design Capstone Final Report

Students in ENAE484
Avionics: Benjamin Adarkwa and Alexander Cochran
Crew Systems: Colby Merrill, Elizabeth Myers, Michael Reed, and Kelly O'Keefe
Loads, Structures, and Mechanisms: Mason Hoene, Kealy Murphy, Olivia Naylor, Jack Saunders, Neal Shah, and Logan Swaisgood
Mission Planning and Analysis: Ryan Allegro, Alberto Garcia-Arroba, and Aidan Sandman-Long
Power, Propulsion, and Thermal: Konrad Shire and Matthew Stasiukevicius
Systems Integration: Ronak Chawla, Hajime Inoue, and Joe McLaughlin

Contents

List of Figures

List of Tables

I. Introduction - Joe McLaughlin

The “Moon to Mars eXploration systems and Habitation” or X-Hab challenge is a challenge posed to various universities with the goal of expanding our knowledge of how to create long term space habitats. This is to be accomplished through challenging various universities to carry out tasks such as designing a food growth system or redesigning an already proven CO2 scrubber. The University of Maryland was challenged with finding “Approaches to Outfitting an inflatable habitat.” From this our team developed the following mission statement: “The goal of this team is to design and test systems which will outfit the existing TransHab allowing it to support a sustained human presence in micro and Lunar/Martian gravity environments.” This mission statement allows us to look at multiple approaches while also creating complete and comprehensive designs for extended human habitation in various environments.

Specifically, as a team we designed the habitat interiors based off of two different environments: microgravity and Martian or Lunar gravity. This allowed for two major designs to be created but also allowed for components of the design to be switched out, upgraded, or changed as needed.

II. Mission Statement - Joe McLaughlin

The goal of this team is to design and test systems which will outfit the existing TransHab allowing it to support a sustained human presence in micro and Lunar/Martian gravity environments.

III. Mission Assumptions - Joe McLaughlin

A. The Transhab Architecture

The assumptions of the project can be split into two major categories: TransHab assumptions and Mission and crew systems assumptions. The first assumption is that we will be using the current TransHab design which is a "lightweight habitation module for space applications" [1]. The dimension assumptions for the TransHab are: 8.23 m diameter (7.62 m interior dimension) with a 12.19 m height for the exterior and a 3.35 m diameter with a 7 meter height for the interior hard core. The TransHab shall be able to house six astronauts (with a surge of twelve) over eight months. Currently, the TransHab has no living or working amenities, source of power generation, or life support system and hence, these systems will have to be designed and implemented. Additionally, all critical subsystems will be stored in the core.

Figure 1: Transhab Design [1]

B. Gravitational Environments

The second mission assumption falls into two main categories. The first category is microgravity, whether that be in interplanetary space or Low Earth Orbit, And the second category is either Lunar or Martian Gravity. There will be one design for each category, each outfitted to allow for ergonomic working and living environments.
In the microgravity configuration, the habitat need to accommodate astronauts translating in all three dimensions. To do this multiple floor panels will be removed and handrails placed in various locations.
In the Lunar/ Martian Gravity environment, both the structure and the layout of the Transhab must accommodate the environment. The structure was designed to sustain loads on the martian surface and during launch. Therefore, this structure is used throughout both the designs, as the structure will perform just as well in microgravity as it would in martian gravity. The layout changes from micro to lunar/martian gravity to include ladders, a freight elevator/winch, and a change in the storage configuration.

Figure 2: Lunar/Martian Gravity Configuration

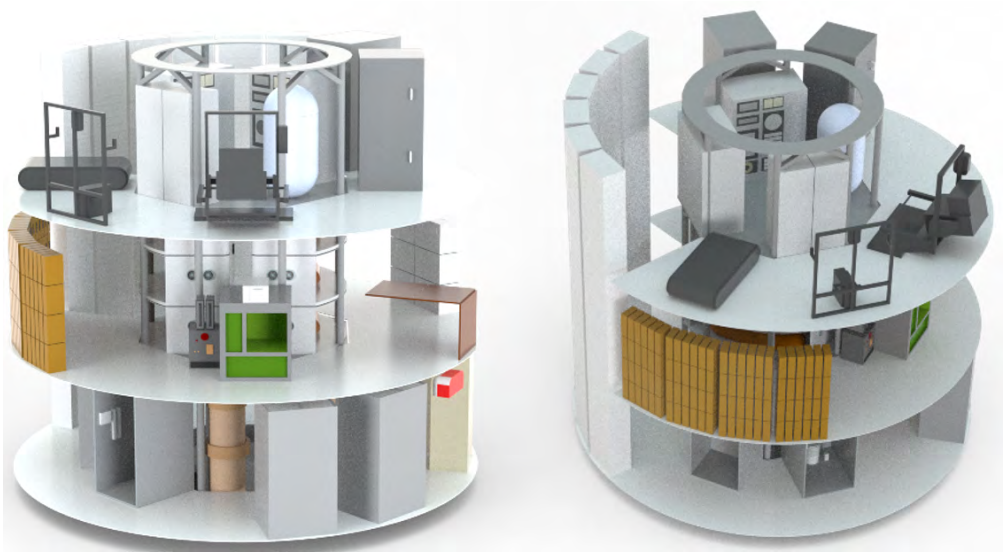

Figure 3: Micro Gravity Configuration

IV. Scope of Project - Ronak Chawla

The scope of this project is to research methods to outfit the existing TransHab architecture to allow for habitation and research of structure, communications, life support and power. The scope also includes testing and evaluating the feasibility of the design and its deployment process by analyzing astronaut comfort and timing of during deployment. In addition, the team defined theoretical mission architectures the design could perform in.

V. Mission Requirements - Ronak Chawla and Joe McLaughlin

The top level mission requirements (M-#) were developed from both NASA X-HAB requirements and requirements from the 484 capstone project. These requirements range from general habitation regulations to detailed loading restriction.

Requirement- ID	**Requirement**	**Source**
M-1	Design Shall Integrate into the Existing TransHab Architecture	NASA X-Hab
M-2	Design shall allow for extended human habitation	UMD ENAE484 & NASA X-Hab
M-3	Outfitted Habitat Shall be Able to Launch on a Current or Near-Term Launch Vehicle	UMD ENAE484
M-4	Design Shall Allow for Flexibility in Mission Objective and Research Goals	UMD ENAE484
M-5	Life support and crew systems shall be able to operate with maximum 6-month resupplies	UMD ENAE484
M-6	No loads may be transferred to the inflated walls	NASA X-Hab

VI. System Requirements - Ronak Chawla

The top level system requirements (S-#) were derived from the Mission Requirements and Mission Reference Architecture. These requirements cover the high-level needs for the system.

Requirement- ID	Requirement	Source
S-1	Shall continuously support 6 crew members and with a surge of 12 people [2]	M-1, M-2
S-2	Shall be designed with two configurations: Microgravity and Lunar/-Martian gravity	M-2, M-4
S-3	Shall have a deployable floor mechanism to the inflated area	M-2, M-4, M-6
S-4	Shall be able to communicate and facilitate data transfer internally and externally	M-2, M-4, M-5
S-5	Shall provide a working laboratory environment for scientific research and crew experiments	M-4
S-6	Shall provide power to meet habitation and working needs	M-5

Subsequently, additional system requirements that are more specific to the sub elements of the design were derived from the top-level system requirements. These include requirements for: Crew Systems (CS); Mission Planning and Analysis; Loads, Structures and Mechanisms; Avionics; and Power, Propulsion and Thermal sub-teams.

A. Crew Systems Requirements

Requirement- ID	Requirement	Source
CS-1	Shall provide a breathable atmosphere to allow for a max load of 12 working astronauts	S-1
CS-2	Shall provide potable water through recycling and resupply	S-1
CS-3	Shall provide temperature control	S-1
CS-4	Shall protect crew from radiation	S-1
CS-5	Shall provide waste management (Human and Other)	S-1
CS-6	Shall provide fire protection	S-1
CS-7	Shall monitor critical systems	S-1
CS-8	Shall provide private and comfortable crew quarters for long duration habitation	S-1
CS-9	Shall provide food, both supplied and habitat grown to sustain the max load of inhabitants	S-1
CS-10	Shall provide crew with options to exercise	S-1
CS-11	Shall provide sufficient lighting for crew living (Simulated Day/Night)	S-1
CS-12	Shall be comprised of interchangeable parts and easily repaired in emergency	S-1
CS-13	Shall abide by NASA-STD-3001: ”Crew Health” & ”Human Factors, Habitability, and Environmental Health” [3]	S-1
CS-14	Shall provide minimum lab space and capabilities to meet mission requirements	S-5, S-2
CS-15	Shall provide the internal aspects of EVA support	S-5

B. Mission Planning and Analysis Requirements

Requirement- ID	Requirement	Source
MPA-1	Both designs shall provide ergonomic working and living amenities given their respective gravities	S-2, S-5
MPA-2	Both designs shall allow for easy transitioning through various spaces throughout the Habitat	S-2
MPA-3	Shall provide protection from various space phenomena and environmental hazards within our scope	S-2
MPA-4	Both microgravity and Lunar/Martian gravity designs shall be able to support their respective missions for a duration of 180 days	M-5, S-2
MPA-5	Each design shall accommodate deployment and unpacking of the core for their respective gravities	S-2

C. Loads, Structures and Mechanisms Requirements

Requirement- ID	Requirement	Source
LSM-1	Shall be autonomously deployed to the inflatable area	S-3
LSM-2	Shall have three floors that match the levels of the core	S-3
LSM-3	Shall be able to support working load of equipment, amenities and inhabitants	S-1, S-3, S-4
LSM-4	Shall not deflect more than 5.9 mm [4]	S-3
LSM-5	Shall adhere to NASA-STD-5001 for all safety factors	S-1, S-3, S-4

D. Avionics Requirements

Requirement- ID	Requirement	Source
AV-1	Shall provide robust and redundant internal communication methods	S-4
AV-2	Shall provide robust and redundant communication to ground stations	S-4
AV-3	Shall support video and audio communication per CCSDS standards	S-4
AV-4	Shall provide communication methods while on EVA	S-4
AV-5	Shall provide sufficient lighting for working on mission systems	S-5

E. Power, Propulsion and Thermal Requirements

Requirement- ID	Requirement	Source
PPT-1	Shall provide 12.5 kW of power under normal operating conditions	S-6, S-1
PPT-2	Shall provide 15.5 kW of power during maximum demand	S-6, S-1
PPT-3	Shall include redundant batteries to support the system for 24 hours under emergency conditions	S-6

VII. Design Reference Mission - Hajime Inoue

The design reference mission guides through the basic overview of the TransHab missions in different configurations we designed for.

A. Microgravity Configuration

Figure 4 visualizes the journey of the TransHab. Following its launch from Earth, the TransHab will enter the parking orbit of Earth. It will then be rendezvoused with the crew. The crew, as illustrated, will be launched separately and dock on the TransHab in order to allow crew members to ultimately move into the habitat. The Transhab will be deployed and outfitted to house the crew in the inflated region of the TransHab. Once the TransHab is successfully in orbit, inflated, and outfitted, crew members will move in. The TransHab will be supplied food, water, and other resources on a recurrent basis.

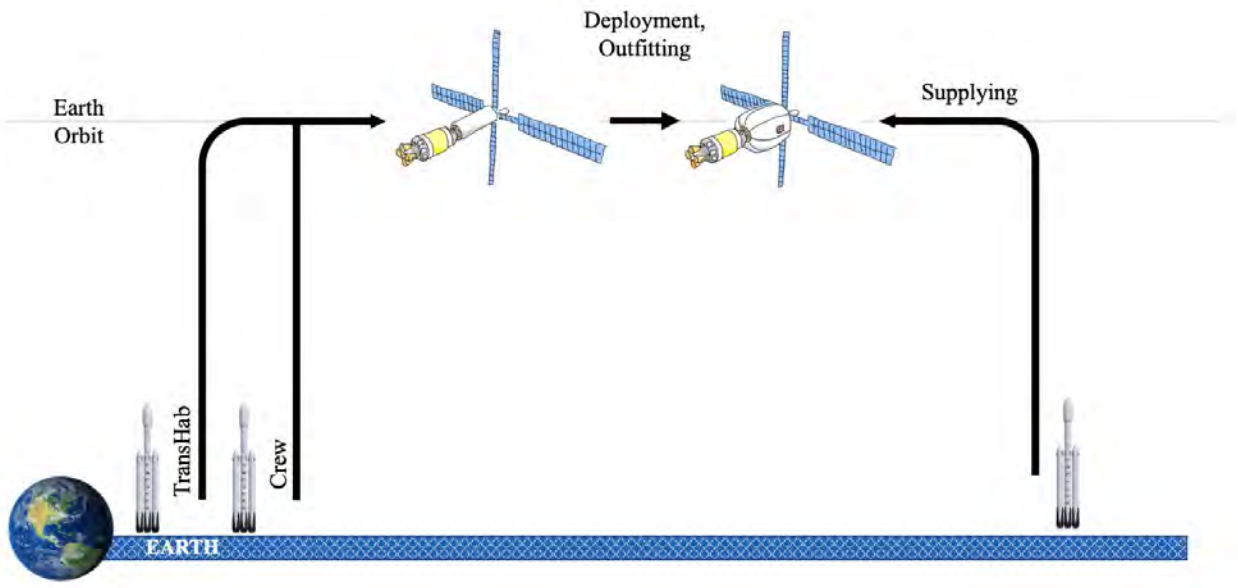

Figure 4: DRM: Microgravity Configuration

B. Lunar/Martian Gravity Configuration

Figure 5 provides an overview of the TransHab being launched from Earth to enter a different destination orbit then land on either Mars or the Moon. Like in the design reference mission for microgravity configuration, it indicates the process by which crews will rendezvous the TransHab via a separate launch once the TransHab enters the parking orbit of Earth. Once the TransHab enters the destination orbit—that of Mars or the Moon—it will enter the Entry, Descent, and Landing (EDL) phase. Once the landing is successfully performed, the TransHab will undergo its deployment process and inflate to allow crew members to move into the habitat. While remaining on Mars/the Moon, the TransHab will be supplied food, water, and other resources on a recurrent basis.

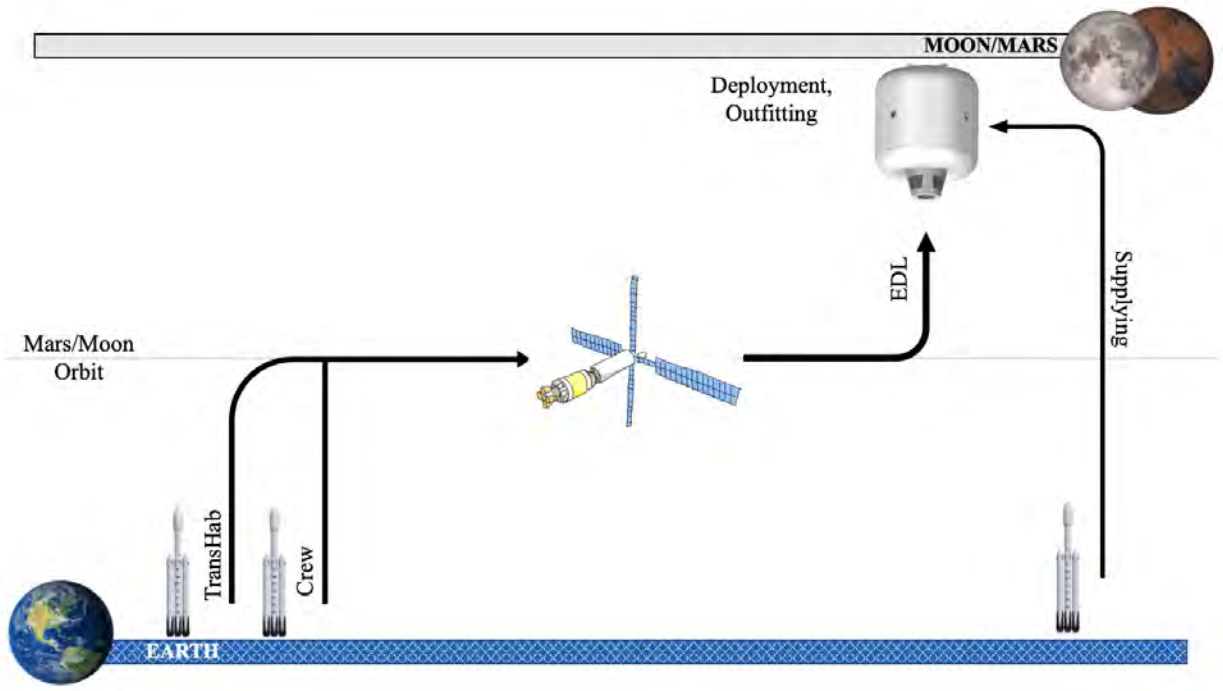

Figure 5: DRM: Lunar/Martian Gravity Configuration

VIII. Interior Layout

A. Interior Design

1. Functional Area Placement - Colby Merrill

The interior design was conducted based on a ranked list from the most difficult designated areas to place to the areas that could effectively work anywhere. The layout is not designed with well-defined rooms, but rather functional areas. That is, the consideration to place an area was based on what people would need to do in the area and where a crew member might have to go after finishing their task. Top priority was given to the placement of the airlock, crew quarters, and life support systems, as they have significant constraints on where they can be placed. The mid-priority placements are defined as being constrained and dependent on the high priority placements. They are the laboratory, kitchen, and food storage areas. The lowest priority placements were the exercise area and bathrooms, as the equipment can be deployed to fit anywhere in the habitat. Figure 6 depicts the final layout of the habitat, color-coded based on priority placements.

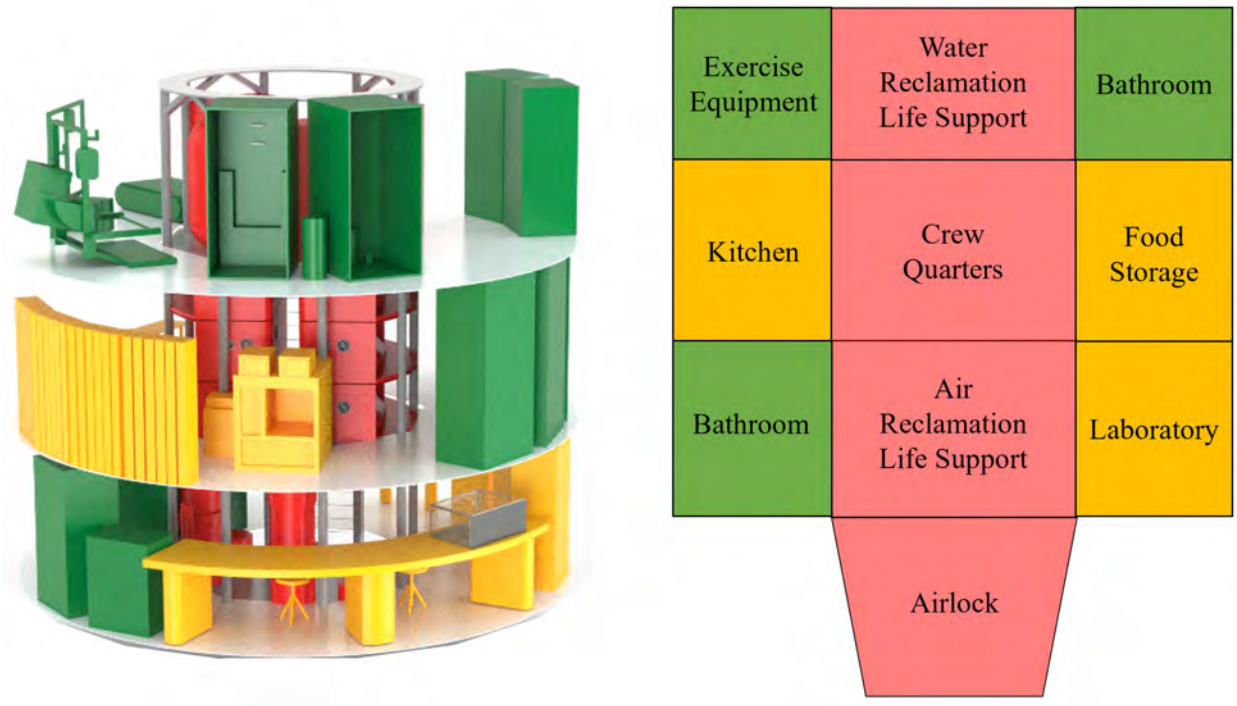

Figure 6: On the left: A colored render of the final layout with coinciding colors to the right image. All storage areas are green as well, as they have the lowest priority of all placements. On the right: Side view of final layout of TransHab displaying the areas of the habitat based on the priority of placement. Red = high priority, Yellow = mid priority, Green = low priority.

The airlock was the first placement considered, as the TransHab architecture includes three main floors interior to the inflatable volume, and only the core structure protruding beyond the inflatable envelope along the central axis. For planetary surface applications, the core structure was extended at the lower end to allow the placement of the airlock there, as it allows direct access to the surface at that location. It is distinct from the rest of the habitat in this position, which provides an advantage in limiting surface regolith intrusion into the rest of the habitat. An airlock placement was investigated on the first inflated floor as well, but would require a more intensive exterior design to accommodate.

The crew quarters was the next priority item, as this area also has many considerations. In order to shield the crew from radiation, the crew quarters are placed in the core where they will have the maximum amount of material between them and the outside environment. The walls of the individual sleeping compartments for the crew will also include extra radiation shielding. Located on a planetary surface, most radiation will approach from the sides or top of the habitat. With this consideration, there were two options left for crew quarter placement: the first floor core or the second floor core. The first floor is very appealing from a radiation shielding standpoint, but there would be no way

for the crew to enter/exit the airlock if the crew quarters were placed there. With this in mind, the final decision was to place the crew quarters in the second floor core, which is also the tallest floor, providing the most volume to fit the six crew members. The downside to this placement is the limited volume which cannot be rectified unless the crew quarters are moved outside of the core, increasing the potential for radiation damage. The crew quarters design section of this paper will further develop the considerations that went into designing the individual crew quarter cubicles.

The life support systems have some of the tightest constraints for placement of any item in the habitat. These systems are highly interconnected in terms of power, data, fluids, thermal, and air handling, and therefore should be pre-installed in the core prior to launch and should also be operational before the crew enters the inflated habitat. That is, they will not be deployed from the core after inflation. Therefore, there are two potential places left for the life support systems: the first floor core and the third floor core. The water recovery system is placed on the third floor, along with the large water supply tank, to provide additional radiation shielding for the crew in the crew quarters. The oxygen recovery system, particulate scrubbing system, CO_2 scrubbing system, and all other atmospheric/air systems will be placed on the first floor core. The oxygen recovery system and CO_2 scrubbing and reduction systems are among the highest-mass components of the system, so placing them nearer to the bottom helps with distributing the structural loads. Additionally, placing all of the high-mass life support fixtures in the center of the habitat helps to maintain a favorable center of mass. There is a drawback of separating the life support systems, in that if maintenance is required for all of the components, crew members will have to ascend and descend the levels of the habitat to get to the systems.

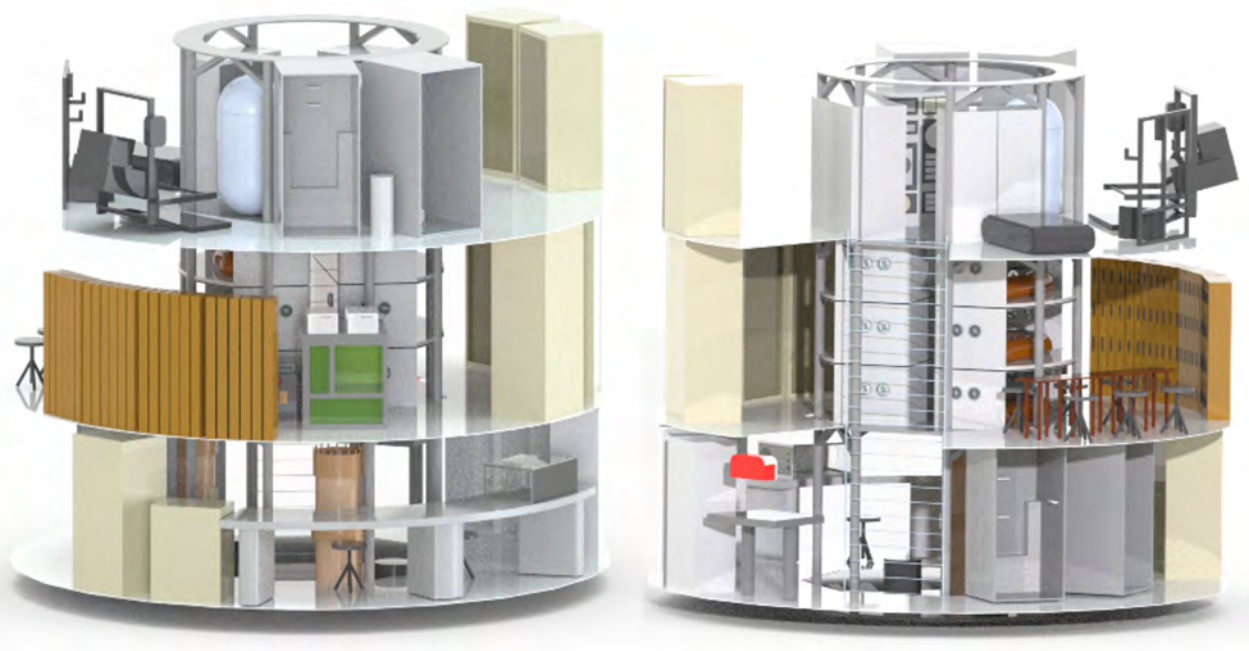

Figure 7: CAD diagram of the fully deployed and outfitted inflatable habitat configured for the lunar surface.

The laboratory area was placed on the first floor in the deployed volume, as it is advantageous to be close to the surface. The crew will be taking extensive regolith and rock samples, and should be able to analyze the samples in a glovebox or other controlled environment within the habitat. Earth analogue habitats such as the NASA DSH/HERA facility have scientific airlocks accessible from the exterior that open directly into the internal glovebox. Since only the airlock is directly adjacent to the surface, it would require an extended staircase or ladder to have the same external science airlock to a laboratory, even if it is on the lowest level. The glovebox will be placed at least 3.5 m off the surface, as the crew requires extra headspace as they walk under TransHab's inflated bladder. Without a robotic or mechanical operating device, transferring samples into the glovebox externally becomes a significant issue. It is likely that a more convoluted system will evolve for in situ sample testing, such as sealing them into containers (as in Apollo), bringing the containers inside the habitat and transporting them to the laboratory, and sealing it to the glovebox before accessing the samples. In any case, it would be advantageous to locate the laboratory on the lowest level of the inflated volume, both for ease of access to the airlock, as well as minimizing any potential contamination from EVA operations. The laboratory will also be used for more extensive spacesuit maintenance, so again, proximity to the airlock is key. Experience from ISS shows that air regeneration systems are among the highest maintenance

components in the habitat; adjacency to the laboratory will provide a more comfortable and productive environment for this category of maintenance activity as well. Ideally, a laboratory area would be placed as close to the lunar surface as possible so that the samples could enter from the surface directly into the glovebox without significant struggle.

The kitchen and dining area is located on the inflated second floor, and the rest of that floor will be dedicated to food storage, general storage, and crew recreation. This floor is coupled with the crew quarters, which conveniently creates a floor strictly dedicated to more relaxed time. One waste management compartment will be placed on each of the first and third floors, with a wash station next to each one. Including more than one bathroom is extremely important for crew accessibility. It is important to place the bathrooms away from the crew quarters, as they will be potentially loud and odorous areas. However, placing them away from the crew quarters also means that it is difficult to get to one when the crew needs to use one during their sleeping hours. Each bathroom is coupled with a wash station. Having a wash station (likely a sponge bath) next to the bathroom on the first floor is helpful, as it might become one of the areas that the crew goes to remove any regolith contamination from suit maintenance. The exercise equipment was the second-lowest priority item, which will sit on the top floor. This is also close to a bathroom and wash station so the crew can clean up after they exercise. The rest of the habitable volume will be dedicated to storage. The second floor storage will be personal crew items, as it is near their sleeping quarters. The first floor will be laboratory equipment storage. The first and third floor also have volume to store other random supplies.

2. Vertical Mobility - Elizabeth Myers

When considering options for vertical mobility within the lunar gravity habitat, the primary choices were a standard ladder or a steep staircase. Concepts for how staircase angles and step distances change with gravity level have been studied at the SSL in the past, and with further research an ideal system could be designed [5]. The primary benefit to using a staircase over a ladder is that the crew members would have at least one of their hands free to carry items between floors. Climbing a ladder requires the use of all four limbs, so crew members would have to resort to other methods of transporting objects within the habitat. However, due to the limited distance between the outer edge of the core and the inflatable wall (2.1 m), the staircase angle would be close to 70°, at which point it is steep enough to be classified as a ship ladder on Earth. Staircases between 50 and 70° are considered to be ship ladders, so the TransHab staircase would reach the upper limit of this category. For a ship's ladder with a width of 0.6 m (24 in) between the rails and a distance of 0.46 m (18 in) between the bottom of the ladder and the wall of the habitat, the angle would indeed be 70°. At this steep of an angle, it would be more difficult and potentially hazardous for the crew to have items in their hands while using the ship's ladder, therefore negating the primary benefit of the choosing the staircase. With the thought of lowering the necessary staircase angle, the use of two separate staircases was also considered. Although using two separate staircases would decrease the angle of each to about 50°, this design would require twice as much floor space and nearly double the amount of habitable volume. Additionally, given the nature of TransHab, any staircase exterior to the core would have to be manually installed by astronauts and it would occupy valuable real estate while packed in the core for transit.

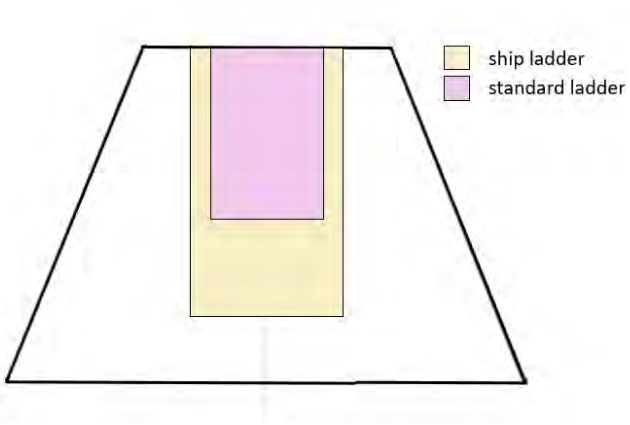

Figure 8: Top view diagram of the available floor space vs the floor space required for the standard ladder (pink) and the ship's ladder (yellow).

As such, vertical ladders were favored for their lower volume and their ability to be permanently installed in the core by only occupying wall space. Another benefit of implementing a standard 90° ladder may also be the conservation of available floor space after core deployment. A ladder with a width of 0.46 m (18 in) between rails and the required 0.18 m (7 in) distance between the rungs and the wall would require 0.6 m^2 of floor area, including the size of the ladder and the 0.76 m (30 in) of space necessary for the user [6]. Comparatively, a single ship's ladder would require an estimated 1.2 m^2 of surface area on the first floor, and dividing this into two staircases would double this number. Figure 3 displays a visual representation of the surface area comparison. Overall, the benefits of a vertical ladder's low volume and lack of installation led to its selection over a staircase.

As previously mentioned, the standard ladder would not allow crew members to carry things between floors. Small and lightweight items such as food packages and clothing could easily be placed in a small bag or a pocket while a crew member is ascending the ladder. Furthermore, a motorized hoist system could allow for the frequent lifting of cargo transfer bags (CTBs) and heavier objects within the same ladder volume that is necessary for human use. Previous research conducted in the SSL determined that test subjects struggled to carry a CTB up a staircase at an angle of 57°, which demonstrates that a hoist system would likely be necessary even if a 70° ship ladder was chosen instead due to the high angle [7]. According to the crew systems mass budget, the heaviest life support system equipment that may have to be moved in the event of an emergent repair would be a Bosch reactor, which has a mass of 500 kg. To transport a maximum mass of 500 kg, the hoist system must be able to move a load of up to 800 N in lunar gravity. The chosen lift design has a max load of 2420 N which allows for a safety factor of 3. In order to transport items from the first floor to the third, this hoist has 4.9 m of lifting capability with a power requirement of 400 watts during operation. With a lifting speed of 0.13 m/s, this 11.3 kg hoist will be able to move objects from the first to the third floor within a minute [8].

Figure 9: CAD design of motorized hoist.

3. Microgravity Configuration - Kelly O'Keefe

The microgravity version of this habitat will keep the same general layout as the surface habitat, with the exception of a few minor changes. Due to the nature of the inflatable design, a 3-floor design was kept in place because load bearing items could not be attached to the walls. So, floors were necessary to keep in order to have a structure to attach all equipment to. A general bottom to top layout was also implemented in order to help the astronauts keep a sense of direction while in the microgravity environment.

All floors will hold the same functional areas as previously outlined in the surface design (lab on 1st floor, kitchen/-food storage on 2nd, exercise on 3rd, bathrooms on both 1st and 3rd floors), however all storage with the exception of a few places for personal storage on the second floor will be moved off of the surface area of the floors and into the gap designed for astronauts to move between the floors. Figure 10 shows this layout. This was done to most effectively use the space as the astronauts will be able to easily access this wall of storage with the assistance of handlebars. This characteristic of having storage line the entire length of the habitat was not achievable in the gravity design, where all items need to be confined to areas that are reachable from the floor space. This wall of storage will be composed of CTBs that will be secured vertically with the first row secured to the first floor and every consecutive row attached to the one below it. They will also be secured horizontally with all CTBs being attached to the sides of each other, and the outer column will be attached at points where it passes the 2nd and 3rd floors.

In addition to the storage layout being changed from the surface habitat, the vertical mobility concept was changed for microgravity. A strict ladder will no longer be necessary for astronauts to move between floors and will instead be replaced by numerous handlebars placed throughout the habitat. Handlebars will be placed on each floor as well as in the space between the floors so that astronauts can move around efficiently. An additional floor panel was also taken out in the microgravity configuration. In the gravity habitat, only one floor panel (1/8th of the entire surface area or 4.6m^2) was removed whereas two floor panels (9.2m^2) were removed for the micogravity habitat. This was done to allow the astronauts to have more space to maneuver when moving between the floors, and to allow the astronauts to feel like they had more headspace when looking up or down (to prevent feelings of claustrophobia). Each functional

area also has small design changes between the surface and microgravity habitats which will be described in their respective functional area design section of this paper.

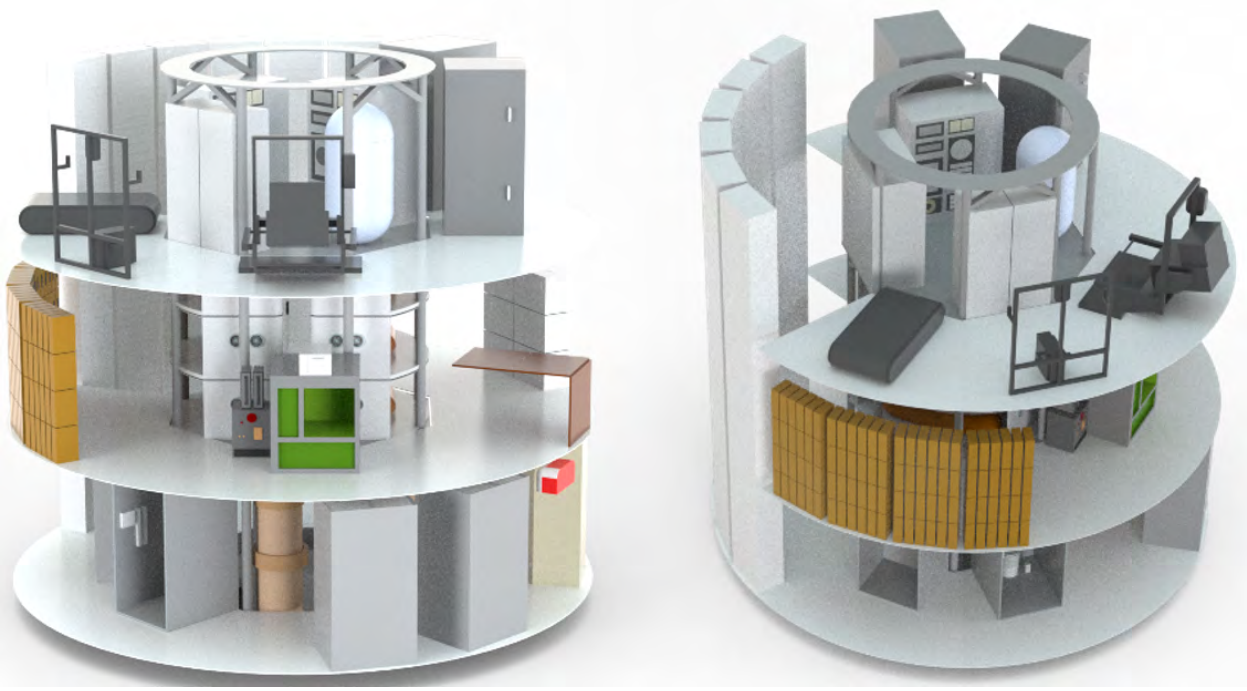

Figure 10: CAD diagram of the fully deployed and outfitted inflatable habitat configured for microgravity environment.

B. Functional Area Designs

1. Crew Quarters - Colby Merrill

The crew quarters needed to be placed in an area of significant radiation shielding, as previously discussed. The design of the crew quarters was particularly challenging, as it is important to maximize the utilization of the available volume throughout the core. This particular section of the core has a 1.7 m (5ft 6in) radius and 2.4 m (8ft) height, and needs to accommodate six crew members with the highest attainable level of comfort. Dividing the total volume of the core (21.5 m^3) by six, the maximum personal volume of a single crew quarter was 3.6 m^3, a more than comfortable volume for an individual crew compartment. However, this number represents the absolute maximum limit that the crew quarter volume can be. There are many additional items required for crew quarter safety and habitability including but not limited to: access corridors, air flow mechanisms, lighting, tablets and/or a personal communication device, radiation shielding walls, and noise mitigation material.

The final design for the crew quarters includes all of the previously mentioned components, and also an ability to control them based on the crew member's specific desire. A tablet is placed above their bed so that they can control the brightness of the lights and speed of airflow inside their personal space. The tablet, not included in Figure 11, will be attachable to multiple surfaces inside their personal volume. The volume itself was designed such that wires and air tubes can fit in the middle of the crew quarter volume. This decreases the total volume for the crew quarters, but is a vital consideration for habitability. The final crew quarters volume ended up being 2.6 m^3 per crew member. The dimensions of a personal space is a 0.8 m height, 2.4 m length, and width that ranges from 1 m to 1.5 m as the area curves. Fans and lights are placed on the walls of each crew volume and can be turned on and off individually based on personal comfort. The bed will be outfitted with straps for the microgravity configuration that can be removed for lunar/Mars configurations. The height of the crew quarters is a significant constraint that limits the activities a crew member can pursue in their personal space. Though they have ample room to lay on their side to read or use their tablets, they will not likely be able to comfortably sit up in their beds.

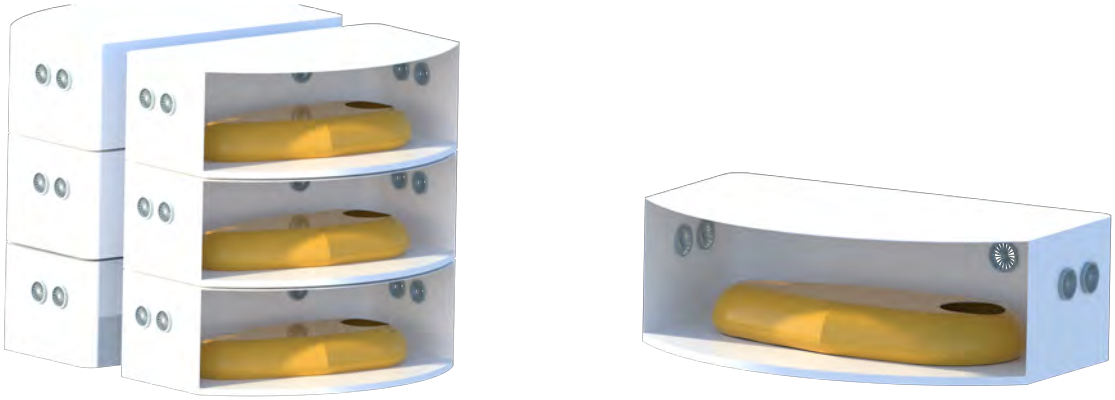

Figure 11: CAD model of the six crew quarters in the second level of the core with doors removed for visibility (left) and single crew quarter cubicle zoomed in with door removed (right). The sleeping pods simply display a representative size rather than a final design specification.

2. Lab Space - Kelly O'Keefe, Colby Merrill

The term "laboratory" is used as a shorthand designation for a general operations area, including (as mentioned above) bench space for working on habitat and EVA systems in need of maintenance or repair. For planetary applications, though, it will almost certainly have dedicated facilities for geological and exobiology investigations. On the lunar surface, characteristics of the regolith are important to study such as the cohesive and electrostatic forces, composition, and porosity.

A glove box is the most important part of this lab, which can minimize contamination of samples by providing a vacuum or, more likely, nitrogen atmosphere around the samples. A geological work station would include microscopic imagers, various spectrometers, and sample preparation equipment, with crew access via isolated gloves and arms. As such, the laboratory will require extensive data links for relaying experimental results to Earth, as well as more mundane tools and equipment for general-purpose repair and operations. The size and shape represented in the CAD model shown in Figure 12 was modeled based on the GEOLab glovebox [9]. The front of the glovebox has two 10-in. ports installed in the polycarbonate window for crew access to the samples using 32-in. hypalon gloves. There will also be one 10-in diameter chamber on either side of the box to allow samples to pass into the box. Finally, various small holes will be placed on either side of the box to allow for any necessary equipment such as Nitrogen inlets and outlets.

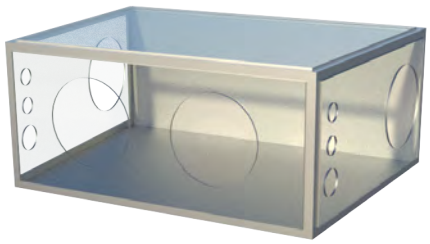

Figure 12: CAD design of a glovebox for lunar sample experiments

In addition to the glovebox, a surface habitat lab space will also include a lab table large enough for miscellaneous experiments to be conducted as well as for any other needs such as maintenance. Maintenance needs could include suit maintenance, life support systems upkeep, as well as any other repairs the astronauts deem appropriate for general care of the habitat. Suits will be stored on this level so astronauts will have easy access to them whenever necessary, and the lab space will be adjacent to the atmosphere life systems in the core so all maintenance needs for that equipment will also be conducted in this space. All necessary tools for maintenance will be housed in the lab storage. Additionally, a lab is an extremely hazardous environment, so in order to keep it as safe as possible, a medical station will be installed in this area. A small space will be equipped to handle all medical emergencies and will contain any necessary supplies such as bandages, topical medications, and items for stitches or other small injuries. A conceptual design for the layout of the lab is shown in Figure 13.

The general concept of the lab stays the same for a microgravity habitat, but some of the specific equipment is switched out for equipment more appropriate for a zero gravity environment. A microgravity habitat no longer has any need for a glovebox as there are no surface samples that need to be contained or experimented on. A dedicated lab table is also no longer necessary and is replaced by express racks which can house multiple small experiments.

Figure 13: CAD depiction of the layout of the lab in a surface habitat.

Space for suit storage and a medical station is still allocated in the microgravity habitat as well. The layout of the microgravity lab can be seen in Figure 14.

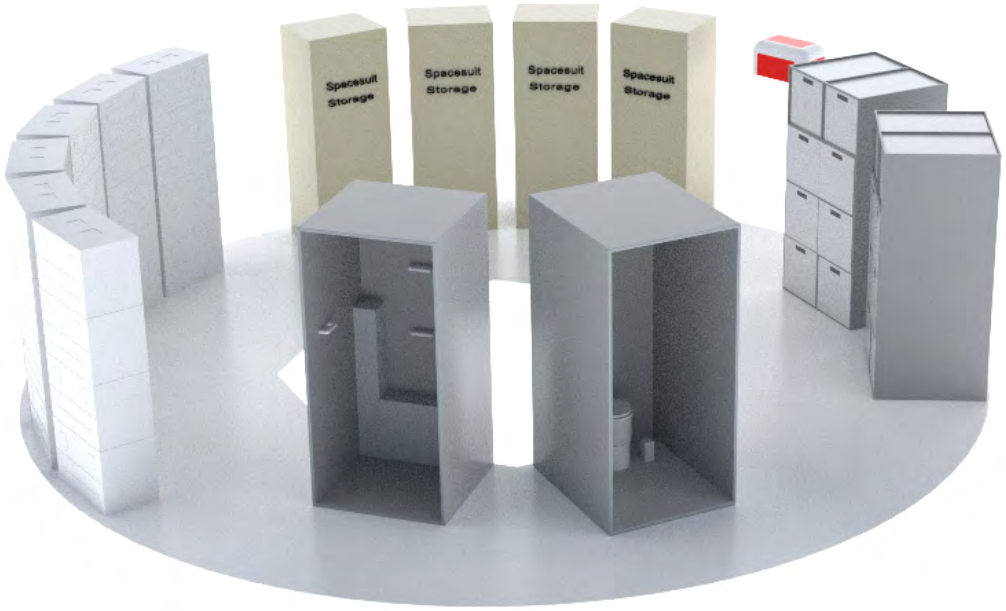

Figure 14: CAD depiction of the layout of the lab in a microgravity habitat.

3. Kitchen and Food Storage - Michael Reed

On the second floor in the inflated area is a "kitchen" for the crew in addition to storage for food, general storage, and a crew recreation area. The "kitchen" is not a kitchen in the traditional sense in that it consists only of a potable water dispenser, a food warmer, and plant habitats. The plant habitats provide fresh produce items for the crew to

consume, and the potable water dispenser and food warmer are for food preparation. The food is stored in food lockers similar to those used on the ISS.

For the lunar habitat design, the crew recreation area has a table and six stools for the astronauts to meet and also share meals together. The remainder of the space is dedicated to general storage for astronauts' personal items and any other equipment that may need to be stored in the habitat.

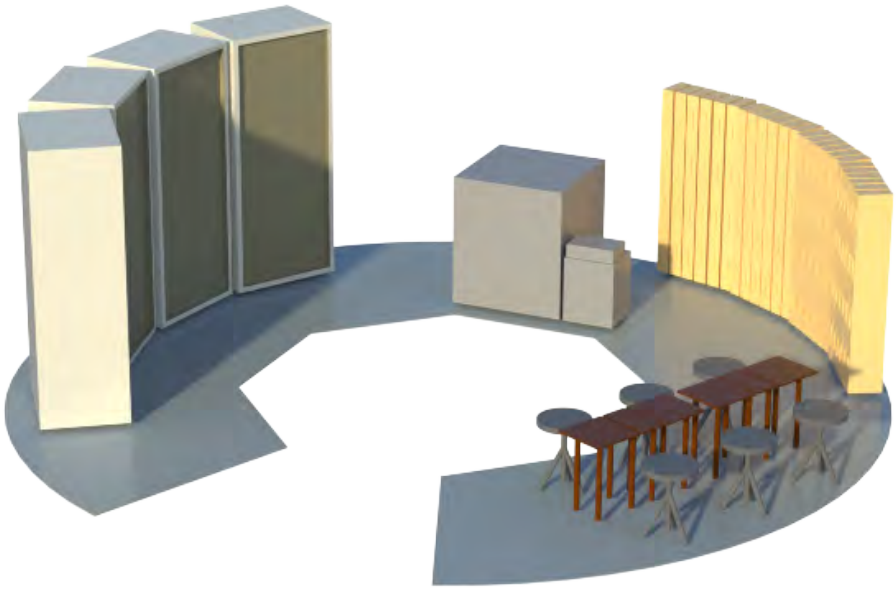

Figure 15: CAD depiction of the second floor layout of the lunar habitat.

This layout changes slightly for the microgravity design. Instead of a table and stools, there is a foldable surface present to serve as a sort of table for meals and other recreational activity that astronauts can affix food and other items to so as to keep them in place. There is also less general storage on the floor since most of the general storage in the microgravity design is stacked through the openings in the second and third floors. The storage that remains is mainly for astronauts' personal belongings since it is right outside the crew quarters.

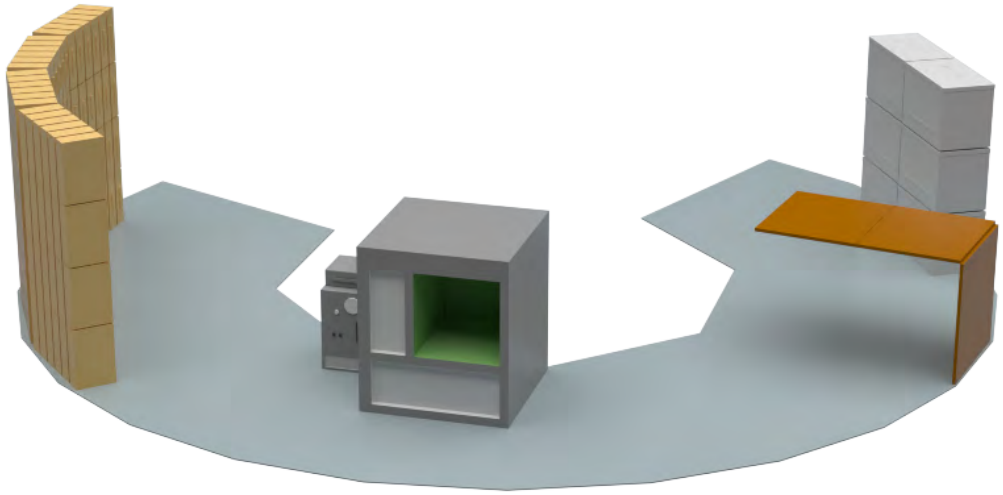

Figure 16: CAD depiction of the second floor layout of the microgravity habitat.

4. Bathroom and Wash Stations - Elizabeth Myers

With a crew of 6, an important decision to be made was determining the number of bathrooms in the habitat. One bathroom would not be sufficient for a crew this large, and there was also a need for redundancy in case one requires repairs or maintenance. Due to the volumetric constraints of TransHab, installing more than two bathrooms would require excessive space and more effort from the crew during the deployment and installation process.

When choosing the location of the bathrooms, placing one on the first and third floors was the most effective way to ensure the crew would have easy access to a bathroom regardless of their location within the habitat. Additionally, having bathrooms near the airlock and exercise equipment will allow the crew to wash up quickly after strenuous activities such as EVAs and exercising. On each floor, the bathroom and wash station stalls will be secured directly outside of the core so the plumbing lines can remain within the core and not occupy valuable floor space.

As shown in Figure 17, the design of the each bathroom includes one stall with a waste collection system and one stall with a wash station to be used for sponge bathing. The waste collection system design was modeled after the Universal Waste Management System (UWMS), which consists of a urinal hose and tank, a seat plate, and a fecal cannister [10]. The output from the urinal tank will be directed to the urine water reclamation system, and the plumbing lines will run through the core. The area surrounding the UWMS will require frequent cleaning, as the device is not perfectly efficient in trapping all waste. Each waste collection system has a mass of 54 kg and a volume of 0.17 m^2 [11].

A stall with amenities for a sponge or towel bath was chosen as the primary method of full-body cleansing for the crew. Although designs for a microgravity shower have been tested and implemented in space, astronauts prefer the simpler method of sponge bathing or wet washcloths. The Skylab 2 mission carried a collapsible shower on board, however; only the first crew members ended up using it due to the general hassle of the device [12]. Each spray shower required at least an hour for setup, bathing, and cleanup because the crew member had to vacuum up all the water droplets from the shower after each use. Feedback from astronauts concluded that systems such as the Personal Hygiene System (PHS) used on the shuttle missions was generally preferred over microgravity shower designs [13].

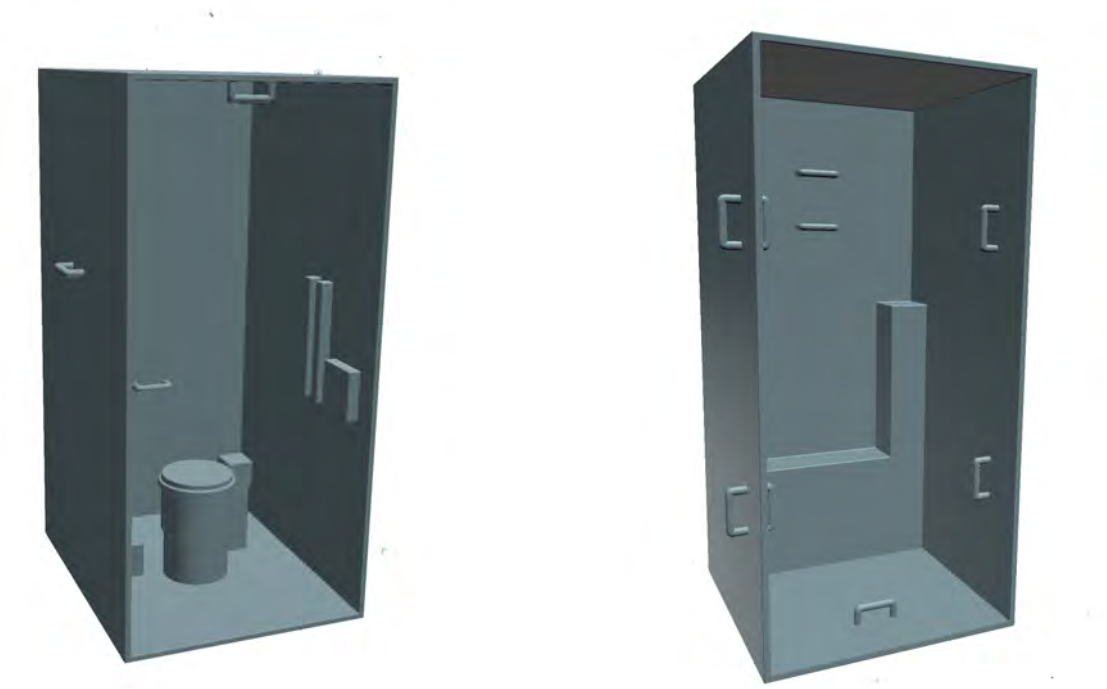

Figure 17: CAD models of the bathroom (left) and the wash station (right) used in the full habitat model.

5. Exercise Space - Elizabeth Myers

Any space habitat housing crew members will require exercise equipment in order to maintain the health of its occupants. Spending extended durations of time in lower gravity levels, such as lunar or microgravity, can lead to loss

of muscle mass and reduce overall muscle function. It can also increase a person's resting heart rate and reduce their exercise capacity. Microgravity in particular leads to cardiovascular deconditioning, which is dangerous as it causes heart weakness and palpitations upon the astronaut's return to Earth [14]. The length and intensity of the workout plans for the crew depend on the level of gravity in their environment. For a lunar gravity habitat, each crew member must exercise for 1.5 hours every day to preserve muscle mass and strength. In a microgravity environment, this time increases to 2.5 hours daily [15].

There are several types of exercise equipment used in space to maintain astronauts' musculoskeletal integrity. For cardiovascular exertion, the most reliable devices are the treadmill and the cycle ergometer (pictured in Figure 18) designed for use in space. The treadmill includes a vibration system to protect the structural integrity of the habitat and a harness system to keep the user in place during the workout. The vibration isolation system counteracts the treadmill and user's movements and prevents these forces from impacting the structure of the habitat. Similarly, the cycle ergometer includes a vibration isolation and stabilization system (CEVIS) to protect its surroundings. This device allows the crew members to exercise in multiple positions, including upright and reclined cycling.

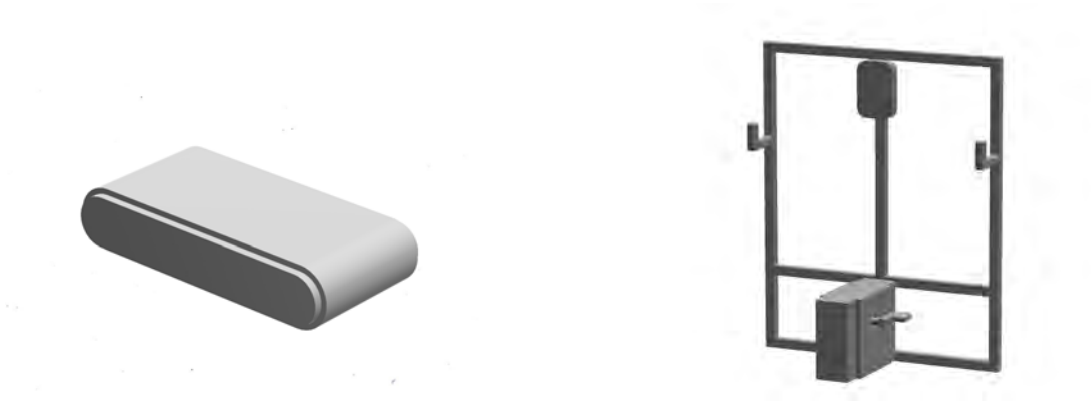

Figure 18: CAD models of the treadmill (left) and the cycle erogmeter (right) used in the full habitat model.

The other important aspect of exercise is weightlifting. The advanced resistive exercise device was designed to allow for a variety of exercises on the targeted muscle groups. There are over a dozen resistive exercises that can be performed using this machine to promote bone generation and use of both primary and secondary muscle groups [16].

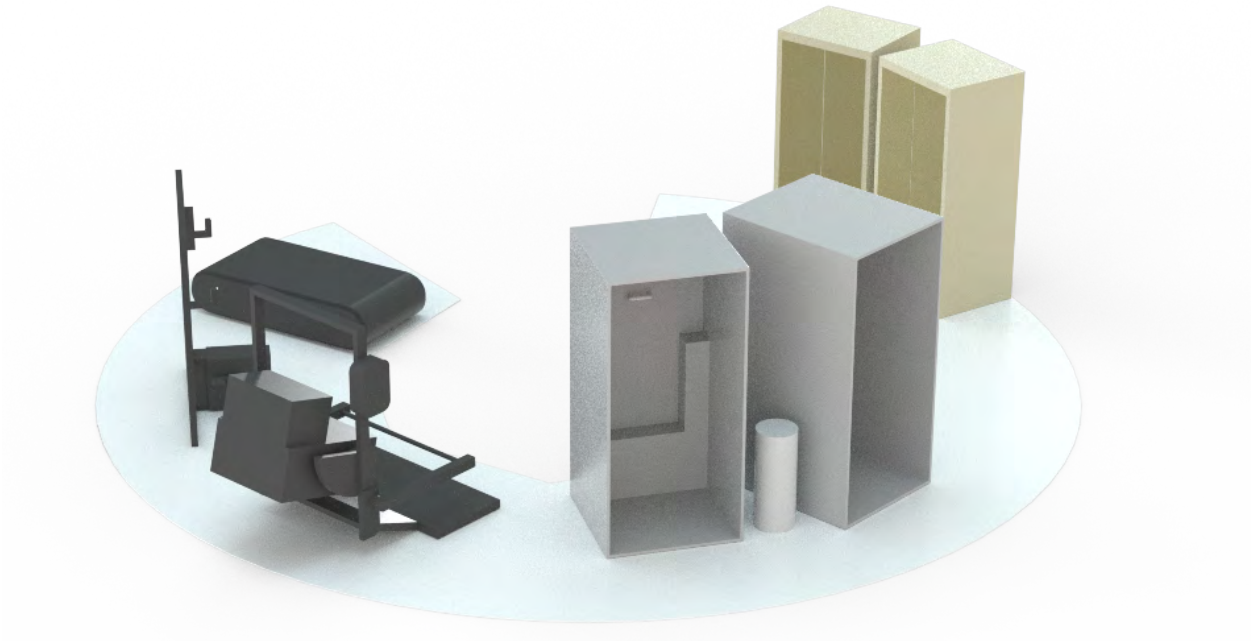

Figure 19: CAD depiction of the third floor layout in a lunar habitat.

The exercise space is located on the third floor of the habitat. This placement prevents the noise generated by the exercise equipment from disturbing any astronauts who may be resting in their quarters or working below in the lab. In addition to this equipment, the third floor houses one toilet and one wash station, for easy access after the completion of a workout. In the lunar gravity design, the rest of the third floor is dedicated to storage space as shown in Figure 19.

In the microgravity version of the habitat, the exercise space and one bathroom remain on the third floor as shown in Figure 20. However, the storage cabinets were removed and replaced by CTBs, and additional handles were added to the toilet and wash stalls in order to improve maneuverability.

Figure 20: CAD depiction of the third floor layout in a microgravity habitat.

6. Airlock - Kelly O'Keefe

Due to the nature of TransHab the airlock was constrained to sit below the first level core to allow astronauts to easily reach the surface when exiting the habitat. The airlock was designed to have a height of 2.5m, and will sit approximately 1m above the surface on a support base designed by the Mechanisms and Loads team. The aforementioned dimensions of the airlock creates a 3m displacement between the surface and inflatable bladder of the habitat, which allows astronauts walking on the surface to have enough space to walk under the habitat without any problem.

The airlock itself will be split into two separate sections. The first section will be kept at a constant pressure consistent with the rest of the habitat (14.7 psi). This area will contain the ladder that allows astronauts to descend into the airlock from the first floor core. There will be a distance of 1.353m from the ladder to the sectioned wall which is just enough space to allow astronauts to access and maneuver into the suitports. There will be two suitports stationed in the airlock, each with a mass of 70kg and operated at 8.3psi [17], while the other four suits will be stored in the lab until needed. A suitport was chosen over a traditional airlock because it allowed the volume to be used most effectively and has many distinct advantages over a traditional airlock including a reduction in both airlock consumables and contamination from the surface getting into the habitable volume [18]. However, unlike sitting completely outside the habitat and exposed to the external elements like many current suitport designs detail, this airlock will have a second dedicated space surrounding the suitports. This area will be able to be kept at vacuum for the majority of the time during normal operations when astronauts are using the suitports to exit the habitat, but it will also have the capability of being pressurized to allow crew members to enter the space to do light maintenance on the suits when needed. This section has a volume of $2.59m^3$ and will need to be pressurized to 14.7 psi when in use. A depth of 1m was maintained between the suit and the exit to allow for a crew member to stand in front of the suit with their arms halfway extended for any necessary work. While light maintenance can be done in this volume, there will also be a pulley system in place similar to the one described in the vertical mobility section which will attach to the bottom of the second floor

core and will allow suits to be hoisted out of the airlock and into the first floor lab space when necessary for heavy maintenance. A diagram of the airlock layout can be found by referencing Figure 21.

Another consideration when creating the airlock design was sample transport into the habitat. Due to the inflatable habitat sitting 3m above the surface, samples are not able to be passed directly into the glovebox in the lab from the outside. This method of sample transport would have been ideal, because it allows for the lowest possible risk of contamination since the surface samples never enter the habitable volume. However, an alternative approach had to be devised which is to have a sample transport chamber in the airlock. When the astronauts enter the airlock from the surface they will put any samples they have collected into this chamber which will pass through to the pressurized volume and into a closed container. The astronaut will then take that container and transport it to the glovebox where he or she will transfer the sample into.

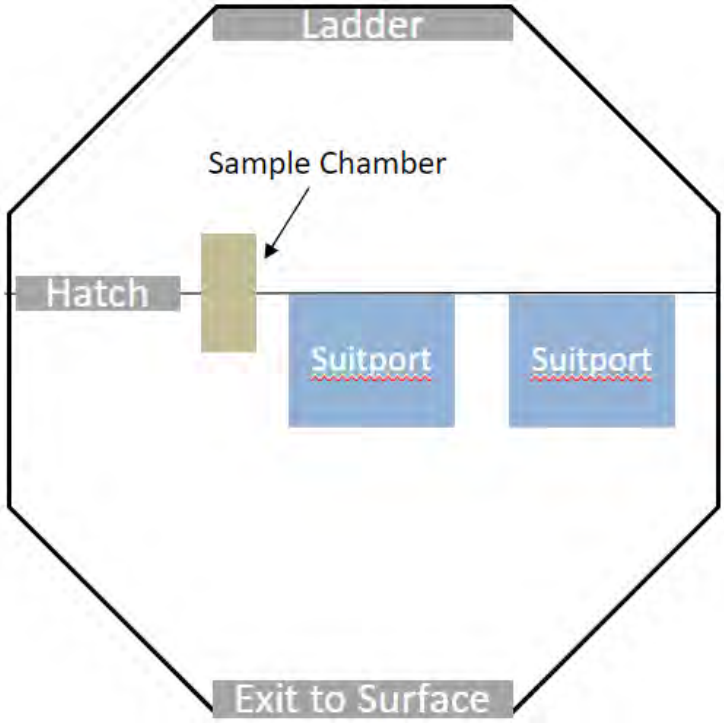

Figure 21: Diagram depicting layout of airlock

7. Core - Kelly O'Keefe

The core structure will be the only volume that initially exists prior to and during launch; this is opposed to the inflatable volume which will expand once the habitat is in orbit or on the surface. Due to the nature of the inflatable mechanism, the core will be the only space allocated for packing items prior to launch. Out of all the equipment needed for the outfitted habitat, the life support systems were determined to be the hardest items to deploy. Because of this, it was determined that these systems needed to be installed prior to launch which gives them top priority for placement in the core. The water reclamation systems will sit on the top floor of the core (as determined by a surface habitat), because this configuration will allow the water tank to dually serve as a mitigation technique for radiation into the habitat. The water tank as well as the machinery for the water reclamation system takes up the majority of the volume of the top floor core, so the atmosphere systems were placed on the first floor of the core. Splitting up the two life support systems also served to distribute the large mass of both the water and atmosphere systems.

In addition to the life support systems, the crew quarters are placed in the second floor of the core to keep the crew shielded from the outside elements as much as possible. The crew quarters also contains equipment that is hard to deploy, which is another reason for why it was placed in the core. The design of the core stays the same for both a surface and microgravity habitat, and the configuration is shown in Figure 22.

Figure 22: CAD model of core structure and layout

C. Concept of Daily Operations - Colby Merrill

Initially, the crew members will dedicate their time to set up the habitat from the configuration for launch and inflation. (It is a prime objective of this study to better understand how long this will take.) In this time, they will be transporting extra supplies in CTBs to the inflated habitat, and organizing the interior based on a planned procedure. Beyond the initial setup time, in order to keep the habitat up and running, life support and other habitat systems will need to be maintained with continuous servicing. Based on ISS experience, at least half of the crew members will likely spend their working hours each day servicing, repairing, and controlling these systems, depending on what is necessary. Maintenance must also be performed on the spacesuits before and after EVAs, as the suits will have to be reused almost daily. A planetary habitat could have EVAs nearly every day. Other crew members will support the science in the habitat by experimenting with the lunar samples delivered to the glove box.

Each morning after an eight hour rest, the crew will spend one hour preparing for the day with breakfast, washing, and some free time. At some point every day, each crew member will spend about two hours exercising to maintain muscle mass in lower-gravity environments. Much like it is on the ISS, the upkeep of the habitat itself will be of the highest priority - simply maintaining the onboard machines will take a significant portion of astronauts' time. EVAs and science will be a second priority, although on planetary surface environments EVAs will likely be far more frequent. The expected work day of a crew member will average to 9 hours with ample time for three meals and some relaxation/personal time. If involved with an EVA, that particular work day may last longer, as each EVA will be scheduled to meet some objective. The nighttime routine will be similar to that in the morning, with approximately an hour allotted for washing and hygiene, and pre-sleep personal activities.

D. Extravehicular Activities - Colby Merrill

The EVAs will occur most frequently on the martian or lunar surface and, as previously discussed, will be for geological or astrobiological exploration and/or support the experiments run in the on-board laboratory. Sample collection and curation will be enhanced by the ability to do in situ analysis and down-select samples to be returned to Earth with the crew for further analysis. Seismometers and other instruments will need to be deployed, and some samples may need to be brought back for analysis as explained in the lab space section. It is likely that experiments will also be conducted on the surface for various purposes, such as to determine the electrostatic charge of regolith in different

areas, or to measure the plasma sheath and dust pluming near the spacecraft landing are to see how it differs from ambient conditions. EVA will of course be critical for sample collection and soil penetrometer tests to analyze surface composition and compaction. Initial maintenance on solar panels and the structure used to hold the habitat will also likely be necessary at the beginning of the mission. Whether for planetary surfaces or for in-space applications, EVAs will always be required for habitat maintenance, repair, and upgrades. An inflatable habitat could form the basis of an upgraded Gateway station in an extended Artemis program, and like ISS, be continually expanded and improved by the integration of new hardware externally.

Figure 23 depicts the denitrogenation time required to safely perform an EVA. Because the suit is held at 8.3 psi for this design, there is not a time where it is considered an unsafe denitrogenation. Equation 1 depicts the R value, which needs to be below 1.6 to be considered safe [19]. P_{N_2} is the partial pressure of nitrogen and $P_{ambient}$ is the ambient pressure in the atmosphere at the moment of denitrogenation. In this case, P_{N_2} is 0 psi (the partial pressure of N_2 in the suit and $P_{ambient}$ is 8.3 psi (the total pressure in the suit).

$$R = \frac{P_{N_2}}{P_{ambient}} \tag{1}$$

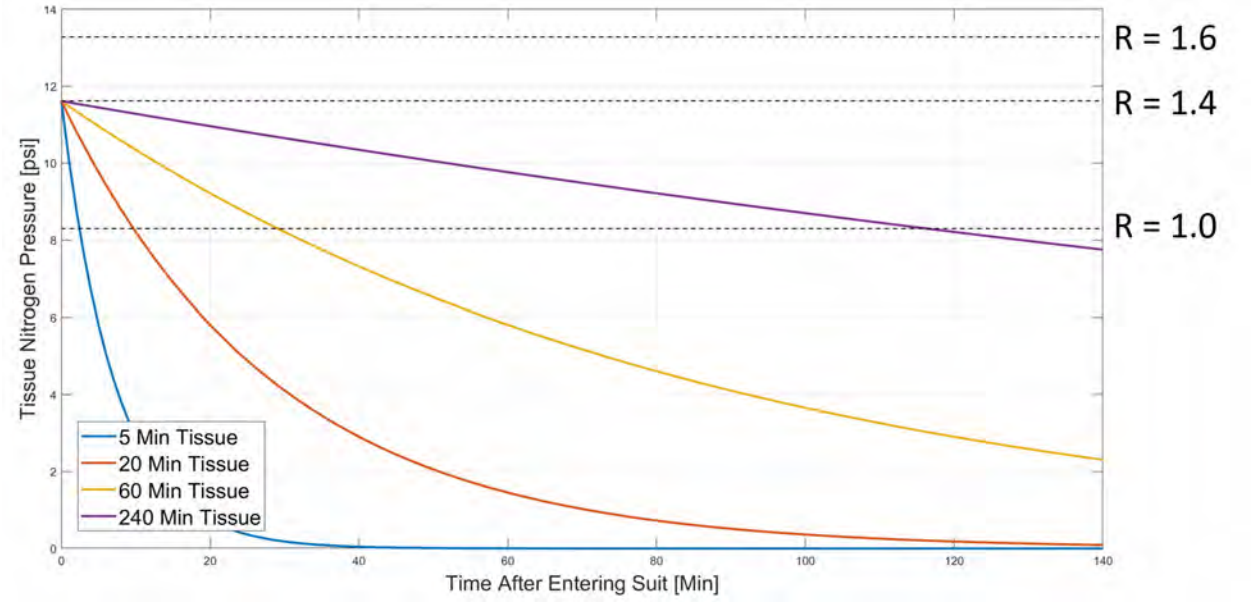

Figure 23: The rate of denitrogenation for EVAs. The suit is held at 8.3 psi and the in-habitat atmosphere is 14.7 psi [17]. An R value less than 1.6 is considered safe, and this sits under an additional safety factor of R = 1.4.

E. Dust Mitigation - Colby Merrill

There will not be any situation where a crew member will intentionally bring in a lunar sample into the habitable volume. Despite efforts during the Apollo missions to remove dust, many were unsuccessful [21]. However, there are a few technologies that have promising results for removing lunar regolith by leveraging the inherent cohesion and electrostatic charge. Both an electrostatic dust shield and adhesive roller or brush will be utilized to remove the residual finer grains [22].

In order to enter the habitat from the outside, the crew members will first move into an airlock and attach to a suitport (both the front and back of the suit will be inside the habitat but the front will be at vacuum most of the time. Multiple degrees of separation will exist between the interior and exterior and the exterior airlock can also be pumped with air when suit maintenance will be required. This design was adopted because it minimizes the volume that needs to be pumped with air for EVA and it also should minimize the lunar dust that enters the habitat. When exiting the suit, adhesive rollers will be readily available to remove the dust from inner clothing and discard once used. Brushes are a good solution to removing dust from something, but when in the habitat the dust will

Figure 24: Gene Cernan of Apollo 17 covered in lunar dust [20].

just end up on the floor (still in the habitat). The robust system of an electrostatic dust shield will be utilized when entering the airlock from the exterior and when moving out of it when doing suit maintenance [21]. Adhesive rollers will be spread throughout the habitat so that cleaning can be accomplished as necessary.

IX. Life Support Design

A. Food System - Michael Reed

A food system is necessary to keep the crew fed and meeting daily nutritional requirements to stay healthy for the duration of a mission. The current food system architecture used for missions aboard the ISS is a prepackaged system where all food items are packaged and brought to the ISS during resupplies. This food mostly consists of natural form shelf stable foods, thermostabilized foods, and freeze-dried rehydratable foods. Some fresh produce is provided during resupplies as well, but it must be consumed quickly due to lack of storage for fresh food items, leaving packaged and dried foods as the main food items to fulfil dietary needs. Under this system the astronauts receive about 1.8 kg of food per person per day. This mass includes the packaging for the foods. So, looking at a lunar mission with a crew of six to receive resupplies every six months, about 1950 kg of food (plus packaging) would be required between resupplies [23]. If a mission to Mars were to be considered, with planned resupplies after 26 months, the required food mass would increase to about 8430 kg. This makes the prepackaged food system for longer duration missions slightly less feasible given mass constraints for the launch vehicle and the mass requirements for everything else in the habitat.

Alternatives for a prepackaged food system where all of the food is included in the launch of the habitat are a prepositioned packaged food system and a bioregenerative food system. Both of these systems would still utilize prepackaged food in some capacity. The prepositioned food system would simply involve prepositioning most of the required prepackaged food in orbit around the destination while bringing only the required amount for transit in the final launch of the habitat and the crew. A fully bioregenerative system would only require the food for transit and potentially an extra supply until food production can be started for a mission. However, since there are currently no fully bioregenerative food systems for space missions above a TRL level of 3-4 [24, 25], a bioregenerative system is not considered for the inflatable habitat. One of the concerns with a prepositioned food supply for longer space missions is the effect of extended radiation exposure. The radiation will be at higher levels and at different spectrums than in low-Earth orbit, and food will potentially be exposed to this radiation for longer periods of time than they would be on the ISS. Limited studies and ground simulations have been performed to investigate the effects of longer radiation exposure and no significant difference in nutritional value has been found. However, these studies have been performed with a limited variety of foods used in the current food system, and further studies or simulations in more relevant storage conditions, over relevant time periods, and in a more relevant environment are needed to verify these results for a greater range of food types [26]. Additionally, regardless of radiation exposure effects, the length of time between the prepositioning of the food and the time at which it is consumed can lead to the degradation of quality and nutritional value since most prepackaged foods have a shelf life of 1.5-2 years. So, this rules out the use of prepositioning food for the inflatable habitat mission for food safety concerns, and since the focus is on lunar and microgravity designs, the food mass required fits within the mass budget for the mission design. The chosen food system architecture for the inflatable habitat is thus the prepackaged food system that is currently in use. A three month margin on food will be added so the crew has extra food in the case of a delayed resupply. This brings the total food mass up to 2920 kg.

One of the other aspects to consider in decisions about the food system is the variety of food and its acceptability to the astronauts. Variety is necessary so that the crew has choices when it comes time to eat. A lack of variety or the consumption of the same foods repeatedly can cause menu fatigue and reduce the acceptability of the food. This in turn can decrease food intake by the crew leading to nutritional deficiency and weight loss among other physiological effects [27]. Acceptability can also be affected by the perceived quality of the food. Fresh produce or food prepared from fresh ingredients is often perceived as having a higher quality than the prepackaged foods. However, due to the challenges associated with a bioregenerative food system that would be able to provide fresh foods and the lack of systems at a high enough TRL, high quality fresh foods are hard to provide for the mission. What can be provided is a minor supplement of fresh produce food items using plant production units aboard the habitat.

The two plant production units being considered for the habitat are the Plant Production System, also know as “Veggie”, and the Advanced Plant Habitat (APH). Both of these habitats are in use aboard the ISS and were designed to test plant growth in the microgravity environment. Veggie is a low power, open air system that can accommodate up to six plants, each started in what is known as a plant pillow, which helps to control water and nutrients delivered to the plant during growth [28]. APH was designed as a fully automated, environmentally controlled, closed-loop system

with about twice the internal volume of Veggie. It has an upgraded light system and over 180 sensors to monitor and assist with plant growth [29]. Numbers for mass, power, internal volume, and produced biomass are reported in Table 1 for comparison. The main advantages of APH over Veggie are its fully automated capabilities and greater growth volume for the plants. These factors reduce the crew time necessary for the maintenance of the plants and allow for a greater amount edible biomass produced per month. However, Veggie requires about a quarter of the power of APH to run and has only about 1/12th of the mass. The same amount of edible biomass can be produced monthly by using two Veggie units instead of the APH while still using about half of the power and having about 1/6th of the mass. The only drawback is the required crew time for plant maintenance when using the Veggie habitat. This comes out to be, on average, about 23-25 minutes per day for one full Veggie unit, which in total is just under an hour of daily crew time. Since this is the only apparent drawback to the system and because Veggie uses significantly less mass and power than APH, two Veggie units were selected to be used in the habitat for purposes of plant production.

Parameter	Vegetable Production System	Advanced Plant Habitat
Mass [kg]	25	300
Internal Volume [m^3]	0.051	0.113
Power [W]	70	280
Edible Biomass Produced [g/month]	156-186	300-400

Table 1: Plant production systems comparison. Numbers reported or calculated from [30, 31, 32].

With just two Veggie units, plant production will result in about 312-372 grams of edible biomass per month. This is equivalent to just a couple fruits per crew member per month, and while this does not seem like a lot, the goal of the plant production units is not to produce significant food mass for the crew since the required food mass is met via the packaged food. The goal of plant production in the habitat is to provide a minor supplement to add occasional variety to the available food for crew to help prevent menu fatigue and decreased food intake, which would lead to nutritional deficiency. The use of Veggie has additional benefits outside of the crew's physical health as well. While there are no bioregenerative food systems that were considered due to low TRLs, the continued use of plant habitats for space missions will further assist with the study of plant growth in microgravity and in reduced gravity (on the Moon) and can potentially contribute to the development of bioregenerative food systems for future missions to farther targets, such as Mars or asteroids. The required crew time for plant maintenance in Veggie will also provide mental health benefits for the crew. There are several factors that contribute to stress and anxiety during spaceflight, including isolation, confinement, proximity to a hostile environment, and physiological effects of a micro- or reduced gravity environment [33]. Anxiety and annoyance were identified as the most frequent behavioral symptoms for astronauts post Space Shuttle missions. Gardening has been shown to have a therapeutic effect that could ease these symptoms on space missions. Studies have shown statistically significant reductions in anxiety and depression as well as increases in attention capacity and self-esteem. The presence of plants also promotes cooperation and group cohesion, which is especially important in the maintenance of a space habitat. The application of these ideas for psychological benefits in a space environment are supported by previous astronauts' anecdotes about the plants produced on the ISS as well. So, having the Veggie units in the habitat is important for both the mental and physical well-being of the crew.

Beyond the food and the plant production units, the habitat will require methods for food preparation. For the rehydration of the freeze-dried foods, a potable water dispenser is required. Some foods will need to be heated before consumption and so will require a food warming device. The food warming device to be used in the inflatable habitat is a forced air convection oven. A summary of the parameters for all of the food systems is given in Table 2.

System	Mass [kg]	Power [W]	Volume [m^3]
Prepackaged Food	2920	-	-
Veggie (x2)	50	140	0.102
Forced Air Convection Oven	7	200	0.03
Potable Water Dispenser	390	280	0.06
Total	**3367**	**620**	**0.192**

Table 2: Food systems summary. Numbers reported or calculated from [23, 30, 34, 35]. The mass reported for the prepackaged food includes the three month margin as discussed.

B. Waste Management - Michael Reed

When considering any space mission, one must also consider how to process the waste generated over the course of the mission. Current waste management system architecture for the ISS involves packaging and storing waste until resupplies occur, which is when stored waste is unloaded off the ISS and burnt up in Earth's atmosphere upon re-entry. This system works for resupplies that occur every month, but for a lunar inflatable habitat mission, resupplies will occur every six months (or 180 days). Using an estimated waste production of 1.69 kg per crewmember per day, a 180-day, 6-crew mission will generate about 1830 kg of waste [36]. If this waste were to be stored at the highest achieved density on the ISS, this would require about 28.5 cubic meters of storage space before a resupply comes to retrieve the waste. This makes the current waste management architecture unfit for the inflatable habitat mission purposes. Instead, a system that will process the waste and reclaim water and gasses is considered.

The three systems chosen for consideration were ozone oxidation, gasification, and incineration. These were chosen based on the end products produced compared to other options. These three systems all produce both water and carbon dioxide, which can be fed through the water reclamation and air systems, respectively. All three systems were compared using their required mass, volume, power, operating temperature, operating pressure, and destruction removal efficiency (DRE) scaled to a system size necessary for a 180-day lunar mission. Equivalent system masses (ESM) were calculated for all three systems for a normalized comparison. DRE was comparably similar between the three systems and so was not included in the ESM calculation. The system parameters and calculated ESMs are reported in Table 3. Based upon the normalized comparison of these systems, an ozone oxidation system was chosen since it has the lowest ESM.

Parameter	Ozone Oxidation	Gasification	Incineration
Mass [kg]	402	450-500	310
Volume [m^3]	0.18	0.15	0.4
Power [W]	600	600-800	1500
Pressure [atm]	4.3	1	1
Temperature [^oC]	125	400-800	300-1000
DRE [%]	99.7	99.9	98-99.9
ESM [10^6 kg]	1.39	2.75-5.36	2.12-6.67

Table 3: Waste systems comparison. All numbers reported for systems scaled to the requirements for a 180-resupply mission. Equivalent system mass (ESM) calculated using all parameters presented except destruction removal efficiency (DRE). All data gathered from [37, 38, 39].

Two waste systems will be aboard the habitat to adhere to the 2-fault tolerance standard. If one waste system were to fail, the other can be used until the first is fixed. This will minimize storage of waste in the case of a failure.

C. CO_2 to O_2 System - Colby Merrill

There are three components to turning CO_2 into O_2: a CO_2 scrubbing system, a CO_2 reduction system, and an O_2 generation system. CO_2 scrubbing systems remove the CO_2 from the air but does not chemically alter the air at all. The CO_2 is then directed to a CO_2 reduction system, which chemically alters the CO_2 and extracts the O_2 from it with H_2 atoms, creating H_2O. The third and final step of this process is an O_2 generation system, which separates H_2 from O_2 and feeds the H_2 back into the CO_2 reduction system, while the O_2 is sent into the atmosphere for crew members to breathe again.

The first portion of the CO_2 to O_2 system is the CO_2 scrubbing system. there were four technologies compared in a trade study to find the optimal system for the outfitted habitat. The four options are found in Table 4, which quantifies the important characteristics of each system. Based on the parameters given in Table 4, it was decided that an electrochemical depolarization concentrator (EDC) would be the ideal CO_2 scrubbing system. The EDC unit pulls CO_2 from the air and directs it toward the CO_2 reduction system. The EDC is also capable of creating water, which is directed to the third component of the CO_2 to O_2 system, the O_2 generation system.

The second component of the CO_2 to O_2 system is the CO_2 reduction system. Three systems were investigated for this task: the Bosch reactor, the Sabatier reactor, and the Sabatier-Pyrolysis pair system. The final decision was to use a Bosch reactor, despite its lower TRL. There are significant upsides to a Bosch reactor, as it has the lowest total mass of the three system configurations investigated. It also has the effect of creating a closed loop system for the CO_2 to O_2 system. The reason why a Sabatier reactor requires so much more H_2 than a Bosch reactor is because

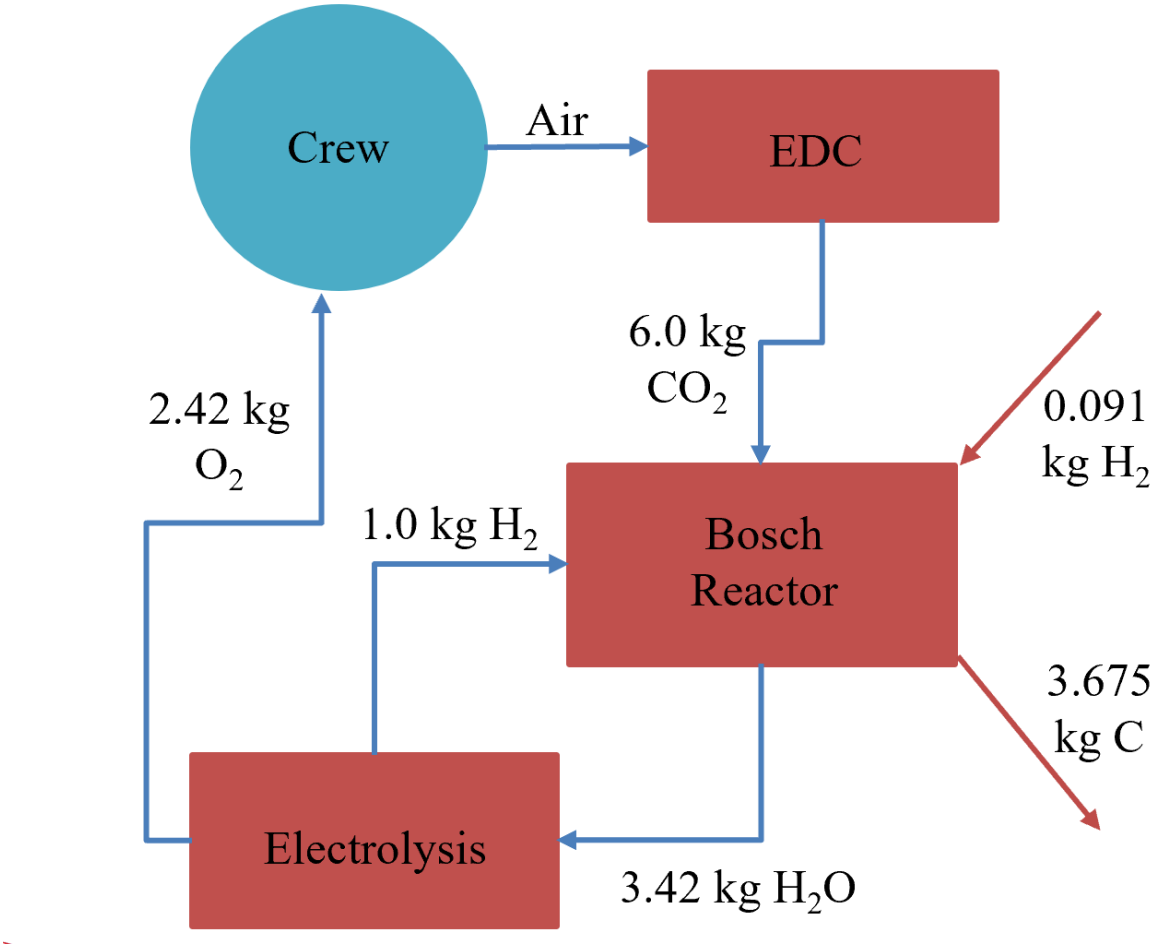

Figure 25: The masses of the CO_2 to O_2 system. The numbers represent the mass that flows through the system on a nominal day [40]. There is also an H_2O line that runs from the EDC to the Electroylsis system, but it is not important to the regenerative cycle (shown above). The expected 0.091 kh of H_2 comes from an external H_2 tank supply and the 3.675 kg of C will likely be vented to space.

System	Mass [kg]	Power [W]	Volume [m^3]	TRL
Electrochemical Depolarization Concentrator	88	480	0.16	6
4-Bed Molecular Sieves	616	128	0.72	9
2-Bed Molecular Sieves	1360	240	0.88	8
Solid Amine Water Desorption	1200	136	0.56	6

Table 4: CO_2 scrubbing systems comparison. All numbers are presented for a 180-day resupply mission. All data was gathered via [41, 42, 43, 44, 45].

the Sabatier reactor ejects CH_4 gas whereas the Bosch reactor ejects solid C. The Bosch reactor requires half the H_2 running through the system that the Sabatier needs at any given moment because the Bosch reactor is able to pair the H_2 with O_2 to produce liquid H_2O. The Sabatier produces CH_4 and H_2O, meaning that it splits up the H_2 that is input into the system between the two chemical products. Because the Sabatier reactor creates CH_4, the H_2 output must also be considered when measuring the masses of the systems. Figure 26 displays the three different configurations and with the lost H_2 included in the total mass. The slope of each of the lines in the table reflects the H_2 loss per day. The H_2 lost by the Bosch reactor is due to inefficiencies in the system; It does not intentionally eject H_2. Similarly, the H_2 rate loss of the Sabatier and Pyrolysis combo system is also a result of inefficiency, as the Pyrolysis system changes CH_4 into solid C and H_2, which is then recycled back into the Sabatier reactor.

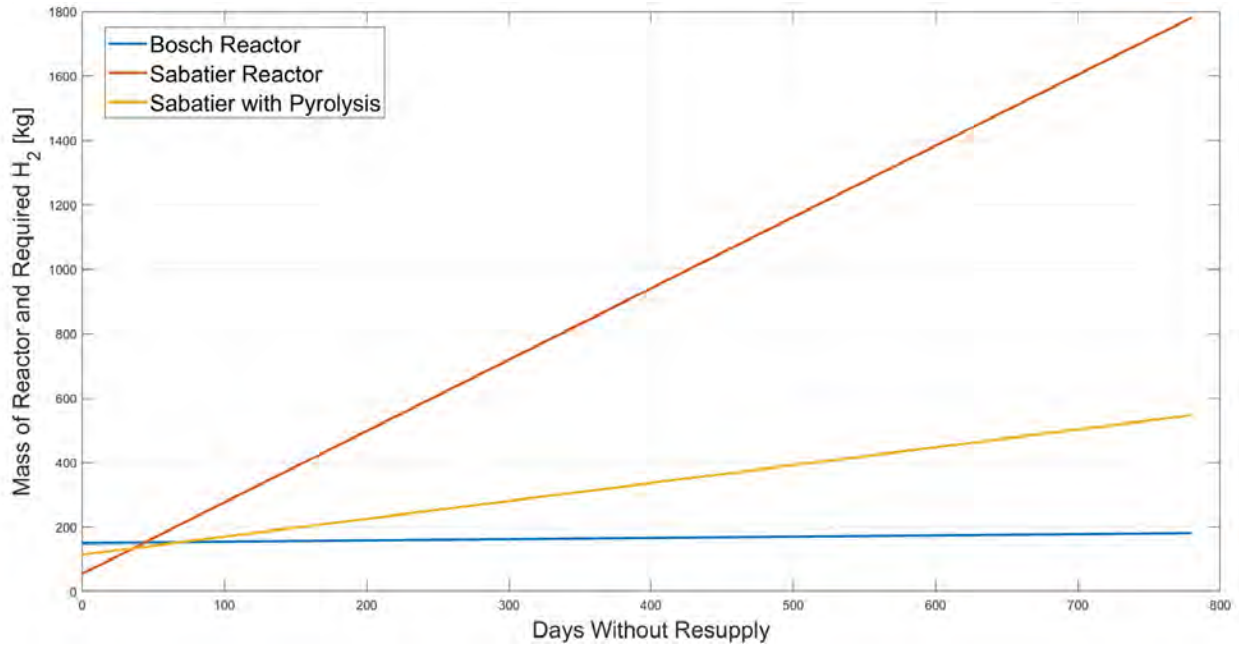

Figure 26: The masses of the three different CO_2 reduction systems as a function of days without resupply. The plot extends to the resupply length of a Martian mission (780 days).

Parameter	Bosch Reactor	Sabatier Reactor	Sabatier Reactor with Pyrolysis
System Mass [kg]	138.2	42.6	102.6
H_2 Provisions and Tank Mass [kg]	19.2	411.4	122.1
Total Mass [kg]	157.4	454	214.7
Temperature [°C]	600	480	850
Power [W]	450	950	1500
TRL	6	9	6

Table 5: CO_2 reduction technologies. The H_2 provisions row is required when comparing these technologies and is reported for a 180 day resupply mission. The H_2 provisions mass increases linearly with resupply time length. All data was extrapolated using [41, 46, 45].

System	Mass [kg]	Power [W]	Volume [m^3]	TRL
Electrochemical Depolarization Concentrator	88	480	0.16	6
Bosch Reactor and H_2 Tank	157	450	0.57	6
Electrolysis System	120	120	0.14	9
Total	**365**	**950**	**0.87**	**6**

Table 6: CO_2 to O_2 system using the discussed technologies. The numbers are representative of the configuration used in the habitat. There is a single mode of failure already included in the numbers. That is, there are multiple reactor chambers inside a single Bosch Reactor, multiple reactive surfaces inside the EDC, and multiple electrodes inside the Electrolysis System. Additionally, there will be two of each of these systems included to provide at least 2-fault tolerance. [47].

The final component of the CO_2 to O_2 system is the oxygen generation system: the Electrolysis system. A tabular trade study was not conducted for this component, as the Electrolysis system is the only oxygen generation system above a TRL of 4. It is simple, as it includes two electrodes and a filter and does not require repairs often. The Electrolysis system is currently used on the International Space Station and has a TRL of 9. Only having a single system that does the job in an effective manner made this was a very simple choice.

The final configuration of the CO_2 to O_2 system is an Electrochemical Depolarization Concentrator, Bosch reactor,

and Electrolysis system. The EDC takes the air of the habitat as its input and outputs liquid H_2O and separates the gaseous CO_2. The CO_2 is fed into the Bosch reactor, where it is combined with H_2. The Bosch reactor outputs solid C, which is vented to space, and liquid H_2O is fed into the Electrolysis system. The Electrolysis system takes liquid H_2O in as its only input and separates it into gaseous H_2 and gaseous O_2. Table 6 displays the final and total configuration quantities.

D. Particulate Scrubbing - Elizabeth Myers

There are a variety of options for particulate scrubbing on long duration human spaceflight missions. Filters, activated charcoal, and chemisorbant beds were researched for this aspect of life support.

The first aspect of particulate scrubbing is the removal of dust, debris, and other particles from the air through the process of filtration. There are two primary options for multistage filters that can be used to remove particles and debris from the air, known as the Bacterial Filter Element (BFE) and the Scroll BFE Filter. The BFE used on the ISS has 3 stages, each with a different type of filter, while the scroll BFE element has two required stages and the third is optional [48].

Data	Bacteria Filter Element	Scroll BFE Filter
Stage 1	Screen roll filter (2.1 kg)	Screen roll filter (2.1 kg)
Stage 2	Impactor filter (3.5 kg)	HEPA element (2.6 kg)
Stage 3	Scroll media filter (6.2 kg)	Impactor filter (3.5 kg)
Total mass	11.8 kg	8.2 kg
Efficiency	99.95%	99.98%
TRL	9	5

Table 7: Particulate Scrubbing Filter Comparison [49, 48]

The first stage of the BFE is the screen roll filter. This filter consists of a screen mesh that captures particles and debris found in the air. This filter is low maintenance because the only requirement is for the roll of mesh to be replaced when necessary for long duration missions. It also decreases the number of cleaning tasks that need to be done by the crew since they will not have to vacuum as often when using this filter. However, it does have a higher mass than other types of screen filters [49].

The second stage, known as the impactor filter, gathers unwanted particles in the air using regenerable collection bands. It can capture small particles that are only a few microns in diameter. This filter does not require regular maintenance other than yearly inspections with cleaning, and the parts do not need to be consistently replaced. Due to the required mechanisms within the filter, it is more complex than other options, higher mass, and more difficult to assemble [49].

The third and final stage is the scroll media filter, which is a pleated filter designed to capture particles that are less than a micron in diameter. This purpose of this filter is to trap any particles that may remain after the air passes through the first two stages. With the combination of these three stages, the BFE has an efficiency of 99.95%, and as it is currently in use in space, its TRL is nine, making it a reliable choice for our habitat [48].

The scroll BFE filter is a newer design currently in the testing phase, giving it a TRL of 5. The first stage of this design is also a screen roll filter. The second stage is a replaceable HEPA element designed to capture a wider range of particle sizes; however, it needs replacement filters more frequently and occupies a greater volume than other filters. The scroll BFE filter also has an optional third-stage impactor filter, which may or may not be necessary depending on the requirements of the area it is filtering [49].

There are several concerns to consider when reviewing this newer filter. Due to the inclusion of the HEPA element, this filter will require larger housing than the previous BFE. Additionally, the design is still in the testing phase so it has not yet been certified. As a result, our habitat design will use the standard BFE for its filtration system.

The required air flow for the ISS laboratory module is 11.9 m^3/min, and this is the air flow we chose to maintain in TransHab as well [48]. Since the floors of our habitat will allow for open air flow between the levels, it is best to use the same air flow throughout the habitat. To determine how many BFEs must be placed throughout the ventilation system of the habitat, a volumetric comparison was done. The ISS lab module has 6 BFEs for a volume of 108 m^3. This was scaled up to calculate that there will be 20 BFEs required for our volume of 347 m^3.

While the general airborne debris can be removed solely using regular filters, chemical contaminants require a more complex filtration system. This is a three-stage system designed to remove trace hazardous chemicals from the air, and it will be located on the first floor by the laboratory area.

The first stage is an activated charcoal bed. Activated charcoal removes heavier compounds, such as ammonia, and helps with odor control [50]. The bed is treated with 10% phosphoric acid to increase its ability to absorb toxins, and then the temperature is raised to several hundred degrees Celsius to complete the treatment process. Phosphoric acid is a preferred agent due to its milder reaction conditions and recyclable properties. Methane and carbon monoxide are not effectively removed by this absorption process, so additional methods are implemented [51].

The second stage of this system is a catalytic oxidizer. This device oxidizes compounds that were not absorbed by the activated charcoal bed. It also converts various carbon compounds such as CH_4 and CO into carbon dioxide, which can then be removed by the CO_2 scrubbing system. The temperature of the catalytic oxidizer reaches a maximum of 400°C so this device must be insulated carefully to ensure the safety of the crew [52].

The third and final stage of the chemical contaminant removal system is a lithium hydroxide bed. This bed removes chemical contaminants such as nitrogen or sulfur compounds, metals, and lighter compounds not removed by the charcoal [48].

Element	Quantity	Mass [kg]
Bacteria Filter Element	25	369
Activated charcoal bed	3	110
Lithium hydroxide bed	3	12
Catalytic oxidizer	3	22
Cartridge replacements	10	118
Total	**44**	**631**

Table 8: Particulate Scrubbing Mass Breakdown [49, 48]

Table 8 displays a mass breakdown of the entire particulate scrubbing system with redundancies included. To adhere to NASA's standards for two-fault tolerance, there will be three of the chemical contaminant removal systems on board and additional BFEs, as well as extra filter replacements for each stage of the BFE. Table 9 shown below lists the summary of the total required values for the particulate scrubbing life support.

Quantity	Value
Mass [kg]	631
Volume [m^3]	1.8
Power [W]	900

Table 9: Particulate Scrubbing Summary [49, 53]

E. Nitrogen Replenishment - Elizabeth Myers

Due to the nature of the inflatable TransHab design, the habitat will not be perfectly airtight. Air will be lost to the surrounding environment, particularly during EVAs, and this air will need to be replaced in order to maintain the atmosphere of the habitat.

Currently, there are no studies that have been conducted in relation to nitrogen leakage for the TransHab design. As a result, studies conducted on the ISS nitrogen loss were used in order to estimate the required mass of N_2 that should be brought on each resupply mission in order to replenish the nitrogen in TransHab. According to a 2011 study of the ISS nitrogen leakage, an average of 0.04 kg of N_2 is lost per day. On days when EVAs were executed, this number increased to about 0.06 kg per day [54]. To ensure the safety of our crew, the higher value of 0.06 kg per day was used for our estimations. To calculate the estimated N_2 loss for TransHab, the numbers recorded for the ISS study were scaled by volume. The habitable volume of the ISS is 372 m^3. Comparatively, the volume of TransHab is 347 m^3. As such, the estimated N_2 that would be lost daily for TransHab is 0.056 kg. Due to the uncertainty present in this methodology and NASA's requirement for two-fault tolerance, a safety factor of 2 was implemented as well. As a

result, the lunar mission with a 6-month (180-day) resupply should bring at least 0.12 kg/day of N_2, equivalent to 21.6 kg.

In order to send N_2 to the habitat on each resupply mission, an appropriate method of transporting N_2 must be chosen. Considering the existing technologies available, there were three ideas investigated for this project: high pressure N_2 tanks, cryogenic liquid nitrogen, and storable nitrogen compounds.

High pressure N_2 tanks are normally pressurized to several thousand psi, which requires a substantial amount of power. The most successful example of high pressure N_2 tank used for a spacecraft resupply is NASA's Nitrogen/Oxygen Recharge System (NORS) [55]. Following the end of the shuttle missions, NASA needed a new design to implement for resupplying nitrogen and oxygen to the ISS. This system uses a 42.7 kg tank pressurized to 6000 psi which holds 28.6 kg of N_2 [56].

Cryogenic liquid nitrogen was also considered as an option for N_2 transport. Although using liquid nitrogen would potentially decrease the volume required on the launch vehicle for the N_2 resupply, there are several downsides to this method. First, cryogenic LN_2 must be kept at a temperature of -196°C [57]. However, LN_2 tanks are not perfectly insulated, so there will always be losses during transport as a small percentage of LN_2 will boil off. Furthermore, LN_2 is hazardous to humans, and once the resupply tank arrives at the habitat it will be moved by the crew and housed in close proximity to their living quarters, which is potentially dangerous [57].

Finally, storable nitrogen compounds could be used to bring N_2 to the habitat. However, using a compound also poses various risks to the safety of the crew. For example, hydrazine is a nitrogen compound often used in propulsion systems, and it is highly hazardous to humans [58]. Transporting N_2 as a compound would also require an additional process to convert it to pure N_2 gas before it could be released into the habitat, adding further complications to the resupply process as well as additional mass and volume to the launch mass.

As a result, high pressure N_2 tanks proved to be the safest and most reliable method of transporting N_2 to TransHab for the resupply missions. The NORS tank could easily be utilized for these missions since it is capable of carrying slightly more than our required N_2 mass. To comply with NASA standard for two-fault tolerance, the lunar resupply should bring two NORS N_2 tanks to maintain additional safety measures.

F. Water Reclamation System - Kelly O'Keefe

A robust water reclamation system is a necessary component of any extended term space mission. Water is one of the most basic needs of the human body, and must be supplied in a sufficient amount every day to keep the crew members healthy and functioning. Table 10 details the breakdown of amount of water needed for each crew member. Each crew member requires 5.32 kg of water a day, which quickly adds up for a long term mission if no recycling system is in place. For 6 crew members on a 180-day lunar mission, 5745kg of water is required and for a 780-day mars mission, 24900kg of water is required. This breakdown is shown in table 11 However, with an efficient water reclamation system on board these mass estimates can be greatly reduced.

Type of Water	kg/CM-d
Drinking and Food Preparation Water	2.38
Urine Flush Water	0.5
Wash Water	1.29
Water in Food	1.15
Total	**5.32**

Table 10: The amount of water broken down by what purpose it is needed for and represented in kg per crew member per day. [59]

In order to effectively reclaim all waste water, both a urine water and potable water reclamation system are necessary. Many technologies currently exist that all have their own pros and cons, so a trade study was conducted in order to determine which systems would be the best to use in this habitat. For urine water, Thermoelectric Integrated Membrane Evaporation System (TIMES), Vacuum Compression Distillation (VCD), Vapor Phase Catalytic Ammonia Removal (VPCAR), and Air Evaporation (AIRE) were analyzed. Each technology was compared by the same characteristics: Mass, Volume, and Power Required. Additionally, in order to most effectively compare each system by these characteristics, an Equivalent System Mass (ESM) was calculated to give a clear answer to which system is the most effective. Table 12 details the breakdown between each system. VPCAR had the lowest ESM, which indicates that it is the most effective system. The AIRE system, with a power required of more than double any of the other

Type of Water	kg/day (6 crew)	kg (180-day)	kg (780-day)
Drinking and Food Preparation Water	14.28	2570	11138
Urine Flush Water	3	540	2340
Wash Water	7.74	1392	6037
Water in Food	6.9	1242	5382
Total	**31.92**	**5746**	**24898**

Table 11: The amount of water needed for long term missions with a 6-member crew [59]

systems, had the highest ESM and was immediately eliminated as an option. Both TIMES and VCD were comparable and had similar requirements in each category. VPCAR however had a significantly lower power and mass required than any of the other systems, which is why this technology was chosen as the urine water reclamation system to use. The VPCAR system has an efficiency of 95% requires 105.6kg, 1.17m^3 of volume, and 0.48kW of power.

Technology	Mass [kg]	Volume [m^3]	Power [kW]	ESM [kg]
TIMES	211.2	2.02	1.56	1199
VCD	226.8	1.93	1.32	1148
VPCAR	105.6	1.17	0.48	701
AIRE	207	2.01	4.68	1797

Table 12: The results of a trade study done to determine which Urine Water Reclamation System is the most effective for the TransHab design. All numbers are reported for a crew of 6 on a 180-day mission. All data for each system was obtained via [59]

The potable water reclamation systems chosen to compare were Multfiltration, Reverse Osmosis, and Electrodialysis. Each of these technologies were compared using the same characteristics as the urine water trade study (mass, volume, power, ESM). Table 13 outlines the results of this comparison. While all of these systems were generally comparable, Electrodialysis comes out on top with the lowest ESM. Multifiltration has the second lowest ESM, and Reverse Osmosis has the highest. The Electrodialysis system has an efficiency of 98%, requires 354kg, 1.86m^3 of volume, and 2.16kW of power. The chosen urine and potable water reclamation systems together will combine to have an efficiency of 93.1%.

Technology	Mass [kg]	Volume [m^3]	Power [kW]	ESM [kg]
Multifiltration	348	2.70	2.76	1715
Reverse Osmosis	528	3.00	2.10	1969
Electrodialysis	354	1.86	2.16	1424

Table 13: The results of a trade study done to determine which Potable Water Reclamation System is the most effective for the TransHab design. All numbers are reported for a crew of 6 on a 180-day mission. All data for each system was obtained via [59]

Another important aspect of any life support system is two-fault tolerance. One way the water reclamation system will be fault tolerant is that there will two of each system (urine and potable water) on board. This is so that if one of the machines fail there will be a back up for the astronauts to install and the habitat will incur no significant losses to the water supply. With two of each system on board, the total mass will be 920kg, and the volume required will be 6.06m^3. In addition to the electrical systems for reclaiming waste water, a water tank with an initial amount of water will need to be brought on board. This water tank will have another fault tolerance built into it by assuming a 90% efficient reclamation system as well as a 50% margin of safety.A nominal 5740kg of water is needed for 6 crew members on an 180-day mission, but taking into account the two aforementioned assumptions, 863kg of water will need to be stored. 0.2kg of tank is needed per kg of water [59], which sums to a total water tank mass of 1040kg. Under nominal working conditions, this water tank holds enough water for 12 months, or double the expected mission lifetime. With complete failure of the reclamation system, the crew can be sustained for 27 days with the amount of water in the tank. This means that a repair or replacement of the system would need to be completed within 4 weeks. Ideally, there should be enough precautions in place to prevent this worst case scenario from happening.

G. Resupply Information - Michael Reed

The mission for the inflatable habitat is based around receiving a resupply every six months. The purpose of this is to replenish resources used by the crew and to provide key resources for upkeep of the life support systems. Due to expected leakage in the habitat as well as other losses due to extravehicular activities (EVAs) and suit repairs, resupplies will need to provide 40 kg of gaseous N_2 and 15 kg of gaseous O_2. These are overestimates on losses, which provides a safety margin on these necessary resources [54]. The overestimates are based on leakage rates on the ISS, which is more susceptible to leakage than the TransHab design. Food and water will also need to be replenished, the requirements being 1950 kg of food and 400 kg of liquid water.

X. Core and Deployable Floor Design

A. Core Design and Analysis - Logan Swaisgood

The TransHab architecture is intended to compress into a smaller volume for launch and transit into its mission environment. Crew equipment, life support, and internal structures must similarly fold into a compressed volume, while remaining structurally secure when faced by the loads placed on the structure during launch. This introduces the structural requirement of a solid core to serve as the backbone of the outfitted habitat. The central solid core needs to retain habitat structural members, and allow for stowage of all crew equipment, furnishings, and life support systems.

The overall structure of the central core is an open-faced pillared structure with rigid octagonal floors. When selecting a material for the overall structure, high strength steel alloys, like 4140, and aluminum alloys, such as 6061 and 2024, were considered for this structure. As the overall mass of the habitat is limited by the payload size of the launch vehicle, minimizing the mass of structural members is crucial. Therefore, 2024 aluminum was selected as the primary material of this structure. 2024 aluminum possesses the highest specific strength, defined as ratio of the ultimate tensile strength to the density of the material, of the materials studied. Moreover, 2024 aluminum exhibits better rigidity than competing high strength aluminum alloys and better machinability than many steel alloys. This trade study is summarized in table 14 below:

Core Material Trade Study				
Material Property	6061 Aluminum	2024 Aluminum	4140 Steel	Units
Density	2.7	2.78	7.85	g/cm^3
Yield Strength	276	324	415	MPa
UTS	310	469	655	MPa
Machinability	280%	90%	65%	Based on AISI 1212 as 100% Machinable
Elastic Modulus	69	73	190	GPa
Specific Strength	0.11	0.17	0.083	$MPa/(kg/m^3)$

Table 14: Core material trade study

The central core structure was initially designed to feature rigid hexagonal floors and six vertical members on each corner of the floor connecting the layers together. This design was adopted with the intend to keep the structure as simplistic to model and fabricate as possible. Each of the straight edges of the floor panels will serve as a mounting point for the hinges of the folding floor, allowing for perpendicular storage of the folding floor, flush to the side of the core. A six sided hexagonal design was selected because a hexagonal interior would be simple to replicate using pre-constructed aluminum frames that could be arranged into a configuration that resembled the interior of the core and its vertical structural support members. These frames would be provided by the Space Systems Lab for migrogravity and lunar gravity testing. A rendering of this design is displayed in figure 27.

When analyzed using Finite Element Analysis in Autodesk Fusion 360, the core was analyzed under a load case with an applied applied load on each floor to represent a fully packed core, and the vertical and lateral accelerations placed on the structure by launch loads. The Falcon payload users guide anticipates a maximum axial acceleration of 8.5 g's and a maximum longitudinal acceleration of 3 g's [60]. Estimating the applied load of the stored equipment and furnishings, and multiplying by the axial acceleration yields an estimated applied load of 0.068 MPa. Assuming

Figure 27: The first iteration of the core design with hexagonal floors and simplified construction

that the core would be fixed at its base to the fairing of the launch vehicle, the the load case was analyzed, and the results of the FEA are discussed in figures 28 and 29

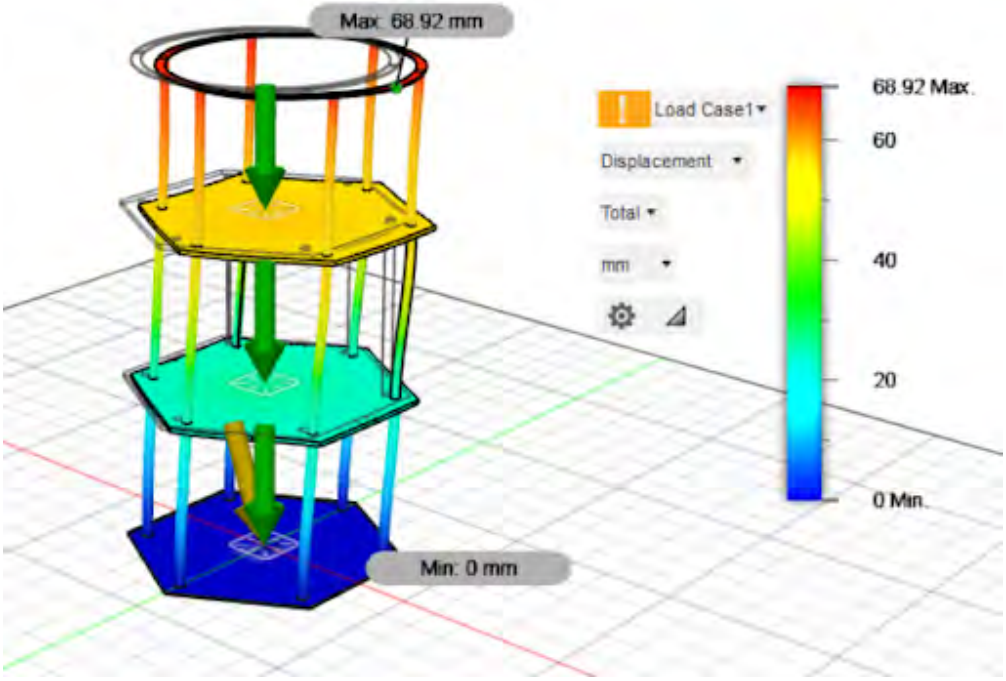

Figure 28: FEA results detailing the maximum deflection of the hexagonal core structure under launch loading conditions

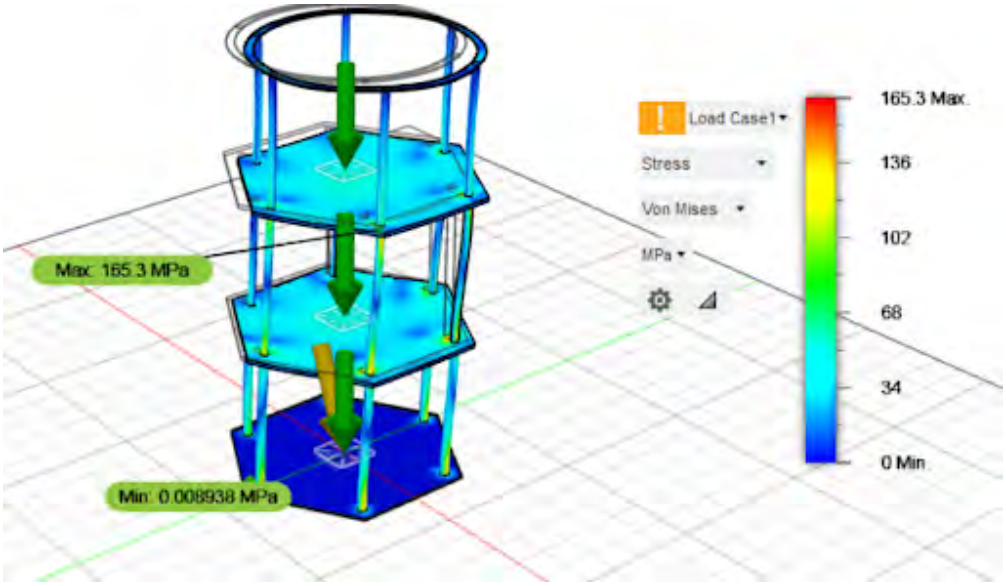

Figure 29: FEA results detailing the stresses inside the hexagonal core structure under launch loading conditions

This original design was deemed insufficient due to the excessive weight of the design, with estimates based on material density and volume placing the weight of the structure around 5730 kg, and the large lateral deflection of 68.92 mm at the top of the structure. The safety factor of this proposed core design is 1.66. Since the TransHab structure is inflatable, the expandable pressure vessel walls cannot be relied upon to retain the structure laterally, and large deflections run the risk of deforming or damaging the inflatable walls. The floors were redesigned into an octagonal shape, because it was more desirable to use an octagonal floor plan instead of a hexagonal floor plan, as the size of the interior enclosed by frame pieces was more accurate to the dimensions proposed for the interior core of the TransHab. Lateral deflection was addressed by implementing members that would connect diagonally between the vertical supports and the solid floor panels. In order to reduce the weight of the structure, the thickness of the floor panels was reduced, and the center of each vertical member was hollowed out. This updated design is shown in figure 30.

This version of the core was then subject to the same load cases as the first design iteration, and the stresses and displacement present in the updated structure under launch conditions were studied. The results of the FEA can be observed in figures 33 and 34

Using this design philosophy, the lateral displacement of the structure was nearly halved, but reducing the thickness of the flooring to save weight, particularly the uppermost floor, introduced greater axial deflection of the core flooring. The safety factor of this design is 1.54 in launch load conditions, and the maximum deflection of the uppermost floor reaches nearly 50 mm. The weight saved by using somewhat thinner floors was counteracted by the additional support structures required to transition the design from a hexagonal to an octagonal structure, and this updated design is expected to weigh approximately 5100 kg.

The maximum weight of the core structure must be minimized such that the entire outfitted TransHab and all necessary crew equipment can be launched in a single Falcon Heavy payload. One proposed method of reducing the core's weight included hollowing out the vertical support members. Studying the FEA proved that the loads developed in the vertical support members was primarily concentrated in the outer edges of the members. The structural capabilities of this weight saving method were analyzed using the same launch load case, and the FEA is shown in figures 33 and 34:

Following this modification, the safety factor of the core under launch loads is 1.54, with maximum deflection occurring in the center of the thin, uppermost floor. However, the mass of the core is reduced to 4500 kg. The major contribution to the weight of the core structure are the solid aluminum panels. In order to prevent deflection of the upper panels, the upper two floor panels were each increased to a thickness of 2 inches. Combined with the 1 inch thick bottom floor, these floors would weigh a collective 3200 kg. A significant contribution to the deflection of the floors is caused by the weight of the floor panels themselves. For this reason, it was proposed to use an aluminum honeycomb composite panel for each of the floors. With two panels, 5 mm thick, on the upper and lower portions of each floor, with the center of each floor panel made up of a composite with an average density of 86 kg/m^3, it was estimated that the total mass of the core structure could be reduced to approximately 1800 kg.

The design of the vertical members would be changed to better accommodate the mounting of the floor trusses

Figure 30: The second iteration of the core design with octagonal floors and support members to limit lateral deflection

and support architecture. Data acquired from testing in the NBRF suggested that the vertical support structures should serve as mounting points to retain the trusses. This eliminates the additional structural weight of horizontally aligned members, and does not limit astronaut and equipment passage between the vertically aligned members. Moreover, a solid, flat surface ensures that the truss will be supported across the entire member in contact with the core, keeping it aligned for retention by way of a linear actuator, attached to housing on the sides of the vertical support members. Retention and connection of the truss structure is described in greater detail in the Secure Connections for Truss Support section of this report. The vertical members were redesigned. The cross sectional area of the structures was increased, and two flat faces have been cut into the members, parallel with the sides of the octagonal base. The final iteration of the core design is shown in figure 35:

The final iteration was tested using Finite Element Analysis, with the same launch load case. With entirely solid aluminum components, the structure is expected to weigh 6600 kg, but with weight saving techniques like hollow vertical members and honeycomb composite flooring, the weight is expected to be reduced to a maximum of 3000 kg. Additional diagonal support members were implemented to combat a design oversight that arose due to the limits of Fusion 360's method of modelling acceleration on a body. The same acceleration vectors were used for each iteration, which failed to account for deflection in the event that the octagonal core and its support members are not oriented in the expected configuration when lateral acceleration is experienced. The FEA detailing the stresses and deflection experienced by the core during launch are included in figures 36 and 37.

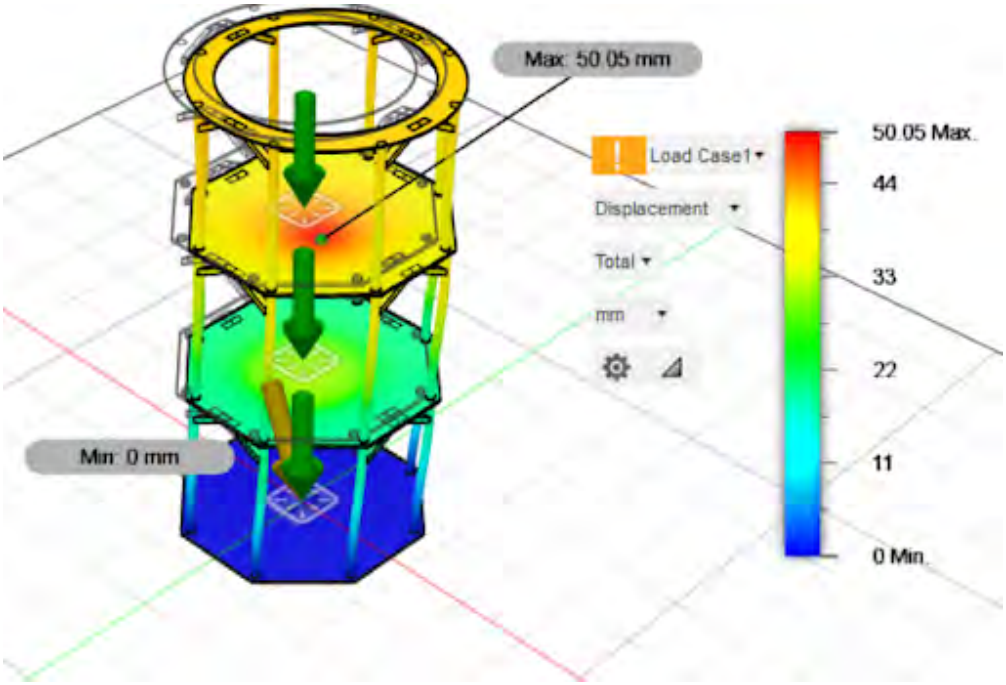

Figure 31: FEA results detailing the maximum deflection of the octagonal core structure under launch loading conditions

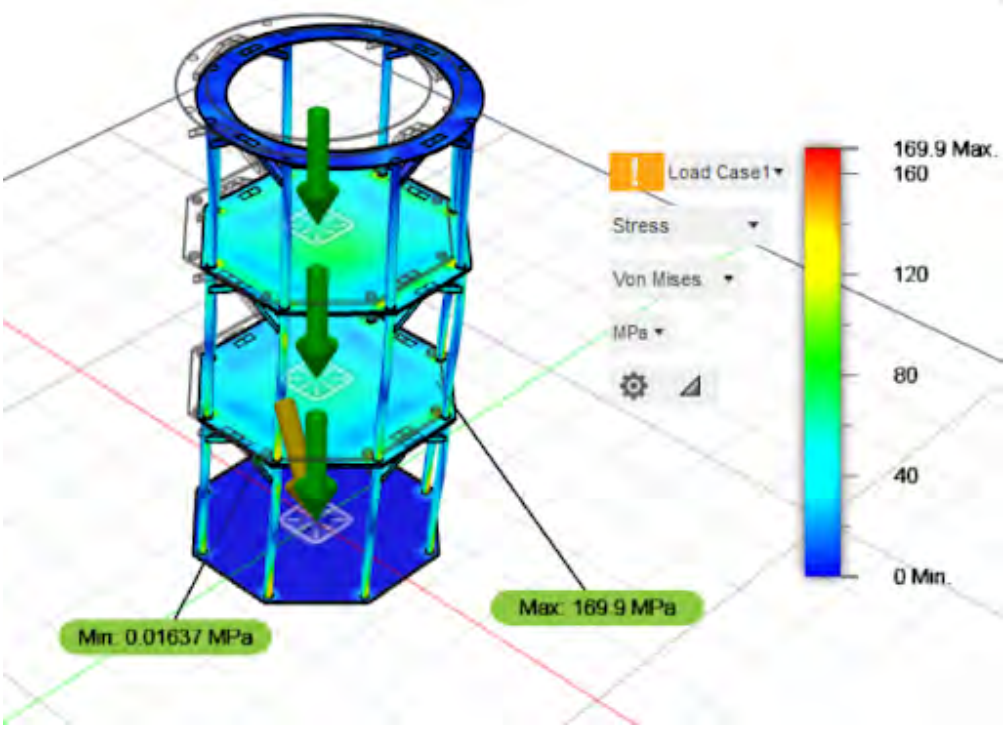

Figure 32: FEA results detailing the stresses inside the hexagonal core structure under launch loading conditions

B. Floor Panel Design and Analysis

1. Initial Floor Panel Design - Olivia Naylor

The floor panel and the overall floor layout has gone through multiple design updates based on added requirements, recommendations, and analysis. the initial design was to have 6 floor panels around the core with 2 side flaps (similar

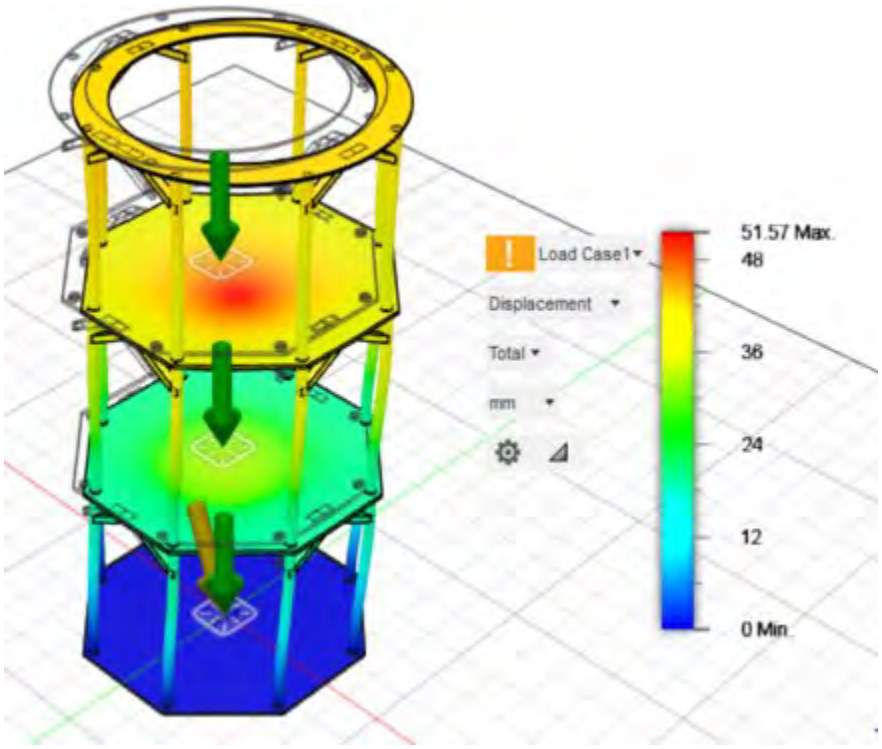

Figure 33: FEA results detailing the maximum deflection of the octagonal core structure under launch loading conditions, with hollow vertical members

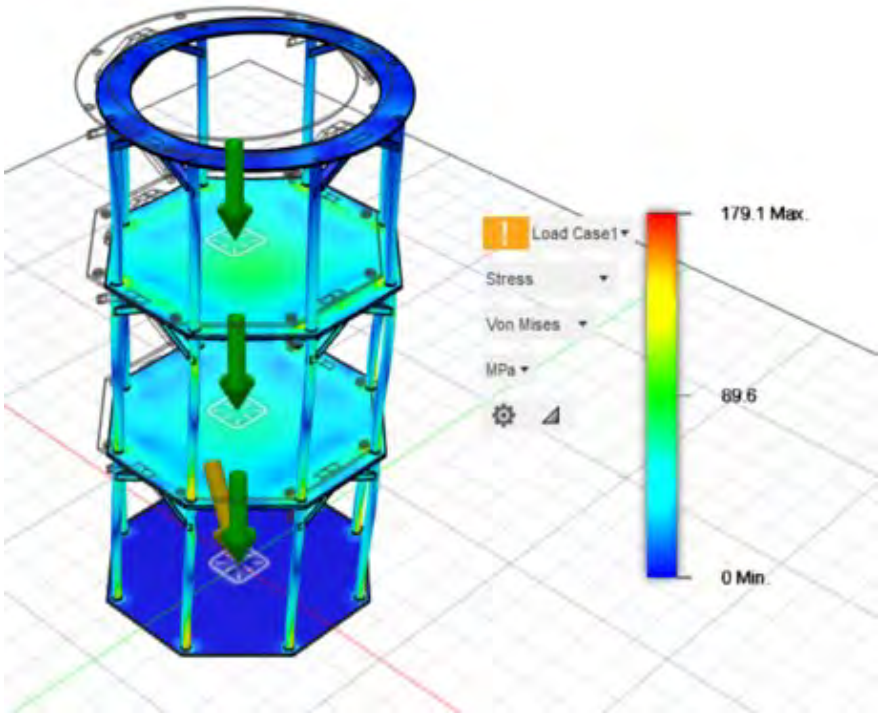

Figure 34: FEA results detailing the stresses inside the hexagonal core structure under launch loading conditions, with hollow vertical members

Figure 35: The final iteration of the core design with octagonal floors, more diagonal support members, and vertical supports meant to accommodate structural trusses

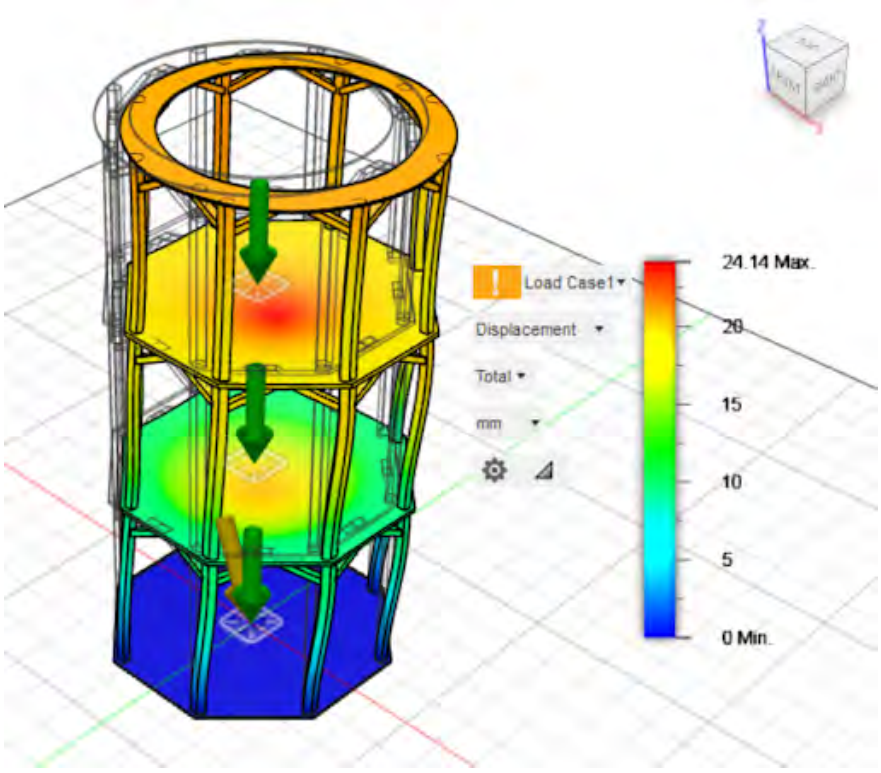

Figure 36: FEA results detailing the maximum deflection of the final core structure under launch loading conditions

to the current design) that were supported by cantilevered beams connected to it. The analysis of these support beams is completed in section D, under *Initial Design*. The reasoning for having six panels at this point is because of the original hexagonal core design that the team planned on. The basic layout of a deck at this point in the design process

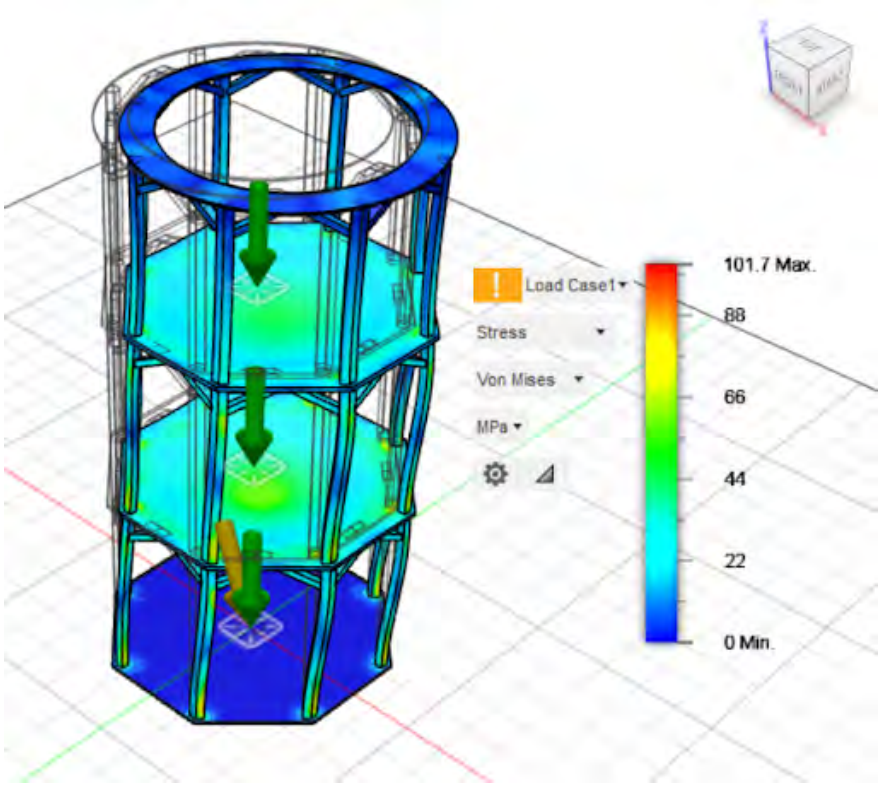

Figure 37: FEA results detailing the stresses in the final core structure under launch loading conditions

was to have 6 floor panels made of a Nylon plastic material connected to the hexagonal core with the support beams underneath that were folded with the floor before deployment. The two folded sides were connected to the central piece via hinges, which is the same as the current design. The dimensions of the floor layout is a hexagonal inner radius of 3.35 m and an outer circular radius of 7.62 m, to align with the dimensions provided by the TransHab [1]. There is also a 5 mm gap between the central piece of the panel and the side pieces. The initial design that was the 6 panel floor is shown in Figure 38 and a single panel is displayed in Figure 39.

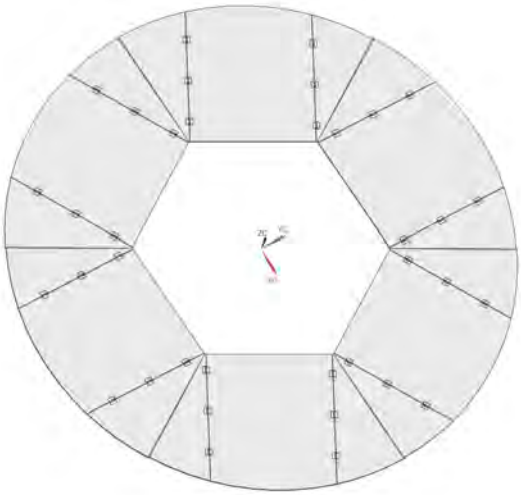

Figure 38: The initial floor layout using 6 panels.

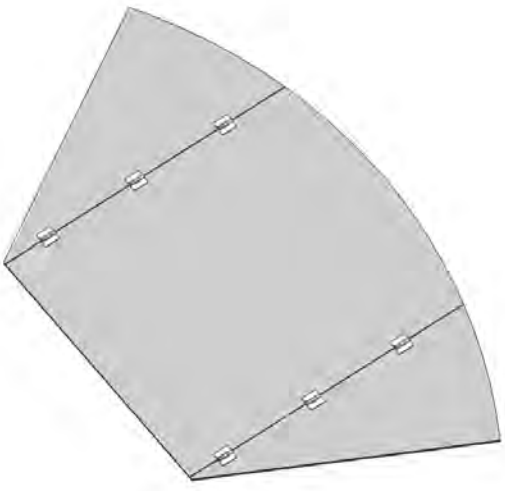

Figure 39: The initial panel design (single panel).

2. Final 8 Panel Floor Design - Olivia Naylor

The team ultimately realized that an octagonal core structure was better suited for the inflatable habitat, which prompted a change in the floor design. With the octagonal core, as discussed in section A, there needed to be 8 floor panels supported by the trusses for lunar and martian gravity detailed in D in *Analysis of Truss and Frame Layouts*, and the beam supports for microgravity in the same section under *Microgravity Floor Support*. Similar to the 6-panel design, the 8-panel one connects two side flaps to a central one using three hinges per flap. The outer and inner radii dimensions are the same, but the overall surface area of a panel for this design is smaller – it is equal to about 9 square meters. Also, a requirement of the habitat is that astronauts are able to move between floors, so one of the floor panels can be removed on the middle and top set to account for enough space to add a ladder or stairs. In the case of the 6-panel design, there would need to be one panel of half the area that is removed, so the 8-panel design provides some ease in the way that an entire panel can be removed and there is no re-design necessary. The 8-panel floor design is shown in Figures 40 and 41.

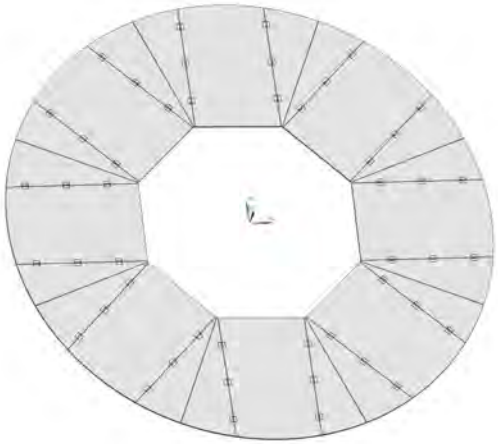

Figure 40: Final floor panel design using 8 panels.

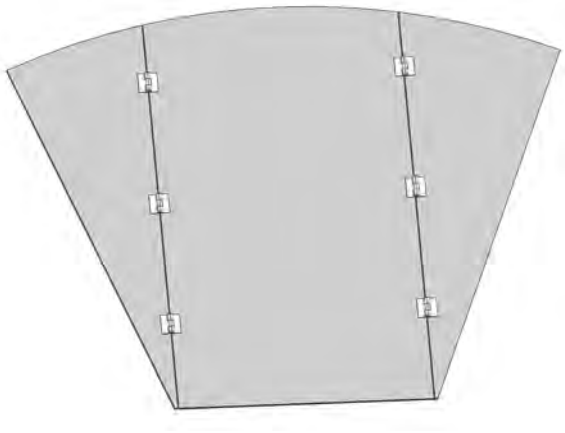

Figure 41: The final panel design (single panel).

3. Honeycomb Floor Panel Design for Martian and Lunar Environments - Kealy Murphy

In order to reduce weight, but maintain stiffness, the team decided to implement honeycomb sandwich panels for the martian and lunar environments. This design is also a candidate for micro-gravity applications, but was not chosen for maneuverability purposes as discussed in sub-subsection 4. Honeycomb sandwich panels consist of an inner honeycomb core layer, and two outer facing skins (a solid sheet), held together with an adhesive layer. To perform mathematical analysis of this structure, the following equations derived in [61] were used:

$$teq = sqrt(3 * hc^2 + 6 * hc * tf + 4 * tf^2)$$

$$Eeq = 2 * tf * Ef/teq$$

$$Geq = 2 * tf * Gf/teq$$

$$d = P * (a^3)/(48 * E * If) + P * a/(4 * Ac * Geq)$$

Where *teq* is the equivalent thickness of the panel, *hc* is the height of the honeycomb core, *tf* is the thickness of the facing skin, *Eeq* is the equivalent Young's Modulus, *Geq* is the equivalent shear modulus, *d* is the estimated deflection, *P* is the applied load, a is the length of the panel, *E* is the actual Young's Modulus of the material, If is the moment of inertia of the facing material, and *Ac* is the cross-sectional area of a core cell in the vertical direction. As per the trade study performed in section A, *Core Design and Analysis*, Aluminum 6061 was chosen as the material for the panels. The results of this analysis are summarized in the table below *Honeycomb Panel Properties*.

Honeycomb Panel Properties		
Thickness of Facing Skins	3	mm
Thickness of Cell Wall	.02	mm
Height of Honeycomb Core	47	mm
Breadth of Hexagon Panel	30	mm
Hexagon Inner Angles	120	degrees
Mass	74.5	kg
Effective Young's Modulus	4.78	GPa
Effective Shear Modulus	1.80	GPa
Applied Load in Analysis	3140	kg
Safety Factor	2	–
Estimated Deflection	5.85	mm

To estimate the greatest load a single panel would experience, the mass of the exercise equipment (2000 kg) and the mass of all 12 crew members in the males 95-percentile for weight (1140 kg) were used. Analysis was performed to produce an optimized design for both martian and lunar environments. However, the lunar panel only weighed 0.2 kg less than the martian design. Therefore, to reduce manufacturing costs the team decided to choose the stronger martian design for both applications.

4. Perforated Floor Panel Design for Micro-gravity Environments - Neal Shah

The floor panel for the micro gravity environment will be a perforated panel made of aluminum 6061. This floor panel will have the same footprint as the the honeycomb panel that will be used in the Lunar and Mars gravity environment. The thickness however will be different. The thickness for the perforated panel will be 12.7 mm. This thickness is thinner than the honeycomb panel because it will be a solid aluminum panel instead of a honeycomb sandwich. The mass of each of these panels will be 103 kg. With all 20 panels taken into account the perforated flooring will add a total of 2060 kg of mass to the entire habitat. In comparison to the honeycomb panel design the perforated panel weighs about 27 percent more. The reason we chose to go with this perforated panel design for micro gravity instead of the honeycomb design is because the perforations will allow for better mobility in a micro gravity environment. The astronauts will be equipped with special shoes that have a raised texture on the bottom sole that matches up with the perforations on the floors. This raised texture will allow for the astronauts to dig into the flooring and push off in multiple directions. Perforating the honeycomb structure is not possible as it will compromise its structural integrity. In addition to the increased mobility, the thinner panel takes up less internal volume than the thicker honeycomb design.

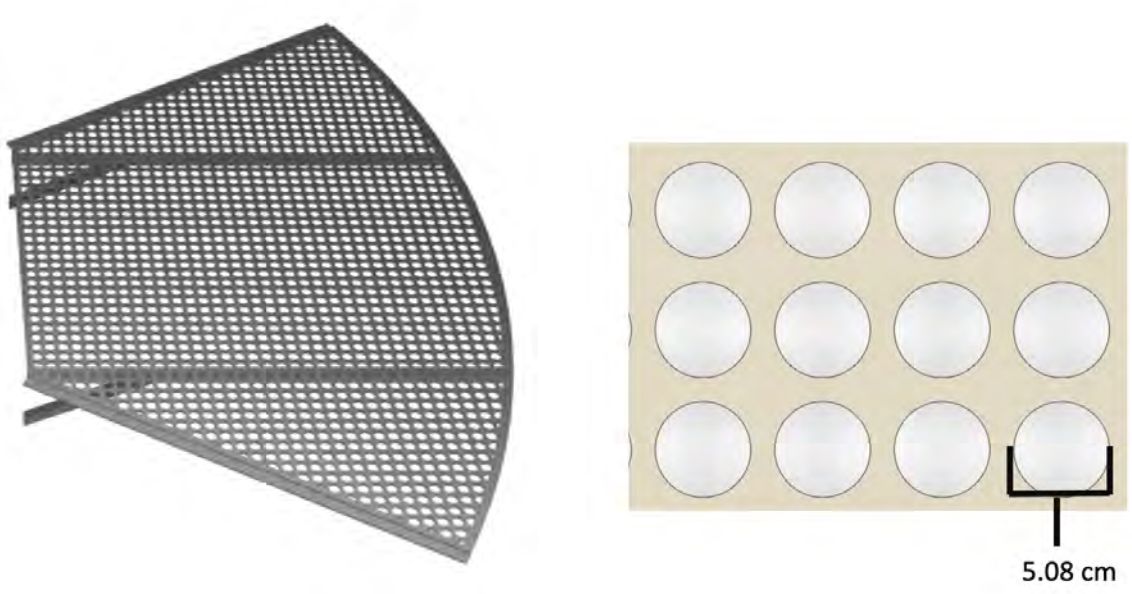

Figure 42: Image on the right is one perforated panel. Image on the left is the perforation dimension.

C. Floor Panel Deployment

1. Floor Panel Deployment Summary - Olivia Naylor

The largest structural outfitting task will be the installation of the deck and ceiling structures for the various levels in the inflated volume. Results from the scale model design exercises showed that it should be possible to have the integrated floor/ceiling panels hinged to the decks of the central core, and folded up alongside the core underneath the pressure envelope for launch.

The overall concept for deck deployment is shown in Figure 43. Each deck (consisting ultimately of both a floor and the ceiling of the deck below) consists of eight rectangular panels hinged to the central core structure (left image). Triangular truss structures will rotate out from the central core to hold up the primary deck panels (center image). A triangular secondary deck panel will be hinged on each side of the primary panels, and will unfold and interconnect to form the contiguous floor/ceiling structure (right image). This deployment system is the stacked version of that of the Constellation project [62].

The deck deployment test set-up focuses on one primary deck panel, along with one support truss along the center and hinged secondary panels. For time and cost savings, the central core structure is represented by an assembly of rectangular modular racks, developed in past X-Hab programs to allow quick reconfiguration of habitats for testing of habitat size and shape[63]). The panels are hinged upward from the upper edge of the rack 2m above the local floor. For testing, the panel is made of 2cm thick PVC sheets because it is waterproof and close to neutrally buoyant for underwater testing. The set-up has a motorized deployment system that lowers the panel using a cable that can then be detached after it is in place. For microgravity testing, the panel will be neutrally buoyant, and will be used to investigate manual deployment using ISS-type hand rails mounted in various positions around the surface. The panels for lunar and potential Mars gravity cases will be ballasted to reflect the local gravitational weight.

The test procedure in 1g and lunar gravity begins with the floor panel folded up and flush to the rack as it would be in the inflatable habitat, and then autonomously deploying the floor panel using the motorized cable system. Then, the support truss is manually locked into place on the rack. In microgravity, the test will start similarly, however the panel will be manually deployed using the previously mentioned hand rails. This manual deployment should start with the center panel piece, followed by the right flap, then the left. The trusses will then be locked into place in the same manner as the 1g and lunar tests. For all tests, the entire process will be timed to allow the estimation of how long the entire floor deployment will take in the various gravity forms. This test is useful because it will confirm the operation of the floor deployment design, and ensure it can be completed in a safe and timely fashion.

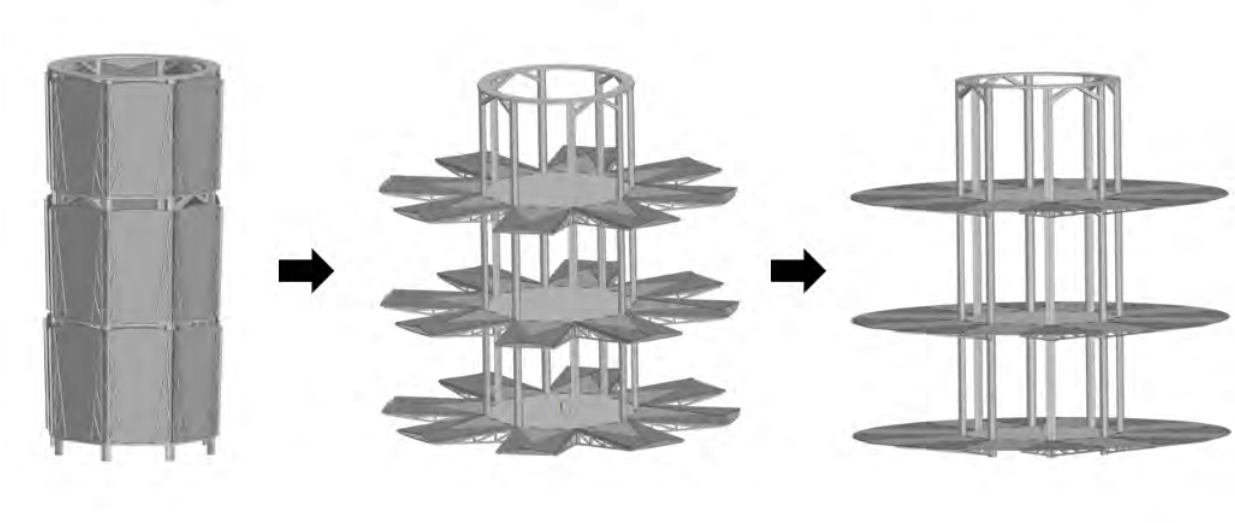

Figure 43: Design for the three steps necessary when deploying the floor panels. The leftmost image displays the pre-deployed configuration where the core will be packed. The center image displays the floors after being lowered from the packed configuration. The rightmost image displays the fully-deployed floor after the trusses are flipped and the panels flush to one another. (Created by Mason Hoene - previous iterations shown in Appendix E)

2. Spring-Loaded Hinge Floor Deployment - Mason Hoene

One objective of the mission is to deploy the floors autonomously so that the habitat is completely deployed and ready for habitation before the astronauts arrive. To achieve this, it was necessary to create a mechanism that would lower the floors in a safe and controlled manner. This mechanism also needed to function in a micro gravity environment, so we determined that it could not rely on gravity to lower the floor automatically.

To solve this problem, we decided to use spring-loaded hinges that will be compressed when the floors are in the upright position. Initially, the floor panels will be pinned to the core with the springs compressed. When the habitat reaches its final destination and is ready to begin deployment, the pins connecting the floor panels to the core will be automatically retracted and the springs will begin decompression. This will initiate the lowering of the floor and damper hinges connecting the floor panel to the core will allow the floor to lower in a slow and controlled fashion.

This method allows the floors to be deployed autonomously and has the added benefit of minimizing the power requirements and added mass for the system without the need for motors. In addition, it eliminates the hazard of additional mechanisms external to the floor panel to lower it, such as cables used for lowering. However, it is only effective in a microgravity environment because the significant weight of the floor panels requires unreasonably high damping coefficients to prevent the floor panels from slamming down during deployment. The analysis for determining the resulting motion of the floor panels during deployment was done in MATLAB and is shown in Figures 44-50.

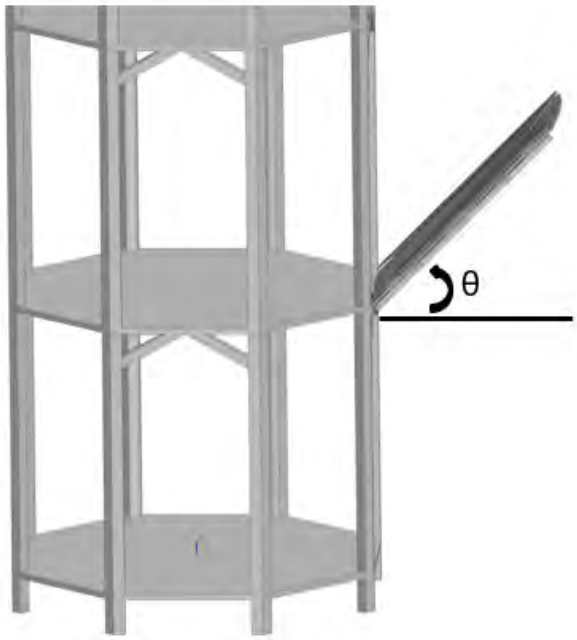

Figure 44: Definition of θ for deriving the equation of motion of the floor during deployment.

The following equation was derived using the free-body diagram shown in Figure 45 and is based off of the angle between the floor of the core and the floor panel shown in Figure 44. The equation was derived with respect to rotation around the hinge pivot point and took into account drag experienced by the panel under standard pressure [64].

$$\frac{mL^2}{3}\ddot{\theta} + c_\theta\dot{\theta} - \frac{L}{8}\rho C_d A L^3\dot{\theta}^2 + k_\theta\theta = 0$$

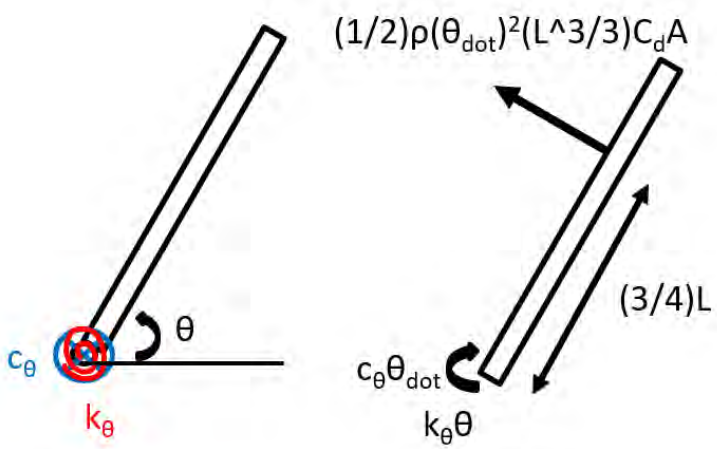

Figure 45: Free body diagram of floor panel deployment in a microgravity environment.

After deriving the equation of motion for this system, the motion of the floor panel could be determining through integration in MATLAB using ode45. This allowed for the generation of angular position and velocity plots to show how the floor panel would move depending on the spring constant and damping coefficient of the hinge. By varying the spring constant and damping coefficient, an over-damped system was created so that the panel would slowly lower into place without overshooting its target end position of zero degrees. The angular position and velocity graphs for

$k_\theta = 2\,N*m/rad$ and $c_\theta = 40\,N*m*s/rad$ are shown in Figures 46 and 47, respectively. From these graphs, it can be seen that the floor panel gradually lowers into place over the course of about 90 seconds for an average angular velocity of 1 degree per second. It can also be seen that it reaches a maximum angular velocity of under 3.5 degrees per second, showing that the floor panel is lowered in a slow and safe manner. In addition, the spring constant can stay relatively small for this application because the floor panel needs to be lowered slowly into place. With $k_\theta = 2\,N*m/rad$, the springs needed for this system do not need to hold dangerously high levels of torque because the torque produced just needs to give a slight push to start the motion of the panel. The code used to create the angular position and velocity plots is shown in Appendix F.

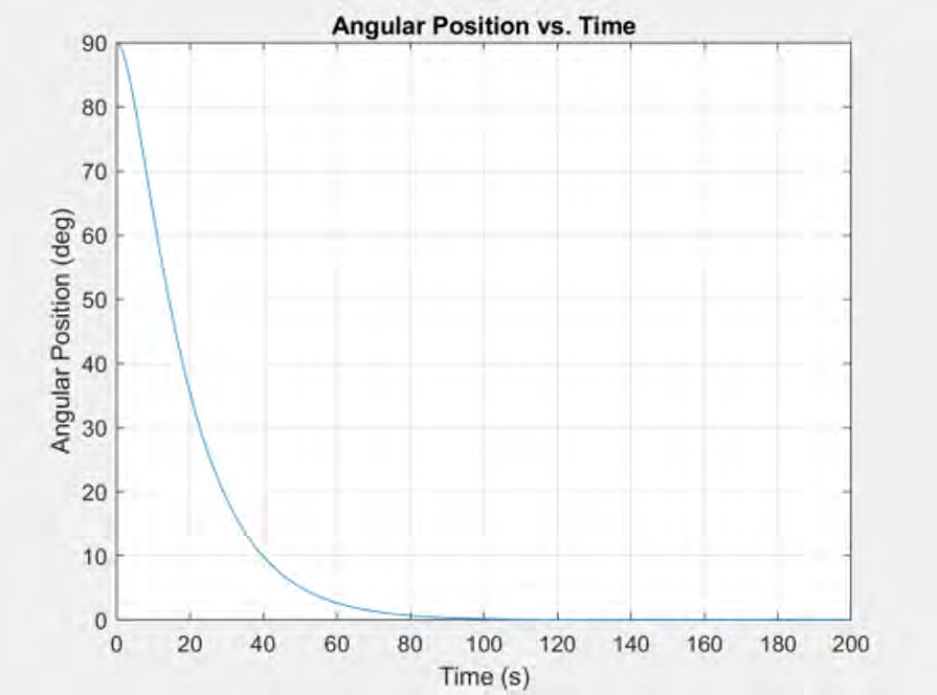

Figure 46: Angular position of floor panel with spring-damper hinges under microgravity with $k_\theta = 2\,N*m/rad$ and $c_\theta = 40\,N*m*s/rad$.

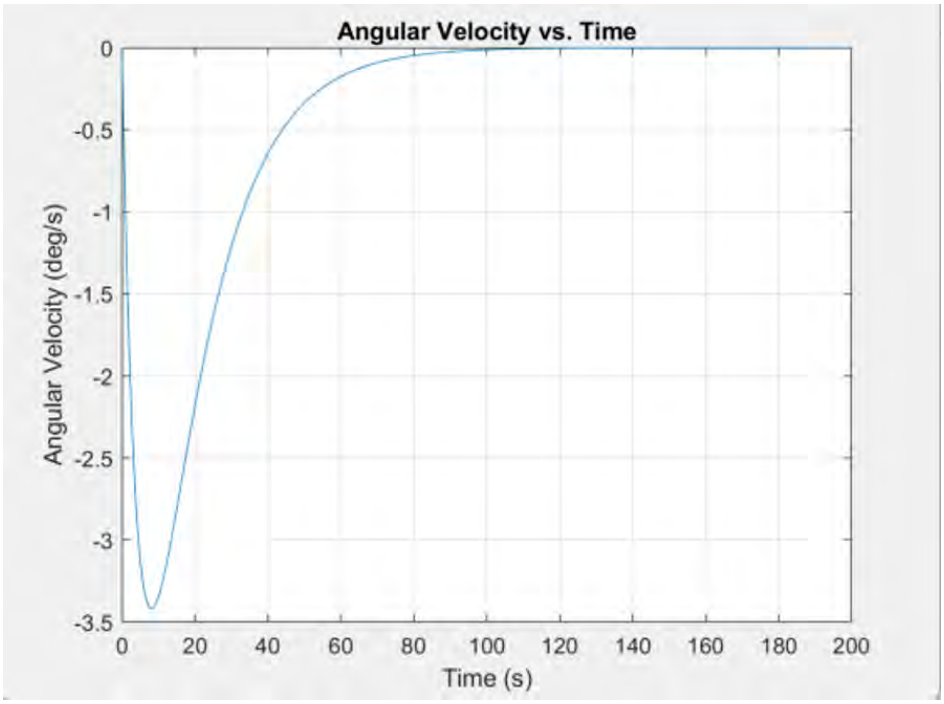

Figure 47: Angular position of floor panel with spring-damper hinges under microgravity with $k_\theta = 2\,N*m/rad$ and $c_\theta = 40\,N*m*s/rad$.

While the spring-damper hinge system works effectively in a microgravity environment, it is not as effective in non-zero gravity environments. To determine this, a similar equation was derived but with the added force of gravity as shown in Figure 48. This force was then incorporated into a new equation of motion, shown below.

$$\frac{mL^2}{3}\ddot{\theta} + c_\theta\dot{\theta} - \frac{L}{8}\rho C_d A L^3\dot{\theta}^2 + k_\theta\theta + \frac{L}{2}mgcos\theta = 0$$

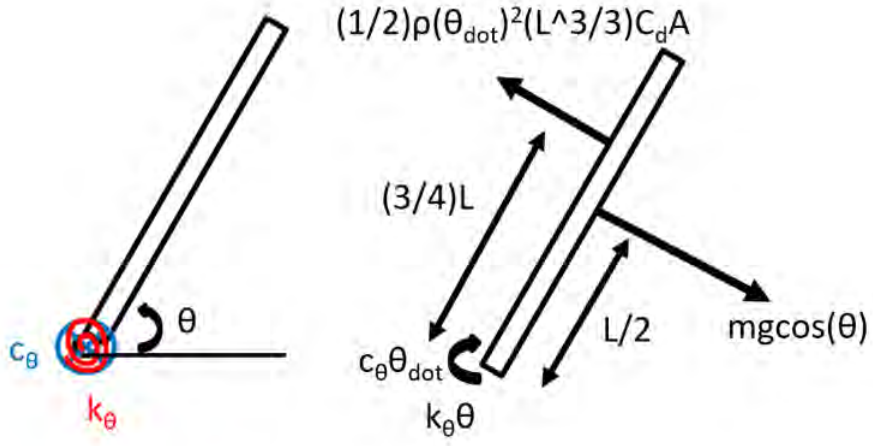

Figure 48: Free body diagram of floor panel deployment in a gravity environment.

Integrating this equation of motion again using ode45 using Mars gravity, it can be seen that the floor panel will violently slam down with the same spring constant and damping coefficient. Based on the graphs in Figures 49 and 50, the floor panel would fall down in less than 5 seconds with an a peak angular velocity of well over 100 degrees per

second. This motion is highly unsafe and would not be an effective method of floor deployment in the Xhab on Mars or the Moon. To achieve similar results to the motion in microgravity, it would require dampers with 100 times higher damping coefficients, which is unreasonable to implement in our deployment system. For this reason, we explored other methods of floor deployment that would use gravity to lower the panel with a cable used to deploy it in a safe and controlled manner. The code for computing these plots is also shown in Appendix F.

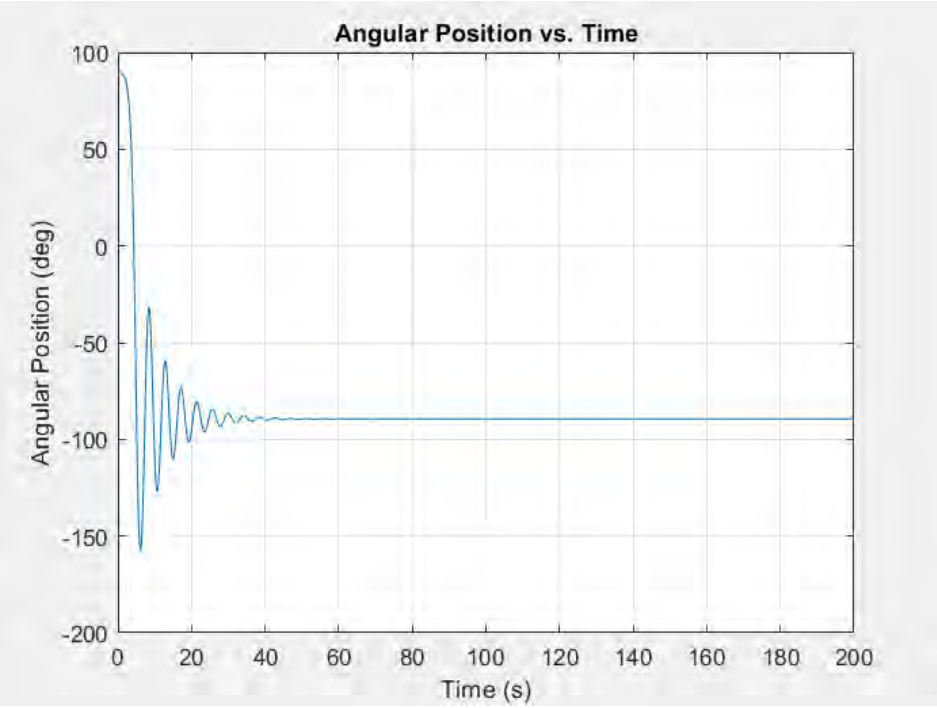

Figure 49: Angular position of floor panel with spring-damper hinges under Mars gravity with $k_\theta = 2\,N*m/rad$ and $c_\theta = 40\,N*m*s/rad$.

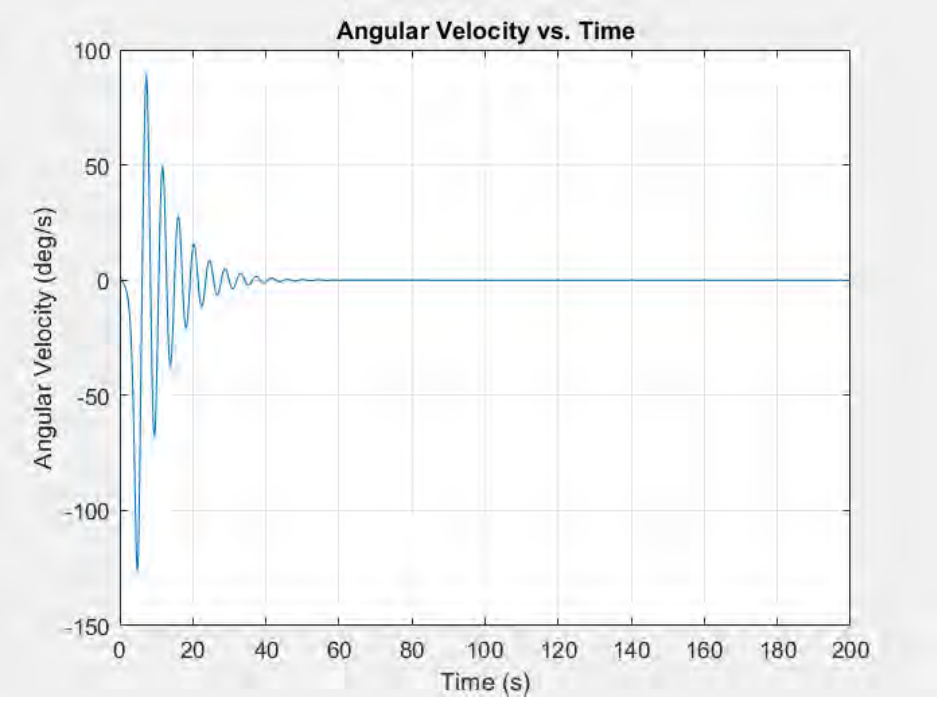

Figure 50: Angular velocity of floor panel with spring-damper hinges under Mars gravity with $k_\theta = 2\,N*m/rad$ and $c_\theta = 40\,N*m*s/rad$.

3. Winch-Driven Floor Deployment - Neal Shah

Figure 51: Mars and lunar gravity floor deployment winch

For the floor lowering system in mars and lunar gravity we chose to use a system of winches. For this system, each panel would be lowered by its own winch. In total this equates to 22 winches. The first floor will have 8 winches in total while the 2nd and 3rd floor of the habitat will have 7 winches. The attachment point for the winches will be inside the core on the ceiling of the floor above it. The configuration for the winches can be seen in the figure below.Each winch will have a cable that connects to the outer radius of the corresponding floor panel. When switched on, the winch will unwind this cable allowing the panel to lower in a controlled manner.

Figure 52: Winch Configuration

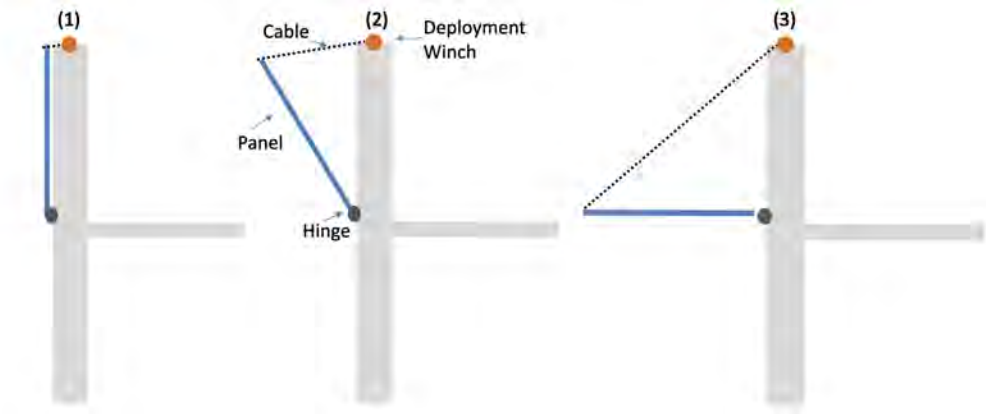

Figure 53: Winch Deployment Sequence

Each winch will be driven by a high torque DC motor. This winch will need to provide a max torque of 7.84 N-m of torque in Mars gravity and 3.41 N-m of torque in Lunar gravity. To reduce the current draw of the motors we incorporated a 4:1 gear reduction. This gear reduction will reduce the RPM of the winch by a factor of 4 but the input torque from the motor is also reduced by a factor of 4. Thus the needed max input toque of the motor will be 1.96 N-m in Mars gravity and 0.85 N-m in Lunar gravity. For a 240RPM motor the output RPM will be 60 RPM. Based on the cable length and winding shaft diameter the total time it will take to lower the floor panel will be close to 90 seconds. Once the winches deploy the floor panels they can then be removed from the inner core to free up space.

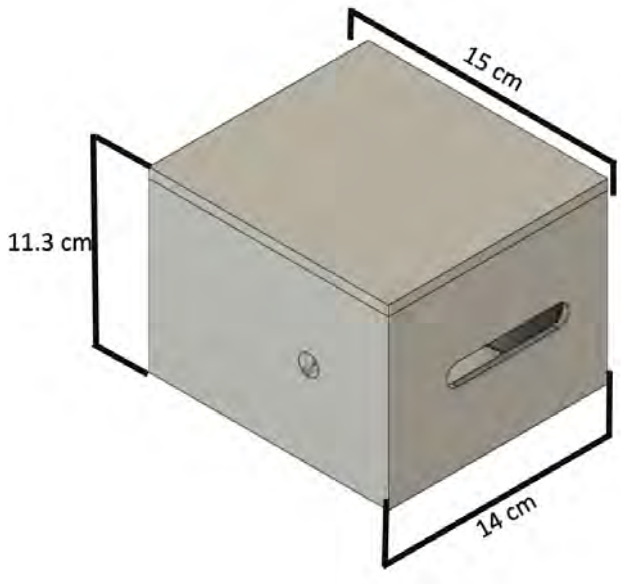

Figure 54: Winch Housing

The housing for the winch was made to be as compact as possible so that the core volume can be used to store other items. The dimensions for the winch housing can be seen in figure 8 above. Aluminum 6061 will be used as the material for the housing as it is light yet robust enough to withstand vibration and small impacts. The total volume that the winches will take up in the habitat is 0.053 m^3. In regards to the mass of each winch, each winch will have a mass of 6.58 kg and the total mass of all the winches combined equates to about 145 kg. The components that lie within the winch besides the DC motor are two gears which will be made out of steel and a winding shaft that will also be made from steel. After the floor panels are lowered by the winch spring loaded hinges will finish deploying the flaps and trust structure.

D. Floor Support Design and Analysis

1. Floor Support Requirements - Jack Saunders

Once the floor panel is deployed into its proper location, it will need additional support to avoid failure. Designing a proper floor support is important as it ensures the safety of the crew and equipment on each floor panel. Design requirements drove the design of the floor supports. The first design requirement is that the support cannot extend further than the outer wall. This limited the design to be less than 2.14 m, which is the distance between the inner core and outer wall. The floor support additionally has a maximum deflection requirement. The limit of floor deflection was determined based off of International Residential Code. The code states that floors should have deflection less than the total unsupported length divided by 360 [65]. This would be a maximum value of 5.93mm, based on the maximum possible length of the support. The floor supports were also required to hold all loads without yielding. The expected weight loads includes expected weight of crew and equipment. This value was updated throughout the design process. Due to the changing nature of this value in the design, there is no exact value to claim as the requirement. The process of determining weight load estimates is discussed in the *Floor Support Load Estimation* and *Refined Loads* sections. The support must also be designed for martian and lunar gravity as well as micro-g. While working through the project, NASA directly gave the additional requirement that the outer pressure bladder wall must not hold any structural loads. In terms of design, this meant the support structure needed to be supported by the core. These requirements are summarized in the following table:

Floor Support Design Requirements		
Requirement	Description	Value
Length	Support cannot extend beyond outer wall	$\leq 2.14m$
Deflection	Must be less than total $length/360$	$\leq 5.93mm$
Weight Load	Must be able to support weight of crew and equipment	TBD
Load Support	All loads must be held by central core	N/A

2. Floor Support Load Estimation - Jack Saunders

In the early stages of designing the floor support, the weight loads were not precisely defined as the layout of the X-Hab interior was not yet determined. In order to proceed with preliminary designs of the floor supports, an estimation was required. Building codes were used as a reference for typical expected floor loads on earth. According to International Residential Code, floors are required to support a pressure of 40 psf for most rooms, with the exception of those used for sleeping [66]. To determine the live load, the following equation was used:

$$F = pA(g/g_{earth})$$

In this equation, F is the live load per floor panel, p is the live load pressure, A is the floor panel area, g is either lunar or martian gravity, and g_{earth} is earth's gravity. This equation solves for the expected live load per floor panel for its desired gravitational environment, based on the residential code. In addition to the live load, the floor support also needs to hold to the dead load, which was the weight of the floor panel that had an initial mass of 156 kg. A safety factor of 2 was then applied as NASA recommends this value for untested structures[67]. The initial calculated loads are summarized below:

Initial Load Estimation		
Load (N)	Mars	Moon
Live Load	8910	3880
Dead Load	1160	510
Total (N)	10070	4390

3. Initial Design - Jack Saunders, Olivia Naylor

The first design of a floor support that was analyzed was a simply supported beam that ran across the underside of the floor panel. This beam would be supported by a pin connection at the core and rest on an additional support attached to the inflatable wall. These connections would allow the support to rotate into position while the floor panel is lowered into position during deployment. It is also important to note that this design came before NASA imposed the requirement for the inflatable structure to carry no structural loads. However, it is still important as it influenced future iterations. This initial design primarily focused on the martian load case, as it is worst load case that would be experienced. It was determined that each floor panel would need 3 support beams to keep floor deflection under 5.93 mm and meet the L/360 requirement. Selecting 3 beams per floor panel resulted in a load of 3360 N on each, which was analyzed as a distributed rectangular load.

The maximum shear load and bending moment of the simply supported beam were then calculated using the following equations:

$$V = wL/2 = 1570 * 2.135/2 = 1.68\ kN$$

$$M_{max} = wL^2/8 = 1570 * 2.135^2/8 = 0.896\ kNm$$

In these equations, w is the distributed load and L is the length of the beam. After these values were obtained, the minimum moment of inertia and cross sectional area of the support beam were calculated based off the shear stress and bending stress. The equations that were used to do so are:

$$I = M_{max}c/\sigma$$

$$A = 3V/2\tau$$

In these equations, M_{max} is the maximum bending moment, c is half of the thickness, *tau* V is the max shear force, *sigma* was the tensile yield strength and *tau* was the shear yield strength. These beams were designed to be solid

Figure 55: Initial support beam with rectangular distributed load and with pinned connection at core (left) and roller support on inflatable structure (right)

Figure 56: Initial floor panel design with rectangular floor supports attached. The floor panel is upside down in the image to provide a clear view of the supports.

rectangles composed of 6061 aluminum. This material was originally selected due to its common use for aerospace applications and high strength to weight ratio compared to other metal alloys. With the selection of the material, the yield strengths became known with $\sigma = 310\ MPa$ and $\tau = 207\ MPa$ and the beam dimensions could be determined [68]. The selected dimensions for this floor support were 2135 mm in length, 100mm in width and 15mm in thickness. This results in a margin of safety of 0.16 for bending stress and 122 for shear stress. Bending stress was the limiting factor for this design by a large margin.

While this design needed to be changed due to new design criteria, it was important as it demonstrated what considerations needed be to investigated further in the future. This included the investigation of different materials and more analysis on the beam sizing. Additionally, the idea to have a support structure run along the underside of the floor panel was kept.

4. Analysis of Truss and Frame Layouts - Jack Saunders

The addition of the requirement to have all loads carried by the core caused a change in the floor support design. Now that the only attachment point for the support was the center core, cantilevered structures became the focus. After conducting some research, it was determined that cantilevered trusses and frames, specifically those with a triangular shape, are commonly used in this application and thus became the framework of the design [69]. Trusses and frames

are similar in design, as they both consist of connected beams that support a load. The key difference is that truss members are connected by pins and frame members are rigidly attached to each other. Truss members also only hold axial loads while frame members can hold axial loads, shear loads, and bending moments[70].

The frame and truss analysis started by determining the overall dimensions of the designs. The length was decided to be 2.14m, which was carried over from the initial design. The maximum height of the support was difficult to precisely determine, due to the balance between reducing its mass and reducing the safety threat for the crew. Ultimately, the maximum height of the design was determined to be 0.3 m. This height would provide 1.82m of minimum clearance on the first floor and 2.13m on the second floor. Clearance is not an issue on the third floor as there is no support structure located above. It is important to discuss that a 95th percentile male, which measures 1.89m in height, would be able touch the bottom of the support at its connection point on the first floor with the top of their head [71]. This poses a potential safety issue. However, load analysis, which is discussed further in this section, provides reasoning for this size. If the truss height was reduced to 0.2m giving complete clearance to the 95th percentile male, loads in the support members would increase by 150% and cause the mass of the members to increase 140%. At the selected design height, the 95th percentile male would be able to move around the outer 75% of the floor area with 1.92+m of space and have no worry of hitting their head. This number does not include any usable space in between the truss members that fall below 1.92m, which, if included, would bring available floor space to around 99%. Additionally, furnishing could be arrange in such a manner that areas near the truss obstruction become inaccessible. The mass reduction justifies the use of the slightly larger design. However, to verify this size selection and fully understand how safety is impacted, physical testing should be completed in the future.

Compared to the initial support design, the load case also changed. It was determined that the floor panel would only require 2 floor supports with a larger truss or frame support (see Section B, *Floor Panel Design and Analysis*. This increased the load per support to 5035N in a martian environment. Once again, the maximum martian load case was analyzed first with the intention of repeating the process for the lunar case once a refined design was found. Another estimation was made, as the load was modeled as point loads that were equally distributed at each node across the top surface. For example, a design with 5 nodes along the top, would be modeled with 1007N downward forces at each of those nodes.

After determining overall design dimensions and loads, the layout of the beams needed to be figured out. To accomplish this, multiple truss and multiple frame designs were analyzed and compared. Three critical designs for each will be discussed in this section. For the truss designs, an online program, titled TrussSolver2, was used for load estimation in each member. For the frame designs, an online structural analyser named Strian was used. For a true comparison, the same member layouts were used. The studied beam layouts can be seen in the figure below:

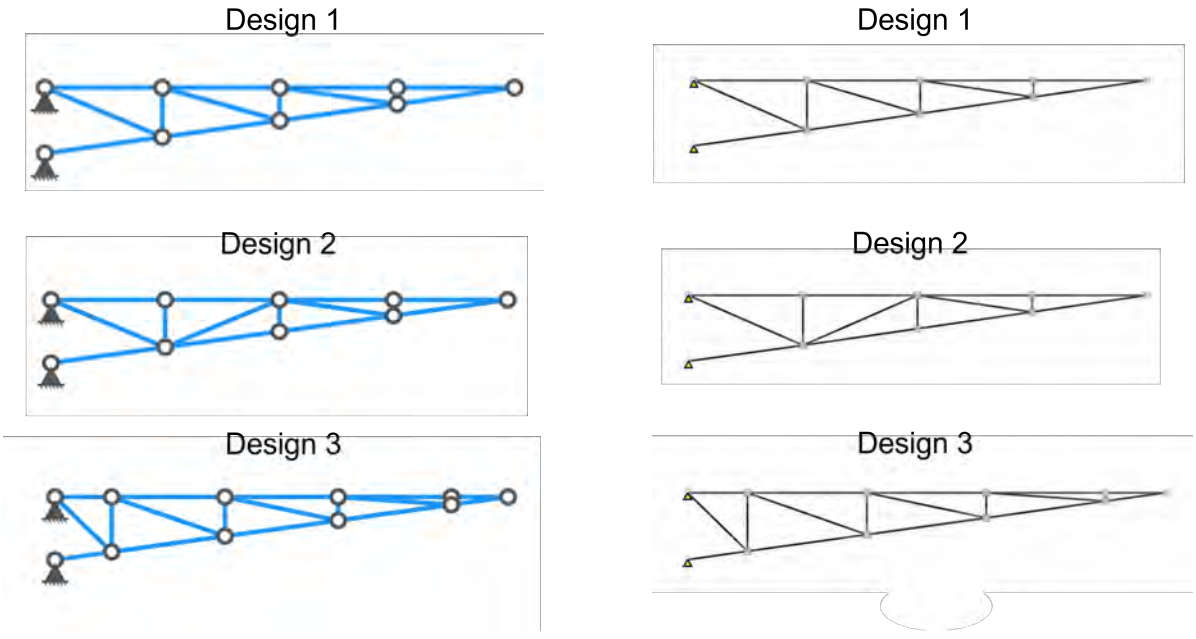

Figure 57: Layouts of the analyzed truss designs (left) and frame designs (right).

The main parameters that were analyzed were the maximum member loads and total length of the beams in the design. These parameters were selected as they influence the size of the beams. Force is proportional to the cross sectional dimensions, and the greater the force, the greater those dimensions have to be. Also, as the total length of beams increases, the amount of material needed increases as well. Minimizing the loading and the total length of the beams would reduce the amount of required material and therefore reduce mass. The parameters for the three studied truss designs are as follows:

Truss Design Summary		
Design	Max Axial Force (kN)	Total Length (mm)
1	17.6	6400
2	17.6	6500
3	17.8	7360

The frame design had similar results, but included additional shear and bending moments. The results for the three frame designs are:

Frame Design Summary			
Design	Max Forces (kN)	Bending Moment (kNm)	Total Length (mm)
1	Axial: 18.1 Shear: 0.38	0.04	6400
2	Axial: 18.1 Shear: 0.98	0.04	6500
3	Axial: 18.3 Shear: 3.83	0.44	7360

Ultimately, the truss and frame designs for each layout acted nearly identical in terms of loading. The frame designs only held very small shear and bending moments compared to the axial loads. Additionally, the axial loads of the truss and frame were nearly identical, varying by less than 1%. Designs 1 and 2 shared the lowest maximum force that was found during analysis of different beam layouts, which was 18.1 kN. Design 3 was not as efficient as it held higher loads with the greatest total length of material. However, it did provide important insight on similar designs. The main point of studying design 3 was to understand how shifting node locations around and how changing the number nodes effected the loads. For this design and other similar iterations, it was determined that adding additional nodes and vertical supports did not reduce the maximum load in the structure. Also, it was found that beams towards the tip were not always able to physically exist. After approximately 75% of the total length, any inner diagonal beams were not physically possibly. The beams are modeled as thin lines, but when adding thickness to the lines they overlap and geometries become altered. So while design 3 was not the optimal choice, it provided insights into other designs and helped to lead to the final selection of a layout. Design 1 was selected as the best option and was used in further analysis. This design has the same forces but is smaller in the total length compared to design 2, which would lead to a lighter support overall.

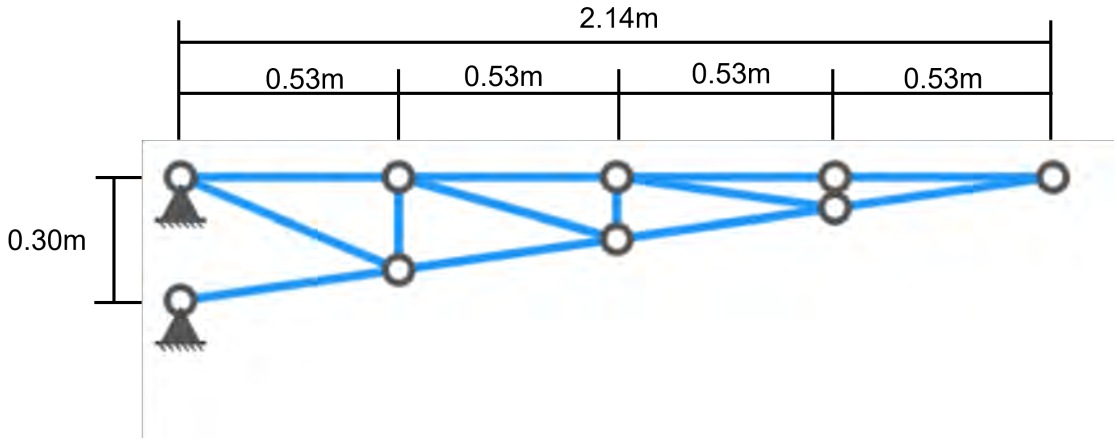

Figure 58: Dimensions of Selected Truss and Frame Layout

With little difference between the truss and frame layout of design 1, more distinguishing features needed to be analyzed. With the loading being nearly identical, the main difference in their design is the process of manufacturing. Understanding how different materials behave during this manufacturing process and the total mass needed to meet design requirements was the factor that allowed for the optimal design to be selected.

5. Analysis of Materials and Beam Sizing for Trusses and Frames - Jack Saunders

To continue the design of the support structure and distinguish between the truss and frame design, sizing the beams became the main focus. To accomplish this, the beam supporting the most load with the longest length would be determined first. This would be be the beam most susceptible to failure and if it is properly sized, then other members will not fail with the same dimensions. The highest load case beam with the longest length had a load of 18.1 kN and a length of 0.54m.

A square shaped tube was determined to be the best shape of the members. This shape is commonly used in support structures as it can be easily cut, drilled and manufactured. It also undergoes less processing than other mechanical tubing making it cost effective[72]. To figure out the outer dimension of this square piping, the size of the hole required to the main pin connection was analyzed. At the pinned connections to the core, there is a 18.1 kN reaction force required to hold the beam in place. To find the size of a bolt capable of holding this force, the following equation was used:

$$d = \sqrt{(4F/\pi\sigma_y)}$$

In this equation d is the diameter of the bolt, F is the force held by the bolt, which would be the reaction force in this case, and σ_y is the shear yield strength [73]. For a 305 stainless steel bolt with σ_y of 150 MPa, the bolt size would be 12.5 mm in diameter. This material was selected as it is commonly used in bolt manufacturing[74]. Using this bolt size, the outer dimension of this square piping was determined to be 50mm in size. The bolt would require at minimum a 13.5 mm hole for a tight fit in a beam member to fit through [75]. Holes must be a minimum of 1.25 times their diameter away from the edge. This required there to be at least 17 mm of space between each edge of the hole [76]. Adding together these distances produces a minimum distance of around 50mm, which became the size of the beam members. This size was kept for all members for easier connections between all the members. Additionally, having a 50mm squared area would allow 25mm of each panel to lay on top of the beam at the hinge location. Having a wider pipe also increases the moment of inertia, which helps avoid failure modes such a bending.

After finding a suitable outer dimension for the beams, an inner dimension needed to be determined. This was accomplished by looking at different failure modes and the required cross sectional area and moment of inertia required for each. These failure modes include buckling and deflection for the truss design and buckling, deflection, and beam bending for the frame design. Calculating the deflection of a system of beams is very difficult without the help of a computer program, which was not available during this analysis. To simplify the analysis, elongation of each beam was used to help estimate the overall deflection. The respective equations used to calculate beam dimensions based on buckling, bending and elongation are as follows:

$$I = P_{cr}(KL)^2/\pi^2 E$$

$$I = M_{max}c/\sigma$$

$$A = FL/(\Delta L)E$$

With the known information calculated up to this point, these equations can be simplified. The known values including the critical buckling load P_{cr} and compression force F which is 18.1 kN, the maximum bending moment M_{max} which is 0.04 kNm, and the length L which is 0.54m. Additionally, it is known that the k variable in the buckling equation is 1 for pin-pin connections like in a truss and 2 for fixed-fixed connections like in a frame. For the truss, where only buckling and elongation applies, the equations simplify to:

$$I = 535/E$$

$$A = 9774/(\Delta L)E$$

For the frame, the equations simplify to:

$$I = 2140/0.7E = 3060/E$$

$$I = 1/0.7\sigma = 1.42\sigma$$

$$A = 9770/(\Delta L)(0.7E) = 13900/(\Delta L)E$$

It is important to note that the frame equations include an additional 0.7 term for the values of E and σ. This is a result of the manufacturign method required to create a metal frame. The members of metal frames are connected by welds. When both aluminum and steel are welded, their yield strengths decrease to approximately 70% of their original value, which is why the additional 0.7 is included [77, 78]. Since Young's modulus is also proportional to stress, its value would also decrease to 70% of its original value after welding. These material change, separates the truss and frame designs. Now comparing the two, it can be seen that the moment of inertia needs to be 5.7 times larger and the area needs to be 1.42 larger for the frame as compared to the truss. To support the same loads, the frame members must be larger to overcome the weakening of the base metal and it becomes heavier. It is for this reason that the truss design was selected over the frame design.

After selecting the truss design, the next step was to determine the material that the truss members would be made up of. Similar to the core material selection, steel and aluminum alloys were considered. Specifically, 6061 aluminum, 2024 aluminum, 4140 steel, and A36 steel were analyzed. All of these materials are commonly used in the construction of aircraft and buildings which is why they were selected. The properties of these materials are as follows:

Truss Material Study				
Material Property	6061 Aluminum	2024 Aluminum	4140 Steel	A36 Steel[79]
Density (kg/m^3)	2700	2780	7850	7850
Elastic Modulus (GPa)	69	73	190	200
Yield Strength (MPa)	276	324	415	250
Machinability (Based on AISI 1212)	280%	90%	65%	72%

These material properties were then used to fully solve the truss failure equations for the inner dimension. To determine an estimated value for the elongation (ΔL), finite element analysis (FEA) was utilized. Using Siemens NX, a model of the truss was developed with beams having outer dimension of 50mm and variable inner dimension. After plugging in test values for the elongation, then calculating the required area, and finally running multiple FEA tests, it was determined that an elongation value of 0.09 mm per beam resulted in a total deflection of approximately 5.80mm, which met the design criteria by a margin of safety of 0.02. This value was then used in further analysis. The size of the beams needed to support the maximum load cases for different materials was then calculated based on buckling and deflection and are as follows:

Thickness of Beams for Aluminum and Steel Alloys			
Material	Thickness for Buckling (mm)	Thickness for Deflection (mm)	Total Mass (kg)
6061 Aluminum	0.09	9.80	27.2
2024 Aluminum	0.08	9.09	26.5
4140 Steel	0.03	3.04	28.7
A36 Steel	0.03	2.88	27.3

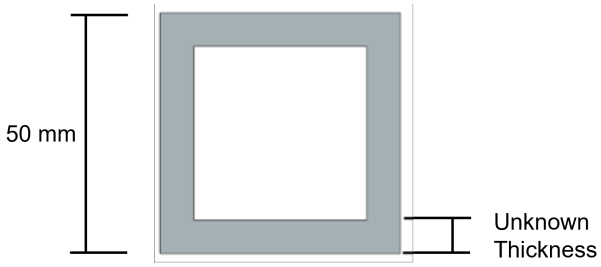

Figure 59: The outer dimension of the square pipe and the unknown thickness which varies with different materials

In the table, the total mass was calculated by using the largest required area and assuming a constant cross section for the entire 6400mm length of the design. This was used to compare the masses for each material. Each beam would need to be optimized, which can be seen in section *Mass Reduction of Truss Design*. However, since sizing each beam will still result in the same percent difference in mass between each material, the comparison being made here still holds. These calculations also demonstrate that deflection is the mode of failure that would occur first, as the needed thickness is around 100 times greater than the thickness needed to prevent buckling. Although the 2024 aluminum is the lightest option, the 6061 aluminum is best material for the truss design. While it is 2.7% heavier, it is over 3 times more machinable. There are 14 beams needed for 44 individual trusses, many of which need to be drilled through and cut at sharp angles. Allowing for significantly easier manufacturing by selecting the 6061 should be worth the slight sacrifice in mass. However, if the mass budget absolutely needs a reduction of mass, the material selection could be revisited in the future. As that is not an issue as of conducting this analysis, 6061 will be selected.

6. Directing Loads to Nodes on Truss Support - Jack Saunders

An important part of a truss is having the loads directed through the connection points of the beams. These systems are not designed to hold high shear or bending loads. To ensure that the loads were being directed to the nodes, the vertical beams were extended slightly so the panel would rest on them rather than on any of the adjacent horizontal members. To allow for a more even distribution of the load, vertical beams were added at each end of the truss structure. Each beam extends above the truss by 5 mm, ensuring the floor panel will not deflect into any members. The new layout is seen in figure 60.

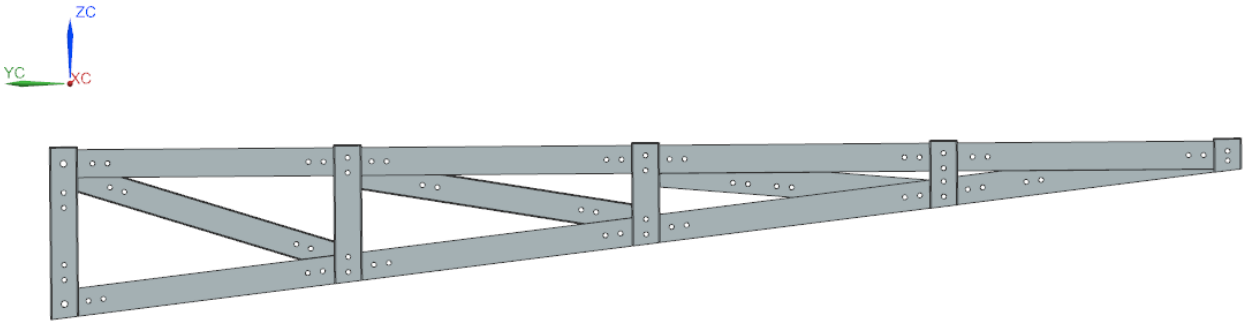

Figure 60: The full truss member layout with new beams on far left and right to help distribute loads to the main nodes

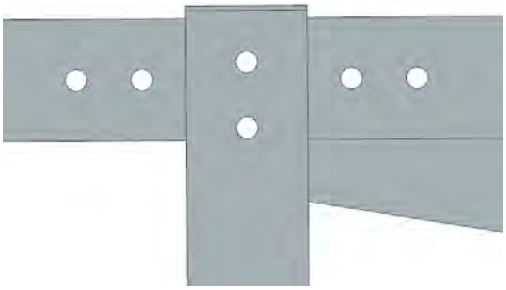

Figure 61: Zoomed in look at the extension of the vertical beam. This connection to the floor directs a compression load to the vertical beam and avoids a risk for high shear loads on adjacent horizontal members

7. Gusset Plate Sizing - Jack Saunders

In a truss design, the members need to be pinned together with some additional piece of material called a gusset plate. These plates are thin pieces of metal that are attached to the beams by bolts. The material of the gussets was selected to be 6061 aluminum for the reasons discussed in the *Analysis of Materials and Beam Sizing for Trusses and Frames* section. The gussets must be able to hold the load from the beam to the bolts, which act in shear along the plate. The worst of these shear forces is equivalent to the force on the bolts holding the reaction force. It was determined that 2 bolts would be used in each beam at each connection point. This would decrease the force by a factor of 2, making each bolt required to hold 9.1 kN. Using the bolt diameter equation, which as previously stated is, $d = \sqrt{(4F/\pi\sigma_y)}$, the bolts are found to be 9mm in diameter.

To determine the thickness of the gussets, shear stress was analyzed. The first important factor in finding the shear stress was determining the area that the bolt force was acting over. An effort was made to keep the gusset plates aligned with the beams to allow for the maximum sight lines for the crew. This limited the width of the gussets to 50 mm. With a hole of 9mm in width, the maximum material area at the hole could be described by the equation $A = bt - ht = 0.05t - 0.009t = 0.041t$, where t is the thickness of the gusset, h is the diameter of the hole, and b is the total width of the plate. Using the knowledge that the shear strength τ of 6061 is 150 MPa, the thickness t could be solved for. The equation $A = F/\tau = 0.041t$ provides a thickness of 3 mm for the gussets. The rest of the gusset dimensions were determined by placing holes 9mm bolt holes 12mm away from the edges of each beam and 22.5mm away from each other. This satisfies the condition to have holes 1.25x their diameter away from the edge and 2.5x their diameter away from another hole [76]. Locating this positions on each beam and mirroring them to a gusset plate is how the shapes were formed.

Using this information a design for all of the gusset plates was determined. Using Siemens NX to model the plates, it was found that the total mass of the gussets was 3.62 kg. It was also estimated that a total mass of approximately 2.5kg of bolts would be required as well. This number was based on the mass of a typical 9mm steel bolt and multiple by the total number needed in the design. The final gusset design is shown below in Figures 62 and 63.

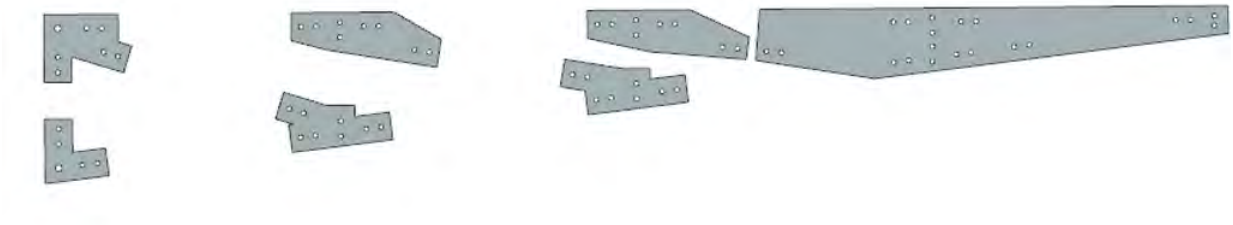

Figure 62: The design of the gusset plates relative to their location on the actual truss model

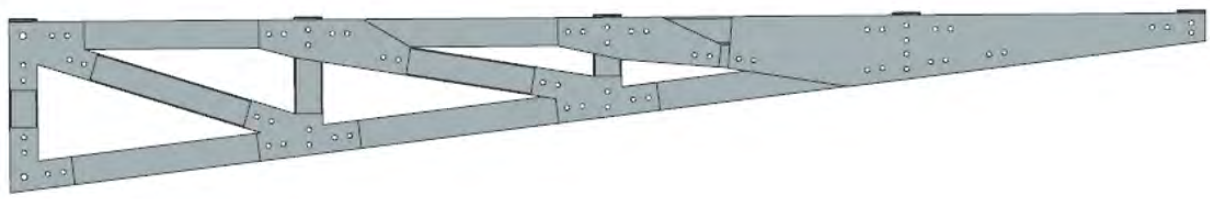

Figure 63: The combination of the gusset plates and truss members

8. Mass Reduction of Truss Design - Jack Saunders

To reduce the mass in the truss structure, each beam was analyzed individually. As it was determined that the deflection requirement was the most strict constraint, satisfying this was the goal for each member. Using Matlab, a code was developed to find the thicknesses required for each beam based off of their lengths and expected loads. Siemens NX was then used to model each member with its calculated thickness and provide an estimated mass for each beam. Also, it was determined that the lower limit of the thickness of each beam member is 1 mm, which is based on the aluminum beams that are currently produced by aluminum pipe manufacturers. Anything smaller than 1 mm would require more laborious manufacturing. After running the Matlab code for martian and lunar gravity, the new thickness and mass of each member is as follows:

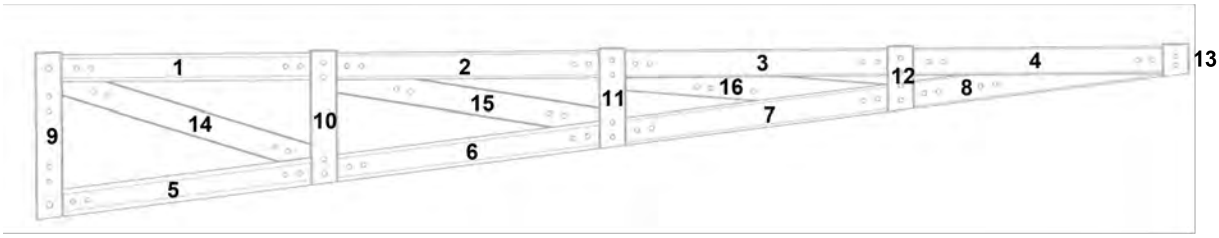

Figure 64: Numbering system used to describe each truss beam

Reduced Mass and Thickness for All Members				
	Mars		Moon	
Beam	Thickness (mm)	Mass (kg)	Thickness (mm)	Mass (kg)
1	7.2	1.48	2.9	0.70
2	5.2	1.17	2.1	0.56
3	3.3	0.85	1.4	0.38
4	3.3	0.80	1.4	0.36
5	9.8	1.91	3.7	0.86
6	5.6	1.67	2.9	0.74
7	5.3	1.21	2.2	0.56
8	3.4	0.47	1.4	0.22
9	1.0	0.40	1.0	0.17
10	1.0	0.32	1.0	0.14
11	1.0	0.24	1.0	0.10
12	1.0	0.16	1.0	0.07
13	1.0	0.08	1.0	0.04
14	1.9	0.44	1.0	0.22
15	1.7	0.41	1.0	0.21
16	1.6	0.47	1.0	0.42
Total	-	12.08	-	5.75

With the new beam thicknesses, the total mass of the truss is 18.3 kg on mars and 12.0 kg on the moon if the mass of the gussets and bolts are included. Before reducing the mass and using all 9.80mm thick beams, Siemens NX calculated the beams to be 19.1 kg and total mass to be 25.3 kg. This indicates that this method reduced the mass of the beams by 36.6%, saving a total of 312.4 kg over the entire structure (44 trusses). To make sure these members were still capable of meeting the design requirements, the deflection of the support systems were tested. Deflection was the strictest constraint and if it was satisfied, the system would pass the other requirements. The deflection of the trusses are demonstrated below in Figures 65 and 66.

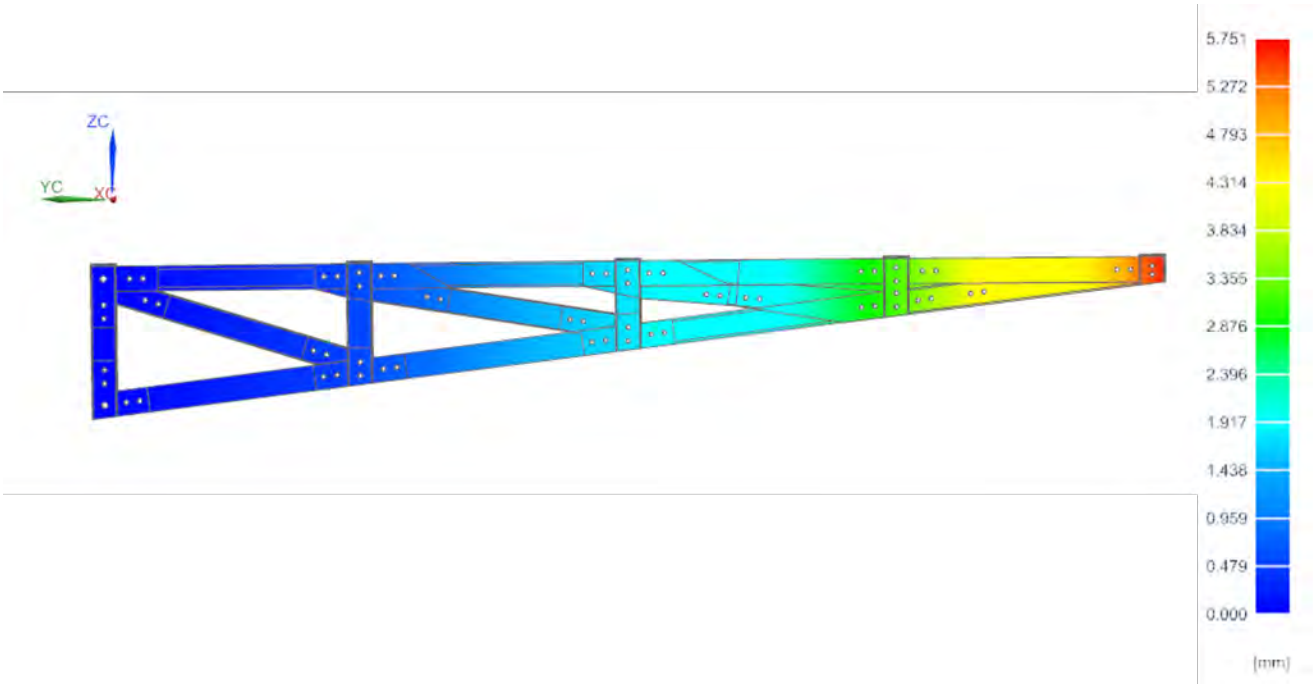

Figure 65: Displacement of the reduced truss model in Mars environment. The maximum displacement is 5.75mm and occurs at the tip

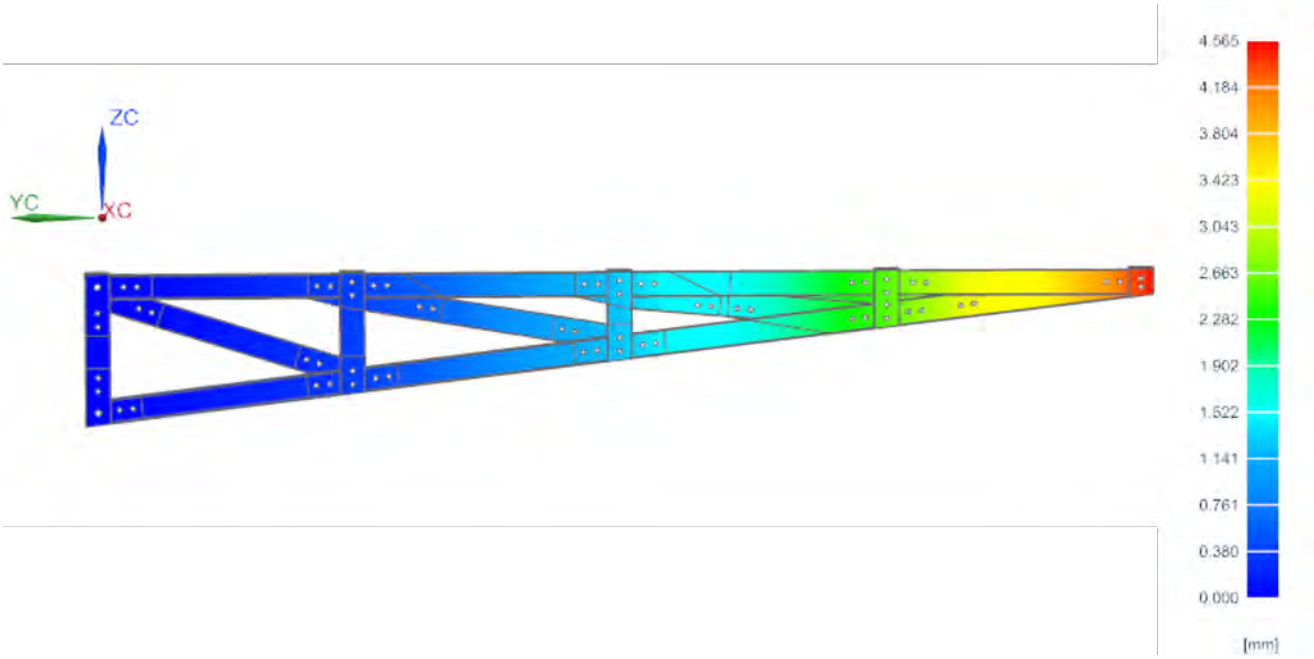

Figure 66: Displacement of the reduced truss model in lunar environment. The maximum displacement is 4.57mm and occurs at the tip

With a maximum deflection of 5.75mm and 4.57mm for the martian and lunar designs, they both fall under the requirement of having deflection less than 5.93mm. The margin of safety for the martian design is 0.03 and for the lunar design is 0.29. While these designs are improvements from previous iterations, they are modeled using the generic load case. The next step in improving the design and loading is found in the following section *Refined Loads and Current Truss Designs*.

9. Refined Loads and Current Truss Designs - Jack Saunders

After the layout of the interior become more understood, the loads on the floor support were able to more accurately predicted. Based on the interior design, the panel holding the most mass was in the exercise area of the third floor. One panel was required to hold the cycle ergometer and ARED which have a combined mass of 1380kg. The weight force of these objects acts approximately the half way point of the floor panel. In addition to the exercise equipment, the support structure must be capable of holding all 12 crew members during a surge period. Each inhabitant can have maximum mass of 95kg, for a total of 1140kg[80]. A safety factor of 2 was applied, consistent with the rest of the load estimations. It was determined that this would be the maximum load on any floor panel. Additionally, the floor panel weight was able to be reduced to 74.4 kg due the inclusion of honeycomb paneling (see section *Floor Panel Design and Analysis*). The updated weight breakdown for martian and lunar environments are as follows:

Updated Loads for Each Panel in Different Gravitational Environments		
Load (N)	Mars	Moon
Exercise Equipment	10270	4470
People	8480	3700
Panel	550	120
Total (N)	19300	8290

These updated loads indicate that the initial estimation was much lower than what the current interior design requires. With two trusses per floor panel, the load per truss is 9650 N on mars and 4145 N on the moon. When modeling the loads on the truss, the exercise equipment was treated as a point load at the halfway point and the load from the inhabitants was treated as a distributed rectangular load across the truss. This results in the following load cases on the truss:

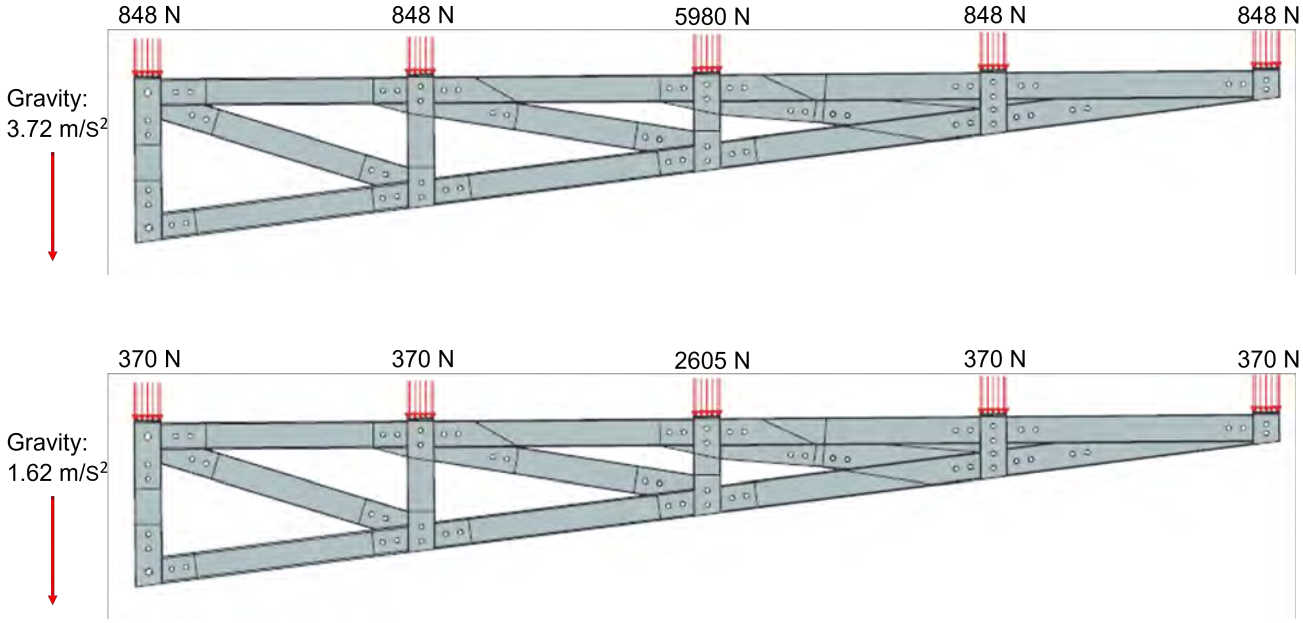

Figure 67: Top: Estimated loads on truss for Mars based on exercise equipment and crew. Bottom: Estimated loads for the moon

Since the martian load case drastically increased from the initial estimation, one of the beams was unable to provide the necessary support. Specifically, the size of beam 5 needed to be increased. This member is responsible for holding the reaction force of 33.6 kN. To successfully pin the truss to the core, a single steel bolt with a diameter 16.9 mm was needed. This required the beam to be expanded to 60 mm in width to maintain a distance of 1.25x the bolt diameter between the edge of the hole to the edge of the beam. The other beams were able maintain the 50 mm outer dimension. The beams in lunar gravity were able to keep the 50mm dimension as well. The gusset plates also needed to be resized to hold the larger loads. Since the max load approximately doubled, the thickness of the gussets did as well. Repeating the beam sizing technique described in *Mass Reduction of Truss Design* results in the current beam sizes for martian and lunar environments. The results are summarized below:

Mass and Thickness for All Members Under Updated Loads				
	Mars		Moon	
Beam	Thickness (mm)	Mass (kg)	Thickness (mm)	Mass (kg)
1	14.8	2.59	5.0	1.21
2	4.3	1.07	1.8	0.5
3	2.7	0.73	1.2	0.38
4	2.7	0.70	1.2	0.36
5*	17.1	3.67	7.5	1.63
6	15.4	2.87	5.2	1.29
7	4.4	1.07	1.8	0.50
8	2.8	0.43	1.2	0.19
9	1.0	0.17	1.0	0.17
10	1.0	0.14	1.0	0.14
11	1.0	0.1	1.0	0.1
12	1.0	0.07	1.0	0.07
13	1.0	0.04	1.0	0.04
14	5.1	1.13	2.1	0.49
15	8.4	1.60	3.3	0.71
16	1.4	0.45	1.0	0.42
Total	-	16.83	-	8.20

Table 15: *Note: beam 5 has an outer dimension of 60mm for martian gravity while the others have 50mm

The deflection of both designs was once again tested using finite element analysis in Siemens NX. The deflection results for the beams described in the table are as follows:

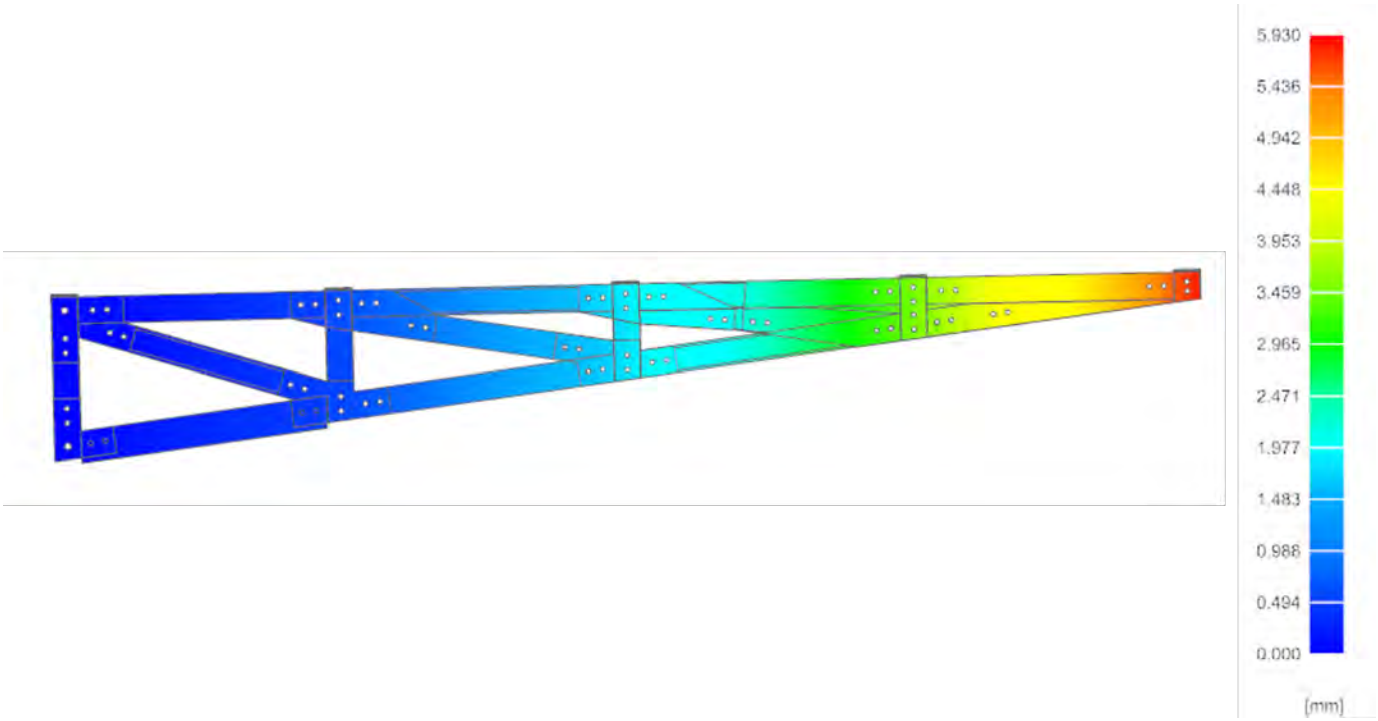

Figure 68: Displacement of the truss model in martian environment with updated loads based on the interior layout of the X-Hab. The maximum displacement is 5.93mm and occurs at the tip

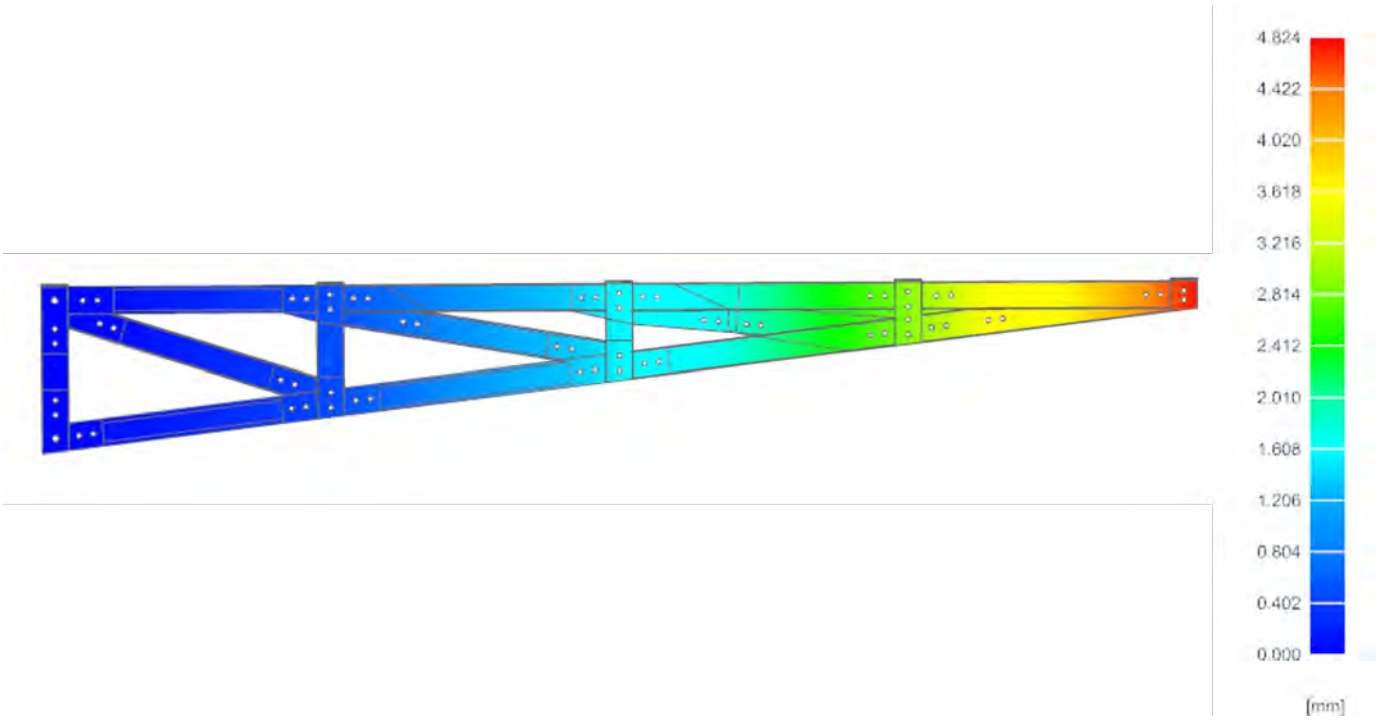

Figure 69: Displacement of the truss model in lunar environment with updated loads based on the interior layout of the X-Hab. The maximum displacement is 4.82mm and occurs at the tip

These thicknesses and masses of the beam members are most current design for the support structure. With the estimated gusset and bolt mass, the total martian truss mass is and the lunar truss mass is 14.4 kg. While these masses

are increased from the initial design, this is expected as the estimated loads increased by almost 2 times. The margins of safety are 0.0 and 0.23 respectively, indicating the martian design passes the deflection requirement perfectly. Moving forward, as the X-Hab layout, loads and requirements continue to change, this model should continue to be updated.

Current Mass Breakdown for Truss		
Support Part	Mars Mass (kg)	Moon Mass (kg)
Beams	16.8	8.2
Gussets	5.7	3.6
Bolts	3.6	2.6
Total	26.1	14.4

10. Micro-gravity Floor Support - Neal Shah

In addition to the gravitational environments, the floor support must also be designed for micro-gravity. For the floor support in micro- gravity we decided to use a simple cantilever beam instead of a truss structure. Our main reasoning for this is because the loads on the floor will not be as extreme as the loads in the mars and moon gravity environments. Based on this fact, using a cantilever beam instead of a truss will reduce launch weight by about 686kg. The location for for each of these support beams will be on the bottom of each floor panel where the seam of the main middle panel and panel flaps meet.

Figure 70: Micro-gravity floor support beam dimensions. Image on the right is the cross sectional dimensions of the beam. Image on the left is the length and height of the beam.

The main loads that the support structure will have to deal with in micro gravity are kick loads from astronauts pushing off from the surface of the floor to move around and vibration loads from the various equipment aboard the habitat. Based on these loads two simulations were run in Fusion 360. The first being a transient load case and the second being a vibration analysis. For the transient load case we applied a 1150 Newton impact load at the far end of the beam. This impact load was based on the average kick load force that an astronaut exerts in space. This transient load simulation yielded a beam deflection of 1.32mm. This deflection is well below the maximum deflection limit of 5.93mm. The vibration analysis revealed that the primary mode of the beam occurs at a frequency of 11.92Hz and at this primary mode there is minimal deflection. Based on the fact that the ISS has a vibration frequency of 0.1Hz - 5HZ at any given moment, this beam design passes the vibration simulation.

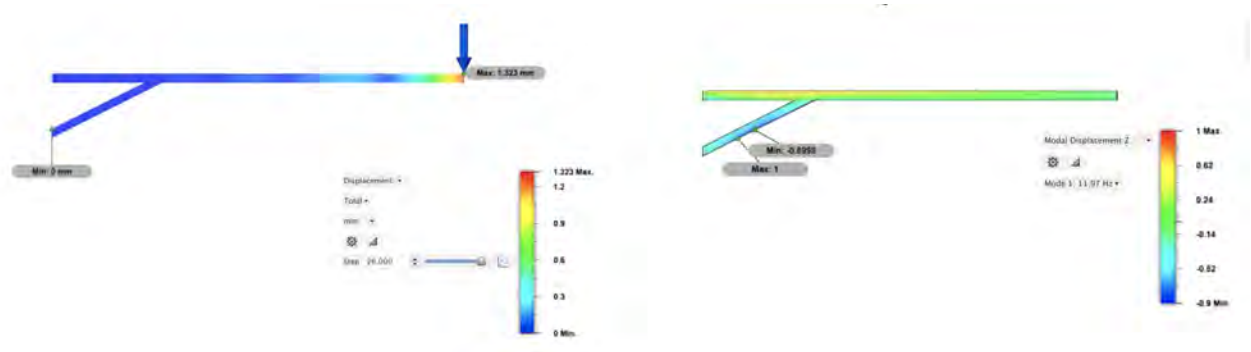

Figure 71: Image on the right shows the results from a vibration simulation run on the beam and image on the beam. Image on the left shows results results from a impact load simulation run on the beam.

11. Truss Deployment - Jack Saunders

The method for truss deployment method is similar to the floor panel deployment. When the floor panel is in an upright position, two trusses will be folded flush along the panel to minimize their extruding distance. This will help minimize the footprint of the X-Hab before it is inflated. The trusses are attached to the underside of the panel by damped hinges. As the floor panel is lowered into the position, the trusses will begin to unfold due to gravitational forces. The damped hinges will slowly lower the truss until it reaches its proper position. In this design, the two trusses will be positioned underneath the folding part of the floor panel. This allows direct support to both the main section and flap of the panels. After deployment, the truss is rigidly attached to the core with pins and the panel with bolts (see *Secure Connections for Truss Support section*). The position of the truss before and after deployment can be seen below in Figures 72 and 73.

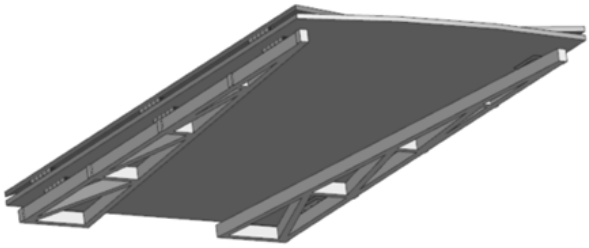

Figure 72: Position of truss before deployment. The trusses lays flush against the floor panel to reduce size of uninflated structure. (Created by Mason Hoene)

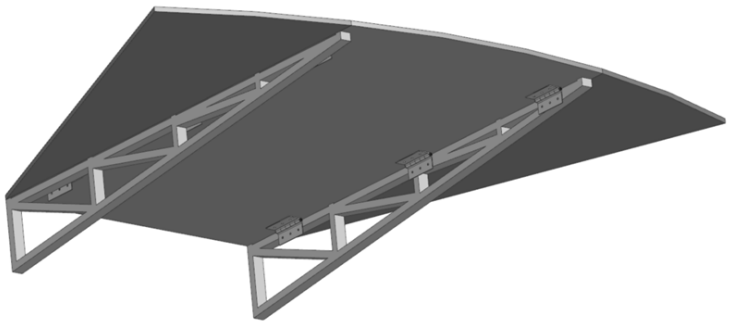

Figure 73: Position of truss when fully deployed. The trusses sit in between the hinged section of the floor panel, providing support to both. (Created by Mason Hoene)

12. Secure Connections for Truss Support - Logan Swaisgood, Jack Saunders

The vertical structural members of the core have been designed with flat faces to align the trusses that support the floor with the flat sides of the octagonal core panels. The vertical members of the truss are meant to be retained in an orientation perpendicular to the floor, such that the top of the floor panels in both micro gravity and lunar gravity align with the flooring of the core. The orientation and positioning of the trusses is shown in figure 74:

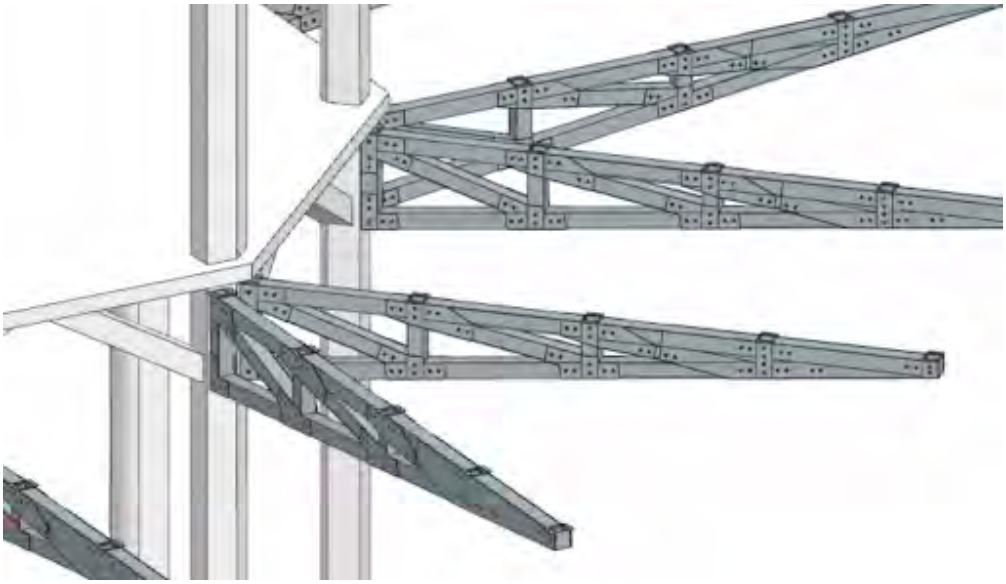

Figure 74: Placement of the fully deployed trusses aligned and flush with the vertical support members in the core

The trusses are retained to the core by two pinned connections. The first of these is a hinge, which connects to the top of the floor panel. The second pinned connection is meant to bear the maximum load acting on the truss. To simplify the architecture, this pinned connection is a shear bolt that slides into place autonomously as the shaft of a linear actuator, mounted to the core. As specified in the Refined Loads and Current Truss Designs section of this report, this shear bolt has a diameter of 16.9 mm. Note that this size was determined by anticipating the greatest reaction forces expected by the support structures. This retaining bolt will serve in both the lunar and microgravity configurations. A linear actuator was chosen to deploy this retaining bolt, because deploying and securing the floor and structural supports must be possible without human intervention. Small-scale linear actuators are ideal for this application because they occupy minimal space, and draw little power. Sample actuators that were available for purchase have a mass less than 100 grams, and are available in closed lengths around 6 inches. Some linear actuator models with a shaft that could serve as the shear bolt and retaining pin for the trusses only require a 12V power source, and draw less than 100 mA [81].

The housing of the actuators may be built into the vertical support members of the core, as shown in figure 75.

This housing will align the actuator and retaining pin with the its corresponding hole in the truss, and supports the loads that pass through the bolt. The retaining bolt is shown connecting the truss structure to the core in figure 76

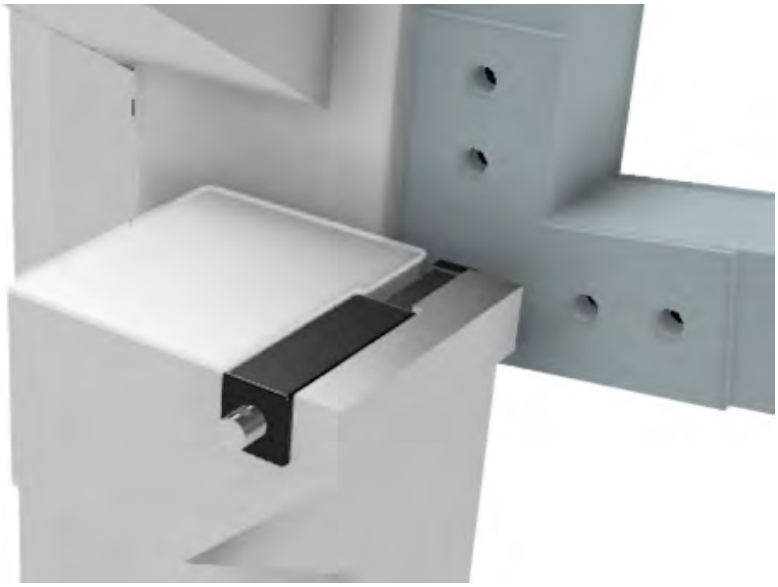

Figure 75: Structural housing for the retaining pin and linear actuator which support the trusses

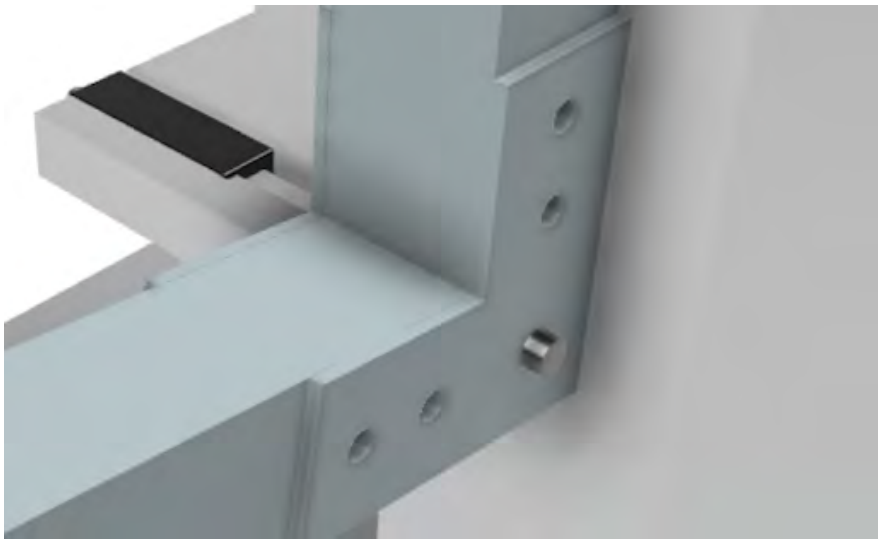

Figure 76: Configuration in which the linear actuator is extended, and the truss is retained by the shear bolt

Along with the connection to the core, the truss must also be rigidly attached to the floor panel. This is accomplished through the use of aluminum extensions off of the vertical truss members. Specifically, the extensions would branch off of the top of the member where the floor is flush with the truss. These extensions would contain threaded holes that would align with holes in the panels. This allows for the installation of bolts through the floor panel directly into the truss, without requiring access to the underside of the floor. Having the ability to complete installation from on top is necessary for the crew on the first floor, where there is no access to the underside. The extensions are depicted in Figures 77 and 78.

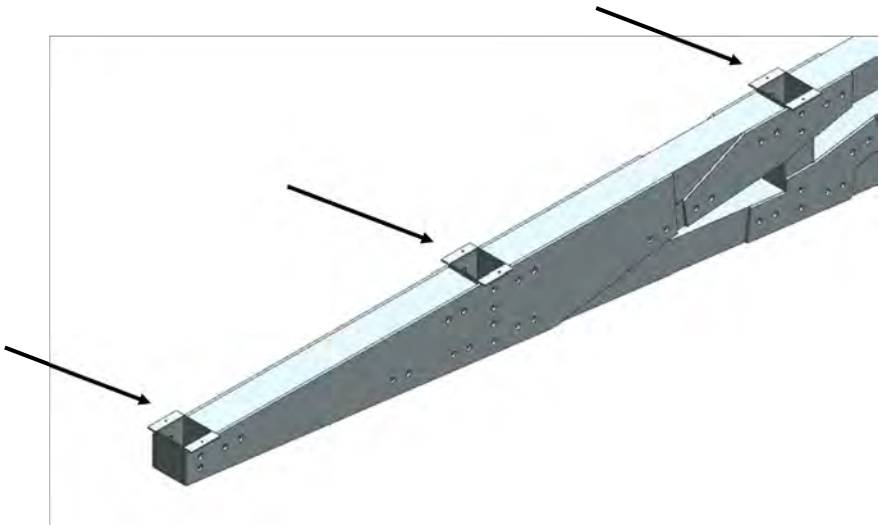

Figure 77: Vertical beams containing extensions for rigid floor connection

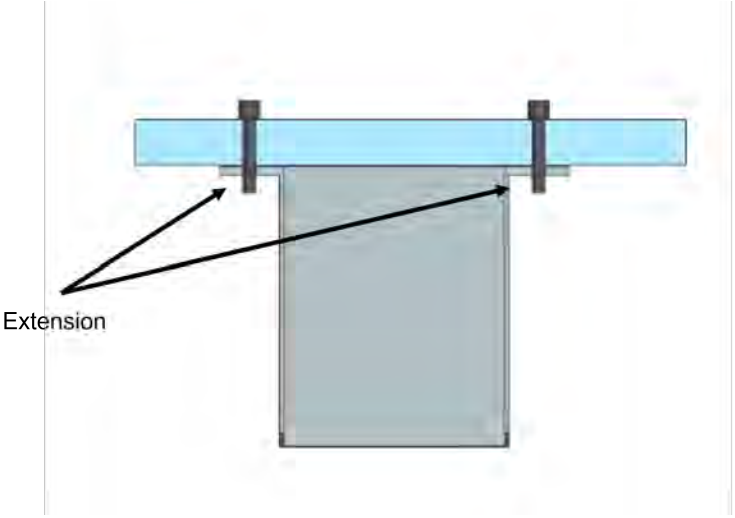

Figure 78: Beam and floor panel (blue) connected by bolts (black) and threaded aluminum extensions

E. Testing of Floor Panel Deployment

1. Floor Deployment Summary - Olivia Naylor

The floor panel deployment test for micro gravity was conducted on April 8, 2022 in the Neutral Buoyancy Research Facility at the University of Maryland. Similar to the testing of the deployment of key subsystems, this test allowed for the team to gain qualitative data. The overall test consisted of the floor panel being lowered into its deployed position and the securing of the truss to the rack. It was originally planned that the panel would be deployed using the mechanical winch system, and then the truss be secured into place by the test subjects. The back-up plan was to have test subjects manually deploy the floor panel.

It turned out that the constructed floor panel for testing was actually buoyant in the tank even though the PVC sheet was chosen due to the material's neutrally buoyant properties, so the mechanical winch system could not be used for deployment. To combat this issue, the second plan was used and the panel was lowered manually by the test subjects and weights were placed on top of it to keep it from returning to its upright position. The truss was then secured to a crossbeam attached to the bottom rack.

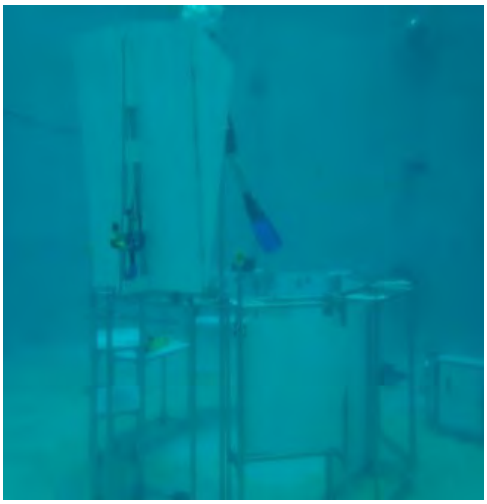

Figure 79: Images from the April 8 test of the floor panel deployment. The left image is the floor in its upright position and the right image is the deployed floor with the necessary weights on it.

Although the test did not go as originally planned, it provided useful information and feedback from test subjects that is being used to update the overall design. Based on the test, the team plans on using two trusses for each panel with one at each folding edge to allow more head space. Attachment panels will also be added to the connection points of the floor panel to allow for more support and decrease deflection, and the hinge bolts will be more staggered in placement so the panel can fold more completely. These changes would allow for a smoother process for future testing.

2. Floor Deployment Testing Initial Design - Mason Hoene

The initial floor deployment testing design aimed to utilize a configuration of 8 racks arranged in an octagon to represent one core floor of the TransHab. This configuration has been used previously in the Space Systems Laboratory Neutral Buoyancy Tank for dive testing. In order to test the deployment of floor panel, the goal of the testing was to create a floor panel that could be lowered and act as a ceiling above this 8 rack configuration. In order to accomplish this, our goal was to create a rack that could stack on top of this 8 rack configuration to allow for the deployment of one full scale floor panel. This testing design also included a truss to support the floor panel, hinges to to lower the panel and to unfold its wings, and a pulley system to lower the panel into place. An initial CAD model of this testing rig is shown in Figure 80.

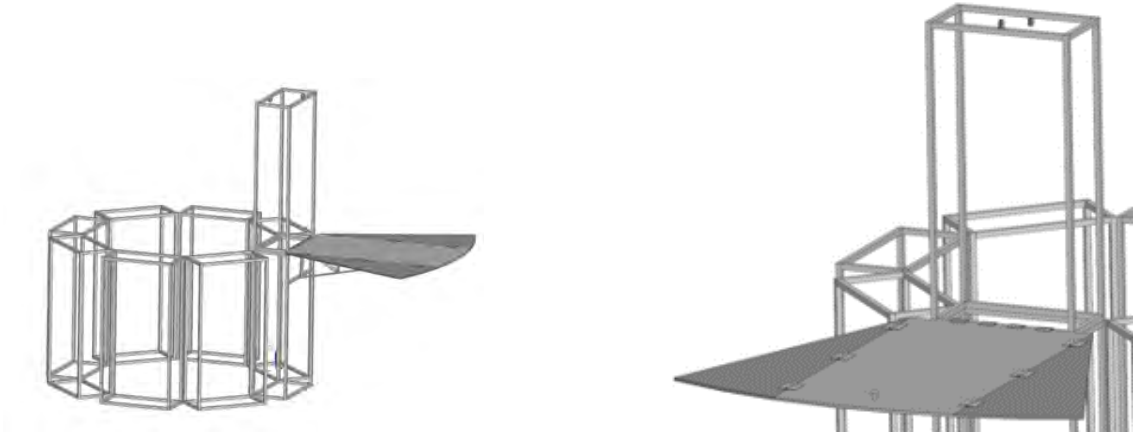

Figure 80: Images of the initial CAD design for testing of the floor panel deployment. (Created by Mason Hoene)

3. Floor Panel Construction - Mason Hoene

To model the overall floor deployment process, we created a full-scale test rig of one floor panel (of the eight floor panels on each floor). The goal for this testing rig was to give a proof of concept of our floor deployment process and gather some qualitative data about deflections and the effect on an astronaut's ability to move around. To create this testing rig, we first cut the floor panel sections out of 4' x 8' PVC sheets. Our design used a floor thickness of around 19 mm, to stay consistent with our design, we used 3/4" thick sheets. To support the floor panel, we created one large truss to span the length of the floor panel. This truss was made by cutting 80-20 beams to fit the dimensions of our designed truss. Gusset plates were then created out of the remaining PVC material and the truss was assembled before attaching to the center of the floor panel. Once the PVC sections were cut and the truss was attached, we then proceeded to connect these sections together using 4" x 1 1/2" steel hinges that had pre-drilled holes. Each panel flap connection was made with three hinges. After the flaps were connected to the middle panel section, we then attached the whole panel to the upper rack of the test rig with four 4" x 1 1/2" steel hinges. An image of this fully assembled floor panel and testing rig is shown in Figure 81.

Figure 81: Images of the floor deployment test rig with a full scale floor panel attached.

4. Test Rig Construction - Neal Shah

The test rig that our constructed floor panel attached to consists of two racks that connect by custom made catches. Both racks are made of 8020 and are 40" wide, 80" tall, and 20" deep. The connection of these two racks occurred in the neutral buoyancy tank as it would be too tall to connect on the deck. Before going into the tank, the upper rack was equipped with two pulleys on the top two bars. The main purpose of these pulleys were to simulate winch deployment. The bottom rack of the test rig was equipped with a crossbeam for the floor panel truss to rest on. Once the bottom rack of the test rig was complete we then had the divers implement it into the rack ring configuration in the neutral buoyancy tank. On testing day the top rack will be lowered on to the bottom rack and divers will close the catches to join both racks together. Figure 82 shows the top rack connected to the 8 rack configuration beneath it with the catches

during the first dive.

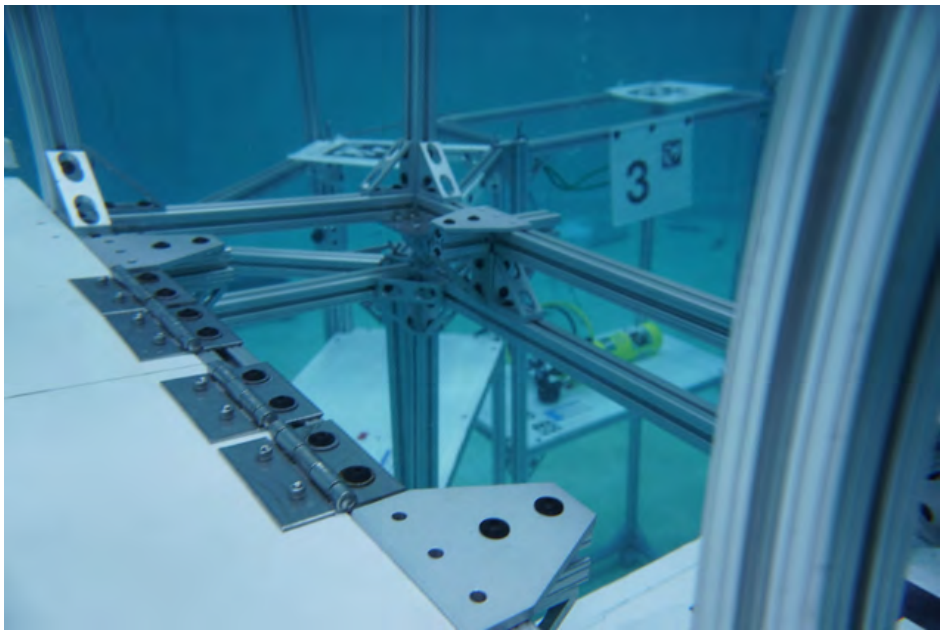

Figure 82: Image of catches connecting the top floor panel rack with the 8 rack configuration resting at the bottom of the Neutral Buoyancy Tank.

5. Floor Deployment Dives - Mason Hoene

The overall objective of our floor deployment testing was to provide a proof of concept for the mechanism, gather feedback from the divers about challenges during deployment, and to qualitatively determine deflections in the floor panel. To test the our floor deployment testing rig in different gravity environments, we utilized the Neutral Buoyancy Tank at the University of Maryland's Space System Laboratory. The goal for the first dive test was to connect a cable to the end of the floor panel and to the pulley system at the top of the testing rack in order to slowly lower the floor panel into place. However, upon beginning the dive we learned that the floor panel floated in the tank, so the pulley system was no longer necessary as the floor panel could be manually lowered due to its buoyancy after adding dive weights. Although the cable system was not tested, we were still able to successfully test the deployment of the floor panel and determine changes necessary to improve the testing rig as well as the design of the floor panel. An image of the floor panel being lowered during the dive is shown in Figure 83.

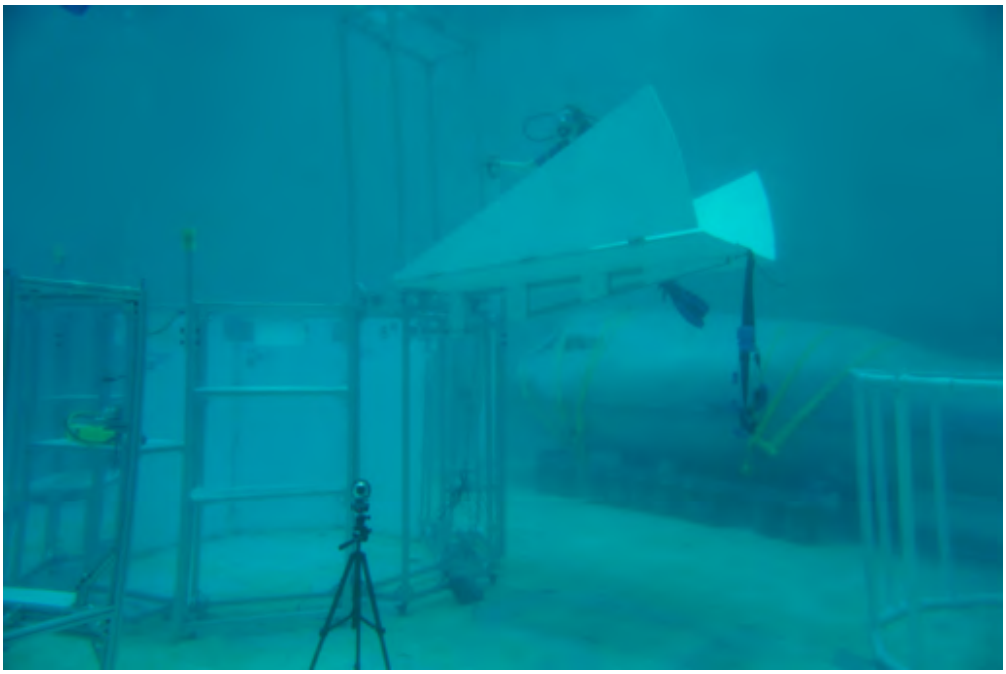

Figure 83: Image of first Neutral Buoyancy Tank dive for testing floor deployment.

After the first dive, we planned to improve the floor panel by adding weights directly to the floor panel to ensure that it did not stay afloat when placing in the tank. We also added handles to the bottom of the floor panel that could be used for divers to attach wires and piping to the floor during equipment testing. These additions to the floor panel are shown in Figure 84. By making these additions to our testing rig, we improved the fidelity of our equipment testing by allowing the divers to have an awareness of what living inside the XHab might be like and to experience moving equipment in and out of the core as well as connecting equipment to the floor panels.

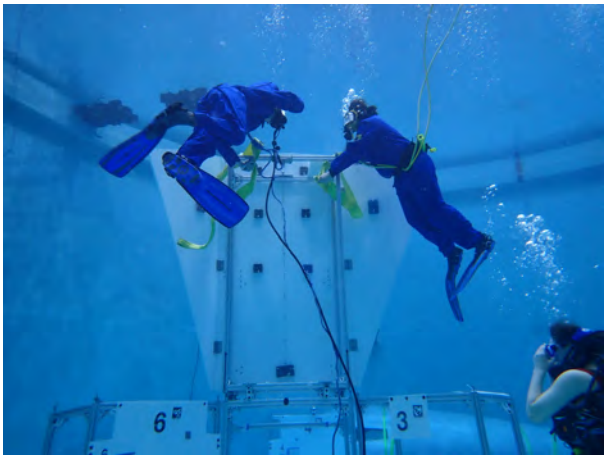

Figure 84: Images of handles and weights added to the floor panel in preparation for the second dive. The image on the right shows the testing rig being lowered into place after being properly weighted.

6. Floor Deployment Testing Lessons Learned - Mason Hoene

After completing two dive tests with our floor deployment testing rig, we utilized the information gathered to make improvements to the design of our system in addition to providing a proof of concept of our system. Based on feedback from the divers, we learned that having a single truss at the center of the floor panel obstructs moving into and out of the core. In order to remedy this, we altered our design by including two trusses, with one at each core pillar to minimize obstruction when moving in and out of the core. We also observed the most significant deflections at the tips of the floor panel wings. To improve this in our design, we included attachment panels between adjacent floor panels to minimize deflections at the edge of each floor panel. An additional issue that we faced was that the floor panel wings could not be closed completely. The main reason for this was that the hinge bolts on the two parts of the hinge were hitting each other because they were in alignment. Based on this, we decided to use hinges with staggered bolt holes to prevent contact between the two sets of bolts.

XI. Habitat Lunar Support

A. Lunar Support Base - Olivia Naylor

There is an additional requirement of a support base for the XHab on the lunar surface due to needed access to the EVA suitport area below the habitat. The EVA suitport section has a height of 2.5m and should sit 0.93m above the lunar surface; this allows for the lowest point of the inflatable bladder to be 3.0m above the surface. The design of the support base structure was completed with the objective that it would travel separately from the habitat because of mass budget constraints. This objective would include having the support base deploy itself on the lunar surface before the habitat arrives. The habitat would then insert itself into the support base as it finishes its arrival on the moon. The design and structural analysis of the support base are described in the following sections.

The team's requirements for the lunar support base were created on the idea that it needs to provide extra structural support to the habitat on the lunar surface and follow the dimensional constraints put in place by the Crew Systems sub-team. It should ultimately be able to withstand the lunar environment and the loads imposed onto it from the fully deployed habitat at worst-case conditions.

B. Lunar Support Base Design Methodology - Olivia Naylor

Upon doing research to begin the design of the lunar support base, the Apollo Lunar Module was observed because of its similar requirements. One of the main structural requirements of the Lunar Module is to have the ability to withstand the loads and conditions of the surrounding environment [82], and this is important for the lunar support base of the habitat also. The most applicable part to the habitat's lunar support base from the Lunar Module structural design is the landing gear. The landing gear on the Lunar Module was designed to meet the requirement of withstanding the environment, as well as be structural support to the Lunar Module while having energy absorbing capabilities. The landing gear of the Lunar Module also needed to have the ability to deploy itself on the moon's surface, which as previously stated is an important aspect to the habitat's lunar support base too. Figure 85 displays the landing gear design of the Lunar Module and its parts that are important to the deployment of the spacecraft.

Figure 85: Image of the design of the landing gear on the Lunar Module. Image is from the report on the Lunar Module landing gear[82]

The shape of the legs is the main design component from the Lunar Module landing gear that is seen in the design of the lunar support base for the habitat. Each leg section on the habitat's lunar support base features a similar pentagonal leg structure and round foot-pad with a lunar-surface sensing probe[82] to assist in its complete deployment on the moon. To fulfil the requirements necessary of the support base, some updates and changes were made that differ it from the landing gear on the Lunar Module that are detailed in the following subsection. Some main differences include the placement of the top members of the leg supports and the overall thickness of each of the legs.

C. Design of Lunar Support Base - Olivia Naylor, Kealy Murphy

The overall design of the lunar support base must be large enough for the EVA area to be secure, as well as have structures to keep the inflated bladder of the habitat supported. Due to this, the current design consists of a large octagonal structure with a cut-out in the center for the EVA suitport area to sit in. With the shape of the EVA area being octagonal, the hole in the center of the structure is that shape as well in order to provide necessary support to its sides. To allow for access to the EVA area, there is a section on the base that comes out as a ramp with folding connections that double as hand rails next to it. The design also utilizes three rectangular beams that come out of the octagonal structure for support of the lowest point of the inflatable bladder. The main base section, without the addition of the support legs is displayed in figure 86. The design of the support legs is shown in figure **??**. There will be three sets of those that attach to the base on the same sides as the three rectangular beams.

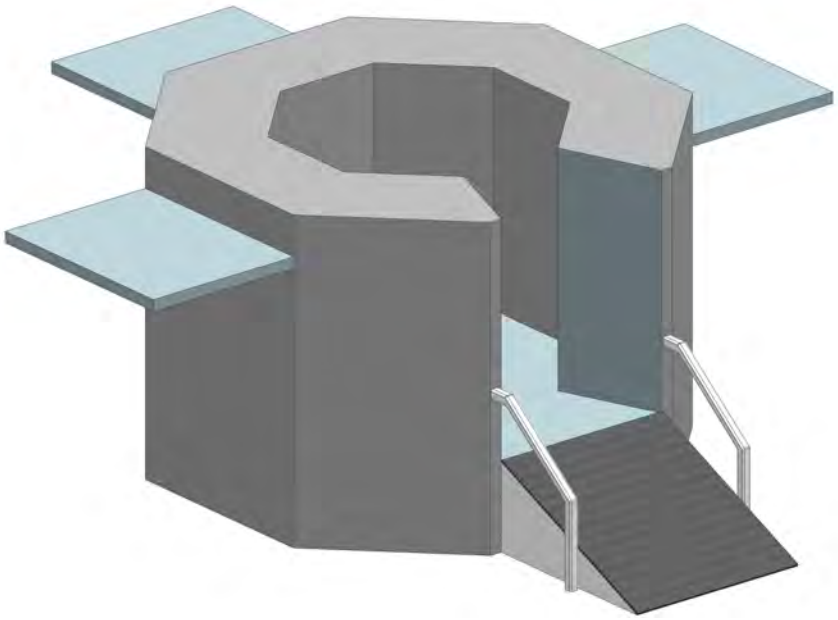

Figure 86: Overall design of the lunar support base without the legs.

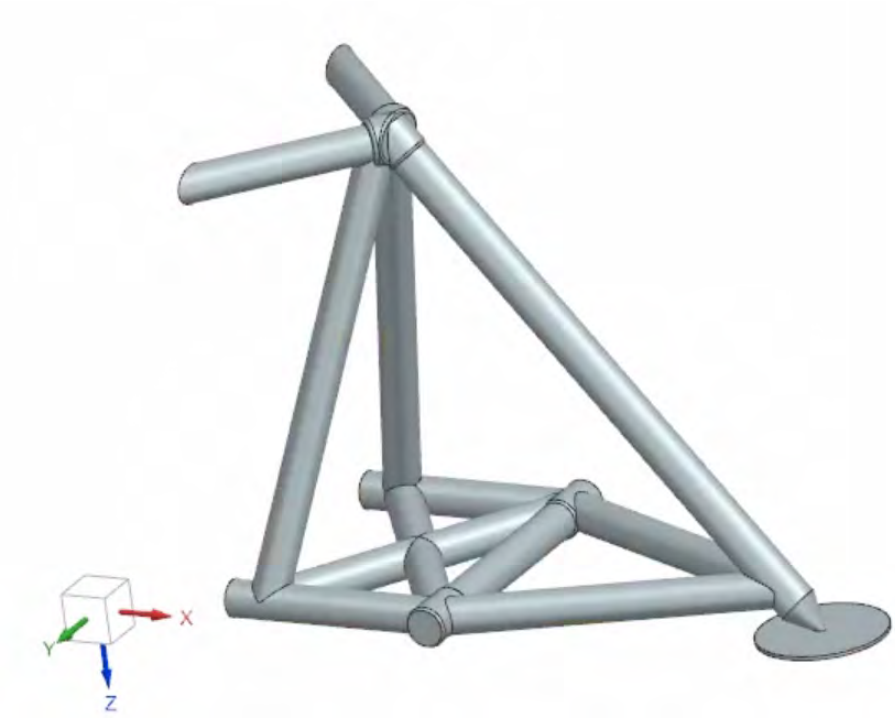

Figure 87: Design of the lateral base support based off of the landing gear on the Lunar Module as shown in Figure 85

D. Analysis of Lunar Support Base - Kealy Murphy

The model used for analysis of the lunar support base began with finding the overall center of mass of the habitat in each direction. The worst case scenario of the center of mass was used because if the habitat and support base can withstand loads in this case, then it theoretically is able to withstand them in any type of mass distribution situation. Using the center of mass as a guideline was selected because of everything that must be deployed from the core and

other items that will be moved around on the habitat. With this, the appropriate distribution of weight from the habitat for the worst case scenario was used to complete the structural analysis on the support base.

XII. Power Distribution - Alexander Cochran

Power distribution for the habitat is broken into three main parts. The first part is the power generation, conditioning, and storage. This portion of the system is responsible for getting power from where it is generated to where it can be properly conditioned and stored for habitat use. The next portion of the system is the primary power distribution. Primary power distribution delivers conditioned power to each of the habitats floors and isolates critical systems from the rest of the habitat loads. The last portion of the system is secondary power distribution, which distributes power to loads that are deployed throughout the inflatable volume. This portion of the system is deployed by the crew. Figure 88 is a diagram of the power distribution system. Blue blocks represent power conditioning and storage which are attached to the power generation system outside of the habitat. The red represents the primary distribution point, while the orange represents the secondary distribution points. Further details on the design of the power distribution system can be found in the Avionics appendix R.

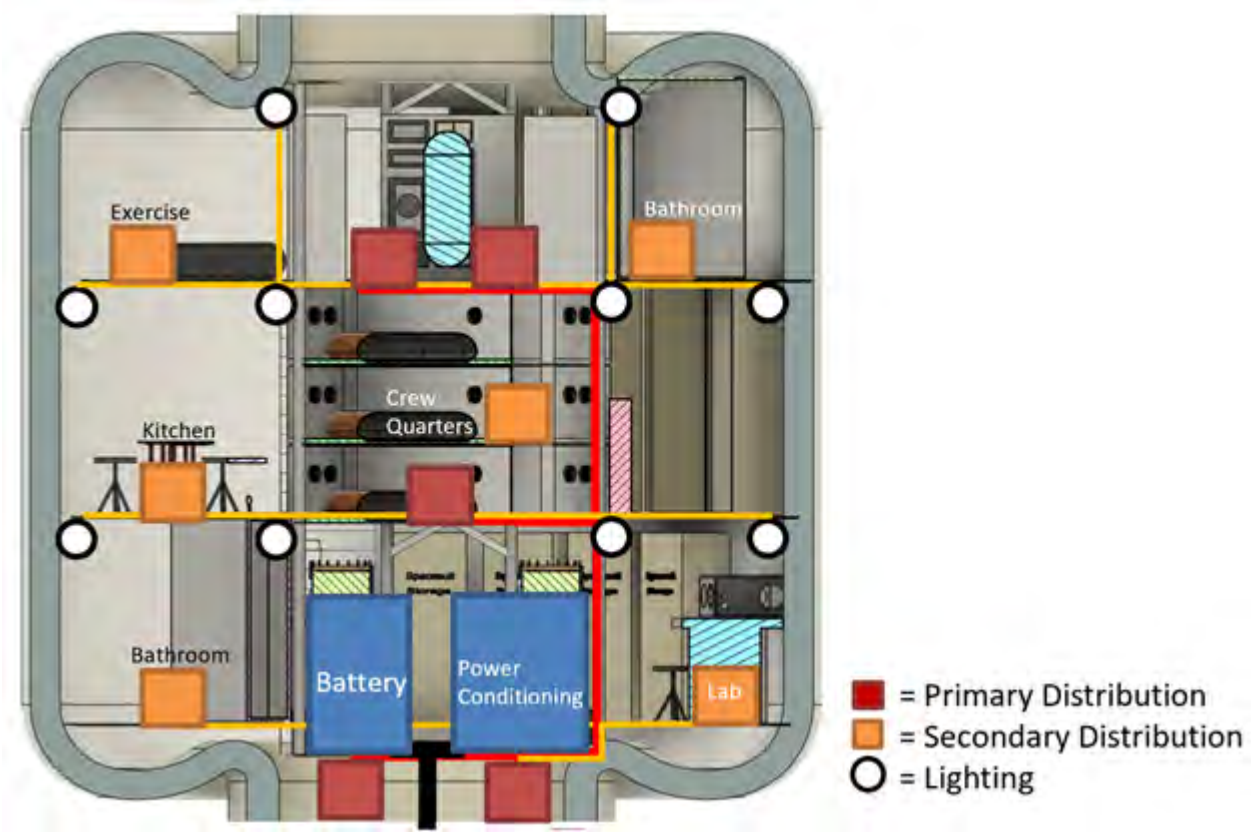

Figure 88: Power distribution diagram with representative placement of power conditioning, storage, and distribution hardware.

A. Power Generation and Conditioning

Once power is generated, it must be conditioned and stored. The power generation for the habitat is external. This is true whether solar or nuclear power generation is used. Wires are unable to be routed through the inflatable layer on the outside of the habitat, so the power must enter the habitat through the top or bottom of the rigid core. The wiring carrying the full 14-20 kW from power generation will be the highest gauge to minimize losses. Conditioning hardware will be necessary to ensure a constant 120 V DC is delivered throughout the habitat regardless of unavoidable variations in power generation. Smoothing out power spikes and drops will prevent any disruption of power or damage to habitat hardware. Since the system must function before and through deployment, associated hardware must be located in the core. The specific location of the hardware in the habitat has very little impact on system mass and complexity. As such, the power conditioning hardware is located at the bottom of the core with the atmospheric life support systems. The portion of the distribution from the top or bottom of the core to the power storage and conditioning hardware

will need to be properly insulated and marked as it could represent a significant safety risk. The wiring connecting the habitat to the nuclear power generation on the lunar surface will need to be attached by the crew following the habitat's landing. The distances required to maintain the safe operation of the reactor can introduce a significant form of loss to the overall power system. This voltage drop can be mitigated through the use of higher voltage for transmission or using a higher gauge or more cables. There are trade-offs in additional mass and losses from voltage conversion and higher mass transmission wires. Once power reaches the conditioning hardware, the power necessary for the habitat's function will be directed to primary power distribution while the remainder is used to charge the habitat's batteries. If there is a disruption in power generation or excess demand, power will be directed from the habitat's power storage to power distribution.

B. Primary Power Distribution

The primary power distribution system consists of all the critical distribution systems for the habitat. This includes the primary power control modules that distribute the required power to each level of the habitat. Each floor has at least one distribution point, while life support systems on each level have separate distribution modules to isolate the critical systems from the rest of the habitat loads. These distribution points and their associated wiring must all be integrated into the habitat before launch as they will be powering the habitat's critical system before deployment.

C. Secondary Power Distribution

Secondary distribution connects the habitat's primary power distribution system to the rest of the habitat's loads. This includes secondary distribution points for loads that are concentrated in different areas around the habitat. This includes the lab, kitchen, and exercise areas. These distribution points and the required wiring will be stored in the core during transit and installed by the crew during deployment. The rest of the secondary distribution system consists of the wiring from the primary and secondary distribution points to the habitat loads. This wiring will also need to be deployed by the crew.

D. Lighting

Lighting the interior of the habitat volume will be required for effective deployment. The wiring for a portion of the lighting system will therefore need to be integrated into the habitat before launch. There is adequate space on the exterior of the core structure and the bottom of the deployable floor to install the lighting for each level of the habitat. This lighting would be sufficient to provide the illumination required while deploying the habitat.

XIII. Lighting System - Alexander Cochran

The lighting system serves to provide adequate illumination for all habitat functions. Illuminance is the total power of light incident on a surface per unit area. The level of illumination required in different portions of the habitat depends on a few different factors. These factors include the schedule of the crew, the task the lighting is illuminating, and the internal layout of the habitat. The specific level of illumination required varies based on the task the lighting is for. For general tasks and illuminating walls and floor surfaces, less lighting is required. When performing technical tasks such as maintenance or health care the lighting requirements are more extreme. Lights inside the habitat will not always need to be at their highest illumination level. When crew members are not using or are not physically in that area of the habitat the lights in that portion can operate at a lower level or turn completely off.

A. Lighting Hardware

The lighting system in the habitat will use solid-state lighting fixtures. Solid-state lighting uses light-emitting diodes that provide a lower mass, power consumption, and heat generation than fluorescent lamps[83]. Solid-state lighting recently replaced the general lamp assemblies on the ISS because of these advantages as well as their longer life expectancy[83]. Solid-state lighting also allows for the control of each light's color temperature which provides benefits to the crew's restfulness and circadian rhythm[83]. The specific solid-state lamps we selected are RGB with a tunable white to take advantage of these benefits. We had initially selected lighting that provided the highest efficiency in terms of lumen per watt as opposed to optimizing for mass. The specification for both these fixtures are located in table 16[84]. However, these power-optimized fixtures have a reduced light output as measured in lumens. This means more fixtures are required for the same illumination requirements. A system with the power-optimized fixtures

would be 7% more power efficient and 44% more massive than one using the fixtures that are optimized for mass[84]. The overall savings in mass and volume for lighting as well as the additional wiring led to the mass optimized fixtures being selected for use in the habitat.

	Mass Optimized	Power Optimized
Light Output (Lumen/m)	1800	1250
Power (W/m)	47	30
Power Efficiency (Lumen/W)	39.3	42.3
Mass (kg)	0.41	0.41
Mass Efficiency (Lumen/kg)	4400	3050

Table 16: Lighting Hardware Specifications

B. Illumination Requirements

The illumination requirements used for the design of the habitat lighting system come from NASA human space flight standards[85]. This document provides an extensive list of minimum illumination levels for various tasks that the crew will be performing. The illumination levels in the NASA human space flight standards are measured at the task or 30 in above the floor[85]. Since these requirements represent minimums, the illuminated area was assumed to be the area of the floor or wall to simplify the analysis. Table 17 contains a complete table of the illumination levels for tasks used in this design broken down by habitat level. Night and emergency illumination levels are 22 and 32 lux respectively. The NASA standards provide a range of 54-108 lux for general task illumination. This general lighting level was taken to be 108 lux for the remainder of the analysis since this represents a more conservative minimum requirement.

	Lighting Purpose	Min. Illumination (lux)
Floor 1	Storage	108
	Bathroom	269
	First Aid	269
	EVA	269
	Workstation	323
Floor 2	Sleeping	54
	Storage	108
	Dining	269
	Food Prep	323
	Reading	323
Floor 3	Storage	108
	Life Support	269
	Bathroom	269
	Exercise	323

Table 17: Habitat Illumination Requirements by Level

C. Lighting Placement

As mentioned in the power distribution section, adequate lighting is critical for habitat deployment by the crew. As such, a significant portion of the habitat's lighting must be installed in the habitat before it is launched. These pre-installed lights will need to be connected to the primary power distribution and fully functional. Since we are unable to put any loads on the inflatable outer layer, the lighting system for the habitat must be installed as part of the core or deployable structure. Lighting the core portion of the habitat is not an issue. However, providing even lighting for critical tasks throughout the inflatable volume while only using lights installed on the core would be difficult. This

was solved by mounting preinstalled lighting to the bottoms of the deployable floor. Once the floor is fully deployed, these fixtures are centered over the habitat area and can be properly positioned to provide even lighting. On the top level, where there is no floor above, lighting will be mounted to the exterior of the core, with supplemental lighting deployed or installed at the edge of the floor. Ceiling mounted lighting will be evenly distributed to provide general illumination to the habitat, with additional task-specific lighting deployed in the form of lamps and additional fixtures deployed by the crew.

D. Lighting System Design

The design of the lighting system starts with the interior layout of the habitat as described in the interior design section. The amount of illumination required in the different spaces of the habitat is driven by the tasks the crew will be performing in that area. Based on the most intensive task that will be performed in that area and the surface area that will be used for that task, the number of lumens that need to be emitted in that area can be calculated. To calculate the surface area of the habitat that needs to be illuminated, the inflatable volume of the habitat was approximated as stacked cylinders as shown in figure 89a. Each floor has an approximate surface area of 200 m^2, for a total area of 590 m^2. The task-specific areas are derived from the internal design of the habitat and listed in the Avionics appendix Q. The location or these areas in the habitat and their illumination levels are represented in figure 89b by the different colors. These lighting requirements and the specification of the selected fixtures result in a total length, mass, and power consumption for the task lighting. Using the crew's schedule, the approximate time each area of the habitat will need to be illuminated and the illumination level can be determined. This gives a duty cycle for the habitat's lighting system that can be used to generate an effective power consumption. The iterative nature of the lighting analysis is expanded upon in the Avionics appendix Q. The final system accounts for the task lighting and crew schedule. The system includes 60 m of lighting with a mass of 80 kg and max power consumption of 2.6 kW. The effective power consumption averaged over the whole day is 1.5 kW.

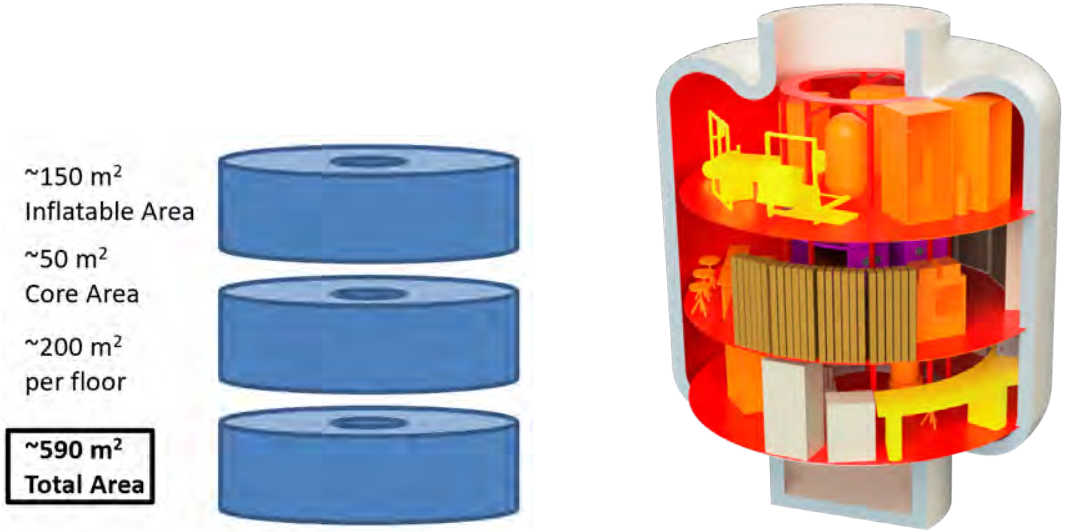

Figure 89: (**a**) On the left: The cylinder approximation of the habitat surface area. (**b**) On the right: The illumination levels throughout the habitat. Purple is a sleep illumination or 54 lux, red represents a general illumination of 108 lux, orange and illumination of 269 lux, and yellow an illumination of 323 lux.

E. Emergency Lighting

In the case of a system failure or power loss, habitat emergency lighting must provide adequate illumination to allow the crew to safely respond to the emergency. This system must turn on quickly once primary lighting has been lost and provide adequate illumination for the crew. A lighting level of 32 lux is required for emergency lighting according to NASA human spaceflight standards. For our habitat with an area of approximately 590 m2, this represents a power requirement of 480W. Lighting control systems to turn lights on and off may not be functioning, so this illumination requirement must be met throughout the entire habitat. If the power distribution system is still functional,

this power could be drawn from the habitat's batteries. Dedicated batteries connected to primary light fixtures could be used; however, depending on the length and criticality of the emergency, the power requirement may be prohibitive. Designing emergency lighting to lead crew members to emergency equipment, including battery-powered flashlights, could alleviate this issue. In the event of a complete power system failure, photoluminescent dots, similar to those used on the ISS will be used to meet emergency lighting requirements. An image of these dots on the ISS can be seen in figure 90[86]. Photoluminescent dots turn on instantly after primary lighting is lost, require no power, and

Figure 90: An example of photoluminescent dots used for emergency egress lighing on board the ISS.

can provide hours of adequate illumination when fully charged. These dots will be used to mark ledges, ladders, and entryways for crew safety. In microgravity, they can also be used to represent orientation to prevent the crew from getting disoriented. Photoluminescent dots that lead to emergency supplies with longer-term lighting solutions could remove the necessity for powered emergency lighting entirely. The emergency system must also serve to guide the crew to emergency egress. For the International Space Station, this requires leading crew to the docked Soyuz or other crew escape vehicle. Our habitat has different emergency egress plans depending on whether it is on a surface or operating in an orbital configuration. Orbital configurations will have the docked vehicle that the crew arrived on, similar to the ISS, that can act as a lifeboat. In this case, emergency lighting can lead the crew to that docked vehicle. There will not be a "lifeboat" docked to the habitat for surface configurations. Lighting in this case will lead the crew to EVA suits and the airlock. Crew members can then egress to the crew return vehicle that will be located close by.

XIV. Communication Design - Alexander Cochran

The communications systems enable the habitat to transmit data and telemetry to Earth, receive commands, interface with other spacecraft and connect internal portions of the habitat. Internally, the habitat will have full wireless network coverage. This network will be resilient to single node failures and crew repairable. Critical and non-critical systems will be isolated and accessible from separate crew interfaces placed throughout the habitat. Inter-vehicle communication will take place with docking spacecraft, relay satellites, and crew on EVA. Generated science data and telemetry will be sent through the ground communication system. This system is required to support HD video communication or video messaging as well as audio communication. Adequate bandwidth for both telemetry and communication with the ground will need to be provided. Ground uplink will allow for communication from the ground as well as commands to be sent to the habitat.

A. Communications Approach

In designing the communication network, we decided to consider only existing communications networks and technology. There are a few important new technologies for deep space communications that are currently in development. Delay tolerant communications networks and optical communication will have improved efficiency and performance compared to traditional RF communications networks. However, the implementation of these new technologies has not yet been finalized. The current relay systems and communications technology will be obsolete by the time this mission launches; however, they will represent a lower bound to communications performance. These

systems can be used to generate a representative power and mass budget for the habitats communications systems. Each habitat configuration represents a different communication environment. The orbital, lunar, and Martian habitats will all have to communicate at some point in the near-Earth environment during launch or transit. There are existing systems for high data rate communications such as the system onboard the ISS capable of 600 Mbps using the Tracking and Data Relay Satellite (TDRS) network. Since this operation is not unique to our design, we focused on the two other communication environments. The lunar and Martian environments are distinct. Current existing NASA network coverage is represented in figure 91[87]. At a lunar distance, there are multiple options for ground stations. The Deep Space Network (DSN) and Near Space Network (NSN) both have options for high-rate communications. The Deep Space Network's 34m diameter BWG antenna can provide up to 150 Mbps downlink at Ka-Band[88], while the 18 m diameter Lunar Exploration Ground Sites (LEGS) as a part of the Near Space Network can provide similar performance or higher performance[89]. There are also some other commercial options available at this distance. At Mars distance, only the Deep Space Network can provide high-rate communication. However, the greater distance will increase the power requirements for given data rates. A link budget analysis was used to quantify and compare the communication systems required for the two environments. A similar analysis was also used to design an emergency communications system.

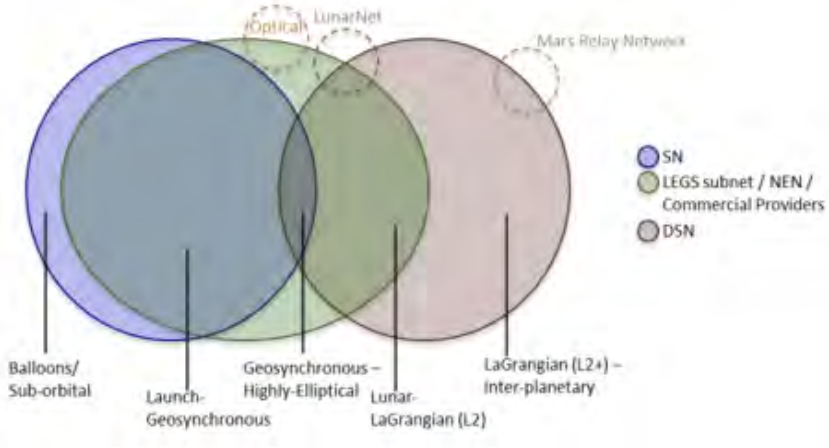

Figure 91: The current and planned coverage of NASA's communication networks.

B. Link Budget Analysis

A link budget accounts for all the power gains and losses in a communication system. The analysis mainly focuses on habitat to Earth downlink performance. Ground stations have fewer limitations in transmit power and the habitat has higher downlink requirements for science data and sensor telemetry. The downlink is therefore likely to fail first. The habitat transmitter was assumed to be a parabolic high gain antenna with an unknown diameter. Transmit powers of 10W and 100W were initially selected for the Moon and Mars respectively to get an idea of the performance of different power levels. A total of 1dB of loss at the transmitter due to pointing and circuits was assumed. The receivers we used were the DSN 34m BWG and NSN 18m Lunar Exploration Ground site. For the DSN, this is their smallest antenna, allowing for performance to be improved by arraying or larger receivers[88]. The NSN receiver is part of a not yet complete network that is representative of the anticipated network performance[89]. The receiver specifications used for this analysis are sourced from the DSN Telecommunications Link Design Handbook[88] and SCaN LEGS documentation[89]. The analysis was conducted as a worst-case communication link. By ensuring an adequate margin at the furthest distance possible, 406,000 km for the moon and 401 million km for Mars, with maximum atmospheric and planetary losses, performance would only be improved in other operating conditions. A minimum link margin of 3 dB at a BER of 10^{-5}, a standard for communication systems, was selected. This analysis was done considering an uncoded BPSK which would again allow encoding gains to represent an increase in performance. The initial analysis was conducted using MATLAB scripts, which can be found in the appendix. The second analysis for lunar and emergency communications was conducted using an AMSAT link model that is also detailed in the Avionics appendix

1. *Lunar Communication*

Initial analysis of the lunar communications system consisted of comparing the antenna sizes as a function of the required bitrate between the DSN and NSN. This was done at a transmit power of 10W for both networks. The maximum considered data rate was the 150 Mbps maximum of the Deep Space Network, though the LEGS are capable of higher bitrate. The results for DSN at S, X, and Ka-band are shown in figure 92. The higher frequency bands, X

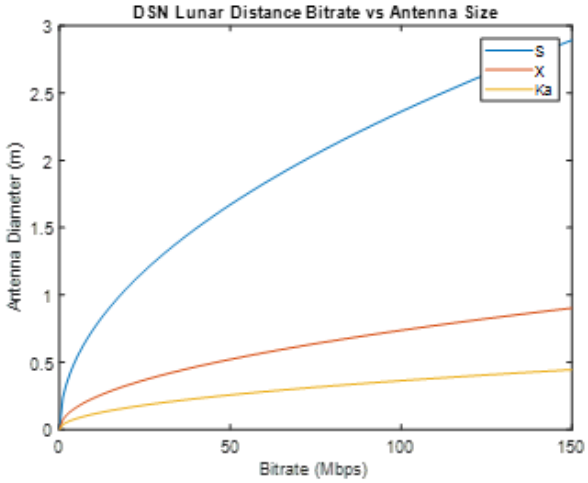

Figure 92: A plot showing the calculated antenna size for a given bitrate and 10 W of transmit power at the maximum Lunar distance for S, X, and Ka-bands.

and Ka, are widely used in space communications. Their higher frequency also means that smaller antennas can be used for a given data rate, which is preferred for lower mass and stowed volume. As such, only the X and Ka-band will be considered in further analysis. The comparison in performance of the DSN and NSN ground stations in the X and Ka-band is shown in figure 93. The NSN ground station's lower diameter means that a higher diameter transmit

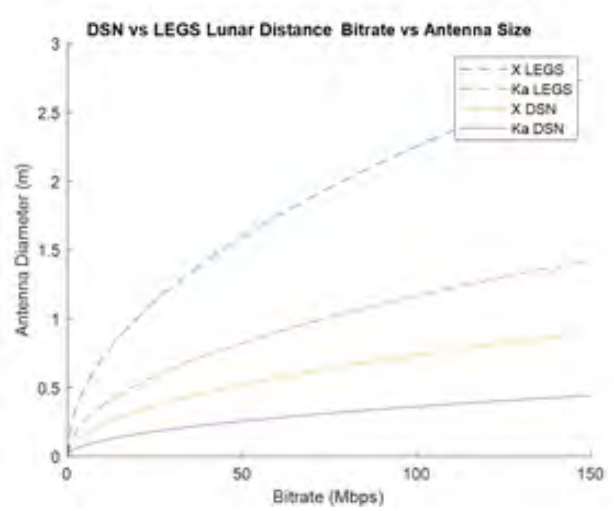

Figure 93: A plot comparing the calculated antenna size for the Deep Space Network (DSN) and Lunar Exploration Ground Sites (LEGS) for X and Ka-bands.

antenna is required for the same downlink bitrate at the same transmit power. For the DSN, the maximum Ka data rate of 150 Mbps can be achieved at 10 W with a 0.5 m diameter antenna. The NSN ground station requires a 1.5 m diameter antenna for the same performance at 10W or an increase in transmit power. Doubling the transmit power to 20 W requires only a 1 m diameter antenna for the same performance. Both ground stations represent viable options for lunar distance communications. A communications system with a wide range of transmit power could

alternate between them based on ground station availability. A higher fidelity AMSAT link model was used to design a lunar communications system for the 150 Mbps maximum data rate of the DSN. This was done to provide a system with maximum performance that could then be scaled down appropriately if extra bandwidth was not needed. The AMSAT model integrates encoding, point, polarization, and atmospheric losses. The losses calculated by the model will be more accurate to the operational link than the more theoretical losses calculated previously. A worst-case link budget was still investigated using the maximum lunar distance of 406,000 km. The Deep Space Network link used an encoding scheme of Conv. R=1/2, K=7, and Reed Solomon (255,223). This encoding scheme supports the network's highest bitrate. Values for receiver losses, such as line, waveguide, and system noise temperature were all sourced from the DSN Telecommunications Handbook for the 34 m BWG antenna[88]. By putting in representative values for the spacecraft that gave 2 dB of transmission line loss and a maximum of 2.3 dB of atmospheric loss. A communications system with a 0.7 m transmit antenna at a transmit power of 10 W was found to be able to robustly provide a 3 dB margin for pointing errors of order 1 degree. The 3dB link margin is maintained up to a 3 deg pointing error. Pointing errors could be caused by disturbances to the habitat or loss of attitude control. Maintaining communications performance without incredibly precise pointing control ensures more reliable communications links. The uplink budget was also calculated for the DSN maximum Ka-Band uplink speed of 40 Mbps. A margin of over 10 dB was calculated verifying the earlier assumption of the increased marginality of the downlink. To investigate the interoperability of this system with the Lunar Exploration Ground Sites, another AMSAT link budget analysis was conducted. The appropriate line, waveguide, and system noise temperature were all sourced from the SCaN LEGS documentation [89]. The same representative values for the spacecraft were used. The same encoding scheme was used for interoperability. At the same transmit power of 10 W, the resistance to pointing error decreased to the order of 0.1 deg. A 3 dB link margin is still maintained for up to a 0.5 deg pointing error. Tolerance to antenna pointing error could be improved by transmitting at a higher power level. Transmitting at 50 W would provide similar resistance to pointing errors as the DSN link. When communication pointing accuracy is high, the NSN and DSN ground stations can be used interchangeably with similar performance. The uplink link budget was also calculated for the LEGS at 40 Mbps at Ka-Band and found to be over 10 dB.

2. Martian Communication

The initial analysis of the Martian communication system consisted of comparing the required antenna size for a given bitrate at different transmit powers. Figure 94 contains a plot comparing DSN performance at X and Ka-band between 100 W and 200 W of transmit power at the Martian distance. In this case, a doubling of transmit power

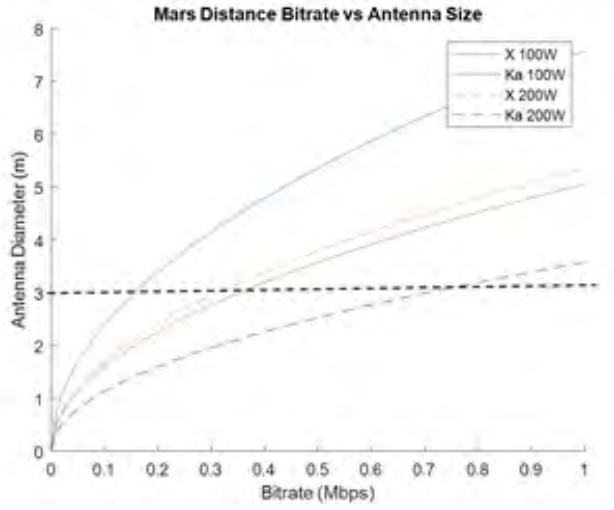

Figure 94: A plot of the calculated antenna size as a function of bitrate using the Deep Space Network (DSN) at Martian distance at a transmit power of 100 W and 200 W for X and Ka-bands.

correlates to a direct doubling of achievable bitrate for a given size antenna. The benefit of using a higher frequency can also be seen here, with Ka providing almost double the bitrate of the X band for a given antenna diameter. A 3 m diameter antenna was selected as a ceiling for the antenna diameter as beyond that size the size of the antenna is larger than the core and would be unwieldy to store and deploy attached to the habitat. This limitation could be lifted

by having the communications antenna deployed at a distance away from the habitat: however, this introduces added complexity in terms of structure and power distribution as well as introduces additional loss from longer lengths of wire. Communication with the habitat must also take place before deployment, so this limit was used. For a 3 m diameter antenna, a 3 m diameter antenna would be able to provide a maximum bitrate of 0.35 Mbps at 100 W and 0.7 Mbps at 100 W. This represents a significant decrease in communication performance compared to a lunar system with both orders of magnitude less mass and power consumption. To get a higher performance link, the power and antenna size would need to be scaled appropriately. Another link budget analysis was done to investigate the trade-off between antenna size and transmit power for a fixed data rate of 1 Mbps. Figure 95 shows the required antenna diameter for a 1 Mbps signal as a function of the transmit power for the X and Ka-band. Considering a 3 m diameter antenna as

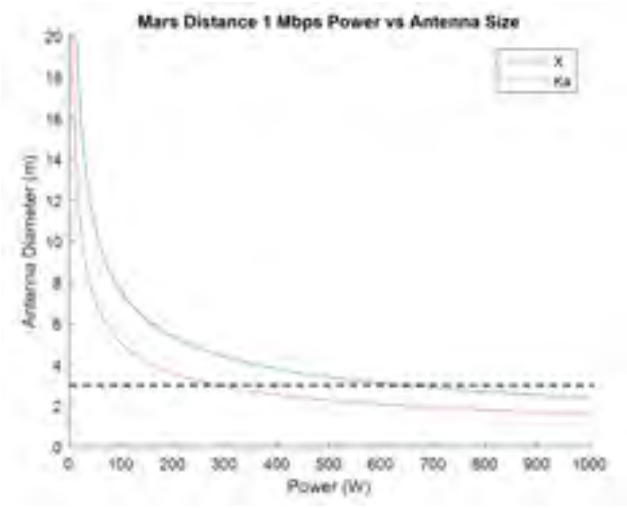

Figure 95: A plot showing the trade-off between antenna size and transmit power for a 1 Mbps signal on the Deep Space Network (DSN) for X and Ka-bands.

before gives a transmit power of approximately 300 W for Ka-band and 600 W for X band. The diminishing returns associated with using higher transmit power and antenna diameter place a significant limit on achievable performance. This is a worst-case link budget analysis, but it represents a bottleneck in communication that would affect the habitat for an extended length of time. Higher rate communications at Mars distance will require using the technological and network improvements that were not considered for this analysis.

C. Emergency

In case of an emergency, such as a loss of antenna pointing or damage to the main communications systems, the crew will still need to be able to communicate with the ground. Communication capability must be large enough for voice communication. Consultative Committee for Space Data Systems (CCSDS) G.711 standards require 64 kbps for two-way voice communication. Compression can reduce this to 8 kbps. The full 64 kbps will be considered the bitrate performance requirement for the emergency system. This would allow multiple voice communication channels open at once and for extra bandwidth to be used for transmitting sensor telemetry, which has a total bandwidth of 180 kbps. This performance will need to be attainable assuming the habitat has lost any pointing capability. Using the Deep Space Network's X Band capabilities would allow for a significant increase in transmit power, up to 17kW, to make up for pointing losses. Medium gain patch antennas were selected for habitat, because of their large beamwidth and their low weight and profile. To quantify the challenges an emergency communication system would face, the AMSAT link model was used to calculate a link budget. For surface configurations, the emergency communications antennas could be mounted facing the general position of Earth. For Mars, this would present a modest 3 dB increase in performance by decreasing the maximum possible pointing loss. On the lunar surface, the Earth stays essentially in one spot in the sky. A medium-gain antenna pointed in the direction of Earth would see only 1 dB of maximum pointing loss, allowing for very robust emergency communications. The most challenging communications environment would be a tumbling orbital habitat that had lost attitude control. Pointing losses will vary as the habitat rotates. By including two medium gain antennas on opposite sides of the habitat, a maximum pointing error of 180 degrees can be set. A pointing error of 180 degrees equates to an antenna pointing loss of 18.6 dB. This is what the system will be designed

around. Assuming the antennas are both 180 degrees out of alignment, the emergency communications system was still able to operate at 64 kbps up and down with a link margin of 20 dB and 3 dB respectively by increasing the habitat spacecraft power to 30 W. The performance could be improved by placing extra patch antennas. However, two antennas are adequate for the minimum performance. Actual performance would be better than what is calculated in this analysis as the antennas would be not always 180 degrees out of alignment.

D. Communication Hardware

To estimate the total mass and power consumption of the communications system, representative hardware was selected. The hardware sizing was done for a lunar environment as it is the most understood communications environment. The communication system has multiple antennas. The high gain antenna, a parabolic 0.7m diameter Ka-band antenna, must be pointed. A deployable 0.7 m Ka-band antenna and the required gimbals for pointing were found to weigh 7 kg and have a max power consumption of 12.5 W. The two X band medium gain patch antennas for the emergency communication system have a total mass of 1 kg, and no power requirement as they do not need to be pointed. The transmit power is provided by an amplifier, which has a maximum power consumption of 50 W to transmit at 30 W and a mass of 2 kg. An ultra-stable oscillator used for setting the transmission frequency has a mass of 2 kg and max power consumption of 8 W. The transponder, which encodes and decodes transmissions, was selected to be a software-defined radio with a mass of 8 kg and power consumption of 65 W. While this represents an increase in power consumption compared to a traditional transponder, it also allows one transponder to handle all the habitats communications, regardless of frequency. Overall, the communication system as designed has a mass of 25 kg, and a peak power consumption of about 150 W.

XV. Internal Networking - Benjamin Adarkwa

A. Data Network overview

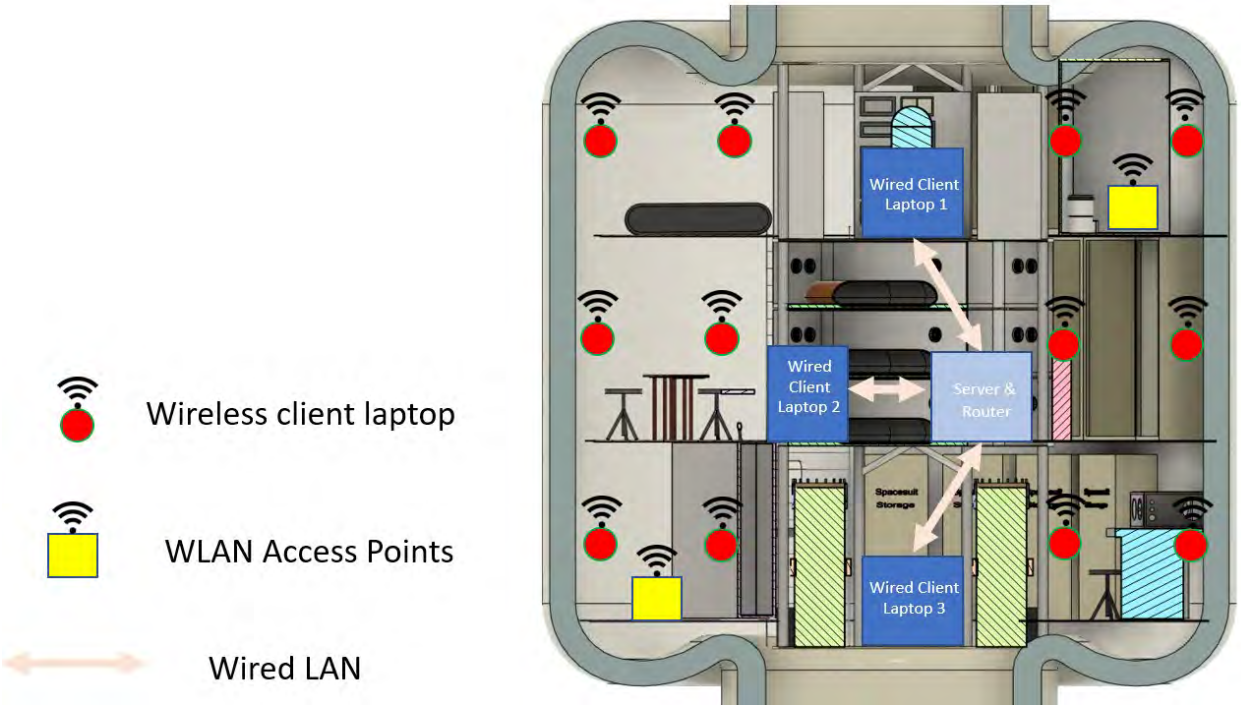

Figure 96: Data network overview

It will be a local area network (LAN) that is built with a hybrid framework. We would have both wired and wireless systems for our network. The wired LAN will connect the local file server, router, and three main client laptops, one on each level. The wireless part of our LAN will consist of two separate wireless access points so as to provide a redundant WLAN for the habitat. In addition to the three client laptops, ten client laptops will be deployed

throughout the habitat for crew use. There would six dedicated devices located in the crew quarters which wouldn't have the ability to interface with the habitat control computers. This is done so we can isolate critical systems in the habitat. All 16 client computers around the habitat will be connected to the WLAN. The WLAN would be built in accordance to the IEEE 802.11ax specifications. Our network's indoor transmission range is in greater than 50 m and a max data rate of 1.2 Gigabits per second[90]. The network will be using a star topology and has a total bandwidth of 80 megabits per second and a power consumption of 3.6 kilowatts.1 Habitat control will be a separate hard-wired network. Six laptops, two for each level, will act as control centers allowing for the crew to interface with and monitor habitat subsystems. This network will include all mission critical sensing and systems. The clients, file server, and router will all be interchangeable laptops to allow faults to be quickly and easily repaired The wireless sensor network consists of three Zigbee base stations and multiple routers that will interface with the habitat control network.

XVI. Sensor Network - Benjamin Adarkwa

A. Framework

One of the most important factors in safely operating and maintaining the inflatable habitat is the sensing system. The systems need some way of knowing important parameters values such as oxygen levels for example or orientation in space so as to process these values and infer if everything is running smoothly or there is something very wrong which needs to be corrected . The way to do this is through a comprehensive sensing system. There were two main choices when tackling the problem on how we want to design the framework of our sensor network.It was a choice between whether wireless or wired framework. The wireless framework would be in the form of a wireless sensor network with sensors in nodes that would communicate wirelessly therefore eliminating the need for any wires. The wired framework, which is more common would require us to physically hardwire all our sensors throughout the habitat and all communication would be over wire like ethernet for example. In order to make the best choice that would fit the needs of the inflatable habitat the advantages of both wired and wireless were taken into account along with their disadvantages that can be found in the appendix

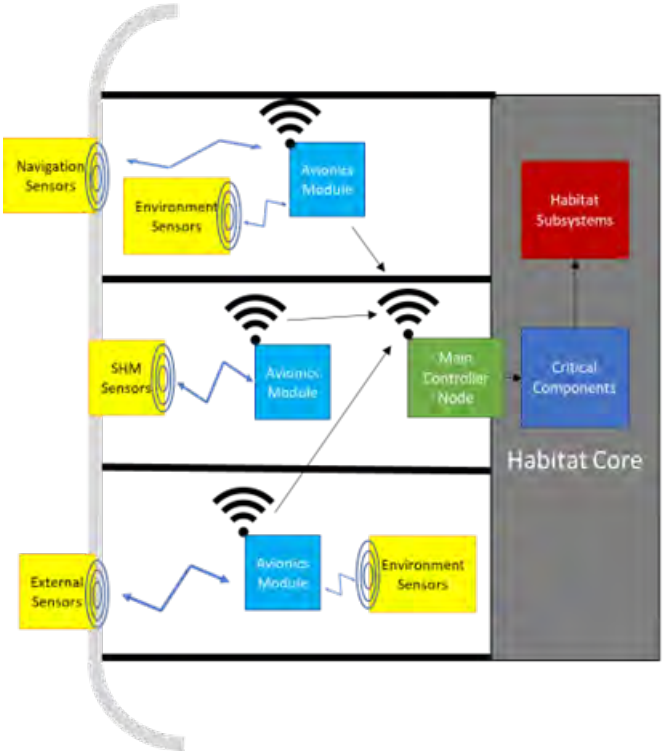

Figure 97: wsn:overview

The sensor network will make use of a hybrid framework so as to benefit from the advantages of both the wired and wireless systems. This network would have a relatively heavy reliance on the wireless framework because the

advantages outweigh the disadvantages talked about in appendix There have been several technological advances in wireless communications which keep making them more reliable and faster. The advantages give it a promising future with expandable applications when compared to wired. There have been successfully applications of a wireless sensor networks in space specifically the German DLR wise-Net on the ISS further proving space readiness of this technology[**dlrarticle**]. The wired framework is also important to our sensor network due to the delicate nature of some critical operations like life support. Wired networks have less latency and are faster than wireless which makes them ideal for systems that have little to no room for error (critical systems). The life support system is a prime example, a delay in a sensor reading could be detrimental to the mission and safety of the crew. It also makes it ideal for backup systems since they have been used several times and longer than wireless networks which has proved their reliability. The main plan was to have the critical and backup systems which use the wired network in the core and while the wireless sensor network would be responsible for the inflatable volume. This hybrid framework as the foundation of our sensor network helped us reach our goal of a comprehensive sensor network with redundancy within wireless network and the wired network also serving as redundancy and reliability.

B. Topology

The next step was to determine best topology for our wireless sensor network. After a lot of literature review on wireless networks and topologies there were two main topologies which emerged that were suitable for our purposes: mesh topology and star topology also known as the wheel and spoke. The picture above shows an overview of both the

Figure 98: Star vs Mesh topology.[91]

star and mesh topology. The star topology is the on the leftmost side and depicted by the picture it connects all of the nodes to a central node called the star coupler. It connects to all the other nodes through a several dedicated full duplex links which allow communication between the node and the star coupler hence the number of links in this topology equals the number of nodes. The nodes in the star topology don't communicate directly to each other but rather the star coupler acts as a mediator and frame-switch device. If a node needs to communicate to another node, they will have to send the data to the star coupler and then the coupler would buffer the arriving frame and retransmit to the intended destination node. The rightmost side of the picture depicts the mesh topology as shown each node is connected to every other node through full duplex point-to point links. This makes the number of links in the topology equal to N*(N-1)/2, where N is equal to the number of nodes. Communication between nodes in this topology does not require a mediator as nodes have direct links to every node, nodes can also act as relays/repeaters and relay information to a nearby node. Both topologies have their strengths and weaknesses which have been summarized in the in appendix N

In addition to their advantages and disadvantages we considered power consumption of both topologies and overall cost in our trade study. Mass was not looked at because topology deals with the physical and logical arrangement of nodes in a network, hence the mass would not be affected.

$$P = aN^3 + bN^2 + cN + d \tag{2}$$

The power consumption for topologies was approximated as third order polynomial under the following assumptions that both topologies[**bounds**]

1. Use the bypass/non-bypass approach
2. Have the same traffic demand
3. Have some sleep and energy efficient protection

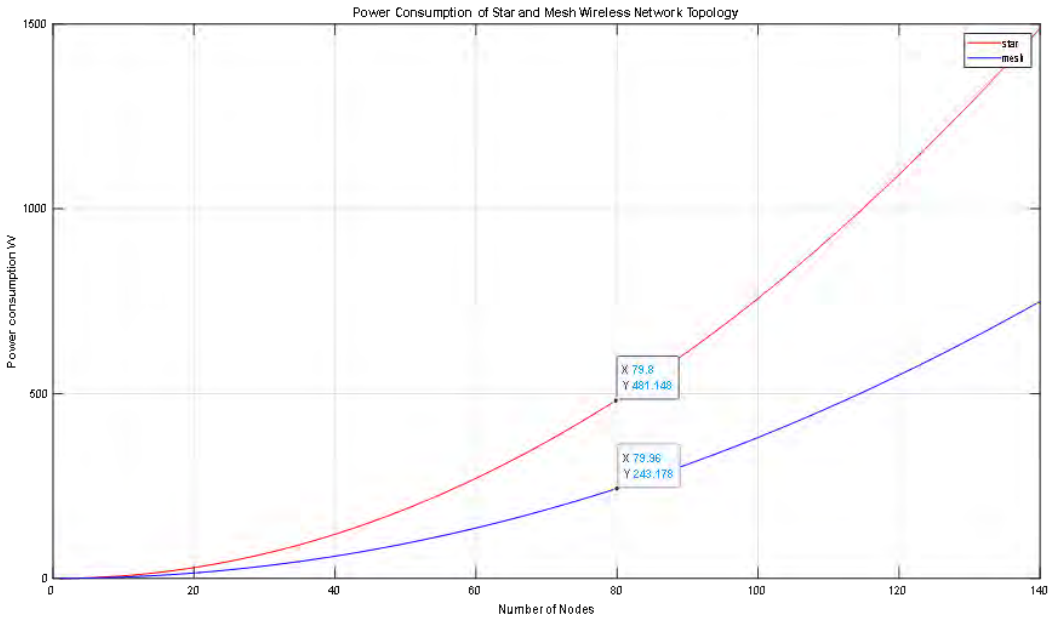

Figure 99: A plot comparing the power consumption of the Star and Mesh topology.

The results from the power consumption comparison show that the mesh topology has a close but lower power consumption to the star topology. As the network gets scaled up and number of nodes increase the difference is very apparent and this is because the b and c coefficients in the power consumption equation are higher in the star topology hence increasing the star topology's power consumptions. After careful consideration we decided to have a mesh topology for our network based on power consumption, scalability, redundancy, and complexity. The redundancy and robustness of the mesh topology is the main advantage since the sensor network is very vital and needs to be as robust as possible. The scalability and power consumption make mesh more suitable when it comes to any future work and expansion of the wireless sensor network for the inflatable habitat. It is important to note that the mesh is not the perfect answer since it has cons the main one being latency issues and the complex nature. As mentioned earlier our sensor system is a hybrid one consisting of a wired network and although the wireless network is bigger than the wired, any sensing that requires high speed sensor readings are classified as critical systems and as such would be on the wired network. The latency levels are acceptable for majority of our non-critical systems and its complex nature is with respect to the star topology which is a very simple topology. Therefore, the pros of the mesh topology far outweigh the cons in retrospect of our project.

C. Sensor Node Design

Every sensor node in the wireless sensor network is made up of four main units[92]: The sensing unit, processing unit, communication unit , reference clock, and a power management unit. The sensing unit consist of all the various sensors and analog to digital converters that digitize the analog signals produced by the sensors which are then sent to the processing unit. The processing unit consist of the microcontroller with short term storage and is responsible for controlling the functionality of the node. The communication unit consist of the omnidirectional transceiver which would wirelessly transmit data of radio and lastly the power management unit deals with power supply to the node. The sensor nodes we are using have very limited computing capacity, the sensing unit consumes very little power,

Figure 100: Four main parts of the sensor node.[92]

and bulk of the power goes into data communication. With such a low power consumption this opens up interesting power management strategies. The main ones we looked were energy harvesting through: micromechanical electromechanical(MEMS) devices and ambient lighting. We couldn't find a way to simulate the mechanical stresses or vibrations that the sensor node would face so MEMS was out of the question. For ambient lighting, we used the lowest general illumination in the habitat which was 54 lux as a baseline[85]. The indoor photovoltaic(IPV) cell has a power generation of at least $1.89*10^{-6}$ Wcm^{-2}[**indoor**].

D. Habitat Sensing

The habitat's sensing was broken down into four main groups: Environmental monitoring, Structural health monitoring, Navigation and Specialty. Environmental monitoring has to do with cabin atmospheric parameters like pressure , temperature, humidity, air composition for example. Structural health monitoring covers micrometeor and orbital debris detection, and leak detection. For navigation we are concern with inertial measurement units and lastly for specialty sensors we are talking about sub teams specific sensors like solar array actuators for the power propulsion and thermal team for example. There is a comprehensive list of sensors for each of the four main categories that can be found in appendix AV. Developing sensing requirements to establish baseline performance benchmarks is very essential since that provides key metrics for the sensor network such as sensor resolution, update rates, total bandwidth, mass, and power budget for sensing. To do this, we took our comprehensive sensor list Kand went "catalog" shopping to essentially find analogous sensors. However, we ran into a lot of difficulties finding analogous sensors, their update rates and resolution. So, we decided to classify all of our sensors according to what we thought their criticality was. Along with that was the order of magnitude approximation of "time to disaster" in seconds. A snippet of our sensing criticality is shown below. This way we could gather all of our data and pick a sensor with the highest criticality and "amount of information found" combination.

Structure Health Monitoring	Criticality	"Time to Disaster" (s)
Wall Temperature	Low	10000
Restraint Layer Accelerometer (MMOD)	Medium	10000
Leak Detection (Ultrasonic)	High	10000
Humidity Sensors (Bladder)	Low	10000
Strain Sensing (Separate from MMOD)	Medium	1000
Radiation Sensors (Solar Weather)	High	1000

Figure 101: Excerpt from the sensor criticality spreadsheet part 1.

Equivalent Sensor	Mass (grams)	Dimensions (mm)	Volume(mm^3)	Power(W)	Voltage	Current(Amps)
TMP461-SP	1.29	7*6*3	126	0.001	3.3	35*10^-6
SDI Model 1527	0.68	9*9*3	243	0.032	5	0.0065
SPU0410LR5H-QB	2.6	4*3*1	12	0.00022	1.8	0.00012

Figure 102: Excerpt from the sensor criticality spreadsheet part 2.

1. Wireless coverage

The wireless coverage of our sensing system was approximated through the disk method. The disk method makes a lot of simplifying assumptions like[93]:

1. Ignoring shadowing and multipath fading
2. Uniform sensing ability of sensor in all directions

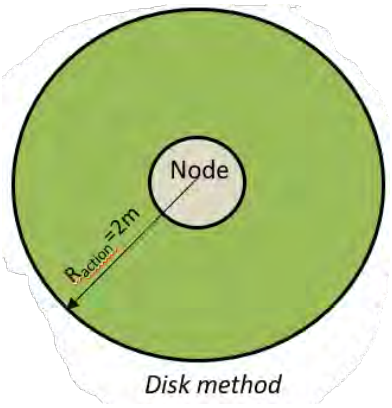

Figure 103: Excerpt from the sensor criticality spreadsheet part 2.

The sensing radius was based on the average radius of action for temperature controlled environments which was around 2 m[2].Based on this each node covers approximately 12.6 m^2 and there is about 58.6 m^2 of surface area per floor. After finding the sensing area of one node it allowed us to find the number of required nodes for the habitat. We

did that through a probability analysis under the rationale that a sensor can only sense the environment and detect the event within its sensing rangeA target is said to be covered if it is within the sensing area of a sensor. The probability of target detection(P_d) by arbitrary sensor is defined as the ratio of sensing area to network area in our case P_d=0.215. The probability of target detection by at least one node on a floor (P_c)=1-(1-P_d))^N, where N is the number of nodes. With a P_c of 0.9 we would need 10 nodes per floor. This puts the total number of nodes for the habitat at 30 nodes.

2. Mass, Power and Bandwidth

With the total number of sensor nodes known we can approximate the mass of each sensor node. Each sensor node is approximately 50 grams which includes a 20 gram margin this brings the total mass of sensor nodes to about 1.5 kg. The power consumption for each node was around 0.3 watts which includes a 0.1 watts margin bringing the total power consumption of the sensor nodes to about 9 watts. The assumptions used in calculating the power consumption were: no low power mode configurations, each node is always transmitting or receiving hence no idle time and lastly the microcontroller is operating on the highest clock frequency. These assumptions are on the extreme end and were chosen for the reason of getting a conservative upper bound. But also, there was not a lot of information on all the sensors that would be in the actual node so, we approximated the sensing unit of the node as two times the parameters for the sensor with highest criticality and "amount of information found" combination. The sensing unit in each node has an update rate of 364 measurements per second and approximately 16 Bits per measurement. This gives each node a data rate of about 6 Kilobits per second. With 30 nodes in the habitat this brings the bandwidth of the sensor nodes to about 180 Kilobits per second.

3. Sensing network standard

Figure 104: WSN:standard.

Our wireless sensor network would be setup according to the IEEE 802.15.4 standards. It will be a wireless local area network with a transmission range in the tens of meters and a maximum data rate of 250 Kilobits per second. A special kind of medium access control(MAC) will be used known MESHMAC.MESHMAC makes use of the a distributed beacon scheduling which enables the mesh network over IEEE 802.15.4[**muthukumaran˙de**]. The direct sequence spread spectrum(DSSS) transmission protocol will used to primarily reduce overall signal interference. There will be three base stations with one base station a the main which will be on the middle floor and the other two as backup which will be on the top and bottom floors. With our network transmission range in the tens of meters each node should be more than capable of communicating which any of the base stations.Although this might bring up some latency concerns with nodes having to communicate over a further distance if the main base station goes down,it is a much better than the alternative to not having redundant base stations and losing the wireless sensing network. Our wireless mesh sensor network will make use of a mesh portal which will serve as the gateway between the it and the internal wired data LAN for habitat control purposes.

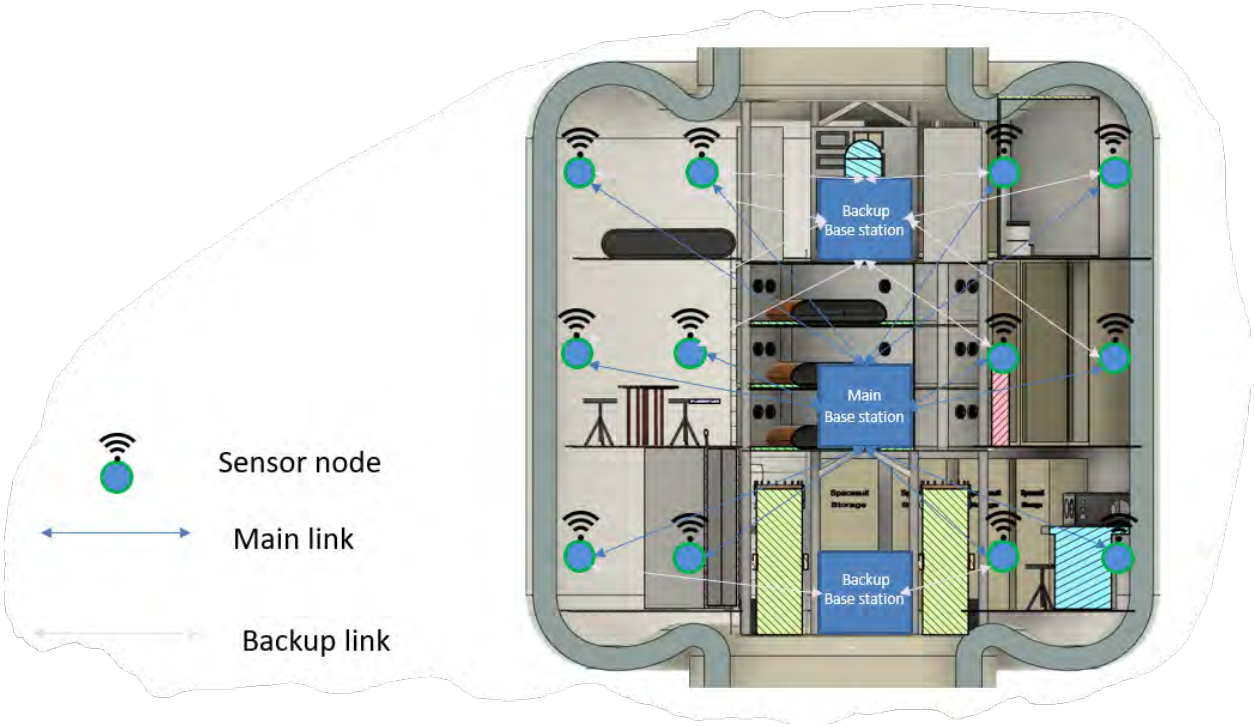

Figure 105: nodes and base station in the habitat.

XVII. Power Generation

1. System Selection - Konrad Shire and Matthew Stasiukevicius

The power generation design began with a trade study where mass was plotted against power for nuclear and photovoltaic (PV) systems. This study, along with the power requirements, was used to determine which system was most appropriate for each configuration. The power requirements are the same for each configuration and are summarized in the table below.

Table 18: Power Requirements and Heat Output with a 30% Margin

Transhab Phase	Max Power [kW]	Average Power [kW]	Max Heat [kW]	Average Heat [kW]
In Transit	0.4	0.35	0.02	0.02
Deployed for Human Use	14	11.4	1.2	1

A. Power Systems

1. Nuclear Power - Konrad Shire

The Kilopower was chosen as the candidate for the nuclear power generation system as it was designed with Lunar and Martian bases in mind. With a TRL of 5 [94], 1 Kilopower unit can provide 10 kW of power with a projected lifetime of 15 years of full power operation [95]. The concept behind Kilopower is among one of the simplest reactor concepts proposed. Its solid core reduces the number of moving parts, thus increasing its reliability. The startup and operation dynamics are additionally easily predictable as a result, and there is no need for a real-time reactor control system. Each Kilopower unit maintains a high level of redundancy in heat transport as every heat pipe can function independently. A 10 kW Kilopower system would have a full system mass of 1500 kg [96].

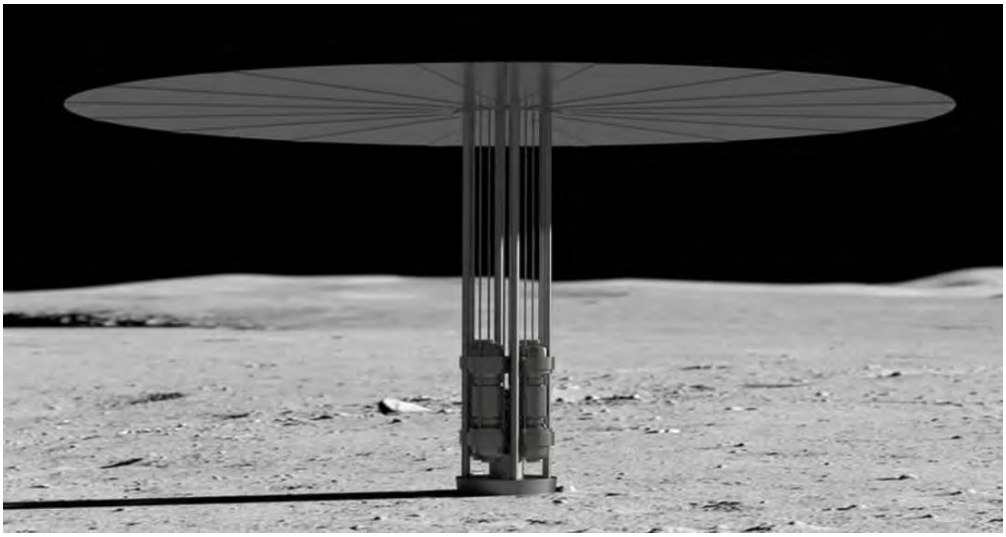

Figure 106: Artist Concept of the Kilopower reactor [97]

For the Lunar and Martian configurations, the habitat will utilize 2 Kilopower units which will arrive on-site prior to the habitat. The excess of 6 kW of power from two units allow for the opportunity to scale up a Lunar/Martian base beyond the inflatable habitat. With the use of nuclear power for a manned mission, the amount of radiation emitted must be considered.

At a distance of 10 m from the reactor, 250 Sv is emitted over 15 years [95]. From inverse square losses alone and the max allowable radiation exposure of 50 mSv per year [98], the Kilopower units would have to be a minimum of 185 m from the astronauts. Additional shielding will be provided by placing the units in a crater such that the Lunar/Martian surface will attenuate this radiation. A model from [99] simulated that a 1 Sv radiation dose could be reduced to 1 mSv with lunar regolith of thickness 150 g/cm^2. With the reactors being placed in a crater away from the habitat, sufficient radiation attenuation measures are in place to keep the astronauts safe from reactor particle emission.

2. Photovoltaic Power - Konrad Shire

The PV system will utilize multi-junction cells for power generation in the orbital configuration. With 30% efficiency [100], the system will charge batteries when exposed to sunlight in addition to powering the habitat. During periods of darkness, the habitat will rely on battery power.

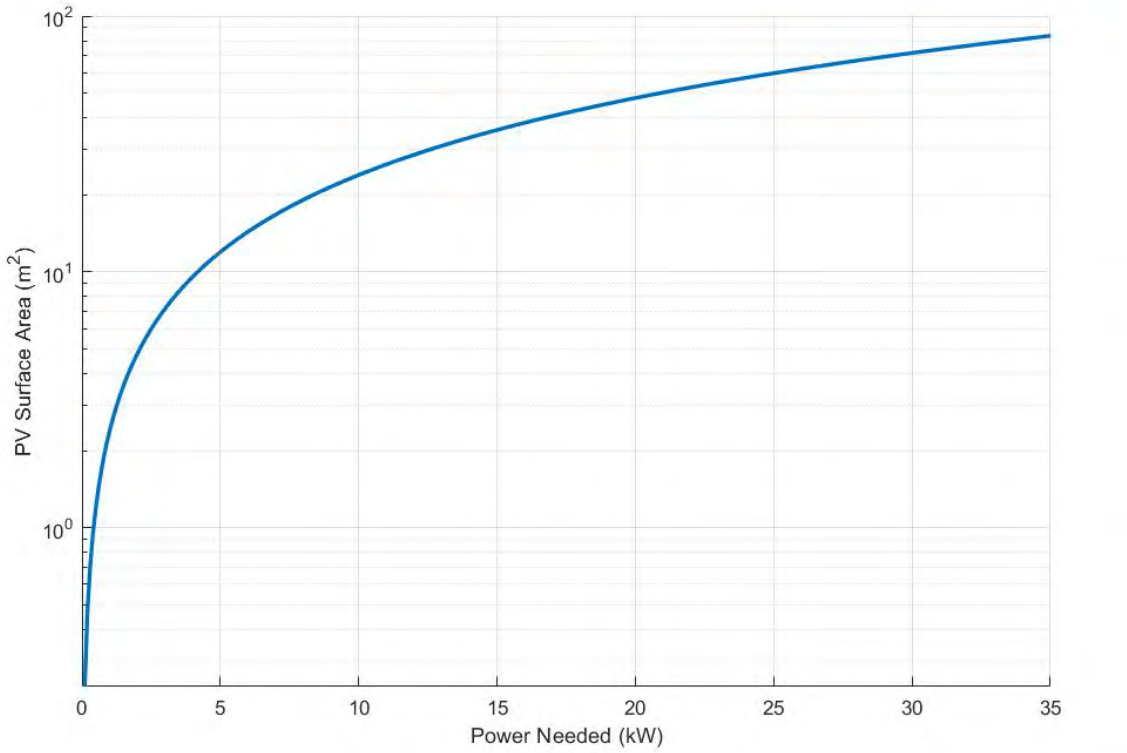

Figure 107: Surface Area vs. Power for a PV System for the Micro-Gravity Configuration

Taking the PV degradation rate of the ISS of 1.8% [101], the PV system for the orbit configuration would function at 83% of their initial performance after 10 years. With the panels initially supplying 14 kW of power, this would lead to a max supply of 11.7 kW. This power is slightly above the average power requirement of 11.4 kW with a 30% margin, about 8% above the maximum power requirement without its margin. Therefore, the panels should be changed after approximately 10 years to continue meeting the habitat's needs.

B. Configurations

1. Micro-Gravity Configuration - Konrad Shire and Matthew Stasiukevicius

As shown in figure 108, the PV system requires less mass for any given power requirement. To provide 14 kW of power, 180 m^2 of solar panels will be needed. Power storage in the micro gravity configuration is heavily dependent on the particular orbit that the habitat is in. It was therefore decided to compare several possible orbits based on how much additional mass they would cost the habitat. All orbits start with the assumption that the habitat could be inserted at a 500km parking orbit from Cape Canaveral. The first class of orbit analyzed was a set of sun synchronous orbits (SSOs) which have inclinations above 90° with orbital altitudes ranging from 275 to 5150 km. The obvious benefit of an SSO is that the habitat could always be facing the sun which means batteries would not be required for nominal habitat operation, they would only be needed as emergency back ups, and solar panel area could be reduced because no batteries would require charging. Launching from Cape Canaveral allows for a maximum parking inclination of 59° [102]. To minimize mass required, ten distinct orbits were considered and we calculated Hohmann transfers with optimal plane changes split between burns from the parking orbit to each SSO. The mass required for the maneuver was then calculated with the rocket equation assuming the 450 second specific impulse obtained from our propulsion

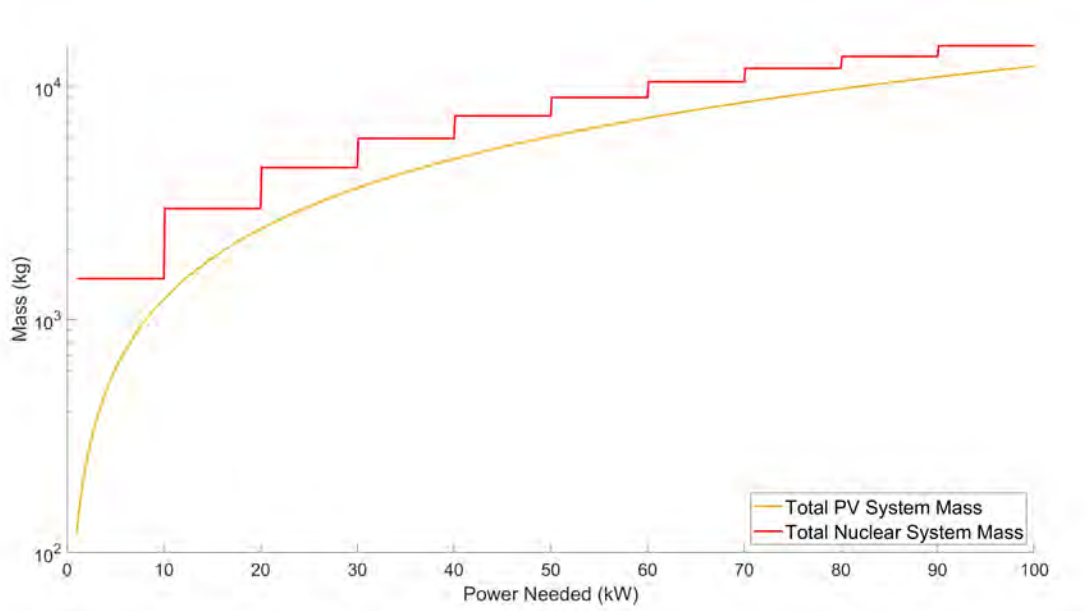

Figure 108: Mass vs. Power for PV and Kilopower for the micro-gravity configuration

analysis. The least intensive maneuver was to an orbit at 96.6° and an altitude of 274 km, and would require about 4.9 km/s of ΔV and therefore about 71 tons of propellant.

Next, we considered a low earth orbit directly from the insertion. Insertions from Cape Canaveral could be as low as about 28.5° which would allow for the most payload to be brought to orbit. No additional propellant would be required to maneuver from this parking orbit, but batteries are required to store power when the habitat is eclipsed by the earth and additional solar panel area is required to charge those batteries when the habitat is sunlit. A conservative estimate is that the habitat will be eclipsed for about 40% of the time in a 28.5° inclination [103]. Based on the time eclipsed and the orbital period at 500 km, a battery capacity to support the 14kW of habitat power could be calculated, and from that capacity a mass of the batteries and a mass of the additional solar arrays could be calculated. In order to perform these calculations we found viable batteries that hold 300 W-hr/kg [104]. Assuming a charging and discharging efficiency of 90% [105], a conversion efficiency of 30% [106], and a photovoltaic cell density of 2.5 kg/m^2 [107] the habitat would require about 330 kg of batteries and an additional 30 m^2 of solar arrays, adding up to a total additional mass of about 400 kg. This is also assuming a depth of discharge of 10% which will help to extend the lifetime of the batteries. At a 10% depth of discharge the batteries are expected to last about 7000 charge/discharge cycles [108] which would last the about 460 days at an altitude of 500 km; this is more than double the time between scheduled resupplies. Drag on the habitat was estimated in these lower orbits to determine how much additional propellant would be needed to counteract drag over the lifetime of the habitat. Given a heuristic equation from [109], the density of the atmosphere was calculated at an altitude of 500 km to be on the order of $8 * 10^{-13}$ kg/m^3.

Assuming at worst case that the broadside of the habitat is normal to the velocity vector, this density would impart a minuscule force that would require about a tenth of a kilogram of propellant to counteract over the course of 6 months.

Finally, a geostationary orbit was considered as a counter example to the other lower altitude options. If drag ended up costing the habitat more mass on the form of propellant this could have been a good alternative. From the 28.5° inclination parking orbit, a Hohmann transfer with an optimal plane change split between burns would require over 4 km/s of ΔV and 55 tons of propellant. On top of this massive propellant requirement, a geostationary orbit would also need the additional mass of a higher batter capacity than in low earth orbit. However, the depth of discharge could be increased in because there are fewer day night cycles.

After analysis of a few different classes of orbits, it became clear that the biggest limiting factor in orbit design for this habitat is maneuvering it because of how massive it is. Therefore, given a fixed orbital injection the most mass can be saved by remaining in an original parking orbit.

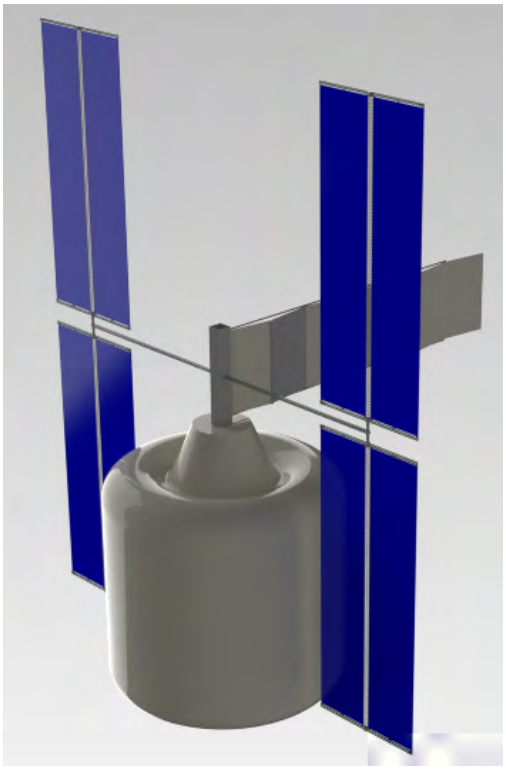

Figure 109: Micro-gravity Configuration

2. Lunar Configuration - Konrad Shire and Matthew Stasiukevicius

The moon presents the challenge of dealing with large temperature ranges that last for a long time at either extreme. With a day length of 709 hours, the temperature at the equator can vary from 90 K to 380 K [110][111]. Assuming 300 W-hr/kg and an average night length of 354.5 hours, a PV system would need 16,500 kg of batteries, adding significantly to the total mass. Given that the nuclear system functions independently of solar intensity, there is less of a need for battery storage. The consequences of the PV battery mass are shown below.

From the stark difference in system mass, it was determined that the mission will utilize a nuclear system to power the lunar configuration. Two Kilopower units will be used to meet the habitat's needs.

3. Martian Configuration - Konrad Shire and Matthew Stasiukevicius

As shown in figure 111, the solar intensity on the Martian surface results in mass vs. power curves which follow each other closely above 10 kW.

The Martian atmosphere presents the additional issue of dealing with wind and thus airborne dust. A PV system would need to be cleaned from dirt for them to function at their maximum potential. With a required PV surface area of 500 m^2, there is also an increased likelihood of damage from wind. For these reasons, it was decided that the Kilopower would be utilized for the Martian configuration.

4. In transit to the Moon or Mars - Konrad Shire

While the habitat is in transit, it will not be able to rely on nuclear power, as the Kilopower units will arrive on site prior to the habitat's launch. The computer system will require approximately 100 W of power, 150 W for communications, and 50 W for network hardware. The mission headed to the Moon will rely on solar panels with a surface area of 1.5 m^2 while the Martian mission will have a surface area of 4.5 m^2. During the propulsive landing of the habitat, the solar panels will be retracted and batteries will power the avionics systems. The solar panels are retracted so they are protected from inertial forces and atmospheric drag on the Martian mission.

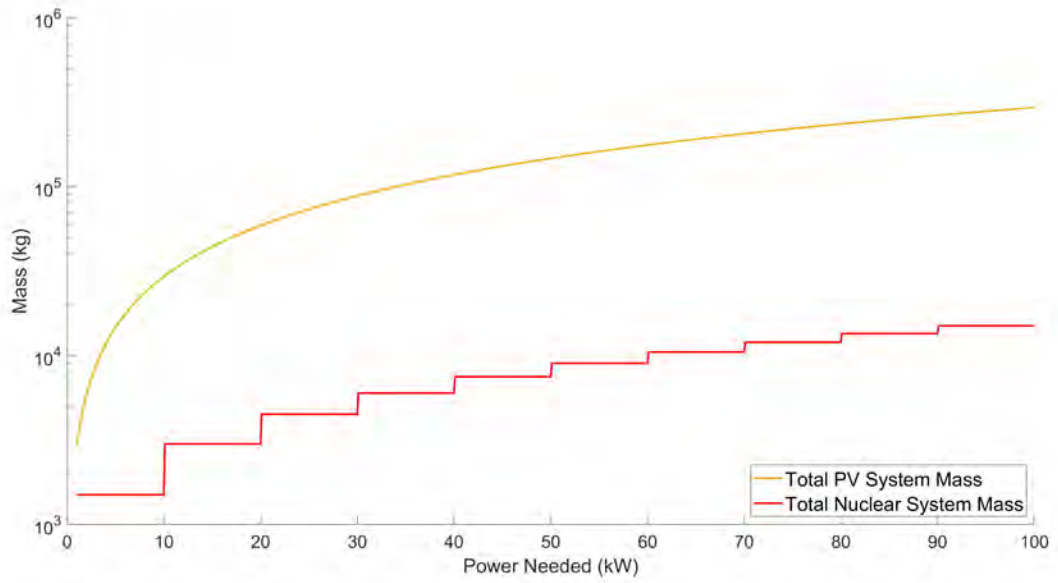

Figure 110: Mass vs. Power for PV and Kilopower in Lunar Application

C. Power Scheming

1. *Power Budget - Konrad Shire and Matthew Stasiukevicius*

To determine the power requirements for the habitat, a spreadsheet was created to list all of the components requiring power. The maximum and average power for each component was found by determining a maximum and average time in use per day. Additionally, each component was listed as either critical, low power, or nominal to determine the power needed in emergency conditions. The critical mode will only power systems that are crucial to the crew's survival while a rescue operation takes effect. This mode uses only 1.4 kW but has life support systems such as scrubbers and electrodialysis machines turned off. As a result, the crew could only survive for approximately seven days in this mode. However, if the power system can provide 2.8 kW of power in an emergency situation, the habitat can function in the low power mode. In addition to the systems powered in the critical mode, the scrubbers, electrodialysis machine, food warmer, and food hydration device are powered. With this additional equipment available, the crew can survive for 14 days before a rescue mission is available. Lastly, the least restrictive life support scheme is the nominal mode. This requires 9.3 kW of power and allows for powered function of all equipment aside from the laboratory, tablets, and normal lighting. In each of these emergency modes, lighting is provided by photo-luminescent dots with a lighting level of 32 lux. In the case of main power generation failure, 550 kg of backup batteries, electronically separate from the main battery system would be able to support the crew in critical power mode for over 5 days in the hope of fixing the issue with the power system or being rescued in that time.

XVIII. Thermal Analysis

1. *Introduction - Matthew Stasiukevicius*

The goal of our thermal analysis is to keep the interior of the habitat at equilibrium temperature of 300 K regardless of where it is in outer space. We need to account for heat generated internal to the habitat by the machinery in the habitat, as well as the external heat loads which can reach a maximum of up to 400 K in direct sun of orbit or on the light side of the moon and a minimum as low 40 K on the dark side of the moon.

2. *Internal Heat - Matthew Stasiukevicius*

To account for the internal heat loads we added a found the electrical efficiencies of the most power consuming devices on the habitat and took the inefficiency to be equal to the heat output of the device. We kept track of this heat

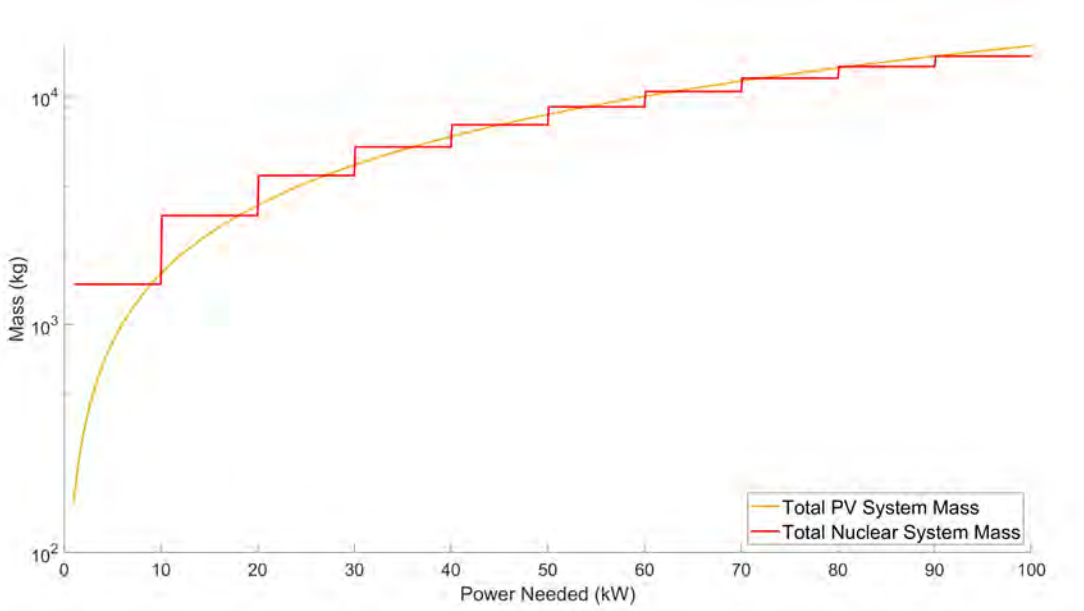

Figure 111: Mass vs. power for PV and Kilopower for the Martian Configuration

output in our power budget to easily keep track of the heat loads. During average operation of the habitat, all of the devices produce about 650 W of heat. When the external heat loads are low, this internal heat can be kept inside the habitat and will help keep the equilibrium temperature up. When the external heat loads are too high, the internal heat must be rejected out to space using radiators.

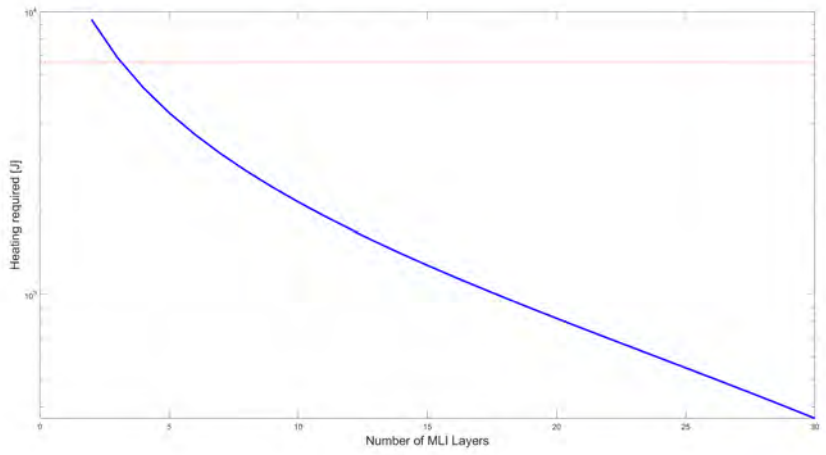

Figure 112: Dark Side of Moon Heating vs Number of MLI Layers

3. *Active Heating - Matthew Stasiukevicius*

In the coldest case of the habitat, being on the dark side of the moon for multiple earth days straight, the multilayered insulation (MLI) outer layer of the transhab design becomes very important to keep what heat is generated inside the habitat. Based on the 6 kW of extra power available from the 2 kilopower units and the 600 W of heat generated internally, we ideally wanted enough layers of MLI to keep the required heating of the habitat below 6.6 kW. Using a heuristic for effective MLI emissivity based on the number of layers [112] we created a plot of the how much heat would need to be generated by additional heaters in the habitat. Based on 112 only 4 MLI layers would be required to

keep the heating under 6.6 kW, but 18 layers could keep the heating under 1 kW and 24 layers could keep it under the passively generated 600 W.

4. Active Cooling - Matthew Stasiukevicius

In order to reduce external heat loads when in direct sunlight, we could cover the habitat in the flight rated paint z93 which has a recorded absorptivity of 0.17 and an emissivity of 0.92 [113]. With this paint applied, direct sun at a distance of 1 AU hitting the broadside of the habitat, and 600 W being generated internally we found that about 25 m^2 of radiator would be required to keep the habitat at 300 K. The radiator itself will have ammonia flowing through its pipes because of the high heat capacity of ammonia and the incredibly cold freezing point of about 200 K. However, no ammonia will enter the pressurized volume of the habitat because it is toxic to humans. Instead, water will flow through cooling loops inside the habitat, because water also has a high heat capacity, and it will go through a heat exchange with the ammonia before the heat is rejected out of the radiator.

XIX. Micro Meteoroid Orbital Debris (MMOD) Shielding - Joe McLaughlin

A. Introduction

The TransHab, while acting as a long term space habitat will not only need to keep the crew warm and ensure the presence of a breathable atmosphere, it will also have to protect them from Micro Meteoroids and Orbital Debris. These particles, when entering Earth's atmosphere, burn up before they reach the ground. This leaves no need to MMOD protection in our day to day life. However, on the Moon, cis-lunar space, or in the orbit of Earth, there is nothing to slow down these particles. Therefore, spacecraft are at constant risk of being impacted by debris or a Hyper Velocity Impact[114]. The Transhab is no different in this respect.

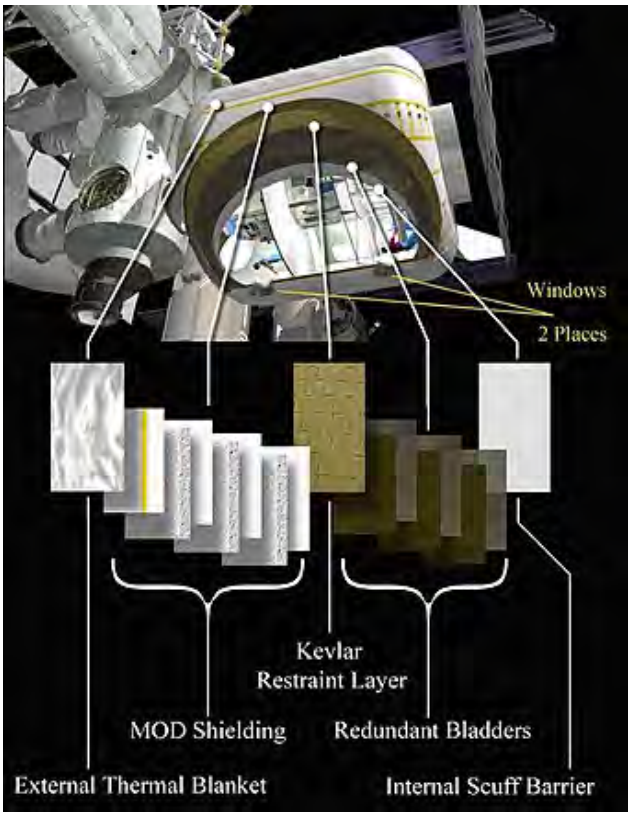

Figure 113: Transhab Design[115]

B. Given Information

The Transhab was originally designed to use its pressure shell as insulation, the inflation structure, and MMOD protection. It accomplished this by having four separate layers: the Multi Layered Insulation (MLA) layer, the scuff barrier/Pressure Bladder, the structural restraint layer, and the MMOD Shield These layers are made out of the following respectivley: a mylar thermal protection blanket, fire retardant Nomex, Combitherm, and multiple layers of Nextel with kevlar backing for the MMOD protection[115]. See Figure 113.

C. Mass information

While the information on materials, and structure of the Transhab is given, the mass of the external pressure shell was not. Therefore, to get an accurate mass of the habitat, this had to be estimated. The Transhab was reconstructed via Figure 114 in Siemens NX to find the surface area of the inflatable portion of the habitat. This model is shown in Figure 115 and Figure 116. The University of Arizona also published a graphic which gave information on mass of MMOD protection per meter squared. For the Multishock protection method, which is what Transhab uses, the mass per meter squared is 4.5kg[116]. For the remaining components including the MLA, the mass per meter squared was estimated to be approximately 1.2 kg. By calculating a surface area of the CAD model and extrapolating those mass numbers, we were able to find that the MMOD protection and outer shell are approximately 2195 kg with a 30% margin.

Figure 114: Transhab Design

XX. Propulsion Design

1. *Propulsion Module - Konrad Shire*

Liquid oxygen and liquid hydrogen were chosen as the oxidizer-fuel combination for takeoff from Earth as they provide an I_{sp} of 390 sec at sea level and 450 sec in a vacuum [117]. Additionally, it will be used to arrive at the lunar surface. Using the methodology in [118] and a heat flux of 0.4 W/m^2 through the MLI, the total boil-off per day was calculated to be 65 kg. This is acceptable for the Lunar mission as the transit would take no longer than four days. For a Martian mission, however, the transit time is on the order of several months and the amount of propellant lost to boil-off is prohibitive. With a much higher boiling point of 114°C [119], liquid hydrazine could be used for the Martian mission, as it would boil off at a rate of 0.3 kg/day. Several previous missions including Perseverance utilized hydrazine to successfully get to the surface of Mars [120]. Unfortunately, hydrazine only produces an I_{sp} of 230 sec [121]. Using the rocket equation, it can be deduced that going from an I_{sp} of 450 sec to 230 sec increases the

Figure 115: Transhab CAD for Estimation

Figure 116: Transhab CAD for Estimation Cut Through

required propellant mass by 248% which is another challenge. The crew systems sub-team additionally found it to be too prohibitive to carry out a Martian mission, so further analysis into propulsion design for Mars was not done.

2. Landing on the Moon - Konrad Shire and Matthew Stasiukevicius

To land on the Moon, [122] provides a conservative estimate of $\Delta V = 2.3$ km/s which corresponds to 27 tons of fuel. The module will propulsively land the habitat on the Lunar surface. The module will have a ladder to allow the astronauts to exit and enter the habitat. This design by was inspired by the Apollo 11 Lunar module with large circular feet and shock absorbers to soften the landing.

Figure 117: Landing Module

3. Attitude Control - Matthew Stasiukevicius

Some form of attitude control is required on the habitat for specific pointing requirements for communication or solar array positioning, if the alpha and beta gimbals don't provide enough degrees of freedom. Attitude control is also required to maintain a stable orientation of the habitat through gravity gradients, propulsive maneuvers, and the moving of astronauts throughout the habitat. In order do some basic attitude system sizing, we started with the notably conservative and bad assumption that all of the mass of the habitat is contained in a thin cylindrical shell with a radius equal to the outer radius of the habitat and of length equal to the height of the habitat. This assumption gives a moment of Inertia about the central axis of the cylinder (z axis) of about 760,000 kg-m^2 and moments about the perpendicular axes (r axes) of about 1,300,000 kg-m^2. We wanted to compare the viability of using reaction control thrusters and control moment gyros (CMGs) for the attitude control of the habitat. We chose to analyze CMGs over reaction control wheels because of the significantly lower power draw that CMGs require [123]. In analyzing the separate systems we wanted to have a system that would control the attitude at angular accelerations slow enough to be not perceivable by the astronauts on board the habitat. Therefore we set maximum angular accelerations to 0.14 deg/s^2 about the z axis, 0.5 deg/s^2 about the r axes, and we also set a maximum angular rotation of 1 deg/sec about any axis [19]. Considering that we can not fasten any materials to the inflatable portion of the habitat, clusters of reaction control thrusters could be placed around the outside of the propulsion module.

For a sizing of the thrusters, a required thrust per thruster could be calculated for a given "pitching" maneuver about the y axis. The maneuver is such that two cluster of thrusters on opposite ends of the y axis fire at the same time in opposite directions to induce a rotation about the y axis, then the same thrusters are fired again in the opposite direction to stop the rotation once the desired angle of rotation has been achieved. Therefore any one maneuver about the y axis, regardless of angle of rotation, would require the same amount propellant, and the same thrust. Given a

desired rate of rotation of 0.1 deg/s and an thrust impulse time of 1 second, (an angular acceleration of 0.0017 deg/s^2) each thruster would have to provide about 280 N of force which is within reason for a helium cold gas thruster. Then assuming a specific impulse of 165 seconds, [124] which has been measured for helium, each maneuver would cost about 175 grams.

A simple CMG sizing was done by relating the desired rotation rate of the habitat, the rotation rate of the CMG, the moments of inertia of the two, and solving for the moment of inertia of the CMG. We again used the more limiting case of the y axis pitch corresponding to the moment of inertia about the y axis, and a desired rate of rotation of the habitat 0.1 deg/s. The rotation rate of the CMG is driven by material properties of the wheel, and 9000 RPM is a sporty but achievable rate [125]. With these parameters, the CMG would need to have a moment of inertia of about 0.25 kg-m^2 which could be achieved with a 15cm wheel that is about 20 kg. Assuming 3 equally massive gyros would be required, the same mass of propellant would not even produce 400 of the above described maneuvers. Furthermore, the CMGs can be placed internal to the habitat and close to the center of mass which should make them significantly more precise than the external thrusters.

A common problem with CMGs is that they can become saturated, which means that it is holding is maximum allowed angular momentum, set by the material of the gyro, in one direction. In order to combat saturation, the angular momentum stored in the gyro can reduced while some external mechanism holds the habitat [125]. In our case, we could keep some reaction control thrusters purely for the purpose of desaturating the CMGs.

XXI. Mass Breakdown - Joe McLaughlin

The following section describes the final Mass breakdown of major components in both the Micro gravity and Lunar Gravity Designs. Each section is broken up by floor and section on each floor, i.e. Floor 3: Lab. At the end of this section there will also be tables summing up the load per floor and total mass of the habitat. All Masses are given with a 30% margin and are in kg

Floor 3

Lavatory 2

Item	Quantity	Total Mass (kg)
Toilet	1	39
Lavatory Walls	1	6.5
Sanitary Consumables	1	46.3
Shower System	1	70.2
Walls	1	65

Exercise Area

Item	Quantity	Total Mass (kg)
Treadmill System	1	1300
Cycle Ergometer	1	260
ARED	1	1120

Core (Water / Life Support)

Item	Quantity	Total Mass (kg)
Water Tank	1	1346
VipCar	1	156
ED	1	2145

Floor 2

Kitchen

Item	Quantity	Total Mass (kg)
Vegetable Growth System (VEGGIE)	2	65
Food Rehydrator	1	507
Food Warmer	1	9.1
Storage Cabinet	1	35.4
Chair	6	23.4
Table	1	7.8
Consumables (Food)	1	3791

Core (Crew Quarters)

Item	Quantity	Total Mass (kg)
Beds	6	39
Bed Structure	1	52

Floor 1

Lab

Item	Quantity	Total Mass (kg)
Storage Cabinet	1	35.4
Chair	2	8
Desk	2	195
Glove Box	1	26
CTB's	120	390
Medical Table	1	13
First Aid Kit	1	23.4

Lavatory 1

Item	Quantity	Total Mass (kg)
Toilet	1	39
Lavatory Walls	1	6.5
Sanitary Consumables	1	46.3
Shower System	1	70.2
Walls	1	65

Core (Air Life Support)

Item	Quantity	Total Mass (kg)
EDC	2	229
Bosch	2	408
Electrolysis	2	312
Nitrogen Tank	2	185

Basement

Airlock

Item	Quantity	Total Mass (kg)
Suits	1	104
Airlock Equipment	1	273
Sample Transport	1	52

Miscellaneous

Structure

Item	Quantity	Total Mass (kg)
Core	1	4960
Floor Panels	22	4719
Truss	44	633
MMOD & Insulation	1	2195

Power

Item	Quantity	Total Mass (kg)
Backup Batteries	1	744
Solar Panels	1	507
Communications	1	104
Lighting	1	169

Floor Summary

Item	Total Mass (kg)
Floor 3	6491
Floor 2	4592
Floor 1	1993
Basement	429
Miscellaneous	14096
Total Mass	**27600**

XXII. Deployment of Core Testing

After TransHab reached to the destination and completed the inflation, several systems including the lab, kitchen, bathrooms, and exercise equipment will need to be moved from the packed core, assembled, and installed on their respective floors in the inflated volume outside of the core. Since the space in the core is limited to critical systems such as life support and crew quarters, the larger inflatable volume outside of the core will be used to house these mid-to-low priority systems. Each system will require a thorough procedure of unpacking from the core, moving to its respective position in the inflated structure, and then being properly secured to the structure. Many systems will require additional interfacing as fluid, power and/or network lines will need to be fed from the core and attached to the subsystem. To get the fundamental idea of the deployment process in the inflatable habitat, the team decided to simulate the environment utilizing the Neutral Buoyancy tank. In this section, we discuss the process of the development of testing plans, test procedures, and test results.

A. Testing Plans

1. Initial Testing Plans - Aidan Sandman-Long (Testing plans) and Alberto Garcia-Arroba (1/3 floor mock-up designs)

Initial testing looked into the deployment of all systems packed in the core to a fully deployed configuration. The purpose of this testing is broken down into two key parts. The first was to determine if all equipment would be able to be completely packed inside the core and able to be efficiently moved out. Time and demand to perform this test would be taken into account and used to determine the optimum methods for how the core would be packed before launch and unpacked to its final deployed configuration. The second was optimizing the fully deployed design to ensure a crew of six people could live inside it for extenuating periods of time. Testers would move around a fully deployed simulated section of each part of the habitat to determine the optimum placement of everything in the habitat.

In order to perform the mentioned testing, the team would have to build structures to represent the core structure, the inflatable exterior structure, and all equipment inside the habitat. A volumetric analysis was performed on all equipment that would be stored in the inflatable habitat to determine approximate dimensions for its packed and deployed configuration. The results of the analysis can be seen below.

The design of a floor mock-up for testing was broken down into two components: the core and the inflated volume. To simulate the core, the SSL racks, sized 1 meter wide by 2 meters tall by 0.5 meters deep, were used. To figure out how many of them would be needed, a trade study was performed based on the maximum radius and area of the original dimensions of TransHab, that is, 1.675 m and 8.81 m^2, respectively [126]. The previously mentioned trade study compared 6-rack, 7-rack, and 8-rack configurations, in which the maximum radius and area were calculated, and a discussion on their pros and cons was included. The results are summarized in Table 19.

Table 19: Core Racks Trade Study Results

Number of Racks	**Max Radius [m]**	**Max Area [m^2]**	**Main Advantage**
8	1.734	9.844	Closest Max Radius
7	1.563	8.07	Closest Max Area
6	Modifiable	Modifiable	Area or Radius can be modified

Although using 6 racks seemed reasonable since it would allow for a modifying area or radius, it would also imply the use of elongated connectors, which were not available in the SSL facilities, and had some drawbacks such as it resulting in less area that would be considered shelving. Since the goal of this test was to find the most efficient container shapes or combination of shapes to pack the core efficiently, the final decision was to use 7 racks as it was the best estimate for the area. However, as the needs and goals for testing hardware shifted with time, it will be explained later why the rack configuration for the core was not significant for the final micro-g and lunar gravity testing.

To simulate the inflated volume, the overall design consisted of building one-third of a floor with a framework made out of PVC encased with plastic wrapping. With a radius of 3.81 m, the same as the actual TransHab [126], this testing configuration would preserve the original dimensions of the habitat and would be interchangeable to test different configurations for the systems found on each floor that needed to be unpacked and secured out of the core.

Once the dimensions for the exterior structure were determined, a comprehensive study was performed to analyze the feasibility of implementing different designs, considering a list of costs for their required hardware, their advan-

tages and disadvantages, the available tools in the NBRF, and the time constraints to have the structure ready to be tested as soon as possible. Based on these premises, two designs were proposed: a curved and a hexadecagon structure.

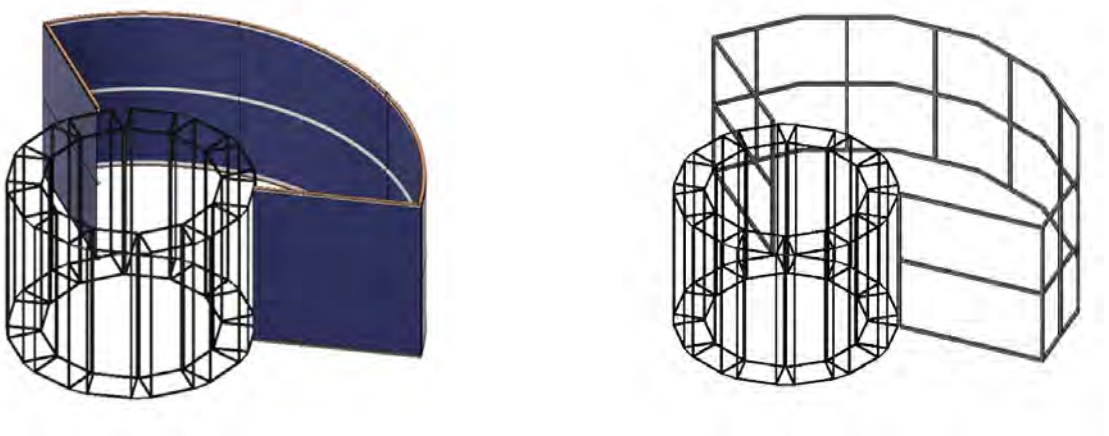

Figure 118: CAD models of the exterior design, curved (on the left) and hexadecagonal (on the right)

The curved exterior, displayed on the left of Figure 118, had the main benefit of allowing for testing of a more accurate inflatable area, with rounded walls resembling the ones in the Transhab. However, it required purchasing a particular device to modify the PVC to the desired shape. For this, three bending devices were considered: an electric PVC Bender Hotbox, a HotBlanket PVC Bender, and a Manual Copper Exhaust Bender Tool, costing $ [127], $ [128], and $ [129], respectively. Due to the budget restriction, reliability, and familiarity with the device, the Manual Copper Exhaust Bender device would be used if the team decided to move forward with this design. After compiling a pricing list, the total cost would be $, as shown in Table 20 below.

The second design, the hexadecanoic exterior, had the main advantage over the curved one in that it would not require the use of any sophisticated machine to bend the PVC, making it faster and simpler to build. After compiling a pricing list, the total cost was set to be $, $ cheaper than the curved configuration. Although it would not be as accurate of a model of the inflatable area, the hexadecagonal configuration was chosen for three main reasons: it would be sufficient for our test purposes, that is, taking metrics regarding the time it would take to unpack the core and secure the equipment to the floor, it would shorten the total expenses, and it would reduce the time spent building hardware prior to testing. This last point heavily conditioned the decision-making process, as the dives in the Neutral Buoyancy tank for testing were limited and needed to be done before hard deadlines regarding the design review.

Table 20: Comparison between the two testing designs

Configuration	**Main Advantage**	**Main Limitation**	**Total Cost [$]**
Curved	More accurate inflatable area	Requires Bending of PVC	
Hexadecagon	Faster and Simpler to build No Bending	Less accurate inflatable area	

2. *Final Testing Plan - Ronak Chawla, Ryan Allegro, Hajime Inoue, Alberto Garcia-Arroba, and Aidan Sandman-Long*

After the feedback from the Preliminary Design Review, as well as discussions between team members, the team decided to change the nature of the testing to be more useful to the NASA sponsors as well as use the unique facilities in the Neutral Buoyancy Facility. Previous ideas of volumetric and spatial testing could be done using a scale model, or CAD. The new tests made use of the ability to simulate different gravity environments in the Neutral Buoyancy Facility. The idea was to perform habitat outfitting tasks and gather data on the time it took to perform these tasks, as well as feedback from the divers on the difficulty of these tasks. From this information, the total time to perform each task on an actual mission in different gravity environments can be estimated.

For the movement testing, the divers moved the item from the core to a designated spot in the deployed floors and the time it took for this task was measured. Next, the time required to secure and screw each equipment was recorded. This represents the first part of the assembly and installation. The last test collected the amount of time it took for the test subjects to properly attach any external wires or fluid lines to the equipment. The fluid and power lines were simulated with hoses and cables to be a representation of the ceiling.

After the equipment is moved to its respective location in the inflatable structure, it will either need to be secured to the bottom of a floor panel or to one of the ceilings from the floor above. Equipment will primarily be secured using simple machine screws, nuts and bolts, and power hand tools. Heavier equipment such as the treadmill may require special tools and support racks to withhold any additional force applied to the floor panels. The floor panels will have threaded holes that will be lined up with the equipment.

Once the equipment is secure, power and fluid lines and network cables will typically be attached to the ceiling or bottom side of the floor panel structure from floor above. The nature of the deployment process and the tools and effort required for deployment and installation of these systems will differ in micro-g versus planetary surface environments.

B. Test Procedures

The capabilities of the Space Systems Laboratory at the University of Maryland allow for testing in various gravity conditions through the use of body segment parametric ballasting in the UMD Neutral Buoyancy Research Facility. By ballasting divers with the appropriate amounts of weight on each of the major body segments, micro-, lunar, martian, or other gravity conditions can be simulated [130]. Design of these experiments for underwater simulation involves attention to detail to maximize adherence to flight conditions and minimize media-specific effects such as hydrodynamic drag. For example, rotating large plates representing floor or ceiling surfaces would involve high drag forces, which could affect the utility of results.

1. Design of Equipment - Ryan Allegro and Hajime Inoue

The final equipment we designed and moved forward with testing was to be a box made of PVC with a cross in the center as shown in Figure 119. The joints are colored in black and PVC pipes are colored in white. The central cross would be used to attach any additional plastic boxes needed to hold water, as well as the place where the weights would be attached in tests in gravity environments. This design encompasses the change in the position of center of gravity for future testing by differentiating the length of the side PVC pipes. For example, to test the equipment with lower C.G., one would need to put longer PVC pipes on the upper side of the T-shaped joints for the central cross, and shorter PVC pipes for the lower. This will minimize the work required for the possible modification of the equipment in the future compared to the fixed C.G. structure we once were designing. The PVC equipment we built also contains holes on the PVC pipes approximately 5 inch apart to fill the water in faster.

To start these designs, a desired volume was determined. The selected volumes were $0.18m^3$, $0.29m^3$, and $2m^3$. $0.18m^3$ and $0.29m^3$ were chosen because the majority of the habitat equipment had volumes between $0.05m^3$ and $0.3m^3$, so we wanted something in the middle of these values, but we also wanted the largest of these values as we felt that larger items would be the hardest to deploy. There were a few larger pieces of equipment and we wanted at least one test that was representative of these larger sized items. For the large equipment, it was appropriate to use $2m^3$ – the approximate volumetric size for the International Standard Payload Rack (ISPR) which used in the International Space Station [131]. The next parameter to find was the inertial mass of the objects. For this we just wanted to evenly space out our three objects, and so aimed to have the equipment at $50kg$, $100kg$, and $150kg$. The majority of our smaller pieces of equipment were $50kg$ or below, which is why this value was chosen. The larger and heavier pieces of equipment were more likely to be split up into smaller loads and assembled in the habitat. These smaller loads could weigh around $150kg$, leading to this being our heaviest structure. Finally, $100kg$ was selected to evenly space out the equipment that was being tested.

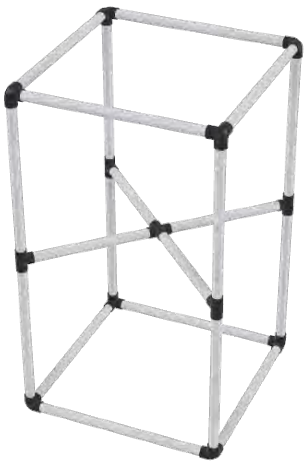

Figure 119: PVC test equipment designed for micro-g and lunar tests. Joint parts are colored in black.

Once we had the desired volumes and masses of the objects, the next step was to design the pieces of equipment we would use. The first step in the design was to calculate the size of the base required for each of these pieces of equipment. One of the key components of this design is its ability to hold water, which will represent the inertia of an object while remaining neutrally buoyant. The initial assumption was that plastic boxes that would hold all of the required water to represent this inertia would be needed. The volume of water needed is calculated from the mass of the object divided by the density of water. From the desired masses of $50kg$, $100kg$, and $150kg$, the calculated required volumes would be $0.05m^3$, $0.1m^3$ and $0.15m^3$. We were able to find plastic boxes that would hold these amounts, so the initial calculations for the dimensions of the bases were made to be large enough to hold these boxes. The PVC bases were calculated to need to be at least $0.75m$ x $0.75m$, $0.9m$ x $0.9m$, and $1.05m$ x $1.05m$ for the small, medium and large boxes respectively. The heights for these PVC structures was calculated to be the amount needed to achieve the desired volume, which were $0.32m$, $0.36m$ and $1.81m$ respectively. Further along during construction of these items it was made apparent that the largest structure would need a smaller base in order to fit through the racks that were used in testing. Its new base was made to be $0.80m$ x $0.80m$ as shown in the Table 21.

Table 21: Calculated Dimensions of Test Structures

Size	**Dimensions [m]**	**Mass [kg]**	**External Volume [m^3]**
Small	0.75 x 0.75 x 0.32	50	0.18
Medium	0.9 x 0.9 x 0.36	100	0.29
Large	0.8 x 0.8 x 1.83	150	1.17

Once the dimensions of the PVC structures were known, we realized that the PVC itself would hold water, and so our calculations for the required water in the plastic boxes would need to change. We had a supply of $1.5in$ PVC from an earlier order, and planned to use this for our structures. The inner diameter of $1.5in$ PVC is $1.593in$ [132], which meant the approximate volume per unit length was $7.97\ in^3/in$. Taking into account the previously mentioned base and height dimensions, as well as the center cross of PVC, it was calculated that the PVC of our structures would hold approximately $0.048m^3$, $0.058m^3$ and $0.096m^3$. From this information it was decided that the small structure would not need a plastic box, as the volume of water in the PVC alone was close to the desired amount. The medium and large structures would both need boxes, but much smaller than originally calculated. A $0.045m^3$ plastic box was found that would work for both structures. This brings the total volume of water in each structure to $0.048m^3$, $0.103m^3$ and $0.141m^3$ as shown in Table 22.

Table 22: Volume of Water in Test Structures

Size	**Length of PVC [m]**	**Inner Volume of PVC [m^3]**	**Volume of Water [m^3]**
Small	9.4	0.048	0.048
Medium	11.2	0.058	0.103
Large	18.64	0.096	1.41

After all the dimensions of the structures were known, construction of them began in the Neutral Buoyancy Facility. Due to some of the limitations in the equipment, the exact dimensions mentioned above were not able to be achieved. The small structure was constructed with dimensions $0.75m$ x $0.75m$ x $0.34m$, the medium structure was $0.91m$ x $0.91m$ x $0.37m$, and the large structure was $0.80m$ x $0.80m$ x $1.82m$. This meant the actual volumes of the structures were $0.19m^3$, $0.31m^3$ and $1.16m^3$ respectively as shown in Table 23.

The actual mass of these structures after construction was calculated by adding the calculated masses of water and PVC, as well as the known masses of the plastic boxes. These were calculated to be $68.4kg$, $127.1kg$, and $169.3kg$. In a lunar test, weights would need to be added to simulate the apparent lunar weight of these objects. This was calculated by multiplying the actual mass by the gravitational acceleration of the moon, then dividing by the gravitational acceleration of earth. The necessary weight was calculated to be $11.3kg$, $21kg$, and $28kg$ respectively. These weights would be attached to the center cross through zip ties or rope.

Table 23: Actual Dimensions of Test Structures

Size	**Dimensions [m]**	**Mass [kg]**	**External Volume [m^3]**
Small	0.75 x 0.75 x 0.34	68.4	0.19
Medium	0.91 x 0.91 x 0.37	127.1	0.31
Large	0.8 x 0.8 x 1.82	169.3	1.16

2. Movement - Ronak Chawla and Ryan Allegro

The outfitting of the inflatable volume was tested by simulating moving, assembling and securing three key subsystems within the mockup. The three subsystems were an approximate representation of the waste management compartment, the advanced plant habitat, and a standard instrumentation rack. These three subsystems not only represented the varying masses, shapes and sizes to be relocated in the outfitting process, but also the different complexities associated with assembly and installation. The data from these three subsystems can be extrapolated to find the time and complexity required for the total deployment of the complete inflatable habitat.

This was far more efficient, saving significant testing costs, time and resources than choosing to test and obtain results for each subsystem individually. For example, a toilet was one of the simulated components that will be deployed outside of the core as a part of the waste management compartment. The toilet requires air, power, and water lines to function. By estimating the time and complexity of installing these lines to the waste management compartment, a similar estimate can be tabulated for other components that will not be tested.

The goal of these tests was to understand and obtain data on the duration and difficulty of operations and subsystem installment. To accurately model the dynamic properties of the hardware in different environments, it was necessary to independently match both the inertia and the perceived weight of the item in the desired gravity field. Inertial mass is simulated for underwater testing by incorporating a closed volume in a neutrally buoyancy structure that encloses a mass of water equivalent to the desired inertia. This step is sufficient for micro-g simulations, assuming the rest of the mockup is neutrally buoyant. The same hardware can be used for planetary simulations by adding ballast equivalent to the calculated weight in the specific gravity field of interest.

The systems inside of the packed core will be carefully marked, preferably by including a color code to easily identify which subsystems will need to be moved and installed outside of the core. These markings will also identify which section the subsystem will be housed in and which larger system it belongs to. The procedure should also include the order that these subsystems will need to be unpacked and moved. Larger equipment will require multiple trips and two or more astronauts to deploy and assemble. To stay at reasonable weights, these systems will be packed into smaller components that can be moved and then assembled and installed during deployment.

Test Procedure for Equipment Movement:

1. Test monitor starts stopwatch
2. Starting with the smallest of the PVC structures move the equipment in the direction of rack 9 and navigate it through the rack to the other side.
3. Navigate along the floor panel using handrails to location at the end of the flooring with 2 large handrails on either side of the location.
4. Place PVC structure at the destination point which is the floor securing site (for small it is labeled with S, medium with M, and large with L)
5. Test monitor stops stopwatch

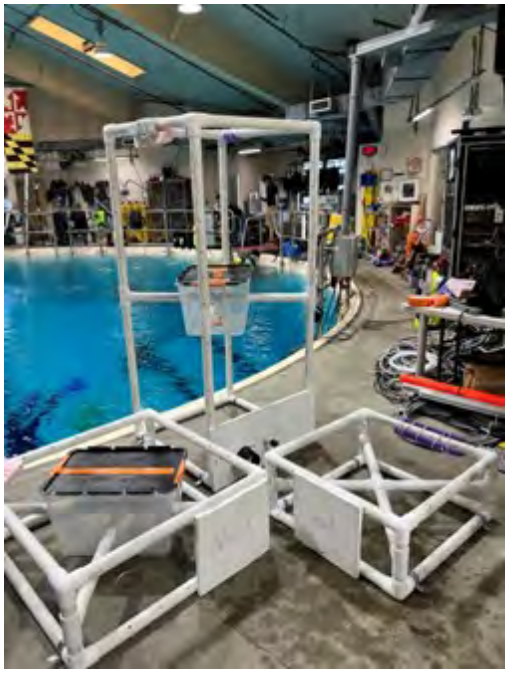

Figure 120: Test equipment used for micro-g and lunar tests. The small, medium, and large PVC structures are displayed.

3. Securing - Alberto Garcia-Arroba

The LSM team designed two floors for the TransHab depending on the gravity conditions: a 37.0 mm thick honeycomb sandwich panel for lunar and mars gravity and a 12.7 mm perforated panel for micro-g. Considering the two different designs, two different methods were considered to develop a securing methodology.

For the lunar and mars floor, the mission plan to secure the equipment to the floor involves using threaded metal inserts. For this, the equipment will have brackets on the bottom with holes in them aligned to the floor. On micro-g, the securing methods take advantage of the perforated floor panel, using threaded holes. To implement this securing methodology in testing, threaded holes were included on the floor, along with rigid conduit straps whose outer hole was aligned with the threaded holes.

Before proceeding with testing, it was essential to figure out how many and what type of bolts would be needed to secure the equipment. Taking advantage of the SSL material inventory and the constraint on the maximum floor's thickness, a Stainless Steel 18-8 1/4" by 3/4" or M6-1.0 by 20 mm long hexagonal bolt was picked. The hexagonal shape allowed the use of tools available in the SSL, such as a hollow shaft nut driver, which was used during testing to help the divers screw in the bolts.

Once the bolt material was chosen, the next step was to perform a preliminary threaded bolt shear and tensile analysis given the maximum loads one unit can hold before failure, considering one piece of the testing equipment under both lunar and micro-g environments. The toilet, 71 cm tall, occupying 0.18 m^3, and weighing 52.2 kg [133], was chosen for this study. Out of the three testing equipment, the toilet was the most likely to tip when experiencing an applied load at its maximum height. Once the testing object was determined, the worst-case scenario was included in the analysis. That is a male astronaut pushing the toilet at the height of 71 cm with a force of 450 N, the average maximum average force an individual can exert under these conditions [134]. From the summarized results in Table 24, it was clear, with an average safety factor of 20, that the actual loads were considerably smaller than their maximums, making it safe to use one bolt on each corner to ensure stability.

Table 24: Results from Bolt Threaded Analysis

Gravity	**Tensile Force [kN]** $T_{max} = 9.9$	**Shear Force [kN]** $V_{max} = 8.9$
Lunar	0.5	0.4
Micro-g	0.6	0.4

The tensile strength of a Stainless Steel 18-8 1/4" by 3/4" is 70 ksi [135]. Subsequent calculations can be found in the appendix.

The previously mentioned analysis allowed the team to move forward, designing a testing procedure for both lunar and micro-g and deciding what metrics would be recorded, namely, the time to complete the test and the feedback from the test subjects through the TLX form.

In both micro-g and lunar tests, two test subjects were used to secure the equipment. However, it is essential to note that, due to the nature of the micro-g environment, one diver had to hold the structure in place while the other would bolt each corner down. This situation did not occur during the lunar test, where both divers could follow the original test procedure, whose outline can be seen below.

Test Procedure for Securing Equipment:

1. Test monitor starts stopwatch
2. Diver navigates to nearest corner of PVC structure (if in micro-g utilize handrails on floor).
3. Diver moves 1/4" by 3/4" long hexagonal bolt out of container to outer hole of 1-1/2" Rigid 2-Hole Conduit Straps with right hand.
4. Diver uses left hand to push conduit strap flush with the floor and aligned with the hole.
5. Diver uses right hand to screw in bolt as much as possible using hex hollow shaft nut driver.

6. Diver navigates to the right most corner unless that corner has already been bolted down (if in micro-g utilize handrails on ceiling and floor).

7. Repeat steps 3 – 5 until all corners are bolted down

8. Test monitor stops stopwatch

4. Line Integration - Aidan Sandman-Long

Once the equipment has been properly secured by the astronauts the next step they undertake is securing all air, water, power, and data lines. In the core, there are separate sources for each of these different lines that will have respective tubes and cords that can be extended from the source to the equipment. For each piece of equipment that is moved out of the core, the astronaut will have to connect all the different lines that are needed in order for it to work. Once this is complete they will then have to secure the lines to handrails on the floor in micro-g and to handrails on the ceiling in lunar gravity. The lines will primarily be secured with Velcro straps. These Velcro straps will be placed such that the load is evenly distributed and the wires are kept taut. The number of Velcro straps needed per wire will be determined by the maximum weight of the lines and the maximum load each strap can hold. Although the loads from these cables and fluid lines should be minimal compared to the load that the floor panel will endure from housing the actual systems, the total weight in surface environments such as lunar and martian gravity need to be considered in the stress analysis of the floor panels.

In micro-g, the maximum weight of the lines is irrelevant so the positioning of the Velcro straps to secure the lines will be focused exclusively on keeping the lines taut. In lunar gravity, the maximum weight of the lines plays a factor in how many Velcro straps are needed to hold all the lines. Velcro straps are rated to hold 2.3 kg [136] so it is necessary to ensure the total weight of all lines, including anything that would be in the lines such as water, does not exceed this value. A volumetric and weight analysis was performed to determine the approximate total weight per meter that would need to be secured and how large the lines would be. The results can be seen in table 37 below.

Table 25: Line Weight and Volume Analysis

Type of Lines	**Diameter [cm]**	**Weight/length [kg/m]**
Power (16 gauge wire)	0.8	0.09
Data	0.2	0.04
Water	1	0.3
Small air	1.3	0.2
Large air	15	0.4
Total		1.0

The Diameter and weight per length of each line [137] [138] [139] [140]

The results of the volumetric and weight analysis established with a safety factor of two, one Velcro strap would be able to hold up over a meter of all the lines which were the guidelines followed when deciding where the lines would be attached to the handlebars.

For the purposes of testing, it was important to have realistic lines that would represent the size and maneuverability of the cords and tubes that would be used by the astronauts. The power and data lines were simulated by an extension cord with a 3D printed connector at the end for attachment to the simulated equipment. The water and small airline were represented by a hose with a quick connect end piece. The large airline was represented by a gutter tube with a gutter connector end piece.

The line securing test was only completed for the large equipment, as attaching lines to any deployed structure should be of the same difficulty. A panel with the connectors attached to it was secured to the side of the PVC structure facing the core. A single diver would start at the secondary structure and follow the outlined procedure below. Two separate divers performed this procedure in both micro-g and lunar gravity. Time to complete and TLX data were recorded after each test.

Test Procedure for Line Securing

1. Testing monitor starts stopwatch.
2. Diver grabs the designated line attached to the secondary PVC structure in the core. Start with black extension cord.
3. Diver navigates towards large PVC structure area where the line needs to be attached while holding designated line.
4. Diver connects line into designated connector.
5. Diver navigates back to secondary structure.
6. Test monitor clicks lap on stopwatch.
7. Repeat steps 2 – 6. The second designated line to be used is the copper piping tube and the third is the large black tube.
8. Diver attaches all 3 designated lines to all handrails (end part closest to the core) to ceiling panel between PVC structure and core using Velcro strap.
9. Diver attaches designated line to the top of the inner core bar in line with the handrail and PVC structure using Velcro straps.
10. Diver assesses if more Velcro straps are needed to be attached designated line in order to fully secure the lines to the core structure.
11. Test monitor stops stopwatch.

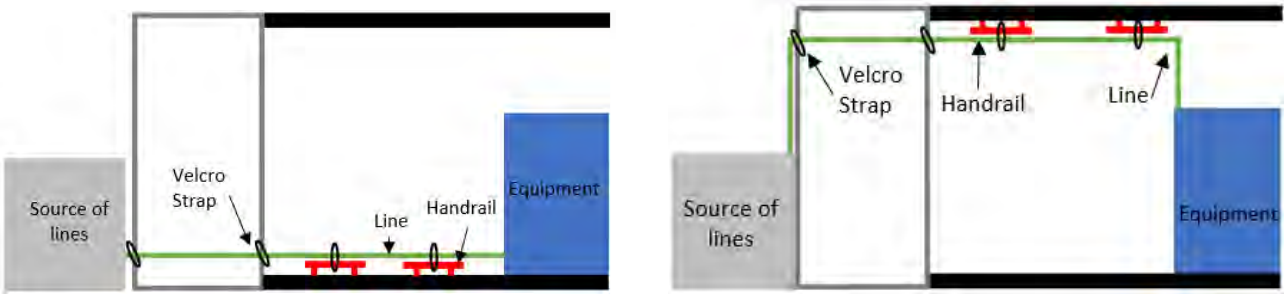

Figure 121: Graphic representation of line securing testing setup in micro-g (on the left), and lunar gravity (on the right).

C. Test Results

1. Micro Test - Ronak Chawla and Ryan Allegro (Movement), Alberto Garcia-Arroba (Securing), and Aidan Sandman-Long (Line securing)

On April 15, 2022, a test to simulate the deployment of key subsystems in micro-g was conducted in the Neutral Buoyancy Research Facility at the University of Maryland. From the test, subjects were able to provide a quantitative assessment using the NASA Task Load Index (TLX) [141] on a scale of 1 to 10 for each of the tasks related to outfitting the inflatable volume of a habitat (10 representing the rating for the most difficult deployment). The time it took the divers to complete each step of the deployment of key subsystems test was recorded and used to determine an approximate time to deploy the rest of the habitat equipment.

The testing followed a 3-step procedure: move the equipment to the designated location, secure the equipment, and attach utility lines to the equipment. The equipment used in the test consisted of three PVC structures, a small structure with a volume of 0.18 m^3 and a mass of 68 *kg*, a medium sized structure with a volume of 0.29 m^3 and a mass of 127 *kg* and a large structure with a volume of 1.29 m^3 and a mass of 169 *kg*. The small, medium and large PVC structures are an approximate representation of the waste management compartment, the advanced plant habitat, and a standard instrumentation rack, respectively.

The time it took the divers to maneuver the small, medium and large PVC structures outside of the core, orient them correctly, and align them with the designated securing location were 47, 35 and 68 seconds, respectively. The designated location was the same for all three sized structures in order to keep the experiment controlled. A possible explanation for the larger time for moving the small equipment versus the medium sized is that the divers faced a learning curve as the small was tested first. Based on the results of the TLX shown in Figure 33, the large sized equipment was the most demanding across all categories.

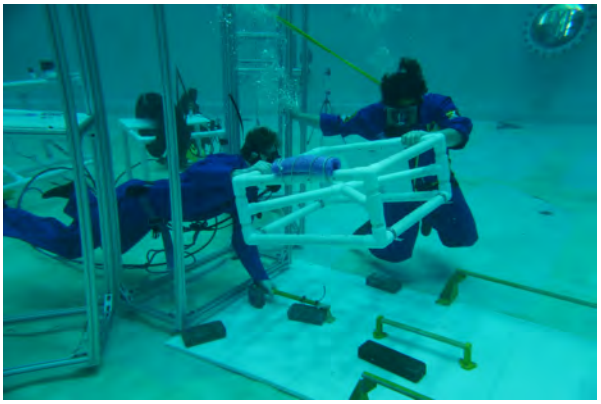

Figure 122: Images from the micro-g test. Divers are shown maneuvering the small and large pieces of equipment out of the simulated core to the securing site, representing the first step in the testing procedure.

Table 26: micro-g Movement Testing Data

Payload Size	**Movement time [sec]**
Small	47
Medium	35
Large	68

Table 27: micro-g Movement Testing TLX

Type of Demand	**Small**	**Medium**	**Large**
Mental	1.5	2.5	3.5
Physical	3	2.5	3.5
Temporal	3	3	4
Performance	1.5	2	3
Effort	3	2	4.5
Frustration	2.5	1.5	4.5

TLX data for Movement Testing in micro-g. Rated on a scale of 1-10.

The securing equipment test followed the same procedure across all three sized equipment where one diver was instructed to use bolts and secure them into the threaded holes, and the other had to hold the PVC structure in place. As discussed in the securing methodology section, each equipment used a total of four bolts, one on each corner. The time it took per bolt to align the conduit strap with the labeled holes and secure each testing equipment is displayed in Table 28. The reason for the medium PVC structure taking longer to secure than the large and small one may be explained in their base area size or the fact that the medium one was not perfectly neutrally buoyant. The second test in lunar gravity conditions would resolve this duality if the relationship held, as the buoyancy issue would not be present because of the addition of weights.

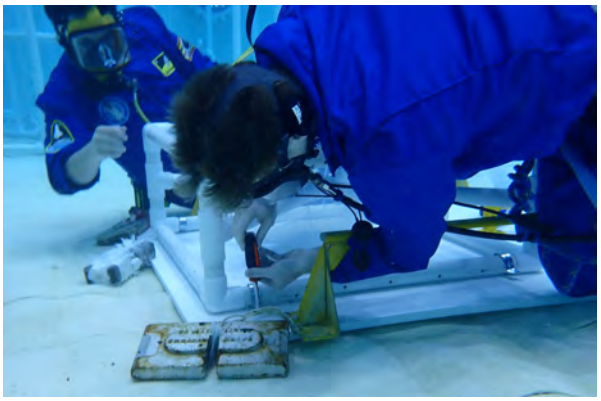


Figure 123: Divers are securing down the equipment, representing the second step in the testing procedure.

Table 28: micro-g Secure Equipment Testing Data

Payload Size	**Secure testing time per bolt [sec]**
Small	23
Medium	45
Large	33

Table 29 shows the average TLX data across the three PVC structures for both divers. As it was expected, the bolter duties were more demanding and frustrating than the holder's. During debrief, the test subjects mentioned the medium and large equipment were not perfectly neutrally buoyant, which increased their frustration, and temporal demand of their respective tasks. For future work, in search of decreasing the divers' demands, it would be interesting to see if switching roles between bolter and holder results in lower TLX ratings. That is, during this test, the same diver was used to secure every PVC structure, which may directly impact their frustration and levels throughout the test.

Table 29: micro-g Secure Equipment Testing TLX

Type of Demand	**Bolter Rating [1-10]**	**Holder Rating [1-10]**
Mental	3	1
Physical	4	2
Temporal	4	3
Performance	3	2
Effort	4	1
Frustration	4	2

TLX data for Secure Testing in micro-g. Rated on a scale of 1-10.

Line securement testing in micro-g was performed by two different divers. The average time it took for both divers to complete the different parts of this test can be seen in the table below. The time it took to attach each line was between 40 to 45 seconds. The preliminary data would suggest that in micro-g the type of line being secured did not have a significant change in time to attach it to the piece of equipment. The largest amount of time in the whole process of line securement was devoted to the securement of the lines to the handrails leading back to the core. As a result future work looking into cutting down total time would best be applied to this part of the test. Based on comments from the divers, possible improvements include a different placement and modification of the handrails lower to the ground to allow for use as footholds and changing the straps used to secure lines to the handrails.

Table 30: micro-g Line Testing Data

Type of Lines	**Line testing time [sec]**
Water/small air	41
Large air	40
Power/Data	45
Secure	162

Time elapsed to connect all lines and secure to handrails.

The TLX results for line securement testing indicate that the divers had the most difficult time during this portion of the testing. In particular temporal demand was given an average rating of 4.5 out of 10 which was the highest across all of the testing. In micro-g, the lines tended to drift around which added a time pressure for our divers. When configuring the design and procedure in the future, more crew ergonomics measures will be included such as additional Velcro straps closer to the start of the line, and possible securement of individual lines instead all at once to decrease temporal demand.

Table 31: micro-g Line Testing TLX

Type of Demand	**Rating [1 - 10]**
Mental	3.0
Physical	2.5
Temporal	4.5
Performance	2.5
Effort	3.5
Frustration	3.5

TLX data for Line Securement Testing in micro-g. Rated on a scale of 1-10.

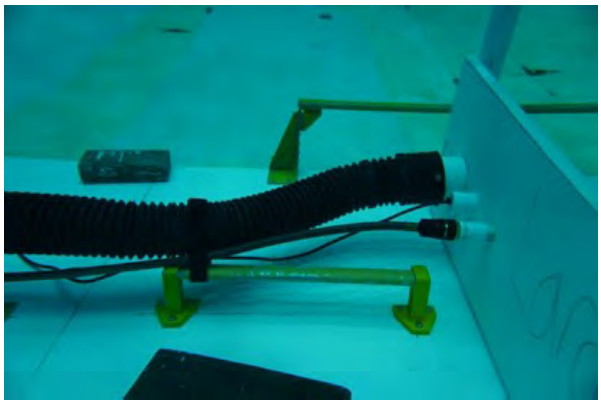

Figure 124: Images from the micro-g test. Diver is attaching utility lines to the equipment, representing the third step in the testing procedure.

2. *Lunar Test - Ronak Chawla and Ryan Allegro (Movement), Alberto Garcia-Arroba (Securing), and Aidan Sandman-Long (Line securing)*

On April 30, 2022, a test to simulate the deployment of key subsystems in lunar gravity was conducted in the Neutral Buoyancy Research Facility at the University of Maryland. This test was designed to obtain results of similar fidelity and allow for fair comparison of results between the micro-g environment (test earlier) and the lunar environment. To configure the test for lunar gravity, small modifications were made from the micro-g test. For example, the

divers had to be weighted to experience lunar gravity in the Neutral Buoyancy Research Facility. Similarly, the test equipment of the physical size and shape was also weighted accordingly. A significant change from the micro-g test was that the lunar test also featured a ceiling which was a part of the floor panel deployment described earlier. The ceiling was represented by the panel from the floor above. This allowed the divers to simulate attaching and running cables and wires along the ceiling rather than along the floor as the design initially intended. It is also important to note that in the actual habitat design, the ceiling would stand at approximately 8 feet high; however, due to the height limitations of the test racks, in the lunar test, the ceiling (floor panel) was 6.5 feet above the floor. Some additional changes to note that were made as a result of recommendations by the divers from the micro-g test were improved positioning and lengths of the handrails.

The time it took two divers to maneuver the small, medium and large PVC structures outside of the core, orient them correctly, and align them with the designated securing location were 19, 24 and 53 seconds, respectively. The time it took a single diver to move the small PVC structure was 20 seconds. That is, having two divers move the equipment versus one diver barely altered the time for the small-sized equipment. Similar to the micro-g test, the results of the TLX stated that the large sized equipment was the most demanding across all categories.

Figure 125: Images from the lunar test. Divers are moving the equipment out of the simulated core to the securing site, representing the first step in the testing procedure.

Table 32: Lunar gravity Movement Testing Data

Payload Size	**Movement time [sec]**
Small	19
Medium	24
Large	53

Table 33: Lunar gravity Movement Testing TLX

Type of Demand	**Small Solo**	**Small Duo**	**Medium**	**Large**
Mental	1	1	2	3
Physical	1.5	1	3.5	3.5
Temporal	1.5	1	2.5	3
Performance	1	1	2	2
Effort	2	1	2.5	4
Frustration	1.5	1	2.5	2.5

TLX data for Movement Testing in Lunar gravity. Rated on a scale of 1-10.

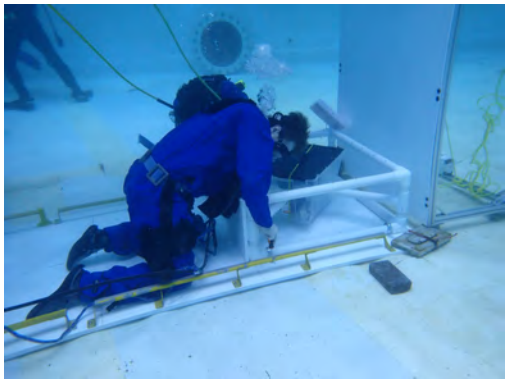

Figure 126: Image from the lunar test. Divers are securing down the equipment, representing the second step in the testing procedure.

The securing equipment test followed the same procedure as the one in micro-g. However, this time, the second diver also had to screw the bolts in, rather than having to hold the structure down to the floor. An extra test was done on the small PVC structure, using only one diver for bolting the equipment. The goal with this added trial was to replicate the conditions experienced in micro-g, where only one test subject was responsible for bolting the corners. The obtained time per bolt was 34 seconds, taking longer than the micro-g case by 11 seconds. Thus, concluding that the figure of the holder in micro-g greatly influenced the results of the tests, and that another diver would be needed in lunar to make it closer to the process the astronauts in the TransHab will undergo. Adding a second diver to help bolt down the the small PVC structure reduced the time to 17 seconds per bolt. The following tests for the medium, and large PVC structures used two divers, and the results are summarized in Table 34. As in the micro-g dive, the medium payload size took the longest to secure, followed by the large one and the small one. Thus, suggesting the linear correlation found in micro-g between equipment base area and secure time per bolt holds regardless of the gravity environment.

Table 34: Lunar gravity Secure Equipment Testing Data

Payload Size	**Secure testing time per bolt [sec]**
Small	17
Medium	34
Large	21

The TLX data for the secure equipment testing in lunar gravity is displayed in Table 35. In micro-g, the purpose

was to distinguish between the bolter and holder duties, and the data obtained for each of them could be averaged across the three PVC structures since the variation on the TLX ratings was minimal. However, this was not the case for lunar gravity, where the PVC structure being tested heavily impacted the feedback received from the divers. Based on the obtained TLX data, and the effort and frustration ratings, the divers had more difficulties to secure the medium structure than the small and large one. An explanation for this phenomenon, along with a direct comparison between lunar and micro-g TLX data will be included in the extrapolation of data section.

Table 35: Lunar gravity Secure Equipment Testing TLX

Types of Demand	**Small Solo**	**Small Duo**	**Medium**	**Large**
Mental	1	1	2.5	2
Physical	2	1	3	2.5
Temporal	3	1.5	2.5	2.5
Performance	1.5	1	3.5	2
Effort	3	1.5	4	2.5
Frustration	2.5	2	4	2

TLX data for Secure Equipment Testing in lunar gravity. Rated on a scale of 1-10.

Similar to the micro-g test, the line securing test was only completed for the large equipment. Unlike the micro-g test results, the time it took to attach each line was very dependent on the diver and the nature of the line or connection. For example, it took the first diver approximately 44, 56 and 109 seconds to attach the power/data, water, and air lines respectively. However, it took the second diver approximately 35, 47 and 61 seconds to attach the power/data, water, and air lines respectively. A similar trend could also be seen with time it took to secure to the handrails on the ceiling. The first diver completed the task in 242 seconds compared to the second diver in 152 seconds. The results can be seen in the table below.

Table 36: Lunar gravity Line Testing Data

Types of Lines	**Diver 1 Line testing time [sec]**	**Diver 2 Line testing time [sec]**
Power/Data	44	35
Water/Small air	56	47
Large air	110	61
Secure	242	152

Time elapsed to connect all lines and secure to handrails.

Based on the TLX data, the second diver also found it much easier and less demanding to do the line securing test than the first diver. One possible justification for this result is that the diver that had a much faster time and lower TLX ratings is approximately 5 inches taller than the other diver. That is, the taller diver most likely had an easier time reaching the ceiling and securing the line. For future testing the use of something to increase the height of divers such as a step stool could be used to remedy this trend.

Table 37: Lunar gravity Line Testing TLX

Types of Demand	**Diver 1 Rating [1-10]**	**Diver 2 Rating [1-10]**
Mental	4	3
Physical	3	2
Temporal	6	2
Performance	2	2
Effort	4	2
Frustration	6	2

TLX data for Line Securement Testing in lunar gravity. Rated on a scale of 1-10.

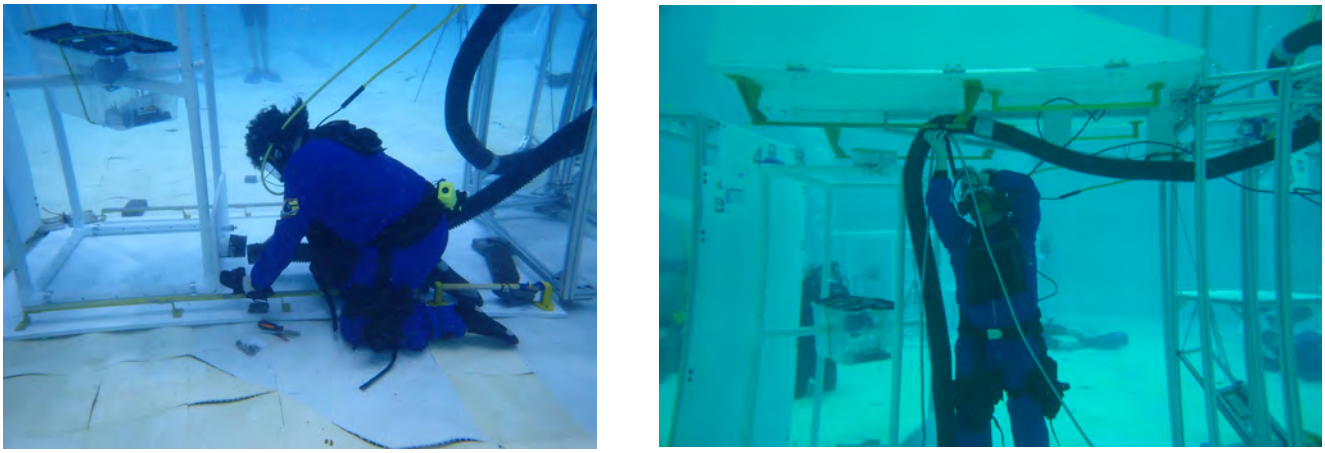

Figure 127: Images from the lunar test. Diver is attaching utility lines to the equipment, representing the third step in the testing procedure.

After discussing results with the divers, they both agreed that they found it easier to test in lunar gravity as compared to micro-g. Additionally, the divers found it easier to move around along the floor in lunar gravity rather than having to monkey-bar and climb in micro-g. The results support the divers' statements, as the times to complete the movement and secure tests were much lower in lunar gravity.

Due to the nature of the tests and its extensive preparation, there was only time to conduct two trials for each equipment (small, medium and large sized). Future testing is required to corroborate the results.

D. Extrapolation of Data

1. Movement - Ryan Allegro

After the tests in the Neutral Buoyancy tank, the timing data was extrapolated to the rest of the habitat equipment to estimate the total time of movement in both micro-g and lunar gravity environments. In all tests, the starting and ending place of the structures was kept consistent. The distance that the actual equipment needs to be moved was determined based on where the equipment in going to be placed in the habitat. The other key factor in movement time was the size and weight of the structures. Larger and heavier objects took longer to move than small and light ones.

For the micro-g test, the small structure took 29 seconds to deploy, the medium took 35 seconds, and the large took 68 seconds. For the lunar gravity test, the small took 19 seconds to deploy, the medium took 24 seconds, and the large took 53 seconds. Comparing these times shows that movement in micro-g took longer than in lunar gravity, which can be seen clearly in Figure 128. This holds true with feedback from the divers, who found it easier to move around the simulated environment when they were weighted down and could walk along the floor. When comparing these times with the mass and volume of the PVC structures, a trend can be seen for both micro-g and lunar gravity, which can be seen in Figures 129 and 130. These linear relationships were used to extrapolate this data to all the equipment in the habitat. Looking at the R^2 values show that the Volume appears to be more closely correlated to the movement

time. Mass may also have some correlation, but it is not as clear from our data. Due to the minimal amount of testing that was able to be done leading to the uncertainty of which was the main cause in the time difference, both mass and volume were used to extrapolate to the equipment for micro-g. However, in lunar gravity, the mass actually drops below 0 seconds for anything less than 20 kg. There are a lot of such items in the habitat, so the volume alone was used to extrapolate the data for lunar gravity.

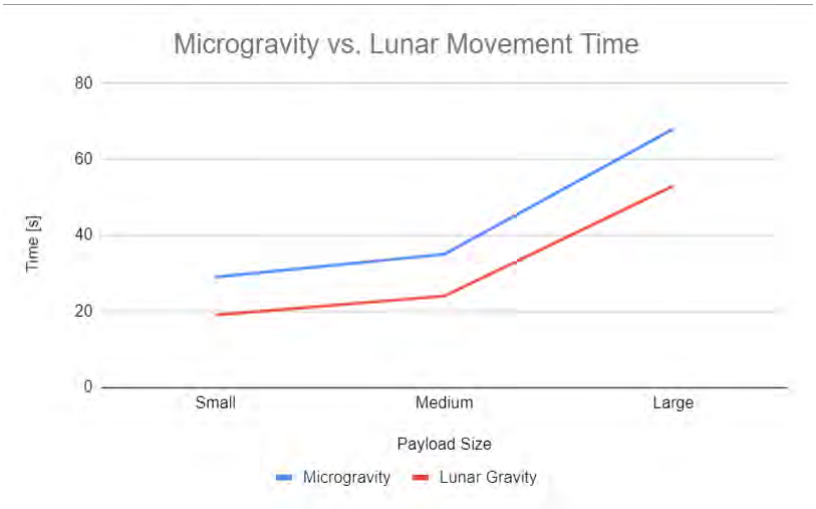

Figure 128: Graph Comparing Microgravity and Lunar Gravity Times for Equipment Movement

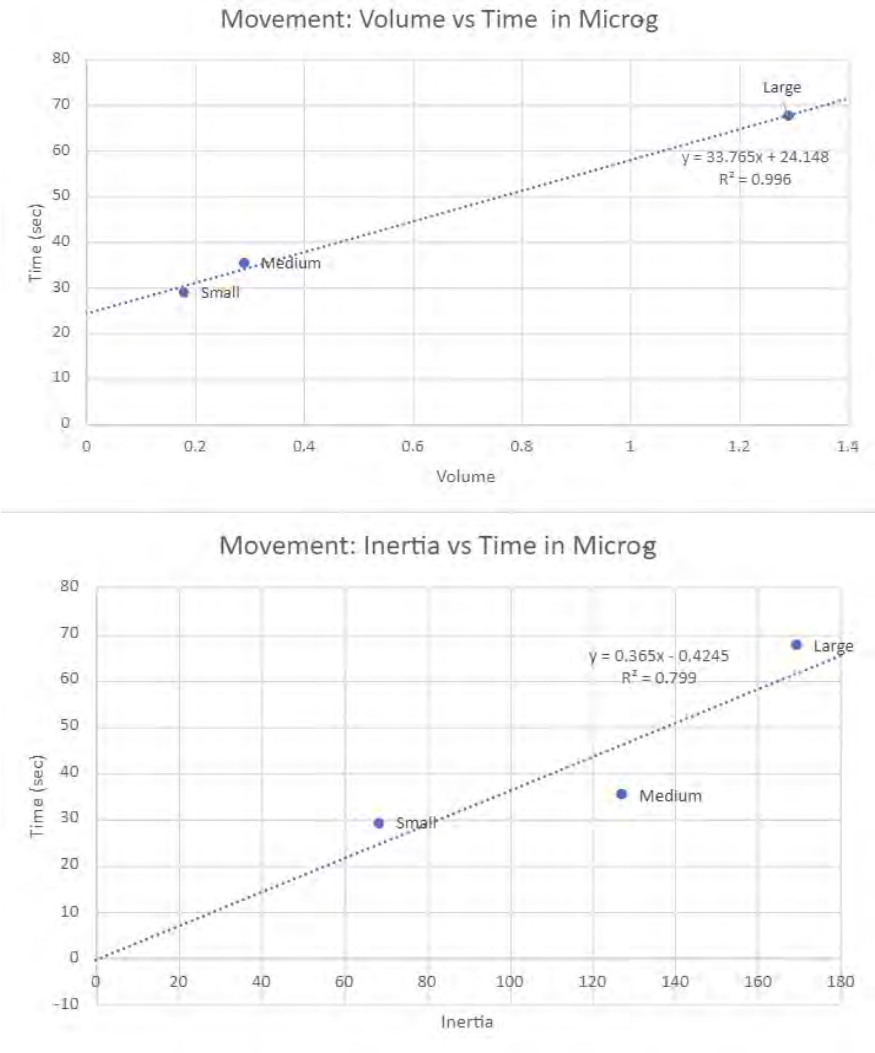

Figure 129: Graphs Depicting Linear Correlations between Volume/Inertia and Movement Time in Micro-g

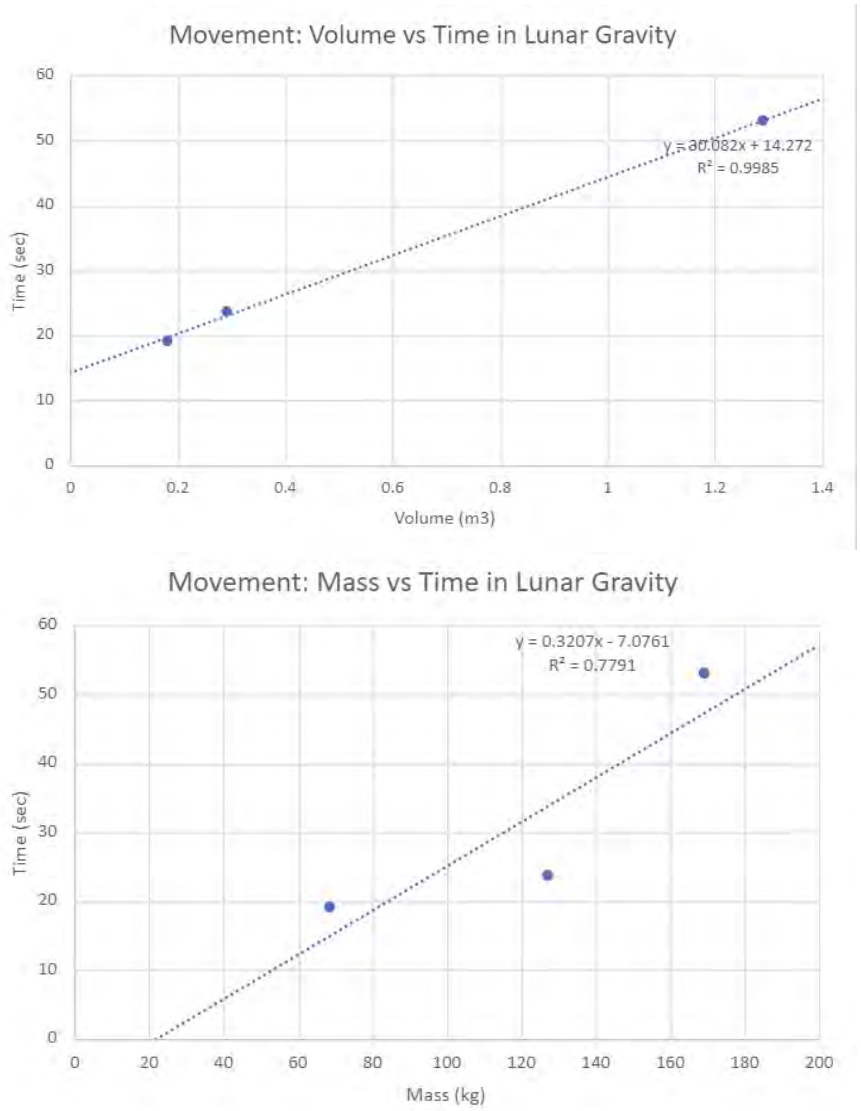

Figure 130: Graphs Depicting Linear Correlations between Volume/Inertia and Movement Time in Lunar gravity

Table 38: Extrapolated Movement Data for Micro-g

System	**Quantity/Trips**	**Distance [*m*]**	**Total Securing Time [*sec*]**
Toilet	2	1.7	51
Sink	1	1.7	21
Wash Stall	2	1.7	46
Treadmill + harness	1	1.7	278
Cycle Ergometer	1	2.5	63
ARED	1	2	321
Storage Cabinet	2	1.7	41
Food Warmer	1	1.8	46
Food Hydration Device	1	1.8	92
Refrigeration Unit	1	2.4	31
Plant Production Unit: Veggie	1	1.8	23
Advanced Plant Habitat	1	1.8	71
Table	1	2.7	37
Desk	6	2.8	225
Chair	12	2.1	343
Astronaut Suits	4	3.1	177
Glovebox	1	3.3	44
CTBs	1	3.6	4789
		Total [sec] Total [hr]	6701 1.9

Table 39: Extrapolated Movement Data for Lunar Gravity

System	**Quantity/Trips**	**Distance [*m*]**	**Total Securing Time [*sec*]**
Toilet	2	1.7	25
Sink	1	1.7	10
Wash Stall	2	1.7	27
Treadmill + harness	1	1.7	292
Cycle Ergometer	1	2.5	51
ARED	1	2	402
Storage Cabinet	2	1.7	53
Food Warmer	1	1.8	21
Food Hydration Device	1	1.8	33
Refrigeration Unit	1	2.4	15
Plant Production Unit: Veggie	1	1.8	11
Advanced Plant Habitat	1	1.8	29
Table	1	2.7	16
Desk	6	2.8	101
Chair	12	2.1	205
Astronaut Suits	4	3.1	68
Glovebox	1	3.3	19
CTBs	1	3.6	2226
		Total [sec] Total [hr]	3604 1.0

When looking at the TLX results for micro-g, shown in Figure 131 below, it is noticeable that there is not much change between the small and medium payloads. In fact, the average TLX result actually decreases slightly from 2.4 to 2.3. This could be explained by the similar volumes and shapes of the two structures. The two heights are within 3cm of one another, and the base lengths are within 15cm of one another. The main difference between the two is the extra water that the medium carries to represent a higher inertia. What this could point to is that the TLX in micro-g is more closely related to the volume of the object, not the inertia. Meaning objects with similar volumes will have similar TLX results. This would mean that when there is little change in volume between objects, like between the small and medium payloads, there is little change in TLX result, but when there is a big change in volume, like the large object compared to the others, the average TLX result increases.

The lunar gravity TLX results points to a different trend. The TLX results appear to move linearly upward, but the first two results are both for the small structure, the first being with both divers, and the second being with one diver. The divers felt it was easier when they were both moving the object. When we look into the trends between objects, we can some other interesting trends. The average TLX results have a bigger jump between small and medium, 1.5 points, than between medium and large, 0.5 points. When we look closer at the structures, we see that the mass changes between objects are almost linear, being 58.7kg between the small and medium, and 42.2kg between the medium and large. While the volume change between objects is not linear, being 0.12m^3 between small and medium, while being 0.85m^3 between medium and large. The TLX results followed a trend more similar to what can be seen in the mass of the objects. This could point towards the TLX being more closely related to the mass of an object, rather than its volume. This would be the opposite of the findings from the micro-g test, where it looked like the TLX results more closely followed the volumes, rather than the masses. Together these two results could mean that in a lunar gravity environment, the mass of an object more closely correlates to the struggles of moving it than the volume. While in a micro-g environment, it is the volume that more closely correlates to the struggles of moving it.

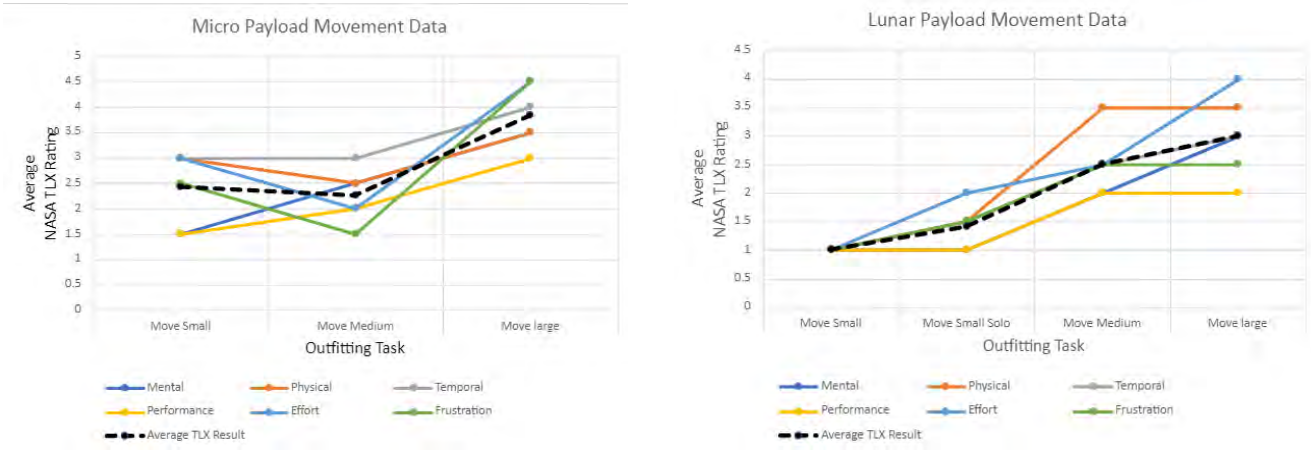

Figure 131: Graphs Depicting Average NASA TLX Rating For Payload Movement Data. Micro-g, on the left, Lunar gravity on the right.

2. *Securing - Alberto Garcia-Arroba*

Once the corresponding dives for micro-g and lunar gravity were performed in the Neutral Buoyancy tank, the obtained timing data was extrapolated to the rest of the systems in the TransHab that need to be unpacked and secured out of the core. To do this, the average time per bolt was used, considering how many units of each system would be in the TransHab, and assuming every structure would have one bolt on each corner, for a total of four. The average time per bolt was found to be 34 seconds for micro-g, and 24 seconds for lunar gravity. Once the securing time was known for every single piece of equipment, the total securing time was calculated. The results are displayed in Table 40, for micro-g, and in Table 41, for lunar. Thus, it would take approximately 1.5 hours to secure all the systems in micro-g and 1.0 hours in lunar gravity. As will be explained in the following paragraph, extrapolation using the average securing time per bolt serves as a good estimate to acknowledge and compare the difference in total securing time between the two gravity conditions but is not as accurate as using the equipment base area.

Table 40: Extrapolated Securing Data for Micro-g

System	Quantity	Total Securing Time [sec]
Toilet	2	269
Sink	1	134
Wash Stall	2	269
Treadmill + harness	1	134
Cycle Ergometer	1	134
ARED	1	134
Storage Cabinet	2	269
Food Warmer	1	134
Food Hydration Device	1	134
Refrigeration Unit	1	134
Plant Production Unit: Veggie	1	134
Advanced Plant Habitat	1	134
Table	1	134
Desk	6	806
Chair	12	1612
Astronaut Suits	4	537
Glovebox	1	134
All Equipment	Total [sec] Total [hr]	5239 1.5

Table 41: Extrapolated Securing Data for Lunar Gravity

System	Quantity	Total Securing Time [sec]
Toilet	2	190
Sink	1	95
Wash Stall	2	190
Treadmill + harness	1	95
Cycle Ergometer	1	95
ARED	1	95
Storage Cabinet	2	190
Food Warmer	1	95
Food Hydration Device	1	95
Refrigeration Unit	1	95
Plant Production Unit: Veggie	1	95
Advanced Plant Habitat	1	95
Table	1	95
Desk	6	569
Chair	12	1139
Astronaut Suits	4	380
Glovebox	1	95
All Equipment	Total [sec] Total [hr]	3700 1.0

The difference in securing time between the two gravitational environments agrees with the pattern found during testing, whose trend line can be shown in Figure 132. During micro-g, one diver had to hold the structure in place while the other bolted all the corners down. However, this situation did not occur during lunar gravity, where the two divers could focus on screwing in the bolts. One relevant aspect to note from Figure 132 is that, in both micro-g and lunar gravity, the medium payload size took longer to be secured than the large one. The explanation for this phenomenon is found in the existing linear correlation between equipment base area and securing time per bolt, as shown in Figure 133. The testing PVC structures had the following base areas: 0.56 m^2 for small, 0.64 m^2 for large, and 0.84 m^2 for medium. Close examination of the R^2 values displayed in Figure 133, it is clear why this relationship between securing time per bolt and base area would result in more accurate extrapolated data than using the average time per bolt between the three payload sizes. However, due to the lack of available information about each equipment's base area, it was not plausible to calculate the total securing time based on this variable.

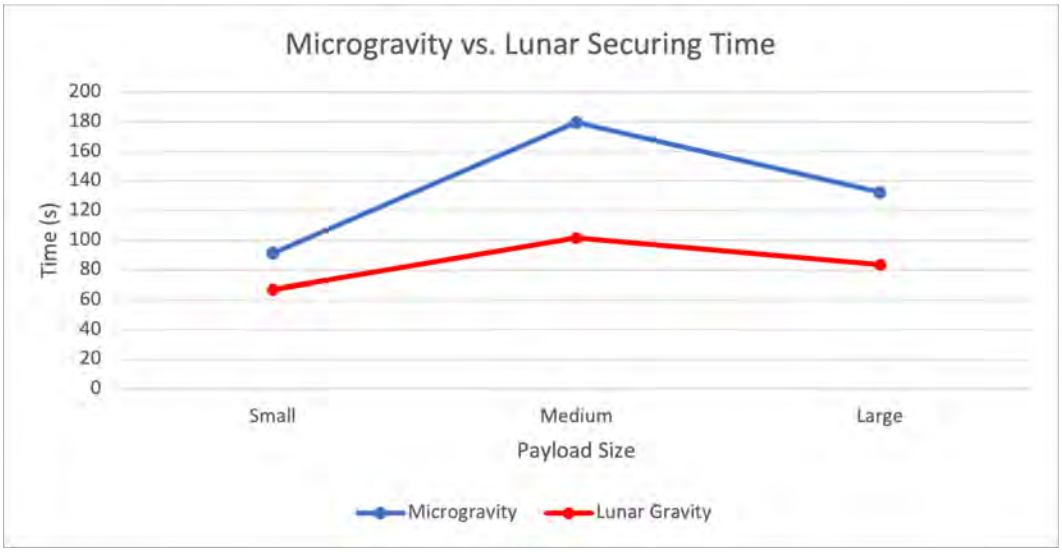

Figure 132: Graph Comparing Micro-g and Lunar Gravity Times for Securing Equipment

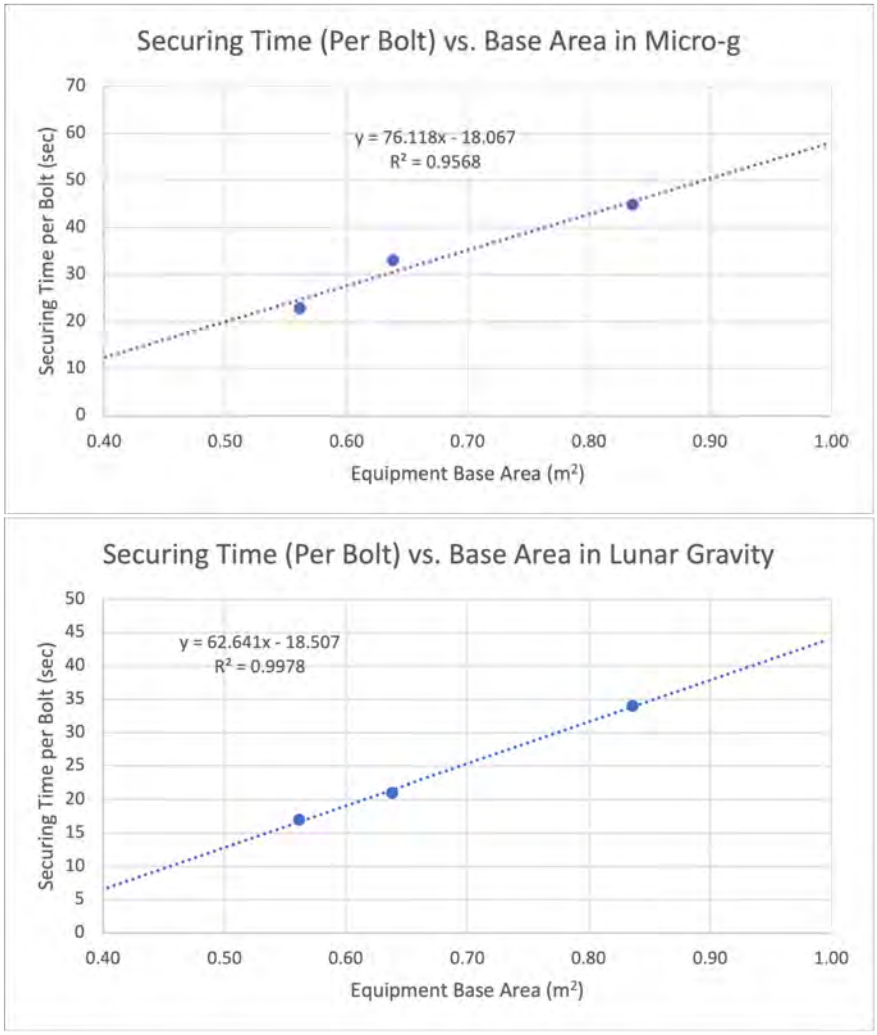

Figure 133: Graphs Depicting Linear Correlation between Base Area and Securing Time per bolt. Micro-g, on the top, Lunar gravity on the bottom

The average TLX data in both micro-g and lunar gravity for securing equipment is shown in Figure 134. From both graphs, it is noticeable that the frustration levels were highest for the medium payload size. During the micro-g dive, testing subjects reported medium was not perfectly neutrally buoyant, which made it harder for them to hold it in place and proceed with securing, affecting their performance. However, this situation did not seem to impact the rest of the parameters involving mental, physical, and temporal demands, where the largest structure ranked higher than both medium and small. During the lunar gravity dive, the higher frustration levels observed in micro-g while securing the medium testing equipment were more acute, extrapolating that annoyance to the rest of the recording parameters. The explanation for this phenomenon is that only two bolts were adequately screwed in, and the third one had to be rotated enough for that corner to be secured. This not only created frustration but it required more mental, and physical effort to finish the procedure. By examining both graphs, it is appreciable the difference in the average TLX trend between the two tests. For instance, the micro-g one shows an almost steady shape, where the same points, 2.7, are allocated for medium and large, and the small one differs by only 0.1, with 2.8 points. In contrast, the average TLX for lunar gravity displays a considerable jump between the medium structure, ranked highest with 3.3 points, with respect to the small and large ones, with 1.3 and 2.3, respectively. Another significant feature to be discussed is how the average trend line of the lunar TLX data follows precisely the one found between equipment base area and securing time per bolt. For future work, it would be interesting to see if this pattern would still hold, assuming no issues were present when securing the medium PVC structure.

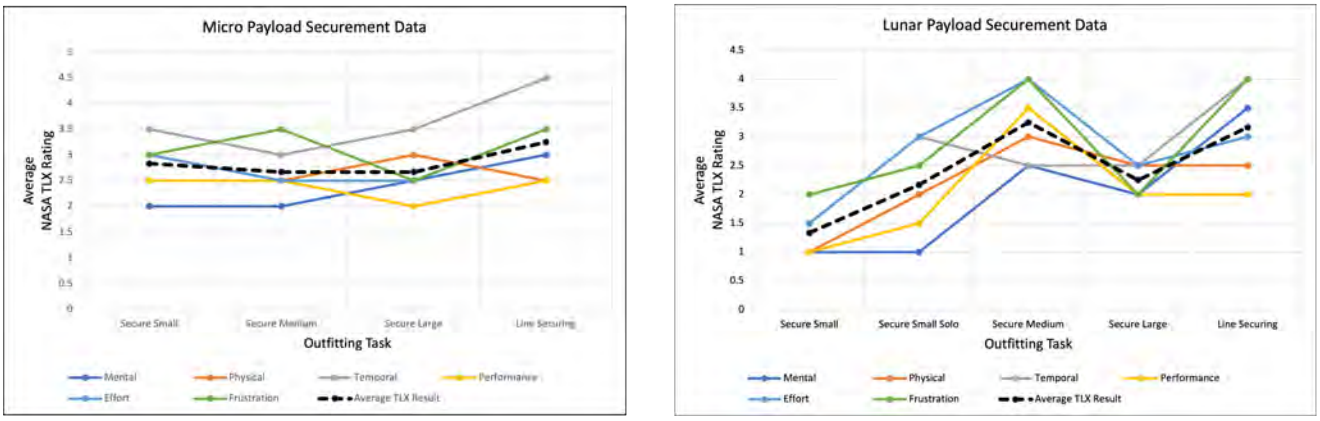

Figure 134: Graphs Depicting Average NASA TLX Rating For Payload Securement Data. Micro-g, on the left, Lunar gravity on the right.

3. Integration - Aidan Sandman-Long

The final part of the data extrapolation estimated the amount of time it would take to secure all water, air, data, and power lines to all equipment that was moved from the core to the inflatable part of the habitat. During testing the time to move each separate line from inside the core, secure it, and then maneuver back inside the core was recorded. In addition, the time to secure all the lines to the designated handrails was recorded. Each of these tests were performed twice in micro-g and twice in lunar gravity. The average of these results were used for data extrapolation.

To accurately extrapolate this data, it is important to account for the distance that lines would need to be run compared to the distance we used for testing. For testing, the divers secured the lines to the large PVC structure 3.3 meters away from the source of the lines. The approximate final location of each piece of equipment was measured from the center of the core to determine the total length that the lines would need to be secured. The center of the core was chosen because the equipment was all moved radially outward in a large enough spread that no matter where the source of the equipment was in the core, the average distance of the equipment from that point would be the same. It is also important to note that not all pieces of equipment required all lines. For all equipment moved outside of the core, it was determined if any water, power, data, and/or which type of airline would be required for the equipment to operate. Given the different lines for each piece of equipment, the time it would take to attach all the correct lines and then secure them to the ground could be calculated and then the resultant would be multiplied by the ratio of actual distance from core over testing distance we used. The results of the extrapolation in micro-g can be seen below on table 42 and in lunar gravity can be seen be seen below on table 43.

Table 42: Extrapolated Line Securing Data for Micro-g

System	Quantity	Total Securing Time [sec]
Toilet	2	297
Sink	1	105
Wash Stall	2	209
Treadmill + harness	1	130
Cycle Ergometer	1	190
ARED	1	152
Food Warmer	2	225
Food Hydration Device	1	135
Refrigeration Unit	1	150
Plant Production Unit: Veggie	1	135
Advanced Plant Habitat	1	182
All Equipment	Total [sec] Total [hr]	1910 0.5

Table 43: Extrapolated Line Securing Data for Lunar gravity

System	Quantity	Total Securing Time [sec]
Toilet	2	349
Sink	1	128
Wash Stall	2	255
Treadmill + harness	1	143
Cycle Ergometer	1	210
ARED	1	168
Food Warmer	2	258
Food Hydration Device	1	157
Refrigeration Unit	1	172
Plant Production Unit: Veggie	1	157
Advanced Plant Habitat	1	207
All Equipment	Total [sec] Total [hr]	2203 0.6

The extrapolation of data from micro-g and lunar gravity testing shows that it would only take approximately 0.5 and 0.6 hours respectively for one astronaut to complete the attachment and securing of all water, data, air, and power lines. The slight increase in time to secure lines in lunar gravity can be attributed to the more difficult task of attaching lines to the ceiling compared to the floor. The preliminary results do suggest that line securement will be the least time intensive part of the total deployment of all equipment and as a result future work should be focused on decreasing the amount of time on other parts of the deployment.

4. Total Deployment - Ryan Allegro

Adding together the extrapolated data for movement, securing, and integration, you get the total estimated time to fully deploy all the equipment. In a micro-g environment it would take 1.9 hours to move everything, 1.5 hours to secure everything, and 0.5 hours to integrate all of the necessary subsystems. This leads to a total estimated time of 3.9 hours. In a lunar gravity environment, it would take 1 hour to move everything, 1 hour to secure everything, and 0.6 hours to integrate all the necessary subsystems. This leads to a total estimated time of 2.6 hours.

Table 44: Total Deployment time

	micro-g	**lunar**
Movement [hr]	1.9	1
Secure [hr]	1.5	1
Integrate [hr]	0.5	0.6
Total [hr]	3.9	2.6

s

XXIII. Appendix

A. Design Iterations - Kelly O'Keefe

1. First Iteration

The first outfitted habitat layout that was proposed consisted of many design decisions that were ultimately changed in the final design. To begin, the core held the crew quarters on the top floor, life support systems on the second floor, and a bathroom on the bottom floor. The core was also used as the primary area for astronauts to ascend and descend throughout each level with a small cut away and a ladder in the core floor structure. This layout is shown in Figure 135. Once more research was conducted to determine how much space was actually needed for both crew quarters and the life support systems, it was determined that there was not enough room in the core to have the ladder placed here, and it instead needed to be in the inflatable volume. We also decided that for safety purposes, the crew quarters should be placed in the center of the core as opposed to the top to keep the crew as far way from the exterior elements as possible.

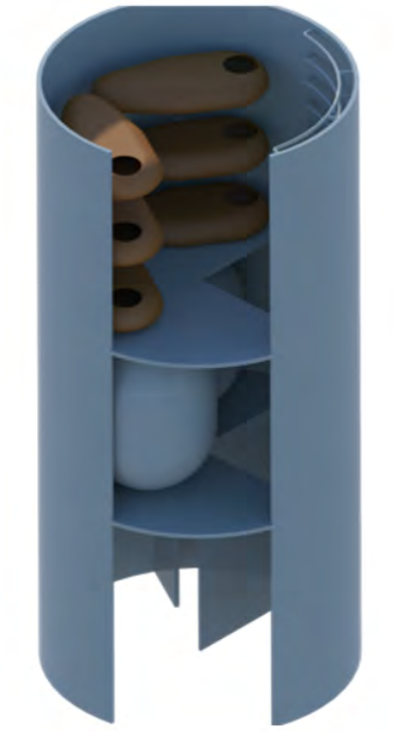

Figure 135: CAD model of the first iteration of the core structure and layout

In this design iteration, the lab was placed on the first floor, the second floor was a dedicated storage space and also housed some electrical systems, and the third floor contained the space for social activities, eating, and exercising. The initial thought process behind these layout decisions was that the lab should be on the bottom floor because it held the heaviest equipment so we wanted to reduce loads on the upper floors. A trade study was also conducted to determine that having one floor of dedicated storage was the most efficient use of the floor space rather than having storage space spread out amongst the habitat. Two floors with storage covering the perimeter of each floor allowed for about 250m^2 of available surface area whereas three floors with all storage on the second floor allowed for about 300m^2 of available floor space. CAD models of this first design iteration are shown in the following figures.

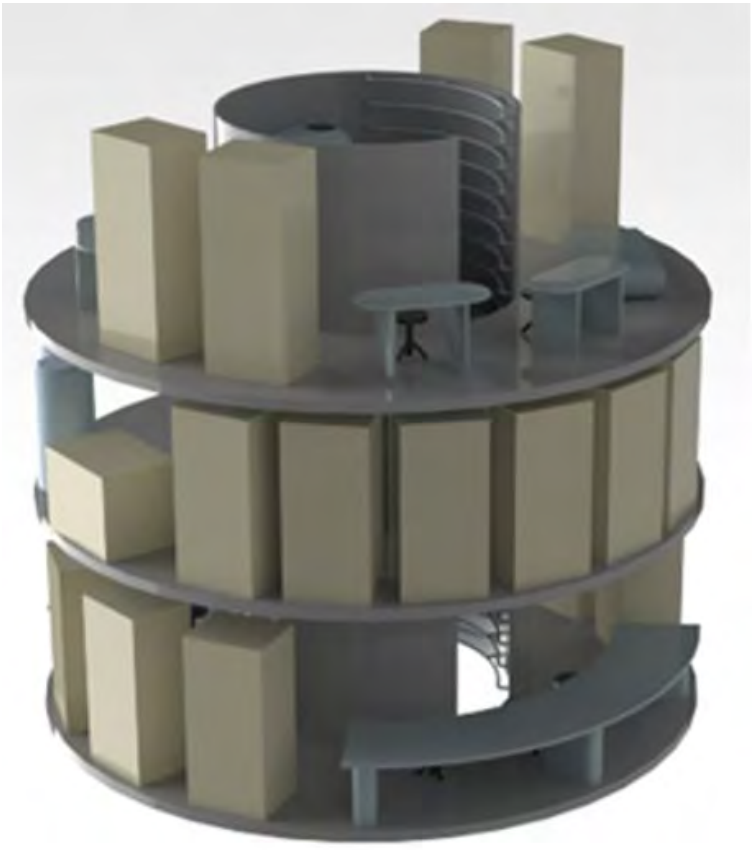

Figure 136: CAD model of the first iteration of the full habitat design

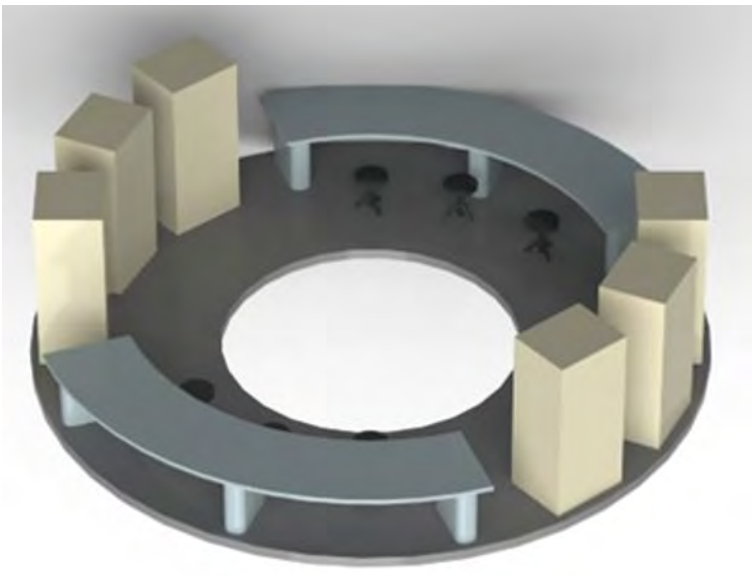

Figure 137: CAD model of the first iteration of the first floor which contained the lab space

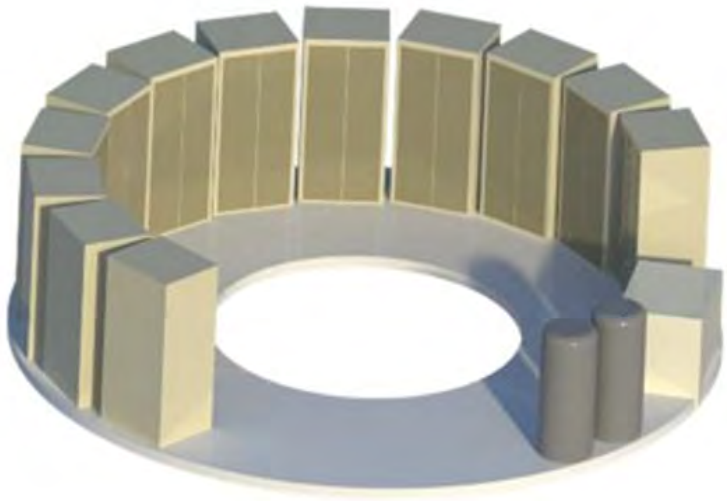

Figure 138: CAD model of the first iteration of the second floor which was dedicated to floor space as well as some electrical systems

Figure 139: CAD model of the first iteration of the third floor which contained space for socialization, eating, and exercising

2. PDR Design

By the time PDR rolled around, we had made significant changes to our first design. As previously mentioned, the method for astronauts to move between floors was taken out of the core and placed in the inflatable volume. A 1/12th of the floor, or 3.06m^2 of surface area, was cut away to allow room for a staircase. A staircase was chosen, because we believed that this would make it easier for the astronauts to carry things between floors as opposed to a ladder. The new full habitat design is shown in Figure 140.

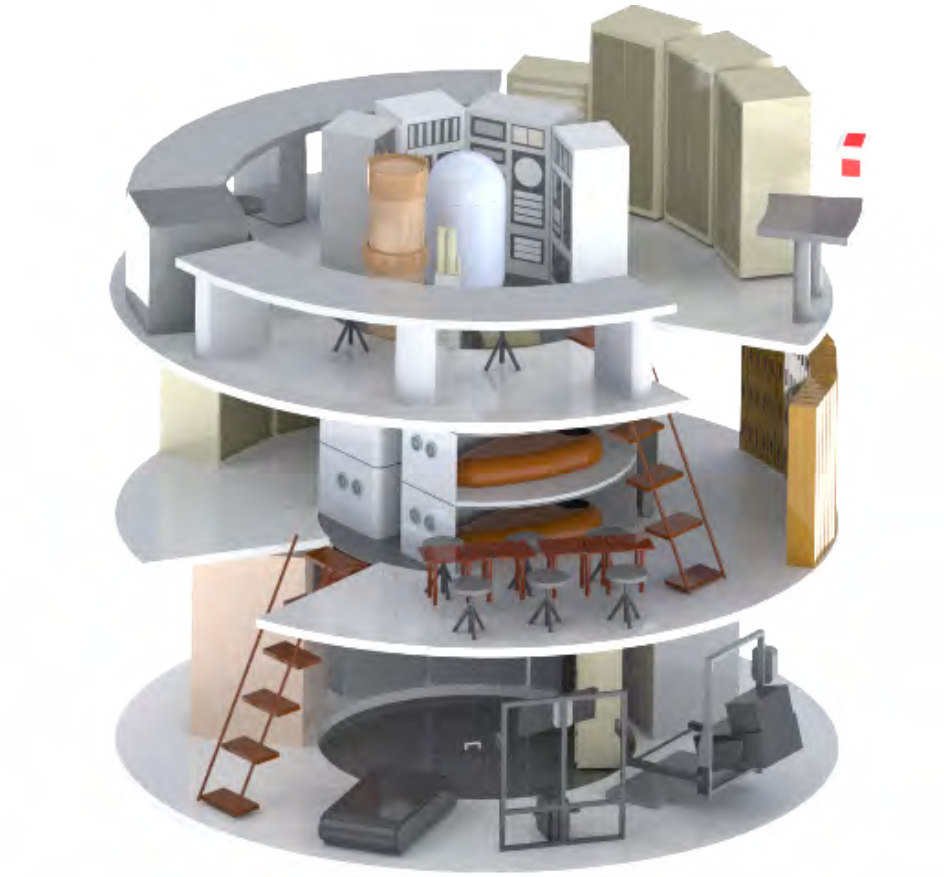

Figure 140: CAD model of the entire habitat design presented at PDR

Additionally, the core now housed all life support systems on the top floor, crew quarters in the middle, and EVA equipment on the bottom. The inflatable volume of the first floor now held the exercise equipment and two bathrooms and two wash stations instead of the laboratory. This decision was made because once we established that the airlock would sit below the first floor core for a surface habitat, we believed that the first floor would be at the highest risk of being contaminated from the the outside. As such, we placed all of our lowest risk items (exercise equipment and bathrooms) on the bottom floor, and moved the lab to the top floor because we did not want any lab equipment being damaged by harmful contaminants. The lab was also moved to the top floor to be the closest to the life support systems. This was done to give the crew ease of access from the lab and its tools to the life support systems that will need constant maintenance throughout the mission. Based on feedback received from PDR, it was determined that the issue of contamination should not have been as big of a concern as we considered it to be because there will be systems in place to effectively mitigate contamination, which is why in our final design the lab was moved back down to the first floor. Finally, instead of a full floor dedicated to storage, the second floor now contained space for food storage, food preparation, and dining. Storage was now allocated throughout the habitat in any available space. CAD models of each floor are shown in the following figures.

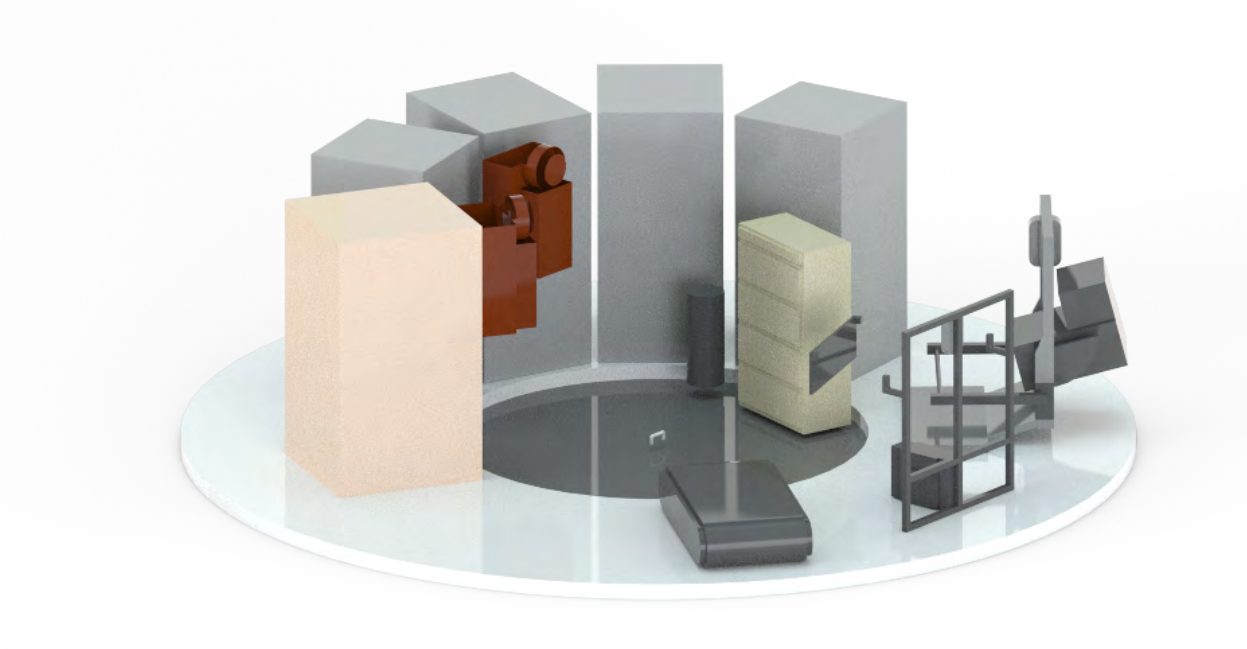

Figure 141: CAD model of floor 1 presented at PDR

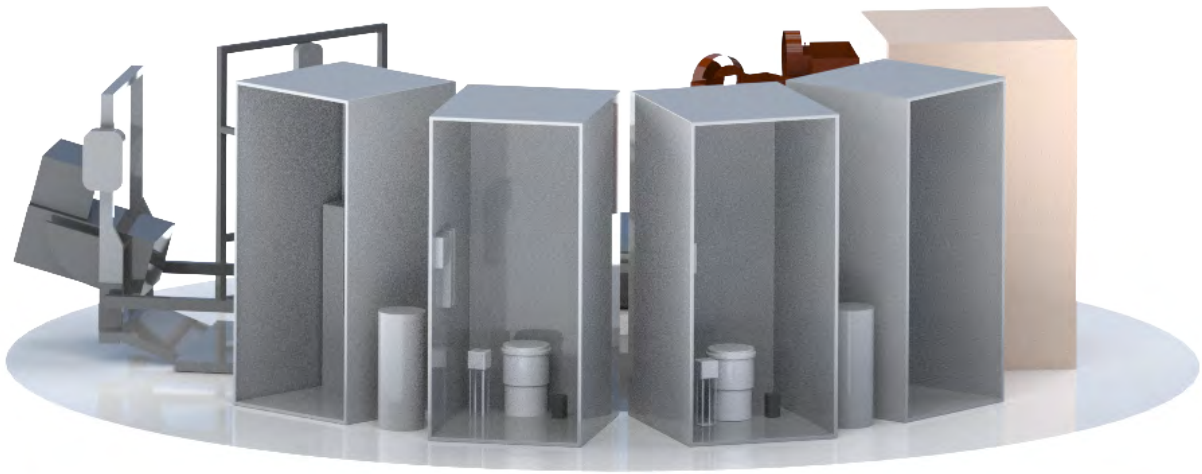

Figure 142: CAD model of floor 1 presented at PDR, shown from an alternate perspective

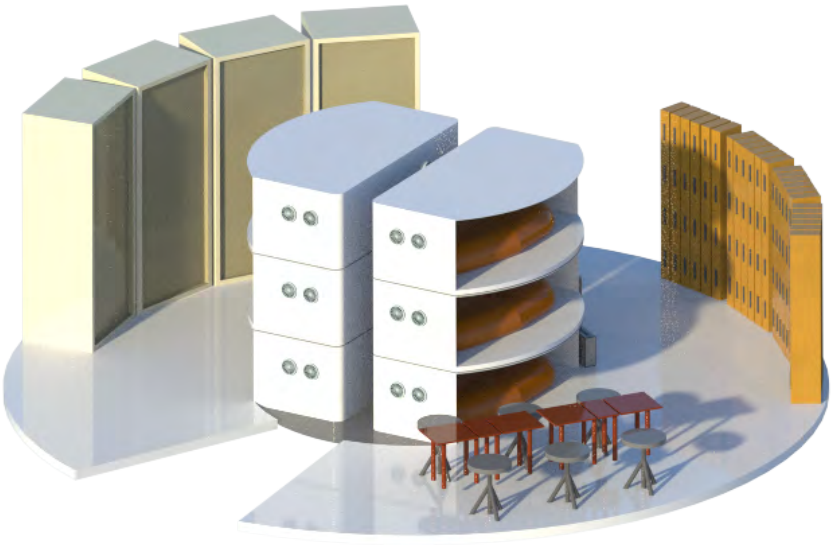

Figure 143: CAD model of floor 2 presented at PDR

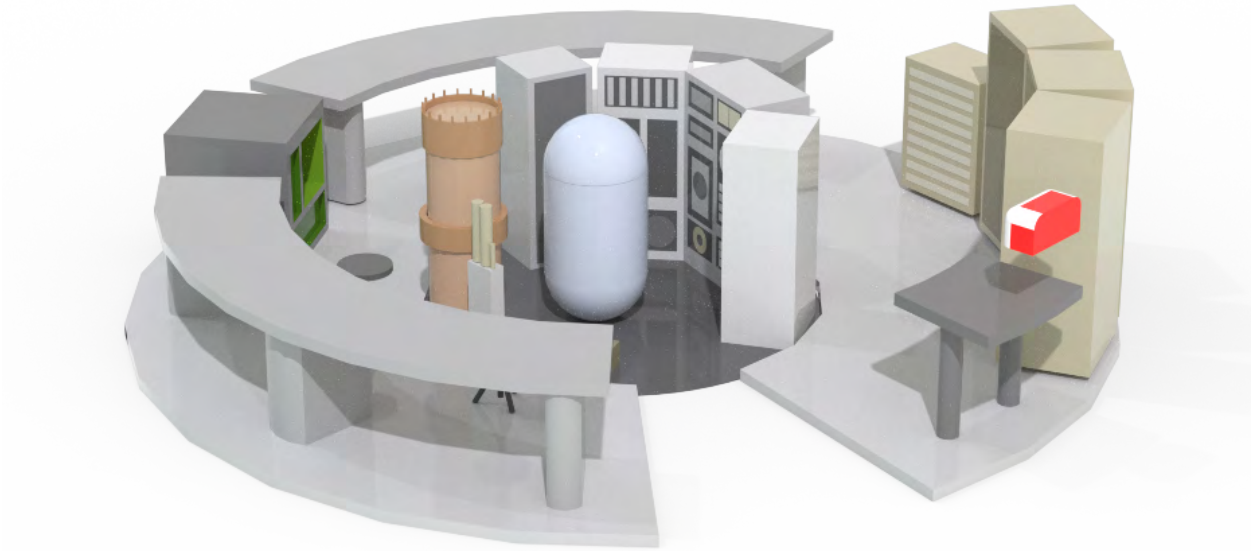

Figure 144: CAD model of floor 3 presented at PDR

B. Equipment Testing in 1g - Elizabeth Myers

For the 1g testing portion of this project, I participated as the test subject in order to assess and give feedback on the testing process prior to the dives. The data collected from these tests was primarily qualitative feedback rather than numerical data, so it was not included with the analysis of the microgravity and lunar dive testing.

Since the MPA team designed the tests and built the equipment, they decided to have another person on our team conduct each of the tests in a 1g environment before attempting to direct the divers to execute the tests underwater. The purpose of this testing was to ensure that all of the testing equipment was functional, to get feedback on the testing procedures they wrote for the divers, and to choose the quantity and quality of any additional tools that may be needed for the tests. It was important to make sure all procedures were clear and easy to follow and the equipment fit together

properly before the dives. The movement, securing, and line connection tests were all conducted in 1g on the ground floor of the NBRF.

As discussed in further detail in the MPA section of the report, there were three PVC structures that were moved and then secured to the floor panel. As the test subject, I moved the small, medium, and large PVC structures from the starting position to the designated position on the floor. The movement testing was simple in the 1g environment, and everything went as planned. The second step was to secure the structure to the floor using four bolts. The most significant feedback I gave for this test was to change the tool that was used. The initial procedure had the test subject use a wrench to secure the bolts, however, due to the design of the structure, using a regular wrench was a slow and slightly frustrating process. Instead, we decided to use a hollow shaft nut driver, which allowed me to screw in the bolts more quickly and efficiently. We also noted that it was easier to align and screw in the bolts when the conduit strap was pressed down to the floor, and this was added to the dive testing procedure. Finally, they added additional labels to clarify which holes in the floor were associated with each PVC structure.

The final test was connecting and securing the air, water, and power lines, as shown in Figure 145. A secondary structure housing one end of each line was placed away from the floor setup, and I had to untangle and connect each of the lines to the large PVC structure that was secured to the floor. The most difficult part of this process was separating the lines from each other and unraveling them. As a result, we determined that the lines would be separated and Velcro-strapped to the structure while they were being lowered into the water for the dive, in order to save time and make it easier for the divers. Once I finished connecting each of the lines, the second part of the test involved securing the lines to the handle on the floor using Velcro straps. This process was simple and easy in 1g since the lines were lying on the ground; however, we recognized that in microgravity the divers may have difficulty holding all of the lines in place while also attempting to secure them. We noted that it would be beneficial to have the diver secure the lines in multiple places to ensure that they would not float out of place. Once all of the equipment and procedures were tested in 1g, the appropriate revisions were made, and the tests were ready to be conducted during the dives.

Figure 145: Images of the setup for 1g equipment testing. The secondary structure housing the lines (left) and the large PVC structure with lines connected and secured (right).

C. Bolt Analysis Calculations for Securing Equipment - Alberto Garcia-Arroba

$$\sigma_T = 70\ ksi$$
$$\sigma_S = \sigma_T \cdot 0.58 = 40.6\ ksi\ [142]$$

$$A = \frac{\pi}{4} \cdot \Phi^2 = 0.049\ in^2$$

$$V_{max} = \tau = 1993\ lb\ or\ 8865\ N$$

$$A_t = \frac{\pi}{4} \cdot \left(\Phi - \frac{0.974}{n}\right)^2 = 0.0318\ in^2\ [143]$$

$$T_{max} = \sigma_T \cdot A_t = 2228\ lb\ or\ 9911\ N$$

In both micro-g and lunar gravity, the sum of forces in the x-direction and moments in the z direction were used to get the actual loads a bolt experience.

Lunar gravity:

$$\sum M_z = 0 \qquad T = 623N$$

$$\sum F_x = 0 \qquad V = 450N$$

Micro-g:

$$\sum M_z = 0 \qquad T = 581N$$

$$\sum F_x = 0 \qquad V = 450N$$

D. Routine Astronaut Schedule - Alberto Garcia-Arroba

Table 45: Micro-g Schedule

Activity	**Weekday**	**Saturday**	**Sunday**
Sleep	8.5	8.5	8.5
Work	9	7	2
Breakfast	1	1	1
Lunch	1	1	1
Dinner	1	1	1
Free Time	1	3	8
Exercise	2.5	2.5	2.5

Table 46: Lunar Schedule

Activity	**Weekday**	**Saturday**	**Sunday**
Sleep	8.5	8.5	8.5
Work	9.5	7.5	2.5
Breakfast	1	1	1
Lunch	1	1	1
Dinner	1	1	1
Free Time	1.5	3.5	8.5
Exercise	1.5	1.5	1.5

Two tentative routines for the astronauts living and working in the TransHab were developed for micro-g and lunar gravity, as shown in Table 45 and Table 46. For micro-g, ISS timelines from past expeditions [144], and testimonies from their astronauts [145] were used as a reference. These sources were also helpful in building a routine for the lunar habitat.

The main difference between a micro-g and lunar routine is the amount of time astronauts need to work out. In micro-g, astronauts have to exercise a minimum of 2.5 hours to mitigate the detrimental effects of weightlessness on the body. The workout time is further broken down into two types of exercise: cardiovascular and lifting, giving the latter a higher priority. For instance, an astronaut working out for 2.5 hours a day should spend 1.5 hours on the weightlifting machine, the ARED, and 1 hour on either the bike or treadmill [145]. Since the consequences of weightlessness are not an issue on the lunar surface, the exercise component takes a secondary role, and more free time is allocated. An astronaut working out for 1.5 hours a day is enough to secure their overall health.

Another significant characteristic to highlight is the differentiation of the weekend days. Namely, a typical Saturday would be focused on work, but technical activities are replaced by housekeeping, while Sundays would be used for equipment inspections and rest.

E. Core and Floor Panel Full Assembly Iterations - Mason Hoene

The design of the core and floor panels progressed as we completed new research, analysis, and testing. The initial design consisted of six floor panels with one truss at the center and one on a wing that folds on the top of the floor panel. This configuration was presented at PDR, with the full process shown in Figure 146 and the unfolding process shown in Figure 147.

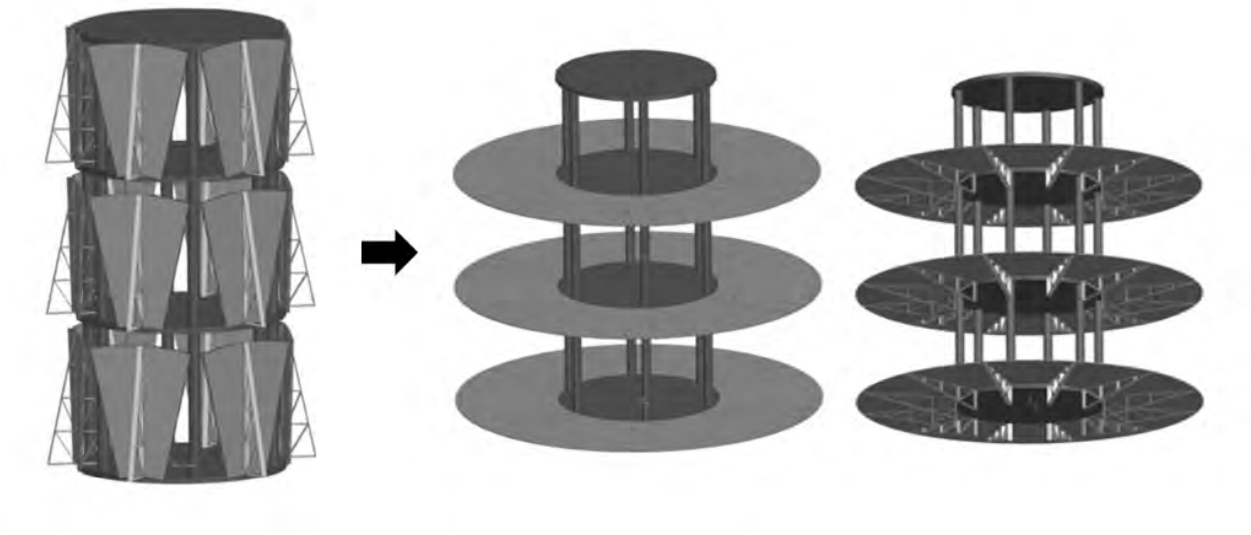

Figure 146: Six panel configuration presented at PDR.

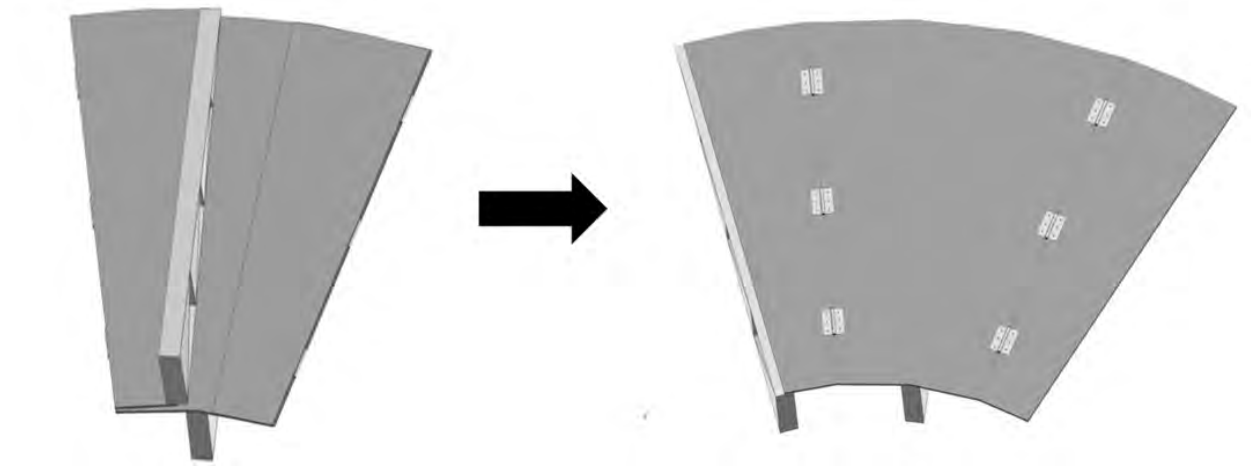

Figure 147: Unfolding process presented at PDR.

After feedback from PDR, the design of the core and the floor panels was altered to have an eight panel configuration to maximum the space available in the core. The design of the floor panel was also altered to make the center panel rectangular so that its area could be maximized and it would fit within the footprint of the core. This configuration is shown in Figure 148.

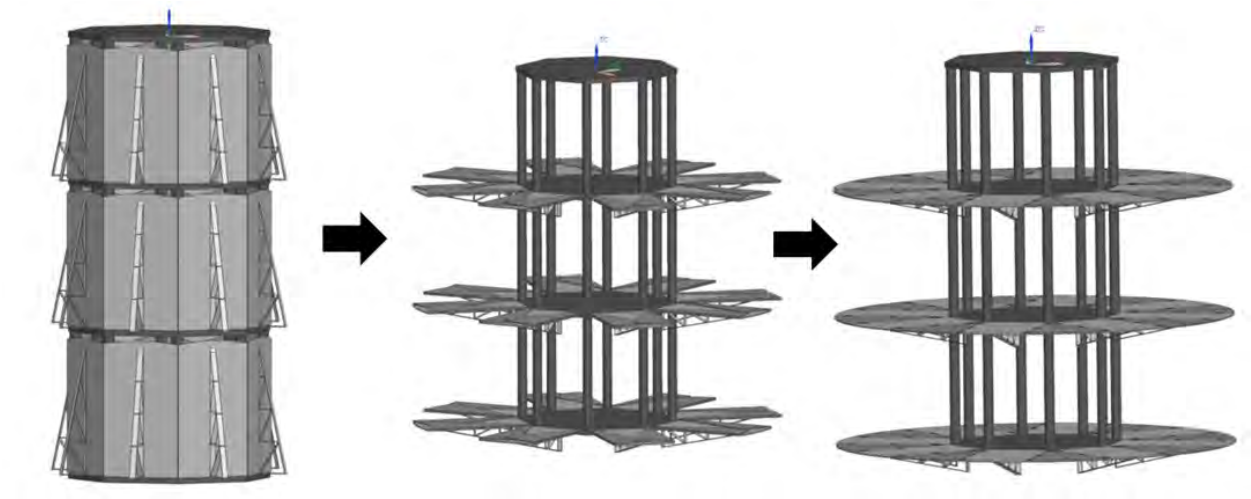

Figure 148: Eight panel configuration with one support truss developed after PDR.

Finally, in preparation for CDR, the design of the core and floor was finalized using feedback from divers during floor deployment testing. Instead of one truss in the center of the main floor panel, there are two trusses, one at each edge of the main floor panel so they align with the core pillars and avoid blocking movement in and out of the core. Also, the trusses were placed on hinges so that they can be flush with the cylindrical footprint of the core before deployment. Finally, the core was updated with further supports and connection points to the trusses of the floor panels. This configuration is shown in Figure 149. In addition to the images of the configuration, an animation of the process was created in preparation for CDR to show the full deployment process and the unfolding of the floor panel wings. Images of the beginning of these animations are shown in Figure 150 and the animations can be found in our CDR presentation.

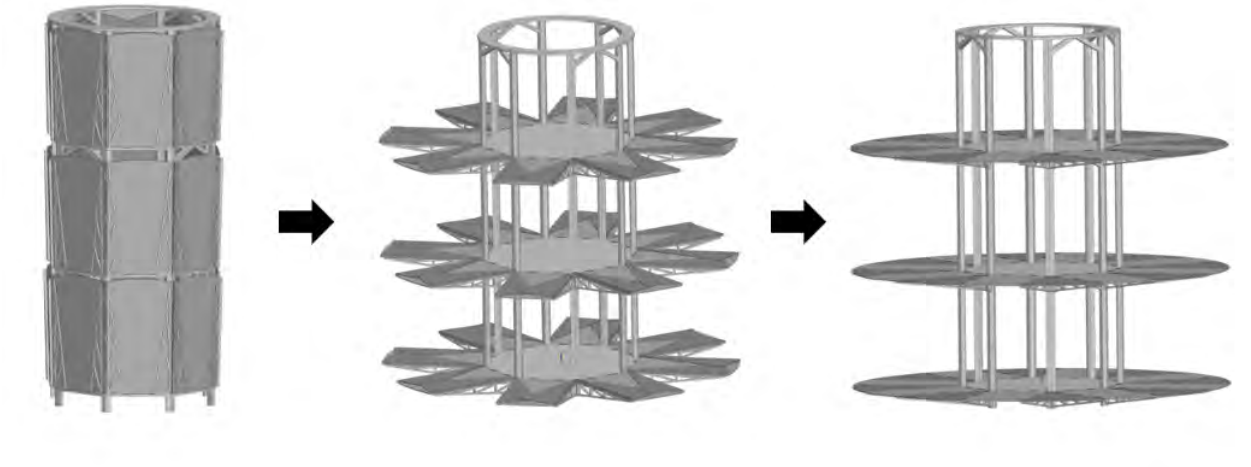

Figure 149: Final eight panel configuration with two support trusses and updated core presented at CDR.

Figure 150: Animations created to show floor deployment process presented at CDR. On the left is a still of the beginning of the full deployment animation and on the right is a still of the beginning of the unfolding of the floor panels.

F. Spring-Damper Floor Deployment MATLAB Code - Mason Hoene

The below MATLAB code shows how the plots of angular position and velocity were produced for the floor deployment spring-damper system in microgravity. It outlines the initial values of the system and shows how ode45 was used to integrate the derived equation of motion. Finally, it shows how that data was output by plotting angular position and velocity.

```
2
3
4
5
6
7
8
9
10
11
12
13
14
15
16
17
18
19
20
21
22
23
24
25
26
27
28
29
```

```
30
31
35
36
37
```

The below code shows a modified version of the previous code to incorporate the effect of gravity on Mars when determining angular position and velocity plots.

```
2
3
4
5
6
7
8
9
10
11
12
13
14
15
16
17
18
19
20
21
22
23
24
25
26
27
28
29
30
31
32
36
37
38
```

G. Winch Max Torque Calculations - Neal Shah

The below code was used to determine the max required torque to lower the floor panels in Lunar and Mars gravity.

```
1
2
3
4
5
6
7
```

8

H. Beam Sizing Analysis MATLAB Code - Jack Saunders

I. Truss and Support Stress Calculator - Jack Saunders, Olivia Naylor

A calculator was created in Excel to complete some of the basic stress calculations for our various supports throughout the design process. By inputting values for dimensions and material properties, it provided moment and reaction, bending and direct stress, and margin of safety calculations. An image of this Excel sheet is displayed in figure 151.

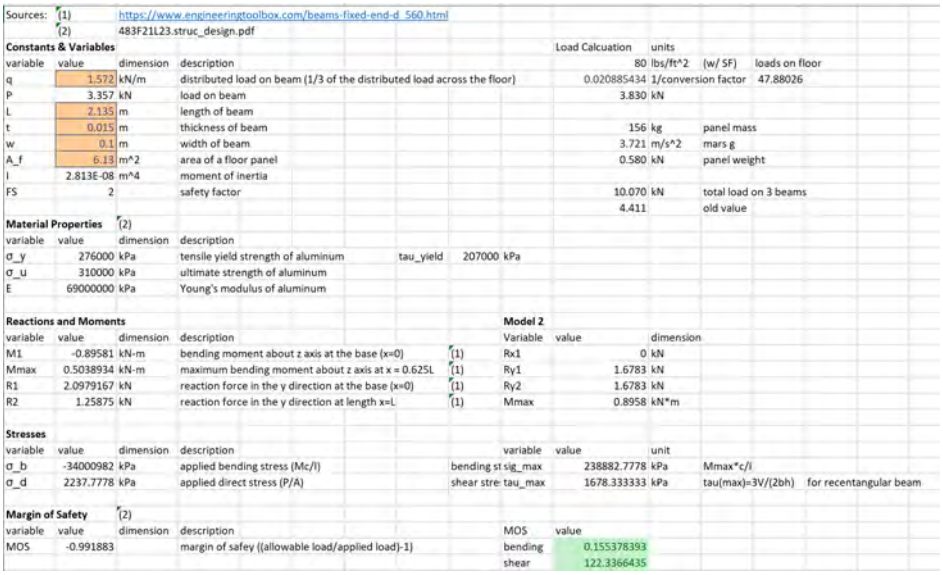

Sources:	(1)	https://www.engineeringtoolbox.com/beams-fixed-end-d_560.html							
	(2)	483F21L23.struc_design.pdf							
Constants & Variables						Load Calcuation	units		
variable	value	dimension	description			80	lbs/ft^2	(w/ SF)	loads on floor
q	1.572	kN/m	distributed load on beam (1/3 of the distributed load across the floor)			0.020885434	1/conversion factor	47.88026	
P	3.357	kN	load on beam			3.830	kN		
L	2.135	m	length of beam						
t	0.015	m	thickness of beam			156	kg	panel mass	
w	0.1	m	width of beam			3.721	m/s^2	mars g	
A_f	6.13	m^2	area of a floor panel			0.580	kN	panel weight	
I	2.813E-08	m^4	moment of inertia						
FS	2		safety factor			10.070	kN	total load on 3 beams	
						4.411		old value	
Material Properties	(2)								
variable	value	dimension	description						
σ_y	276000	kPa	tensile yield strength of aluminum	tau_yield	207000	kPa			
σ_u	310000	kPa	ultimate strength of aluminum						
E	69000000	kPa	Young's modulus of aluminum						
Reactions and Moments					**Model 2**				
variable	value	dimension	description		Variable	value	dimension		
M1	-0.89581	kN-m	bending moment about z axis at the base (x=0)	(1)	Rx1	0	kN		
Mmax	0.5038934	kN-m	maximum bending moment about z axis at x = 0.625L	(1)	Ry1	1.6783	kN		
R1	2.0979167	kN	reaction force in the y direction at the base (x=0)	(1)	Ry2	1.6783	kN		
R2	1.25875	kN	reaction force in the y direction at length x=L	(1)	Mmax	0.8958	kN*m		
Stresses									
variable	value	dimension	description		variable	value	unit		
σ_b	-34000982	kPa	applied bending stress (Mc/I)	bending st	sig_max	238882.7778	kPa	Mmax*c/I	
σ_d	2237.7778	kPa	applied direct stress (P/A)	shear stre	tau_max	1678.333333	kPa	tau(max)=3V/(2bh)	for recentangular beam
Margin of Safety	(2)								
variable	value	dimension	description		MOS	value			
MOS	-0.991883		margin of safey ((allowable load/applied load)-1)		bending	0.155378393			
					shear	122.3366435			

Figure 151: Excel spreadsheet used as the stress calculator for various design iterations of panel support

J. Original Lunar Support Base Design - Olivia Naylor

The original design for the Lunar support base for the habitat is very similar to the current design, however, based on comments and recommendations from the CDR, some revisions were made. There was also not enough time between being given the assignment and the CDR to complete a full FEA analysis of the design, so only a basic, very conservative analysis on the beams of the support base was completed. The initial design of the of the lunar support base was still an octagonal structure, but with a center hole in the shape of a circle. The center hole also had a short support hoop within it for the EVA airlock section. This design also contained 4 doors (there was slight miscommunication among subteams about the design of the EVA airlock), and 4 sets of beams coming from the top of the support base with a leg support structure underneath each of them. The leg support structure is very similar to the current design, however the legs are thinner and the long member is directly attached to the underneath of the beam. This original design is displayed in figures 152 and 153.

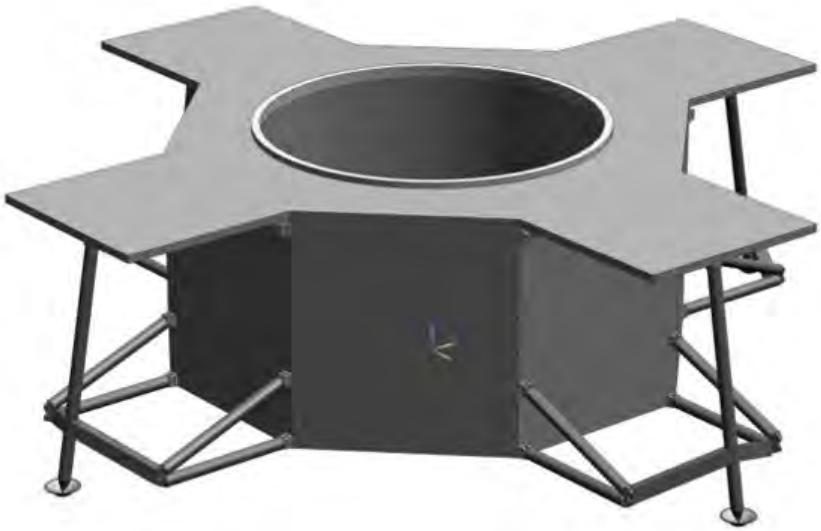

Figure 152: Original design of the lunar support base with the doors closed.

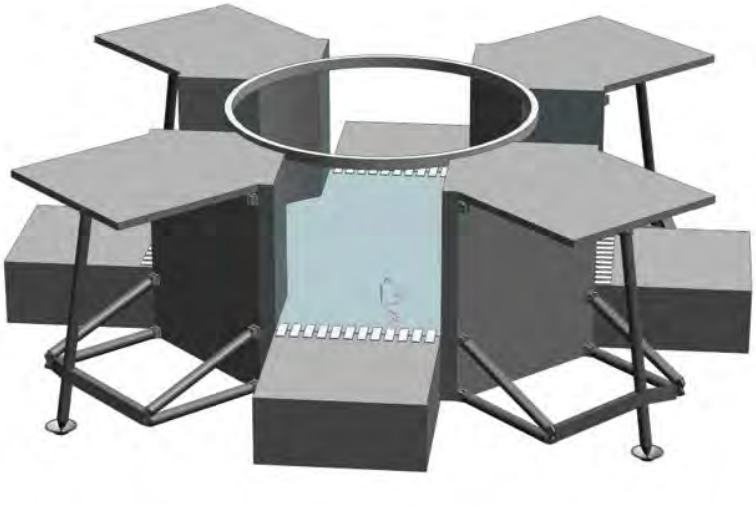

Figure 153: Original design of the lunar support base with the doors open.

K. Sensor List - Benjamin Adarkwa

Environmental Monitoring:

1. Cabin pressure sensor
2. Cabin humidity sensor
3. Cabin temperature sensor
4. Air Quality and Composition

- CO_2 sensor
- O_2 sensors : Percent O_2
- N_2 sensors : Percent N_2
- Ammonia detector
- Smoke detector: smoke
- Ion mobility sensor :Volatile Organic Compounds(VOCs)

5. Radiation levels
    - Radiation Environment Monitor
6. Water Quality and Composition
    - Residual Chlorine sensor
    - Turbidity sensor
    - Conductivity
7. Structural health Monitoring
    - Ultrasonic sensors: Leak detection
        - Ultrasonic is used because a leak may not be sensed early with regular pressure sensors since the volume of the habitat would also shrink resulting in an early unnoticeable pressure drop.
    - Strain Gauge and Accelerometer: Micrometeor and Orbital debris(MMOD) impact detection
    - Embedded fiber optic strain gauge
    - Dosimeter: External Radiation levels
8. Navigation
    - Inertial Measurement Units: Angular and translational acceleration
    - Sun and Star Sensor: Angular velocity
9. Other sensors
    - Tank pressure sensors (Crew systems)
    - Encoders for floor deployment motors(Loads, Structures and Mechanism Sub Team(LSM))
    - Voltmeter, Ammeter, Power Meter (Power, Propulsion and Thermal Team(PPT))
    - Encoders for Solar Array Orientation and deployment (PPT and LSM)

L. Advantages and Disadvantages of wired and wireless networks - Benjamin Adarkwa

Some advantages of wireless networks include[**advantages**]:

1. It is scalable and hence can accommodate any new nodes or devices at any time.
2. It is flexible and hence open to physical partitions.
3. As it is wireless in nature, it does not require wires or cables.
4. Wireless network installation is easy and it requires less time.
5. More area is covered by wireless base stations which are connected to one another.
6. Mobility is not limited, as it operates in the entire wireless network coverage

Some disadvantages of wireless networks include [**advantages**]:

1. It is expensive to build such network and hence can not be affordable by all

2. There are various challenges to be considered in WSN such as energy efficiency, limited bandwidth, node costs, deployment model, Software/hardware design constraints and so on.

3. Wireless sensors networks are very sensitive to obstructions since high frequency electromagnetic waves cannot pass through solid objects without some signal loss.

4.

Some disadvantages of wired networks include[**advantages**]:

1. It is not scalable and hence hard to accommodate any new nodes or devices.

2. As it is wireless in nature, it does not require wires or cables.

3. longer installation time with all the wires. Requires hubs and switches for network coverage limit extension

4. Mobility is limited

Some advantages of wired networks include [**advantages**]:

1. It is cheaper to build such network as cables are not expensive hence can be affordable by all.(initial installation cost)

2. Not sensitive to obstructions.

3. Faster data rate and high bandwidth

M. Sensor node calculations - Benjamin Adarkwa

Below is a table with of how we calculated the mass and power consumption of a general node. For the sensing data rate, the sensor with the highest criticality and "amount of information found" was the 4 in 1 environmental sensor. This sensor contained a pressure, temperature, humidity and a gas sensors. We took the highest data rate of the 4 and doubled that as an approximation of the sensing node. The microcontroller was also assummed to be operating at its highest clock frequency.

Parts of Node	Mass(grams)	Dimension(mm)	Data rate(bit/sec)	Power(W)
Microcontroller (SOC)	0.3	7*7*1.2		.00576W
BME sensor	5	3*3*.93	3000	0.0432
Other sensors(approx)	5		3000	0.0432
omnidirectional RF antenna (comm)	28.4			0.00576
transceiver(comm)	0.009	7*7*2		0.2
			Total Power(Watts)	0.29216
			Total mass(grams)	38.709

N. Advantages and Disadvantages of star and mesh topology - Benjamin Adarkwa

Below is a table with the criteria in which we evaluated both topologies

Base of comparison	Star (Wheel and spoke)	Mesh
Number of Links	Equal to number of nodes	Equal to n(n-1)/2 ,n= number of nodes
Structure	Relatively simpler structure	Relatively more complex structure
Scalability	Easy	Relatively easy
Range	Base station should be in range of radio of all separate nodes	No automatic restriction on network through the range from a single node
Robustness	Not robust enough since it depends on a single node to handle the network	Redundant and robust with self-heal capability
Latency	Communication with less latency among base station	Latency concerns due to multi-hop communication

Figure 154: Star vs Mesh topology:advantages and disadvantages.

O. Topology Power consumption calculations-Benjamin Adarkwa

$$P = aN^3 + bN^2 + cN + d$$

Topology	a	b	c	d
Star	0	$2E_c\bar{L}$	$(\eta_n\frac{p_r}{B} - 2E_c)\bar{L}$	$(2E_c - \eta_n\frac{p_r}{B})\bar{L}$
full mesh	0	$\bar{L}(\eta_n\frac{p_r}{B} + E_c)$	$-\bar{L}(\eta_n\frac{p_r}{B} + E_c)$	0

Figure 155: Star vs Mesh topology:advantages and disadvantages.

Where : E_c= non bypass energy coefficient ; B= Data rate ; $\bar{L}$=Average Traffic Demand; L=traffic demand between node and central hub; P_r=Power consumption of router port

1. *Matlab script for topology power consumption calculations*

P. Internal Data network Calculations - Benjamin Adarkwa

Laptops will be used as routers and base stations. They would be slight spec'd differently but interchangeable to allow faults to be quickly and easily repaired.

1. bandwidth approximation

For bandwidth approximations we considered what the internal data network would be used for. Activities such as video calling, internal communication, video streaming, and Habitat system control were looked at. For video streaming in High definition was about 5 megabits per second[**help**], since we have a 6 crew mission that bring that to 30 megabits per second. For internal communication, the Consultative Committee for Space Data Systems(CCSDS) specifies about 64 kilobits per second so for 6 crew members that brings it up to 384 kilobits per second. Video calling is around 2 megabits per second[**skype**] per a call hence for 6 crew members we need around 12 megabits per second. With 10 crew interfaces for habitat control we get 5 megabits per second. Finally sensor telemetry is about 180 kilobits per second. With a 33 megabit per second margin our approximated bandwidth is about 80 megabits per second which is a lot less than our max internal network data rate

2. Power conusmption of hardware in internal data network

We need a flight computer that is two fault tolerant for a life/mission critical mission.HPSC project (100 times RAD750). Computers must be radiation hardened for the radiation environment of mission. 12-25 W of processor power, 30-100W computer power. High perfomance laptops have a power consumption of 150W, with a total of 24 laptops this brings power consumption to about 3.6 kilowatts.

Table 2 – NASA Applications Requirements Summary

Apps Summary	Processing Type			Criticality	Available Spacecraft Power			Rad Env	Mem Access	Duty Cycle	Mem Rate	I/O Rate
	DSP	GP	P	MC	LP	MP	HP					
Throughput = 1-10 GOPS												
Autonomous Mission Planning		X	X	X	X	X	X	All	R	C,S	1GB/S	100Mb/S
Disaster Response	X	X			X			LEO	R,S	C	200,B/S	1Gb/S
Hyspiri	X	X	X			X		LEO	R,S	C	200MB/S	
Throughput = 10-50 GOPS												
Fast Traverse	X	X	X	X	X			Mars	R, S	C	500MB/S	
Extreme Terrain Landing	X	X	X	X	X			Mars, GEO	R, S	C	50MB/S	
Adept		X	X			X		LEO, MEO	R, S	C	375MB	
Optimum Observation	X	X	X		X	X	X	All	R	C	1GB/S	1Gb/S
Space Weather	X		X		X	X	X	All	R	C	125MB/S	500Mb/S
Robotic Servicing	X	X	X	X	X	X	X	GEO	R	C,S	125MB/S	
Cloud Service	X	X	X				X	All	R,S	C,S	6.25GB/S	10Gb/S
Advanced ISHM		X	X		X		X	All	R	C	6.25GB/S	10Gb/S
Autonomous and Telerobotic Construction		X	X	X	X		X	GEO, Mars, Lunar	R	C,S	12.5GB/S	50Gb/S
Througput = 50-100s GOPS												
Hyperspectral Imaging	X	X	X		X	X	X	All	R,S	C,S	nGB/S	
RADAR Science	X	X	X				X	All	R,S	C	1GB/S	
RADAR EDL	X		X	X	X	X	X	All	R,S	S	1GB/S	
Automated GN&C	X	X	X	X			X	All	R,S	S	12.5GB/S	10GbS
Human Movement Assist	X	X	X		X			All	R,S	S	12.5GB/S	50GbS
Crew Knowledge Augmentation		X	X					All	R,S	S	12.5GB/S	10Gb/S
Improved Displays and Controls		X	X	X	X		X	All	R,S	C	12.5BG/S	50Gb/S
Augmented Reality		X	X		X		X	All	R,S	S	12.5GB/S	50Gb/S
Telepresence		X	X		X		X	All	R,S	S	12/5GB/S	50Gb/S

Q. Iterative Lighting Design - Alexander Cochran

1. First Analysis

The initial lighting analysis considered a uniform lighting level over the whole interior surface area of the habitat. The illuminated surfaces are represented in figure 156 in red. This surface area, the internal surface area of the habitat,

Figure 156: The uniformly illuminated surfaces in the habitat for the first analysis, represented in red.

was approximated by assuming the habitat is empty and constructed of 6 stacked concentric cylinders. Each level of the habitat is assumed to be a cylinder with a radius of 12.5 ft (3.81 m) and the appropriate level heights of 7 or 8 ft (2.13 or 2.44 m). The core and its associated walls on each level are represented by a concentric cylinder with a radius of 5.5 ft (1.68 m). The floor and ceiling area where the cylinders overlap is only counted once. The surface area calculated using this method is approximately 40 m^2 for each core portion per level and 160 m^2 for the inflatable volume portion. The total calculated surface area is 590 m^2 for the entire habitat structure. Since the majority of the core will not have walls as assumed in this calculation, this represents the maximum of the structural surface area. This was done to estimate the maximum power consumption of the lighting system for power generation before the internal

design was finalized, so the surface area of the equipment inside the habitat was unknown. An illumination level of 108 lux was considered as this is the minimum illumination level for general use from the NASA human space flight standards. With this illumination, a total lighting requirement of 64,000 lumens, length of 35 m, a power requirement of 1.6 kW, and mass of 47 kg was calculated for the system. Illumination requirements can be significantly higher than the general use requirement for fine tasks such as maintenance, lab work, or medical procedures. The workstation lighting requirement of 323 lux was selected to provide an upper bound, considering that some portions of the habitat will require higher illumination levels. With this level of illumination over the entire internal surface area, a lighting requirement of 191,000 lumens, a length of 110 m, a power requirement of 4.9 kW, and a system mass of 120 kg was calculated. This analysis has 3 major flaws. First, the lighting in the habitat will not be uniform. The illumination level will vary depending on what that specific area of the habitat is being used for. As mentioned previously, the habitat is not empty. It will contain work surfaces and equipment that will increase the overall surface area that needs to be illuminated. Finally, the lighting in this analysis is assumed to always be on. The lights in the habitat will not function in this way. Lights will turn off when they are not needed to reduce the power requirement.

2. *Second Analysis*

The second analysis of the lighting system addresses one of these poor assumptions by considering varying illumination levels. Each level is split into different sections, with the surface area for each section calculated using the approximation mentioned earlier. Each of these sections is assigned a purpose based on the interior design of the habitat and using the NASA human spaceflight illumination requirements for that purpose an illumination requirement is set. The illuminated surfaces and their illumination requirement are represented in figure 157. While the areas are

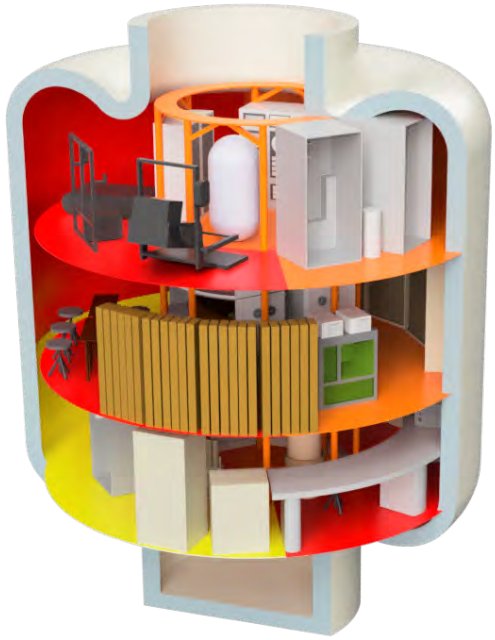

Figure 157: The illuminated surfaces in the habitat for the second analysis with color representing illumination level. Red indicated a level of 323 lux, yellow 269 lux, and orange 108 lux.

still approximate and the habitat is still empty, the distribution of illumination requirements is representative of those in the final habitat design. This analysis was used to approximate the power consumption from the lighting on a floor-by-floor basis. Since each level has a different distribution of lighting requirements, the power draw of the lighting on each floor, and therefore the power distribution requirements, may also differ. The section areas, illumination requirements, and lighting requirements for each floor are broken down in table 47. Using these areas and illumination requirements, the lighting requirement in lumens for each floor was calculated. Floor 1 has a lighting requirement of 58,000 lumens, floor 2 a requirement of 46,000 lumens, and floor 3 a requirement of 52,000 lumens. There is some variation in the lighting requirements between floors, but only around 10%, which was not significant enough to affect power distribution. The total lighting requirement for this analysis is 156,000 lumen, giving a lighting length of 87 m, a mass of 120 kg, and a power requirement of 3.7 kW. This analysis still fails to capture the actual task surface area

	Lighting Purpose	Area (m^2)	Min. Illumination (lux)	Total Lighting (Lumen)
Floor 1	Bathroom	39.4	269	10600
	EVA	43.3	269	11700
	First Aid	39.4	269	10600
	Workstation	78.8	323	25500
Floor 2	Sleeping	43.3	54	2300
	Storage	78.8	108	8500
	Dining	39.4	269	10600
	Food Prep	39.4	323	12700
	Reading	43.3	323	14000
Floor 3	Storage	39.4	108	4300
	Bathroom	39.4	269	10600
	Life Support	43.3	269	11700
	Exercise	78.8	323	25500

Table 47: Second Lighting Analysis Habitat Illumination and Lighting Requirements

that will be introduced by equipment in the inflatable volume and the duty cycle of the lighting

3. Third Lighting Analysis

The third and final analysis of the lighting system is the most complete. The purpose of this analysis was to model the illumination requirements of the habitat as accurately as possible and calculate the max and average power draw for the lighting system. At this point in the design process, preliminary task areas were available for many of the habitat functions. These task areas are estimates of the surface area that will be used for specific tasks based on the habitat design and mission requirements. This includes the floor space dedicated to exercise and the bathrooms as well as the surface area of the lab and dining tables. Task areas for the exercise area, bathrooms, lab space, and food prep area that were used in this analysis are located in table 48. Each portion of the core of the habitat now also

	Lighting Purpose	Area (m^2)	Illumination (lux)	Total Lighting (Lumen)
Floor 1	Workstation	6	323	1900
	Bathroom	4	269	1100
	EVA	43.3	269	11700
	First Aid	3	269	800
	General (wall/floor)	157.6	108	17000
Floor 2	Dining	3	269	800
	Food Prep	8	323	2600
	Galley	78.8	215	16900
	Sleeping	43.3	54	2300
	Reading	3	323	1000
	General (wall/floor)	122.1	108	13200
Floor 3	Exercise	12	323	3900
	Life Support	20	269	5400
	Storage	39.4	108	4300
	Bathroom	4	269	1100
	General (wall/floor)	161.5	108	17400

Table 48: Third Lighting Analysis Habitat Illumination and Lighting Requirements

has an assigned function and associated illumination requirement. With specific areas for more intensive tasks and illumination requirements for the core, the general or a storage illumination requirement was assumed for the rest of the structural surface area. The surfaces of the habitat and their associated illumination requirements are represented in figure 158. As illustrated in figure 158, these task areas act to fill in the previously empty habitat area. The structural

Figure 158: The illuminated surfaces in the habitat for the third analysis with color representing illumination level. Purple is a sleep illumination or 54 lux, red represents a general illumination of 108 lux, orange and illumination of 269 lux, and yellow an illumination of 323 lux.

surface area, representing the walls and floors of the habitat, was still approximated as described previously. The areas and illumination requirements used in this analysis for the entire habitat are broken down by floor in table 48. Using these values, lighting requirements for each section and floor of the habitat were calculated. These lighting requirements are also tabulated in table 48. This gives a total lighting requirement for the habitat of 101,000 lumens, a length of 56 m of lighting, a mass of 75 kg, and a power requirement of 2.6 kW. Since this still assumes all lights in the habitat are always on, the calculated 2.6 kW represents a maximum power draw for the system. As mentioned previously, the lights in the habitat will be cycling on and off as they are needed. When crew members are not using a section of the habitat, the lighting in that habitat will be turned off. A lower power night mode will be used on the second floor while the crew is sleeping. Duty cycles for the task lighting were interpreted from the crew schedule. The general-purpose lighting was assumed to be on during the entirety of habitat "day" while the crew is awake, which lasts 16 hours. Shifts in power consumption due to the shifting color temperature of the lighting was not considered. The duty cycles and calculated effective power consumption for each portion of the lighting system is included in table 49. The first floor has an effective power consumption of 510 W, the second floor 580W, and the third floor 430 W, for a total effective power consumption of 1.5 kW. The third floor has the lowest effective power consumption due to the exercise area on that floor only being in use for 2 hours per day. Since the second floor houses the crew quarters and will have night and sleeping lights on during crew "night," its higher effective power consumption was expected. The night illumination requirement of 22 lux was assumed to only be on for the entire 8.5 hours on the second floor while lighting on the other floors is entirely off. However, short trips to other portions of the habitat may occur. Approximately 100W of power is required to illuminate each floor at 22 lux, so these trips will not significantly impact the overall effective power consumption. Lighting on each floor will periodically cycle on and off to keep the emergency lighting dots on each floor charged in the case of a complete power failure, but this consumes on average less than 40 W of power so it was also not included.

R. Power Distribution Design - Alexander Cochran

Estimating the length of wiring required for power distribution as well as the wiring mass required localizing loads throughout the habitat. Wires for power distribution will run along the structure of the habitat to keep them out of the way of the crew. The distances each of these wires would need to run was determined using the interior design and the load on the wires from the power budget. The power generation was assumed to enter the habitat through the

	Lighting Purpose	Power (W)	Duty Time (Hr)	Effective Power (W)
Floor 1	Workstation	49	9	18
	Bathroom	27	3	3
	EVA	297	16	198
	First Aid	21	1	1
	General (wall/floor)	433	16	289
Floor 2	Dining	21	2	2
	Food Prep	66	2	5
	Galley	431	16	288
	Sleeping	60	8.5	21
	Reading	25	8	8
	General (wall/floor)	336	16	224
	Night	88	8.5	31
Floor 3	Exercise	99	2	8
	Life Support	137	9	51
	Storage	108	16	72
	Bathroom	27	3	3
	General (wall/floor)	444	16	296

Table 49: Third Lighting Analysis Habitat Effective Power Consumption

center of the bottom core, before connecting to the power storage and conditioning hardware located in the bottom core. From there all cables are assumed to only run horizontally along floors and vertically along walls through the power distribution system to the habitat loads. The load per floor was calculated to be 4.5, 2.4, and 7 kW, for floors 1, 2, and 3 respectively. Internal power runs at a constant 120V DC, so these loads correspond directly to the currents carried by the power distribution wires. NEC guidelines on maximum current load ratings were used to select wiring gauges based on the currents. The mass and resistance of the wire are calculated using the length and wire gauge. The insulation for the wiring is assumed to weigh 20% of the conductor mass to give the total mass of the wire. With the resistance, ohmic power losses can be calculated for the entire system. Adherence to NEC guidelines for wire gauges ensures a maximum voltage drop over any cable of 3%. The habitat loads considered, calculated wire lengths, selected wire gauges, masses, and power losses for each portion of the power distribution network are listed in table 50. While the calculated masses for the habitat wiring of 140 kg seems very conservative, the total system length of 400 m (including the 200 m of cable for the nuclear power generation system) represents a lower bound for the power distribution system. It assumes the nuclear power generation is only 100 m away, all cable runs inside the habitat are direct along floors and walls, and that the gauge of each wire is only rated for the load it is carrying. The distribution system has a total ohmic wiring loss of 700W or 3.5% of the total generated power. This does not account for the efficiency of power storage, conditioning, or power conversion losses at load. Most of the losses in the system, 78% or 550 W, occur while transmitting power for power generation and conditioning. The use of a higher voltage for power generation would reduce these losses significantly. Higher voltage would result in a lower current being carried in the wires, and ohmic losses are proportional to the current squared. Splitting current between two parallel cables is another way to reduce losses, as was done with the cabling for the power generation. This does not require the use of higher voltages, however, it comes at the cost of additional cable mass and length.

S. MATLAB Link Budget Calculations - Alexander Cochran

The following MATLAB scripts were used for initial link budget analysis on Lunar and Martian Communication. Using ground station specifications and estimates of the habitat's position and communications system, theoretical losses were used for system sizing. This link budget analysis was used to size the transmit power and antennas for the communications system. All ground station specifications are derived from the respective network documentation.

	P (W)	V (V)	I (A)	Gauge	Length (m)	R (Ohm)	Power Loss	% Volt Drop	Mass (kg)
Primary Power									
Power Generation 1	10000	120	83.33	0	200	0.0640	444.44	0.044	114.00
Power Generation 2	20000	120	166.67	0	6.86	0.0022	60.97	0.003	3.91
Battery	20000	120	166.67	0	5.49	0.0018	48.78	0.002	3.13
Floor 3 Life Support	4800	120	40	8	6.86	0.0144	23.05	0.005	0.61
Floor 1 Primary	3100	120	25.83	10	6.86	0.0224	14.97	0.005	0.39
Floor 2 Primary	2400	120	20	10	3.35	0.0110	4.39	0.002	0.19
Floor 1 Life Support	1500	120	12.5	12	6.86	0.0357	5.57	0.004	0.24
Floor 3 Primary	2400	120	20	10	6.86	0.0224	8.97	0.004	0.39
				Totals	243	0.1738	611		122.85
Secondary Power									
Floor 1									
Lab Secondary	2000	120	16.67	10	3.81	0.0125	3.46	0.002	0.21
	333.33	120	2.78	16	18	0.2376	1.83	0.005	0.25
Bathroom	270	120	2.25	16	3.81	0.0503	0.25	0.001	0.05
Lighting	830	120	6.92	16	30.19	0.3985	19.06	0.023	0.42
Floor 2									
Kitchen	1450	120	12.08	12	4.88	0.0254	3.70	0.003	0.17
	800	120	6.67	16	18	0.2376	10.56	0.013	0.25
Lighting	940	120	7.83	16	29.88	0.3945	24.20	0.026	0.42
Floor 3									
Exercise	1200	120	10	12	5.03	0.0262	2.62	0.002	0.18
	1000	120	8.33	16	10	0.1320	9.17	0.009	0.14
Lighting	820	120	6.83	16	39	0.5194	24.26	0.030	0.55
				Totals	163	1.5144	99		2.64

Table 50: Power Distribution Length, Mass, and Power Loss

1. Lunar Deep Space Network All Bands Antenna Sizing

This script considered free space and estimated line and atmospheric losses for the Deep Space Network (DSN) to calculate the required gain for a given bitrate and transmit power, 10 W, for S, X, and Ka-bands at lunar distance. That gain was then used to calculate the required antenna diameter. A plot of the antenna diameter for the complete range of DSN bitrates, 0 –150 Mbps.

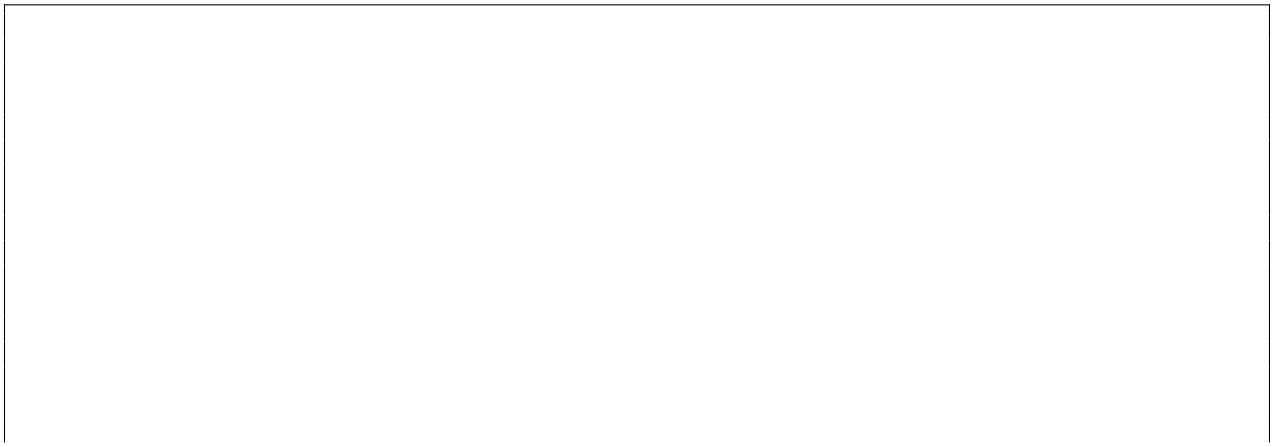

31
32
33

2. Lunar LEGS and DSN Antenna Sizing Comparison

This script considered free space and estimated line and atmospheric losses for the Lunar Exploration Ground Sites (LEGS) to calculate the required gain for a given bitrate and transmit power, 10 W, for X and Ka-bands at lunar distance. That gain was then used to calculate the required antenna diameter. A plot of the antenna diameter for LEGS and the DSN over the complete range of DSN bitrates, 0 –150 Mbps, is generated to compare ground station performance.

28
29
30

3. Martian Deep Space Network Antenna Sizing

This script considered free space and estimated line and atmospheric losses for the Deep Space Network (DSN) to calculate the required gain for a given bitrate and transmit power, 100 W and 200 W, for X and Ka-bands at Martian distance. That gain was then used to calculate the required antenna diameter. A plot of the antenna diameter for a reduced range of DSN bitrates, 0 –1 Mbps, is generated to compare antenna sizes for different transmit powers.

4. Mars Transmit Power for 1 Mbps DSN Signal

This script considered free space and estimated line and atmospheric losses for the Deep Space Network (DSN) to compare the trade-off between antenna size and transmit power at a fixed bitrate, 1 Mbps. A plot showing the range of possible antenna sizes and transmit powers is generated.

T. AMSAT Link Model - Alexander Cochran

The AMSAT link model is a comprehensive Excel sheet created by Jan A. King, W3GEY/VK4GEY. This sheet is distributed by the Radio Amateur Satellite Corporation to be used as a learning tool and for the complete design of a spacecraft's RF system. Information about the ground stations and spacecraft, including the orbit, antennas, and system noise, are input into the sheet which produces a complete uplink and downlink budget. The sheet also provides estimates of various communications system parameters that were used for the analysis. The tool is available at https://www.amsat.org/tools-for-calculating-spacecraft-communications-link-budgets-and-other-design-issues/.

U. Power Generation

1. Initial Trade Study Comparing Nuclear and Solar Systems

V. Altitude Drag Calculation

W. Attitude Control Sizing

X. Geostationary Orbit Maneuver Calculation

Y. Batteries Required for LEO Orbit

Z. LEO to SSO Orbit Calculation

Acknowledgments

This research was supported by the NASA Moon to Mars Exploration Systems and Habitats Academic Challenge program, administered by the National Space Grant Foundation.

The authors would like to thank Charlie Hanner for his testing contributions and the ENAE 100 students who worked on the 1/12 scale model and testing for this project: Mason Eberle, Daniel Grammer, David Labrique, Emily Seibert, and Savyon Stokes.

References

[1] Gary R. Spexarth Gerard D. Valle Horacio delaFuente Jasen L. Raboin. "TransHab: NASA's Large Scale Inflatable Spacecraft". In: 2000. URL: https://ntrs.nasa.gov/citations/20100042636.

[2] NASA. *Mars Facts*. URL: https://mars.nasa.gov/all-about-mars/facts/.

[3] Robert Lewis. *Human Spaceflight Aviation Standards*. 2020. URL: https://www.nasa.gov/offices/ochmo/human_spaceflight/standards101.

[4] TCNA. *Deflection*. 2022. URL: https://www.tcnatile.com/faqs/30-deflection.html.

[5] Lemuel Carpenter, Charles Hanner, and David L. Akin. "Experimental Investigation of Vertical Translation Design Commonality Across Differing Gravitation Levels". In: *48th International Conference on Environmental Systems*. 2018.

[6] Elaine L Chao and John L Henshaw. *Stairways and Ladders: A Guide to OSHA Rules*. U.S. Department of Labor, Occupational Safety and Health Administration, 2003.

[7] David L. Akin et al. "Habitat Design and Assessment at Varying Gravity Levels". In: *44th International Conference on Environmental Systems*. 2014.

[8] Hoists Direct. *J.D. Neuhaus Mini 250/5, 550 pound air hoist with 16'of lift, hook mounted*. URL: https://www.hoistsdirect.com/shop/1234#tab1,addendum=accessed:04.01.2022,year=.

[9] Cynthia Evans. *Glovebox for GeoLab Subsystem in HDU1-PEM*. 2012. URL: https://www.techbriefs.com/component/content/article/tb/pub/briefs/manufacturing-prototyping/12788. (accessed: 03.21.2022).

[10] Zachary Taylor. “A Study of Space Bathroom Design”. In: *Acta Astronautica* 174 (2020), pp. 55–60. DOI: https://doi.org/10.1016/j.actaastro.2020.04.027.

[11] Erin Mahoney. *Help NASA Design a Toilet for Artemis Astronauts on the Moon*. 2020.

[12] Arthur A. Rosener et al. “Space Shower Habitability Technology”. In: *AIAA* 9 (7 1972). DOI: https://doi.org/10.2514/3.61735.

[13] Susmita Mohanty, Michael J. Rycroft, and Michael Barratt. *Design Concepts for Zero-G Whole Body Cleansing on ISS Alpha Part II: Individual Design Project*. 2001.

[14] G. Antonutto and P. E. di Prampero. “Cardiovascular deconditioning in microgravity: some possible countermeasures”. In: *European Journal of Applied Physiology* 90 (2003), pp. 283–291. DOI: https://doi.org/10.1007/s00421-003-0884-5.

[15] Jonathan Michael Laws. “To the Moon, Mars and Beyond: Recommending Exercise Countermeasures Against Musculoskeletal and Cardiovascular Deconditioning During Microgravity Exposure, for Future Spacecraft Applications”. In: *Northumbria Research Link* (2021).

[16] J.A. Loehr et al. “Musculoskeletal adaptations to training with the Advanced Resistive Exercise Device”. In: *Official Journal of the American College of Sports Medicine* 43 (1 2011), pp. 146–156.

[17] Amy Ross. “Z-1 Prototype Space Suit Testing Summary”. In: NTRS, 2013.

[18] Robert M. Boyle et al. “Suitport Feasibility - Human Pressurized Space Suit Donning Tests with the Marman Clamp and Pneumatic Flipper Suitport Concepts”. In: NTRS, 2013.

[19] David L. Akin. *ENAE 483/788d - Fall, 2021 Lecture 14 Aerospace Physiology*. 2021. URL: https://spacecraft.ssl.umd.edu/academics/483F21/483F21L14.physiology/483F21L14.physiologyx.pdf.

[20] NASA. *Gene Cernan Covered In Lunar Dust*. 2013. URL: https://www.nasa.gov/exploration/humanresearch/multimedia/images/hrpg_img_06.html. (accessed: 03.21.2022).

[21] James R. Gaier. “The Effects of Lunar Dust on EVA Systems During the Apollo Missions”. In: (2005).

[22] C.I. Calle et al. “Active dust control and mitigation technology for lunar and Martian exploration”. In: *Acta Astronautica* 69 (11 2011), pp. 1082–1088. DOI: doi:10.1016/j.actaastro.2011.06.010.

[23] Maya Cooper, Grace Douglas, and Michele Perchonok. “Developing the NASA Food System for Long-Duration Missions”. In: *Food Science* 76 (2 2011), R40–R48. DOI: https://doi.org/10.1111/j.1750-3841.2010.01982.x.

[24] Hong Liu et al. “Review of research into bioregenerative life support system(s) which can support humans living in space”. In: *Life Sciences in Space Research* 31 (2021), pp. 113–120. DOI: https://doi.org/10.1016/j.lssr.2021.09.003.

[25] National Aeronautics and Space Administration. *Deep Space Food Challenge: NATIONAL AERONAUTICS AND SPACE ADMINISTRATION (NASA) Phase 2 Competition Rules*. 2021. URL: https://static1.squarespace.com/static/5fd5ab003c1f6275809f31d9/t/61e86f5cb338e40afd183e34/1642622814713/FNL_NASA_DSF_Phase_2_Rules.pdf.

[26] Grace L. Douglas et al. “Impact of galactic cosmic ray simulation on nutritional content of foods”. In: *Life Sciences in Space Research* 28 (2021), pp. 22–25. DOI: https://doi.org/10.1016/j.lssr.2020.12.001.

[27] Grace L. Douglas et al. *Evidence Report: Risk of Performance Decrement and Crew Illness Due to an Inadequate Food System*. 2016. URL: https://humanresearchroadmap.nasa.gov/Evidence/other/AFT.pdf.

[28] National Aeronautics and Space Administration. *Veggie*. 2020. URL: https://www.nasa.gov/sites/default/files/atoms/files/veggie_fact_sheet_508.pdf.

[29] National Aeronautics and Space Administration. *Advanced Plant Habitat*. 2017. URL: https://www.nasa.gov/sites/default/files/atoms/files/advanced-plant-habitat.pdf.

[30] Howard G. Levine and Trent M. Smith. *Vegetable Production System (Veggie)*. 2016. URL: https://ntrs.nasa.gov/citations/20160005059.

[31] Stephanie E. Richards, Howard G. Levine, and David W. Reed. *Advanced Plant Habitat (APH)*. 2016. URL: https://ntrs.nasa.gov/citations/20160005065.

[32] Jess M. Bunchek, Aaron B. Curry, and Mathew W. Romeyn. "Sustained Veggie: A Continuous Food Production Comparison". In: ICES, 2021.

[33] Raymond Odeh and Charles L. Guy. "Gardening for Therapeutic People-Plant Interactions during Long-Duration Space Missions". In: *Open Agriculture* 2 (1 2017), pp. 1–13. DOI: https://doi.org/10.1515/opag-2017-0001.

[34] Laura A. Shaw and Jose L. Barreda. "International Space Station USOS Potable Water Dispenser Development". In: ICES, 2008.

[35] Cheryl L. Mansfield. *Station Prepares fro Expanding Crew*. 2008. URL: https://www.nasa.gov/mission_pages/station/behindscenes/126_payload.html.

[36] Paul E. Hintze et al. *Trash to Supply Gas (TtSG) Project Overview*. 2010.

[37] James A. Nabity, Erik W. Andersen, and Jeffrey R. Engel. *Low Temperature Ozone Oxidation of Solid Waste Streams*. 2010.

[38] Anne J. Meier et al. "Development of a Micro-Scale Plasma Arc Gasification System for Long Duration Space Mission Waste Processing". In: ICES, 2017.

[39] A. E. Drysdale and S. Maxwell. "Waste System Implications for Mars Missions". In: *Adv Space Res.* 31 (7 2003), pp. 1791–1797. DOI: https://doi.org/10.1016/s0273-1177(03)00012-7.

[40] Hannah Ritchie and Max Roser. *CO2 Emissions Data*. 2022. URL: https://ourworldindata.org/co2-emissions.

[41] P. E. Hintze et al. "Sabatier System Design Study for a Mars ISRU Propellant Production Plant". In: ICES, 2018.

[42] E. Fabbri and T. J. Schmidt. "Oxygen evolution reaction—the Enigma in water electrolysis". In: *ACS Catalysis* 8 (2018), 9765–9774. DOI: https://doi.org/10.1021/acscatal.8b02712.

[43] O. Sandru. *New catalyst for electrolysis reduces costs by 97% and increases hydrogen production fourfold*. URL: https://www.greenoptimistic.com/gridshift-electrolysis-catalyst-20100519/,addendum=accessed:02.20.2022,year=.

[44] Zachary W. Greenwood et al. "State of NASA Oxygen Recovery". In: ICES, 2018.

[45] United States Department of Energy. *Advanced closed loop system*. 2022. URL: https://www.energy.gov/eere/fuelcells/hydrogen-storage. (accessed: 02.01.2022).

[46] L. Spina and M. C. Lee. "Comparison of CO2 Reduction Process - Bosch and Sabatier". In: vol. 94. SAE International, 1985, pp. 262–271.

[47] European Space Agency. *Advanced closed loop system*. URL: https://www.esa.int/Science_Exploration/Human_and_Robotic_Exploration/Research/Advanced_Closed_Loop_System,addendum=accessed:04.01.2022,year=.

[48] J. L. Perry, H. E. Cole, and H. N. El-Lessy. *An Assessment of the International Space Station's Trace Contaminant Control Subassembly Process Economics*. 2005. URL: https://ntrs.nasa.gov/api/citations/20170006616/downloads/20170006616.pdf.

[49] Juan H. Agui and Jay L. Perry. "Life Support Filtration System Trade Study for Deep Space Missions". In: ICES, 2017.

[50] J. J. Konikoff. *Space Flight Ecologies*. 1961. URL: https://apps.dtic.mil/sti/pdfs/AD0268509.pdf.

[51] J. L. Perry. *Trace Contaminant Control for the International Space Station's Node 1—Analysis, Design, and Verification*. 2017. URL: https://ntrs.nasa.gov/api/citations/20170005170/downloads/20170005170.pdf.

[52] Ariel V. Macatangay and Rebekah J. Bruce. "Impacts of Microbial Growth on the Air Quality of the International Space Station". In: ICES, 2010.

[53] David L. Akin. *ENAE 483/788d - Fall, 2021 Lecture 15 Space Life Support Systems*. 2021. URL: https://spacecraft.ssl.umd.edu/academics/483F21/483F21L15.life_support/483F21L15.html.

[54] R. Schaezler et al. “Trending of overboard leakage of ISS cabin atmosphere”. In: ICES, 2011.

[55] Gregory J. Gentry. “International Space Station (ISS) Environmental Control and Life Support (ECLS) System Overview of Events: 2016-2017”. In: ICES, 2017.

[56] Harry W. Jones. “Oxygen Storage Tanks Are Feasible for Mars Transit”. In: ICES, 2017.

[57] VCH. *Liquid nitrogen hazards*. 2011. URL: https://www.vchri.ca/sites/default/files/LiquidNitrogenHazards_23June2011.pdf.

[58] P. Wieland. *Designing for human presence in space: An introduction to environmental control and life support systems (ECLSS)*. 2005. URL: https://ntrs.nasa.gov/api/citations/20060005209.pdf.

[59] Harry W. Jones et al. “Developing the Water Supply System for Travel to Mars”. In: ICES, 2016.

[60] *SpaceX*. SpaceX. URL: http://www.spacex.com (visited on 05/17/2022).

[61] Jeom Kee Paik, Anil K Thayamballi, and Gyu Sung Kim. “The strength characteristics of aluminum honeycomb sandwich panels”. In: *Thin-Walled Structures* 35.3 (1999), pp. 205–231. ISSN: 0263-8231. DOI: https://doi.org/10.1016/S0263-8231(99)00026-9. URL: https://www.sciencedirect.com/science/article/pii/S0263823199000269.

[62] K.J. Kennedy and L. Toups. “Constellation Architecture Team-Lunar Habitation Concepts”. In: *AIAA Space 2008 Conference Exposition*. 2008. DOI: https://arc.aiaa.org/doi/pdf/10.2514/6.2008-7633.

[63] David Akin, Zachary Lachance, and Charles Hanner. “Experimental Investigation of Minimum Required Cabin Sizing in Varying Gravity Levels”. In: *50th International Conference on Environmental Systems*. ICES-2021-097. 2021.

[64] *The Drag Equation*. 2021. URL: https://www.grc.nasa.gov/www/k-12/airplane/drageq.html.

[65] International Code Council, Inc. *2018 International Residential Code*. 2017. URL: https://codes.iccsafe.org/content/IRC2018P4/copyright.

[66] John A. Bologna. *Calculating Live Loads*. 2017. URL: https://coastalengineeringcompany.com/knowledge-base/calculating-live-loads.

[67] John Zippay, C. Thomas Modlin Jr., and Curtis Larsen. *The Ultimate Factor of Safety for Aircraft and Spacecraft – Its History, Applications and Misconceptions*. 2020. URL: https://ntrs.nasa.gov/api/citations/20150003482/downloads/20150003482.pdf.

[68] Christian Cavallo. *All About 6061 Aluminum (Properties, Strength and Uses)*. URL: https://www.thomasnet.com/articles/metals-metal-products/6061-aluminum/#:~:text=The\%20shear\%20strength\%20of\%206061,are\%20summarized\%20in\%20Table\%201..

[69] Madeh Hamakareem. *Cantilevered Beams and Trusses- Uses and Advantages*. URL: https://theconstructor.org/structural-engg/cantilevered-beams-trusses-applications-advantages/36236/.

[70] Paul Comino. *Difference Between Truss and Frame Members*. URL: https://skyciv.com/education/truss-vs-frame-members/.

[71] US Department of Defense. *HUMAN ENGINEERING DESIGN DATA DIGEST*. 2000. URL: https://rt.cto.mil/wp-content/uploads/2019/07/HE_Design_Data_Digest-acts.pdf.

[72] HGB Industrial Group. *Advantages and Uses of Square Tubing*.

[73] A. Varma. *Design of Steel Structures*. 2017. URL: https://www.egr.msu.edu/~harichan/classes/ce405/chap5.pdf.

[74] AZO Materials. *Stainless Steel - Grade 305*. 2012. URL: https://www.azom.com/article.aspx?ArticleID=6795.

[75] Harvey Tool Technical Resources. *Clearance Hole Drill Sizes*. URL: http://fpg.phys.virginia.edu/fpgweb/useful_info/Clearance_Hole_Drill_Sizes.pdf.

[76] Idea StatiCa. *Detailing of bolts and welds and anchors according to AS*. 2022. URL: https://www.ideastatica.com/support-center/detailing-of-bolts-and-welds-and-anchors-according-to-as.

[77] S.I Talabi O.B Owolabi J.A Adebisi T. Yahaya. “Effect of welding variables on mechanical properties of low carbon steel welded joint”. In: *Advances in Production Engineering Management* 9 (2014). URL: https://www.apem-journal.org/Archives/2014/APEM9-4_181-186.pdf.

[78] American Welding Society. *STRUCTURAL WELDING CODE -ALUMINUM*. 2014. URL: https://pubs.aws.org/p/1277/d12d12m2014-structural-welding-code-aluminum.

[79] AZO Materials. *ASTM A36 Mild/Low Carbon Steel*. 2012. URL: https://www.azom.com/article.aspx?ArticleID=6117.

[80] The Canadian Press. *Do you have what it takes to go to space?* 2017. URL: https://nationalpost.com/news/canada/do-you-have-what-it-takes-to-go-to-space-retired-astronauts-weigh-in-on-the-gruelling-recruitment-process#:~:text=Aside\%20from\%20being\%20in\%20excellent,(110\%20and\%20209\%20pounds)..

[81] *Actuonix L12-50-50-6-I*. Actuonix Motion Devices Inc. URL: https://www.actuonix.com/l12-50-50-6-i (visited on 05/18/2022).

[82] William F. Rogers. *Apollo Lunar Module Landing Gear*. 1973.

[83] Coyle W. Ayers M. Kemp J. Warfield B. Maida J. Bowen C. Bernecker C. Lockley S. W. Hanifin J. P. Brainard G. C. "Solid-state lighting for the International Space Station: Tests of visual performance and Melatonin Regulation". In: *Acta Astronautic* 92.1 (2013), pp. 21–28. DOI: https://doi.org/10.1016/j.actaastro.2012.04.019.

[84] Solid State Luminaries. *CLCV Interior RGBW Fixture Datasheet*. 2022. URL: https://www.solidstateluminaires.com/downloads/specs/CLCV.pdf.

[85] Jennifer Boyer Whitmore Mihriban and Keith Holubec. "NASA-STD-3001, Space Flight Human-System Standard and the Human Integration Design Handbook". In: *In Industrial and Systems Engineering Research Conference*. 2012. URL: https://msis.jsc.nasa.gov/.

[86] Smithsonian Magazing. *ISS Nightlights*. 2014. URL: https://www.smithsonianmag.com/air-space-magazine/station-nightlights-180965844/. (accessed: 05.17.2022).

[87] NASA. *SCaN Network Coverage*. 2019. URL: https://essp.larc.nasa.gov/EVM-3/pdf_files/SCaN-MOCS-0001\%20Rev\%202_final.pdf. (accessed: 05.17.2022).

[88] NASA JPL. *DSN Telecommunications Link Design Handbook*. 2021. URL: https://deepspace.jpl.nasa.gov/dsndocs/810-005/.

[89] NASA Space Communication and Navigation. *Lunar Exploration Ground Sites (LEGS) LEGS Brochure*. 2020. URL: https://essp.larc.nasa.gov/EVI-6/pdf_files/LEGS\%20Brochure\%20r20.pdf.

[90] Harris Andrea. *All about the new wi-fi 6 standard - 802.11ax explained (tutorial)*. 2021. URL: https://www.tech21century.com/802-11ax-wifi6-explained/.

[91] Tech Behr. *Mesh vs star topology – how to find the right architecture for your IOT Networks*. 2021. URL: https://behrtech.com/blog/mesh-vs-star-topology/.

[92] Feng Xia. *Wireless Sensor Technologies and Applications*. 2009. URL: https://www.mdpi.com/1424-8220/9/11/8824/htm#:~:.

[93] Sushil Kumar and D. K. Lobiyal. *Sensing coverage prediction for wireless sensor networks in shadowed and multipath environment*. 2013. URL: https://www.hindawi.com/journals/tswj/2013/565419/.

[94] et al. Marc Gibson. *Kilopower Reactor Using Stirling TechnologY (KRUSTY) Nuclear Ground Test Results and Lessons Learned*. 2019. URL: https://ntrs.nasa.gov/api/citations/20180007389/downloads/20180007389.pdf.

[95] Patrick McClure David I. Poston Marc Gibson. *Kilopower Reactors for Potential Space Exploration Missions*. 2019. URL: http://anstd.ans.org/NETS-2019-Papers/Track-4--Space-Reactors/abstract-96-0.pdf.

[96] Patrick Ray Mcclure. *Space Nuclear Reactor Development*. 2017.

[97] *Kilopower*. URL: https://www.nasa.gov/directorates/spacetech/kilopower.

[98] *Space Radiation*. 2019. URL: https://www.nasa.gov/sites/default/files/atoms/files/space_radiation_ebook.pdf.

[99] John E. Nealy Lisa C. Simonsen. *Radiation Protection for Human Missions to the Moon and Mars*. 1991. URL: http://citeseerx.ist.psu.edu/viewdoc/download;jsessionid=9A1182C85822037B15B47B45E94BD220?doi=10.1.1.518.6098&rep=rep1&type=pdf.

[100] Dan Lockney. *Cost-Saving Method Yields Solar Cells for Exploration, Gadgets*. 2016.

[101] Eric D. Gustafson Thomas W. Kerslake. *On-Orbit Performance Degradation of the International Space Station P6 Photovoltaic Arrays*. 2003.

[102] *Visual Satellite Observing Chapter 09*. 1998. URL: http://www.satobs.org/faq/Chapter-09.txt.

[103] Sumanth RM. "Computation of eclipse time for low-earth orbiting small satellites". In: *International Journal of Aviation, Aeronautics, and Aerospace* 6.5 (2019), p. 15.

[104] Mark Kane. *Catl breaks into 300+ wh/kg energy density on battery cell level*. 2019. URL: https://insideevs.com/news/343690/catl-breaks-into-300-wh-kg-energy-density-on-battery-cell-level/.

[105] Sonja Caldwell. *3.0 power*. 2021. URL: https://www.nasa.gov/smallsat-institute/sst-soa/power#3.3.4.

[106] *Cost-saving method yields solar cells for exploration, gadgets*. 2016. URL: https://spinoff.nasa.gov/Spinoff2016/ee_5.html.

[107] Kwangbok Jeong et al. "A prototype design and development of the smart photovoltaic system blind considering the photovoltaic panel, tracking system, and monitoring system". In: *Applied Sciences* 7.10 (2017), p. 1077.

[108] David L. Akin. *ENAE 483/788d - Fall, 2021 Lecture 17 Space Power Systems Design*. 2021. URL: https://spacecraft.ssl.umd.edu/academics/483F21/483F21L17.power/483F21L17.powerx.pdf.

[109] David L. Akin. *ENAE 483/788d - Fall, 2021 Lecture 11 The Space Environment*. 2021. URL: https://spacecraft.ssl.umd.edu/academics/483F21/483F21L11.environ/483F21L11.environ_r1x.pdf.

[110] NASA Goddard. *100 Lunar Days - Parts I and II*. 2017.

[111] Phil Lamarr. *What is the temperature on the Moon?* URL: https://coolcosmos.ipac.caltech.edu/ask/168-What-is-the-temperature-on-the-Moon-.

[112] David G Gilmore, David G Gilmore, and Martin Donabedian. *Spacecraft thermal control handbook*. Vol. 1. Aerospace Press El Segundo, CA, 2002.

[113] John H Henninger. *Solar absorptance and thermal emittance of some common spacecraft thermal-control coatings*. Vol. 1121. National Aeronautics, Space Adminitration, Scientific, and Technical . . ., 1984.

[114] Alexander M. Jablonski Dinindu Gunasekara. "Technical Aspects of Micrometeoroid Impact on Lunar Systems/Structures". In: *ASCE* (2021).

[115] Kriss J. Kennedy. "International Space Station (ISS) TransHab: An Inflatable Habitat". In: (2000).

[116] Micael Ekstrom Stephen Hofstetter Troy Markes Erich Orzech Andrew Brady Josh Bullock. *Micrometeoroid and Orbital Debris (MMOD) Shielding*.

[117] Mark Wade. *Lox/LH2*. 2019. URL: http://www.astronautix.com/l/loxlh2.html.

[118] V. N. Smelyanskiy C. B. Muratov V. V. Osipov. *Issues of Long-Term Cryogenic Propellant Storage in Microgravity*. 2011.

[119] *Liquid Rocket Propellant*. URL: https://www.sciencedirect.com/topics/earth-and-planetary-sciences/liquid-rocket-propellant#:~:text=The\%20most\%20popular\%20monopropellant\%20today,when\%20we\%20need\%20large\%20impulses..

[120] DLA Energy rocket propellant fuels NASA rover to Red Planet. *Lox/LH2*. 2021. URL: https://www.dla.mil/AboutDLA/News/NewsArticleView/Article/2512550/dla-energy-rocket-propellant-fuels-nasa-rover-to-red-planet/.

[121] Peter A. Van Splinter Forrest S. Forbes. *Hydrazine*. URL: https://pubchem.ncbi.nlm.nih.gov/compound/Hydrazine.

[122] Alan Wilhite et al. "Lunar module descent mission design". In: *AIAA/AAS Astrodynamics Specialist Conference and Exhibit*. 2008, p. 6939.

[123] Ronny Votel and Doug Sinclair. "Comparison of control moment gyros and reaction wheels for small earth-observing satellites". In: (2012).

[124] Hugo Nguyen, Johan Köhler, and Lars Stenmark. “The merits of cold gas micropropulsion in state-of-the-art space missions”. In: *The 53rd International Astronautical Congress, IAC 02-S. 2.07, Houston, Texas*. 2002.

[125] Thomas R. Coon and John E. Irby. “Skylab attitude control system”. In: *IBM Journal of Research and Development* 20.1 (1976), pp. 58–66.

[126] Kriss J. Kennedy. “Lessons from Transhab: An Architect’s Experience”. In: *AIAA Space Architecture Symposium*. AIAA, 2002. DOI: 10.4271/2002-6105.

[127] *Greenlee 849 1/2” - 2” Electric PVC Heater/Bender*. URL: http://web.archive.org/web/20080207010024/http://www.808multimedia.com/winnt/kernel.htm.

[128] *Hotblanket PVC Bender*. URL: https://www.amazon.com/Gardner-Bender-BB5150-Hotblanket-Conduit/dp/B000N50NGI/ref=asc_df_B000N50NGI/?tag=hyprod-20&linkCode=df0&hvadid=309802506143&hvpos=&hvnetw=g&hvrand=14659371732931136639&hvpone=&hvptwo=&hvqmt=&hvdev=c&hvdvcmdl=&hvlocint=&hvlocphy=9007733&hvtargid=pla-593079841154&psc=1.

[129] *GYZJ Hydraulic Pipe Bender 1/2 Inch Manual Copper Exhaust Bender Tool 6 Dies*. URL: https://www.amazon.com/Hydraulic-Exhaust-Adjustable-Rollers-Ratcheting/dp/B09JK4JSG1/ref=sr_1_5?keywords=pipe+bender&qid=1643152911&sprefix.

[130] John Mularski and David Akin. “Water Immersion Ballasted Partial Gravity for Lunar and Martian EVA Simulation”. In: *37th International Conference on Environmental Systems (ICES)*. 2007-01-3145. 2007.

[131] NASA. *ISS User’s Guide*. URL: http://www.spaceref.com/iss/ops/ISS.User.Guide.R2.pdf.

[132] *PVC Pipe Dimensions 1/8” through 24”*. 2021. URL: https://www.pvcfittingsonline.com/resource-center/pvc-pipe-dimensions-18-through-24/.

[133] et al Autrey David. *Development of the Universal Waste Management System*. 2020. URL: https://ttu-ir.tdl.org/bitstream/handle/2346/86292/ICES-2020-278.pdf?sequence=1..

[134] Shrawan Kumar. “Upper body push-pull strength of normal young adults in sagittal plane at three heights”. In: *International Journal of Industrial Ergonomics* 15 (1995). URL: https://www-sciencedirect-com.proxy-um.researchport.umd.edu/science/article/pii/0169814194000628.

[135] *1/4-20 x 3/4” Hex Head Tap Bolts Fully Threaded Stainless Steel 18-8 Qty 50*. URL: https://www.fastenere.com/14-20-x-34-hex-head-tap-bolts-fully-threaded-stainless-steel-18-8-qty-50.

[136] “Which Velcro brand fastener is the strongest”. In: *Velcro Brand Blog* (2022).

[137] T. Thiele. “Choosing the correct extension cord sizes is critical to safety”. In: *The Spruce* (2021).

[138] Alle Rechte vorbehalten. “PTFE convoluted hoses”. In: (2015).

[139] Branelle R. Rodriguez Thilini P. Schlesinger. “International Space Station Crew Quarters”. In: (2013).

[140] “Ever wonder how much a fiber or ethernet cable weigh”. In: *Myriad360* (2011).

[141] *NASA Task Load Index*. URL: https://humansystems.arc.nasa.gov/groups/TLX/downloads/TLXScale.pdf.

[142] Portland Bolt. *Calculating Yield Tensile Strength*. 2011. URL: t.https://www.portlandbolt.com/technical/faqs/calculating-strength/.

[143] The Engineering ToolBox. *Threaded Bolt Stress Area*. URL: https://www.engineeringtoolbox.com/bolt-threads-stress-d_856.html.

[144] *International Space Station Timelines*. 2013. URL: https://www.nasa.gov/content/international-space-station-timelines-december-2013.

[145] *Shannon Walker: A Day in the Life on the International Space Station*. 2021. URL: https://www.nasa.gov/stem/feature/shannon-walker-a-day-in-the-life-on-the-international-space-station.html.